ETC HE Report 2022/12

European air quality maps for 2020

PM_{10}, $PM_{2.5}$, Ozone, NO_2, NO_x and Benzo(a)pyrene spatial estimates and their uncertainties

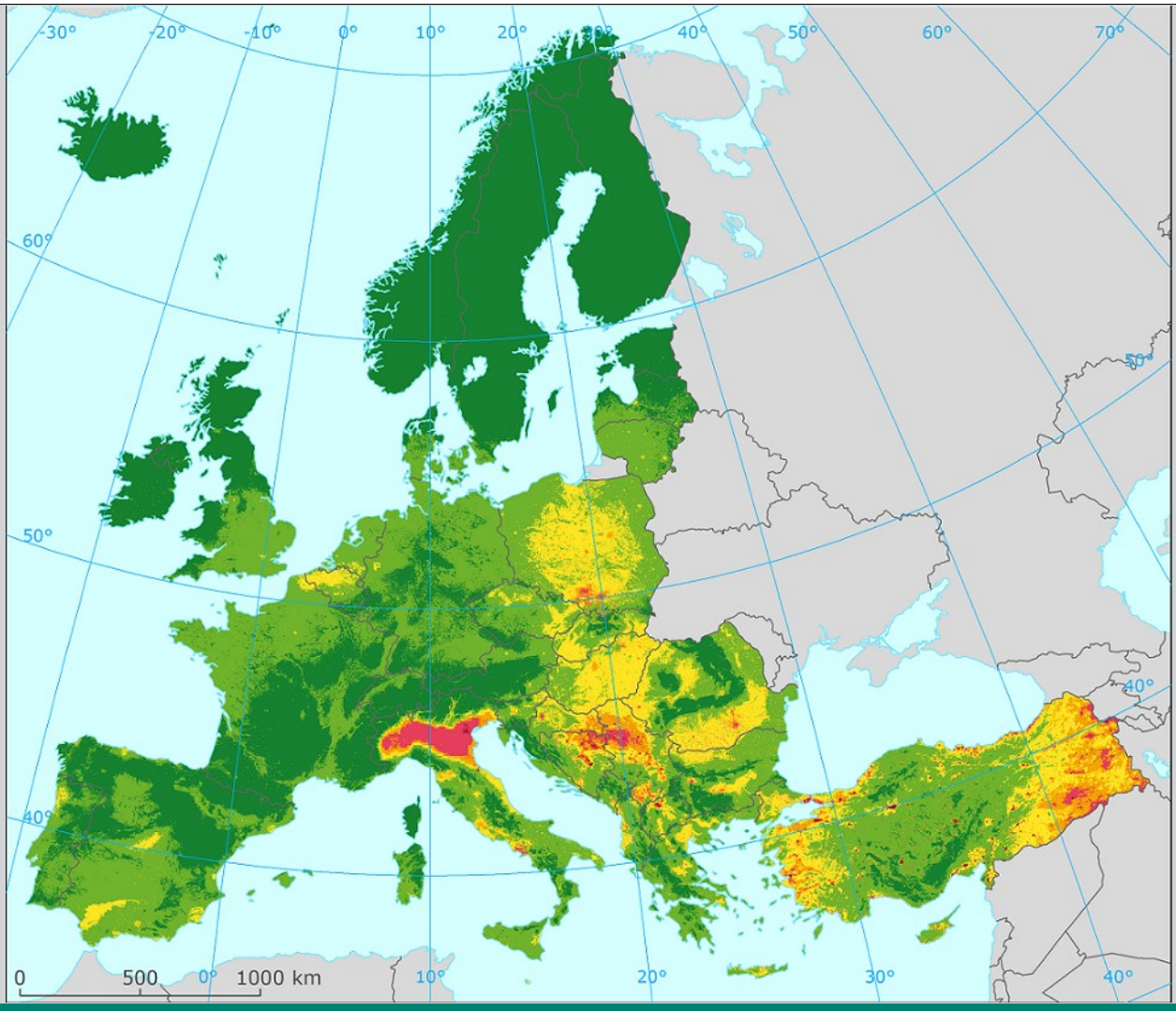

Authors:
Jan Horálek (CHMI), Leona Vlasáková (CHMI), Markéta Schreiberová (CHMI), Jana Marková (CHMI), Philipp Schneider (NILU), Pavel Kurfürst (CHMI), Frédéric Tognet (INERIS), Jana Schovánková (CHMI), Ondřej Vlček (CHMI), Daša Damašková (CHMI)

European Environment Agency
European Topic Centre
Human health and the environment

Cover design: EEA
Cover picture: Concentration map of PM_{10} indicator 90.4 percentile of daily means for 2020. Units: µg/m^3. (Map 2.2 of this report.)
Layout: EEA and ETC HE

Publication Date: January 2023
Revised Version Publication Date: 16 February 2024
ISBN 978-82-93970-39-2

How to cite this report:
Horálek, J., Vlasáková, L., Schreiberová, M., Marková, J., Schneider, P., Kurfürst, P., Tognet, F., Schovánková, J, Vlček, O, Damašková, D. (2022). *European air quality maps for 2020. PM10, PM2.5, Ozone, NO2, NOx and Benzo(a)pyrene spatial estimates and their uncertainties* (Eionet Report – ETC HE 2022/12). European Topic Centre on Human Health and the Environment.

The report is available from https://www.eionet.europa.eu/etcs/all-etc-reports and https://zenodo.org/communities/eea-etc/?page=1&size=20.

EEA activity Human Health and the Environment

Revision note
This is a revised version of the report published in January 2023, which has been prepared due to an error in the ozone measurement data. POD_6 maps (i.e. Maps 3.6-3.8) and the relevant descriptions in Summary and Section 3.4.1 have been updated, as well as Table A3.9 and Figures A3.8 and A3.9 in Annex 3.

ETC HE coordinator: Stiftelsen NILU

ETC HE consortium partners: Federal Environment Agency/Umweltbundesamt (UBA), Aether Limited,
Czech Hydrometeorological Institute (CHMI), Institut National de l'Environnement Industriel et des Risques (INERIS),
Swiss Tropical and Public Health Institute (Swiss TPH), Universitat Autònoma de Barcelona (UAB),
Vlaamse Instelling voor Technologisch Onderzoek (VITO), 4sfera Innova S.L.U., klarFAKTe.U

The United Kingdom exited the European Union in January 2020. Nevertheless, results in this report include this country. In this way, a comparison of the 2020 results with the previous years can be done. This is especially important because 2020 saw an exceptional decrease in the emission of certain pollutants, specifically NO_2, due to the lockdown measures adopted to prevent the spread of the COVID-19.

European Topic Centre on
Human Health and the Environment (ETC HE)
https://www.eionet.europa.eu/etcs/etc-he

Contents

Acknowledgements

The EEA task manager was Alberto González Ortiz. The external task ETC HE reviewer was Joana Soares (NILU, Norway).

The air quality monitoring data for 2020 were extracted from the AQ e-reporting database by Anna Ripoll and Jaume Targa (4sfera, Spain). The CAMS-Ensemble Forecast model results for 2020 were downloaded by Paul Hamer (NILU, Norway). The Obukhov length and the air density data for 2020 were calculated by Florian Couvidat (INERIS, France).

The EMEP modelling data for benzo(a)pyrene as prepared under the Meteorological Synthesizing Centre - East (MCS-E) were provided by Alexey Gusev (EMEP, MCS-E, Russia).

Summary

European air quality concentrations maps have been prepared for the year 2020. The maps are based primarily on air quality data as reported under the Ambient air quality directives by EEA member and cooperating countries and voluntary reporting countries (EC, 2004, 2008). The countries considered for mapping include the most of Europe, apart from its eastern part. Concentration maps have been produced to assess the situation with respect to the most stringent air quality limit values and the indicators most relevant for the assessment of impacts on human health and vegetation.

Methodology

The mapping method follows the methodology developed earlier (Horálek et al, 2022a, and references cited therein); it combines the monitoring data with the results from a chemical transport model and other supplementary data (such as land cover, meteorological and satellite data). The method ('Regression – Interpolation – Merging Mapping') is based on a linear regression model followed by kriging of the residuals produced from that model (residual kriging). Next to this, maps of Phytotoxic Ozone Dose (POD) indicators have been presented since 2018, based on methodology described in CLRTAP (2017a) according to Emberson et al. (2000). These maps are prepared based on hourly ozone rural maps, hourly meteorological data and soil hydraulic properties data.

Population exposure

Concentrations of PM_{10} (i.e. particulate matter with a diameter of 10 µm or less) continued to be above the EU and WHO standards in large parts of Europe. Almost 6 % of the considered European population is exposed to concentrations above the EU PM_{10} limit value of 40 µg/m^3; 35 % of the considered European population is exposed to concentrations above the 2005 WHO Air Quality Guideline (AQG) level of 20 µg/m^3 (WHO, 2005) and 65 % of population is exposed to concentrations above the 2021 WHO AQG level of 15 µg/m^3 (WHO, 2021a). Table 2.2 shows that 17 % of the population is exposed to PM_{10} concentrations above the daily limit value in more than 35 days per year. Figure S.1 shows that the countries with the highest values of annual averages PM_{10} are located in the south-eastern parts of Europe.

Figure S.1: PM_{10} annual mean concentrations to which the population per country was exposed in 2020. The 2021 WHO AQG level (15 µg/m³) is marked by the green line, the 2005 WHO AQG level (20 µg/m³) is marked by the yellow line, the EU annual limit value (40 µg/m³) is marked by the red line

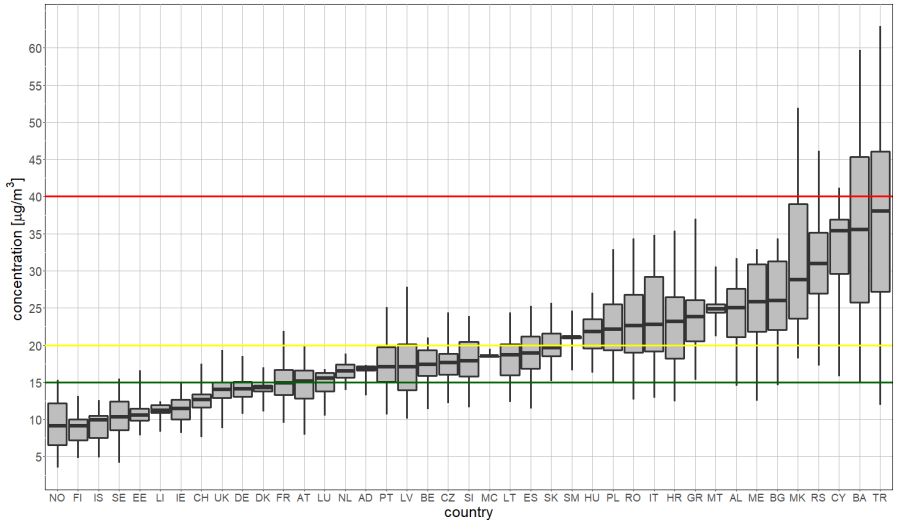

Note: For each country, the box plot shows the concentration to which a percentage of the population was exposed: 50 % in the case of the black marker, 25 % and 75 % in the cases of the box's edges, 2 % and 98 % in the cases of the whiskers' edges.

Approximately 1 % and 6 % of the considered European population (excluding Türkiyein this case of $PM_{2.5}$) is exposed to concentrations above the EU $PM_{2.5}$ limit value of 25 µg/m³ and to concentrations above the EU $PM_{2.5}$ indicative limit value of 20 µg/m³, respectively. Almost 47 % of the considered European population is exposed to concentrations above the 2005 WHO AQG level of 10 µg/m³ (WHO, 2005) and 97 % of the population is exposed to concentrations above the 2021 WHO AQG level of 5 µg/m³ (WHO, 2021a), see Table 3.1. The concentrations of $PM_{2.5}$ and PM_{10} are often highly correlated, with the highest $PM_{2.5}$ exposures found in the central, south and south-eastern parts of Europe similarly as in the case of PM_{10}, see Figure S.2.

Figure S.2: $PM_{2.5}$ annual mean concentrations to which the population per country was exposed in 2020. The 2021 WHO AQG level (5 µg/m³) is marked by the green line, the 2005 WHO AQG level (10 µg/m³) is marked by the yellow line, the EU annual indicative limit value (20 µg/m³) is marked by the orange line and the EU annual limit value (25 µg/m³) is marked by the red line

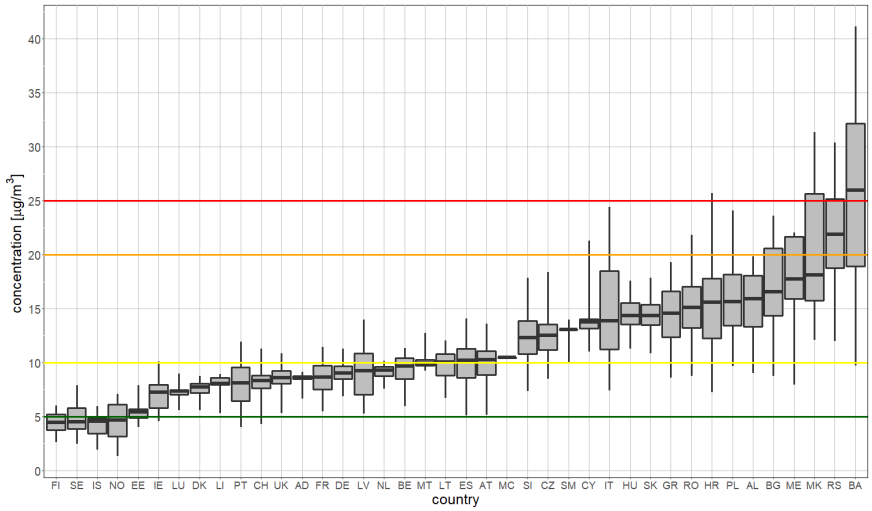

Note: For each country, the box plot shows the concentration to which a percentage of the population was exposed: 50 % in the case of the black marker, 25 % and 75 % in the cases of the box's edges, 2 % and 98 % in the cases of the whiskers' edges.

The nitrogen dioxide (NO_2) annual mean concentration map shows a different spatial distribution than the PM maps. Table 5.1 indicates that in 4 countries (Romania, Italy, France and Greece), a limited fraction of the considered European population (2 % in total) has been exposed to concentrations above the EU annual limit value of 40 µg/m³ (which is the same as the 2005 WHO AQG level). Nevertheless, more than 72 % of the considered European population has been exposed to annual average concentrations above the current 2021 WHO AQG level of 10 µg/m³ (WHO, 2021a). Figure S.3 shows that in all countries, the majority of population lived well below the limit value in 2020, according to the presented assessment.

High exposures to annual mean concentrations of 20-30 µg/m³ are observed in the larger urban areas (e.g. Milan, Naples, Rome, Turin, Paris, Barcelona, Madrid, London, Athens, Bucharest, Ankara, and Istanbul).

Figure S.3: NO_2 annual mean concentrations to which the population per country was exposed in 2020. The 2021 WHO AQG level (10 µg/m^3) is marked by the green line, the EU annual limit value and the 2005 WHO AQG level (40 µg/m^3 in both cases) are marked by the red line

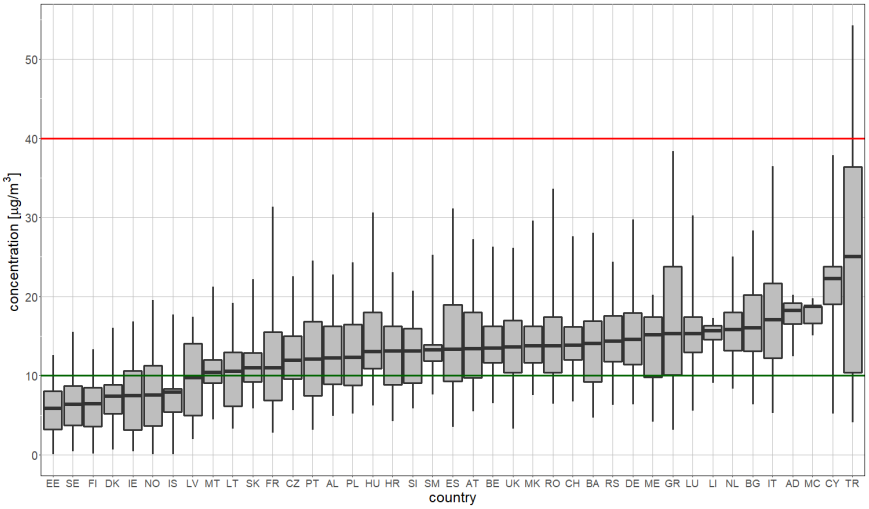

Note: For each country, the box plot shows the concentration to which a percentage of the population was exposed: 50 % in the case of the black marker, 25 % and 75 % in the cases of the box's edges, 2 % and 98 % in the cases of the whiskers' edges.

Exposure to ozone concentrations above the EU target value (TV) threshold (a maximum daily 8-hour average value of 120 µg/m^3 not to be exceeded on more than 25 days per year) occurs in 2020 in a large area of Europe, namely in some areas of Europe, namely in Belgium, France, Germany, Italy, Luxembourg, Netherlands, Portugal, San Marino, Spain, Switzerland and Türkiye. More than 7 % of the considered European population live in areas where concentrations are above the ozone TV (Table 4.1). Figure S.4 shows that the countries with the highest values of SOMO35 are located in the southern and south-eastern parts of Europe.

Figure S.4: Ozone concentrations (expressed as the indicator SOMO35) to which the population per country was exposed in 2020

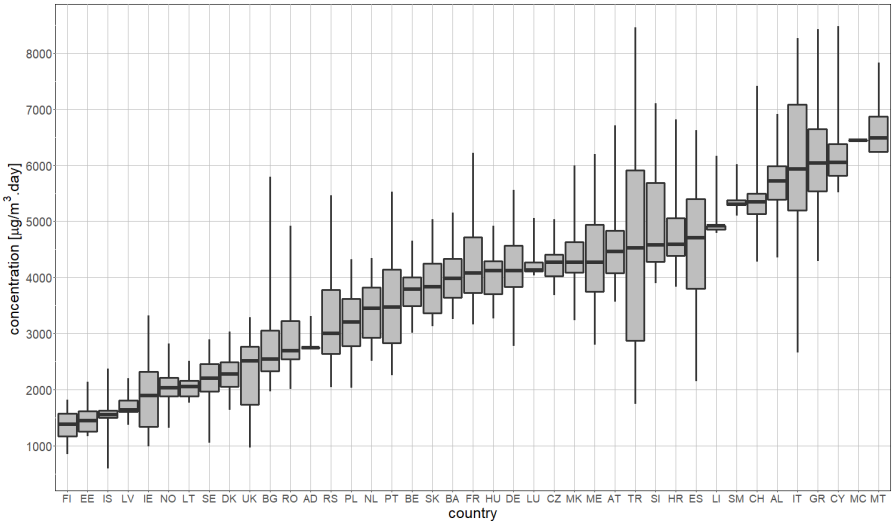

Note: For each country, the box plot shows the concentration to which a percentage of the population was exposed: 50 % in the case of the black marker, 25 % and 75 % in the cases of the box's edges, 2 % and 98 % in the cases of the whiskers' edges.

Based on the experimental map of benzo(a)pyrene (BaP), it is estimated that 14 % of the considered European population live in areas where concentrations are above the EU ozone TV (Table 5.1). The highest BaP concentrations are shown in Poland, north-eastern Czechia and some populated locations in the central and south-eastern Europe and the eastern Po Valley in northern Italy.

Accumulated risks

Although the spatial distributions of PM, NO_2 and ozone concentrations differ widely, the possibility of an accumulation of risk resulting from high exposures to all three pollutants cannot be excluded. The maps for the three most frequently exceeded EU standards (PM_{10} daily limit value, O_3 target value and NO_2 annual limit value) have been combined, see Map S.1.

Map S.1: Exceedance of Health-Related Air Quality Standards, 2020

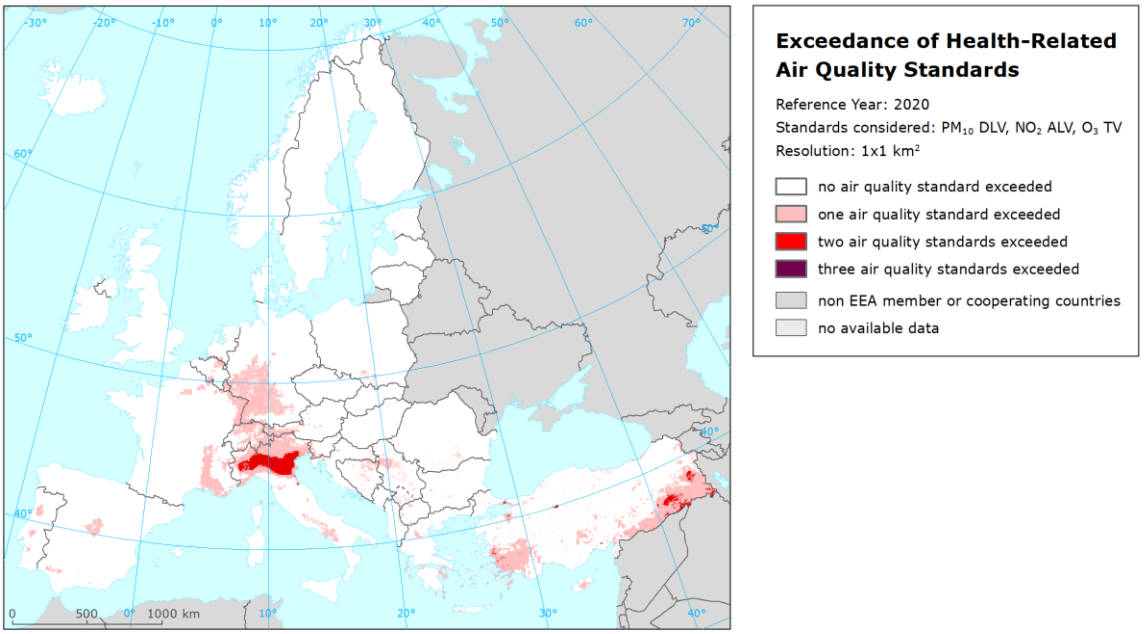

The combined population exposure shows the following results: out of the total population of 623 million in the mapping area, 5 % (34.4 million) people live in areas where two or three of these air quality standards are exceeded; and 0.05 % (314 000) people live in areas where all three standards are exceeded. The worst situation is observed in Italy (in particular the Po valley), where 0.5 % of the Italian population live in areas where all three standards are exceeded; this is followed by Türkiye, where it is also the case for 0.04 % of the Turkish population.

Vegetation exposure

Standards for the protection of vegetation have been set, among others, for NO_x and ozone. In a limited number of cases, concentrations of NO_x are above the critical level, although since most of thoses cases happen in urban areas, this is relevant only if there is vegetation in those areas. A larger impact on vegetation can be expected from the direct exposure to ozone. Ozone concentrations (AOT40 for vegetation) are above the target value for the protection of vegetation in about 5 % of the agricultural areas and above long-term objective in 75 % of the agricultural areas. Ozone concentrations (AOT40 for forests) are above the critical level for the protection of forests in about 61 % of the forested areas.

In 2020, the exceedance of critical levels (CLs) of Phytotoxic Ozone Dose (POD_6) for wheat is most noticeable over large parts of France, the United Kingdom, Poland and Czechia. However, exceedances of the CLs for wheat have also occurred in other areas of varying size in many other countries from the north to the south of the whole mapped area. Most of France, Benelux and Italy showed values of POD_6 for potato above the corresponding CL in 2020. Values of POD_6 for potato above the CL were also found in larger areas of the United Kingdom, Germany, Poland, Portugal, Spain and Hungary. On the other hand, in the case of POD_6 for tomato only in very small parts of the coastal areas (where tomatoes are supposed to be grown in open air) POD_6 values above critical level for tomato have occurred.

Changes over time

Since 2005, maps for most of the pollutants have been prepared in an overall consistent way, although the mapping methodology has been subject to continuous improvement. This enables an analysis of changes in exposure over time. While PM_{10} and ozone maps have been prepared for the whole period 2005-2020, $PM_{2.5}$ maps have been routinely constructed since 2010, NO_2 maps since 2014 and BaP only since 2020, with few maps for older years available. Thus, $PM_{2.5}$ maps are available for the whole period 2005-2020 apart from 2006, while in the case of NO_2 the maps for 2006, 2008, 2011 and 2012 are missing. Throughout the years, some methodology changes have been applied. Apart from minor changes, a major change was introduced for PM_{10} and $PM_{2.5}$ since 2017 maps, taking into account air quality in urban traffic areas, as was done for all the NO_2 maps.

The population-weighted concentration is calculated for the area of all countries considered in the report, both including and excluding Türkiye, because the area of Türkiye has not been mapped until 2016. For changes in population-weighted concentrations, excluding Türkiye, see Figure S.5. For comparability reasons, the results based on both the old and the new PM mapping methodology have been included in Figure S.5.

Figure S.5: Population-weighted concentration of PM_{10} (annual mean), $PM_{2.5}$ (annual mean), ozone (SOMO35), and NO_2 (annual mean) in 2005-2020. For PM_{10} and $PM_{2.5}$, results based on both the old (blue dots) and the updated (red dots) mapping methodology are presented, where available.

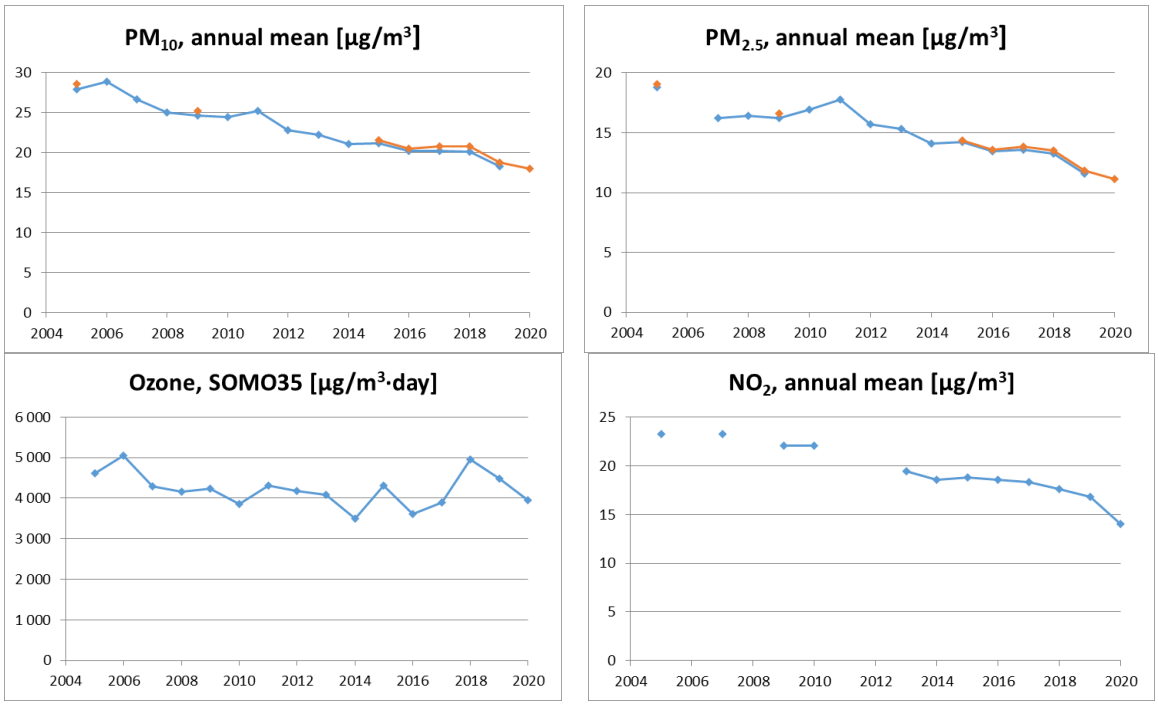

The PM concentrations show a steady decrease of about 0.6 µg/m^3 per year for PM_{10} annual average and 0.5 µg/m^3 per year for $PM_{2.5}$ annual average. It is estimated that the considered European inhabitants have been exposed on average to an annual mean PM_{10} concentration of 18 µg/m^3 and to an annual mean $PM_{2.5}$ concentration of 11 µg/m^3 in 2020, being both the lowest values in the sixteen-year time series.

For the ozone concentration (expressed as SOMO35) no trend is observed for the period 2005-2020, due to the year-to-year variability. The NO_2 concentration (in terms of annual average) shows a decrease of about 0.5 µg/m^3 per year.

Again, the agricultural-weighted concentration is calculated for the area of all countries considered in the report, both including and excluding Türkiye. For changes in agricultural-weighted concentrations (in terms of AOT40 for vegetation), excluding Türkiye, see Figure S.6. No trend is observed for the agricultural-weighted concentration over the period 2005-2020, in terms of AOT40 for vegetation.

Figure S.6: Agricultural-weighted concentration of ozone indicator AOT40 for vegetation in 2005-2020

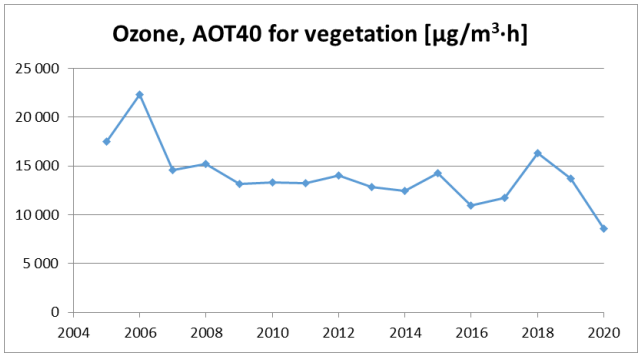

1 Introduction

This report provides European air quality concentration maps, population exposure and vegetation exposure estimates for 2020. It builds on the previous reports (Horálek et al., 2022a, and references cited therein). The analysis is based on interpolation of annual statistics of validated monitoring data from 2020, reported by the EEA member and cooperating countries (and the voluntary reporting country of Andorra) in 2020. The paper presents mapping results and includes an uncertainty analysis of the interpolated maps, adopting the latest methodological developments, see Horálek et al. (2021) and references cited therein. The mapping area covers all of Europe apart from Belarus, Moldova, Ukraine and the European parts of Russia and Kazakhstan. Türkiye([1]) (including both European and Asian areas) is included in the mapping area for all pollutants except $PM_{2.5}$, due to the lack of rural stations in Türkiye for $PM_{2.5}$ in 2020 reported data to the AQ e-reporting database (EEA, 2022a).

In this report particulate matter (PM_{10} and $PM_{2.5}$)([2]) ozone (O_3), nitrogen dioxide (NO_2), nitrogen oxides (NO_x) and benzo(a)pyrene (BaP) are considered for 2020, being the most relevant pollutants for annual updating due to their potential impacts on health and ecosystems. The analysis method applied is similar to that of previous years. Benzo(a)pyrene is presented for the first time in this regular report, based on the method shown in Horálek et al. (2022b).

The mapping is primarily based on air quality measurements. It combines monitoring data, chemical transport model results and other supplementary data (such as altitude and meteorology). The method is a linear regression model followed by kriging of the residuals produced from that model ("residual kriging"). It should be noted that this methodology does not allow for formal compliance checking with the limit or target values as set by the Ambient air quality directives (EC, 2004, 2008).

The maps of health-related indicators of ozone are created for the rural and urban (including suburban) background areas separately on a grid at 10x10 km^2 resolution. Subsequently, the rural and urban background maps are merged into one final combined air quality indicator map using a 1x1 km^2 population density grid, following a weighting criterion applied per grid cell. This fine resolution takes into account the smaller settlements in Europe that are not resolved at the 10x10 km^2 grid resolution. The maps of health-related indicators of PM_{10}, $PM_{2.5}$, and NO_2 are constructed by the improved mapping methodology developed in Horálek et al. (2017b, 2018, 2019): together with the rural and urban background map layers, the urban traffic map layer is constructed and incorporated into the final merged map using the road data. All individual map layers are created at 1x1 km^2 resolution and land cover and road data are included in the mapping process as supplementary data. The maps of ozone and NO_x vegetation-related indicators are constructed at a grid resolution of 2x2 km^2 and applicable for rural areas only. They are based on rural background measurements; in the case of ozone, they serve as input to the EEA's indicator AIR004 (EEA, 2022b). The map of BaP is constructed using the rural and urban map layers that are created at the 1x1 km^2 resolution and subsequently merged. The map of BaP is labelled as experimental (as recommended in Horálek et al., 2022c) to indicate that it does not yet meet the same accuracy standards as the regularly produced maps of other pollutants.

Among the ozone vegetation-related indicators, maps of Phytotoxic Ozone Dose (POD_6) indicators are also presented, following the conclusions of Colette et al. (2018). POD is the ozone flux through the stomata of leaves above a specific threshold accumulated during a specified time; it is calculated based on methodology described in CLRTAP (2017a) according to Emberson et al. (2000) and Jarvis (1976).

Maps of the POD were presented for the first time in Horálek et al. (2021). This indicator takes into account the plant physiology, not only the ozone concentrations in the ambient air (as in the AOT40

([1]) In this report, new official name Türkiye is used for this country, instead of earlier name Turkey.

([2]) PM_{10} and $PM_{2.5}$ is particulate matter with a diameter of 10 µm and $PM_{2.5}$ or less, respectively.

indicators), and reflects the ozone actually absorbed by the vegetation. It is widely acknowledged that the impact of ozone on vegetation is more closely related to the ozone flux absorbed through the stomata than to the exposure to ozone in the atmosphere (Musselman and Massman, 1998; Nussbaum et al., 2003). The POD annual maps are calculated based on hourly ozone rural maps (created similarly to the annual ozone maps), hourly meteorological data and the soil hydraulic properties data. In the report, the maps of POD for representative species of crops in Europe (i.e. wheat, potato and tomato), in agreement with CLRTAP (2017a), are presented.

Next to the annual indicator maps, tables showing the population exposure to PM_{10}, $PM_{2.5}$, O_3 and NO_2, and the exposure of vegetation to ozone in terms of AOT40 indicators are presented. The tables of population exposure are prepared using the concentration and population density maps in 1x1 km^2 grid resolution. For PM_{10}, $PM_{2.5}$ and NO_2, the population exposure in each grid cell is calculated separately for urban areas directly influenced by traffic and for the background (both rural and urban) areas, in order to better reflect the population exposed to traffic emissions. The tables of the vegetation exposure are prepared using the concentration maps in 2x2 km^2 grid resolution and the Corine Land Cover 2018 dataset in 100x100 m^2 resolution (EU, 2020).

Tables give the relative population exposure for particular concentration intervals including above WHO Air Quality Guideline levels (WHO, 2005; WHO, 2021a), limit and target value intervals (EC, 2004, 2008) and population-weighted concentration for each pollutant. Tables in the chapter 4.3 give the absolute and relative agricultural area for each country and for five European regions where ozone concentrations are above the target value (TV) threshold and long-term objective (LTO) for protection of vegetation as defined in the Ambient AQ Directive (EC, 2008). The frequency distributions of the agricultural area and the forested areas over some exposure classes per country is presented as well.

All tables present exposure results for individual countries, for the EU-27, for the whole mapped area and for five large European regions. For the country grouping into the regions, see Annex 1 Map A1.1 and below: Northern Europe (N): Denmark (including Faroes), Estonia, Finland, Iceland, Latvia, Lithuania, Norway, Sweden; 2) Western Europe (W): Belgium, France north of 45°, Ireland, Luxembourg, Netherlands, United Kingdom; Central Europe (C): Austria, Czechia, Germany, Hungary, Liechtenstein, Poland, Slovakia, Slovenia, Switzerland; Southern Europe (S): Andorra, Cyprus, France south of 45°, Greece, Italy, Malta, Monaco, Portugal, San Marino, Spain; South-eastern Europe (SE): Albania, Bosnia and Herzegovina, Bulgaria, Croatia, Montenegro, North Macedonia, Romania, Serbia (including Kosovo under the UN Security Council Resolution 1244/99), Türkiye.

Chapters 2, 3, 4 and 5 present the concentration maps and exposure estimates for particulate matter, ozone, NO_2 and NOx, and benzo(a)pyrene, respectively. Chapter 4 presents only the concentration map for NO_x; concentrations above the critical level for the protection of vegetation occur in very limited areas and, as such, it is considered not to provide relevant information from the European scale perspective. Chapter 6 summarizes the trends in exposure estimates in the period 2005-2020.

Annex 1 describes briefly the different methodological aspects. Annex 2 documents the input data applied in the 2020 mapping and exposure analysis. Annex 3 presents the technical details of the maps and their uncertainty analysis including the cross-validation results. Annex 4 shows concentration change in 2020 in comparison to the five-year average 2015-2019. Annex 5 presents the concentration maps including concentration values measured at the stations, in order to provide more complete information of the air quality in 2020 across Europe.

2 Particulate matter

The Ambient Air Quality Directive (EC, 2008) sets limit values for long-term and for short-term PM_{10} concentrations and for long-term $PM_{2.5}$ concentrations. The EU long-term annual PM_{10} limit value is set at 40 µg/m^3. The Air Quality Guideline level recommended by the World Health Organization (WHO) in 2005 (WHO, 2005) for the PM_{10} annual average was 20 µg/m^3. In September 2021, WHO introduced its new Air Quality Guidelines (WHO, 2021a). The current Air Quality Guideline level for the PM_{10} annual average is set to 15 µg/m^3. The EU short-term limit value indicates that the daily average PM_{10} concentration should not exceed 50 µg/m^3 during more than 35 days per year. It corresponds to the 90.4 percentile of daily PM_{10} concentrations in one year. This daily limit value is the most frequently exceeded air quality PM limit value in Europe. The Air Quality Guideline levels recommended by the World Health Organization in 2005 (WHO, 2005) and in 2021 (WHO, 2021a) for short-term PM_{10} concentrations indicates that the 99 percentile of the daily average PM_{10} concentrations should not exceed 50 µg/m^3 and 45 µg/m^3, respectively (99th percentile means 3-4 exceedance days per year).

The EU annual limit value for the annual average $PM_{2.5}$ concentrations (ALV) is set at 25 µg/m^3. In EC (2008), there is also an indicative limit value (ILV) of 20 µg/m^3 defined as Stage 2, in place since 2020. The Air Quality Guideline level recommended by the World Health Organization in 2005 (WHO, 2005) for the $PM_{2.5}$ annual average was 10 µg·m^{-3}. The current Air Quality Guideline level as introduced by the WHO in September 2021 (WHO, 2021a) for the $PM_{2.5}$ annual average is set to 5 µg/m^3.

This chapter presents the 2020 situation in relation to of two PM_{10} indicators, i.e. the annual average and the 90.4 percentile of the daily averages, and the $PM_{2.5}$ annual average. The 90.4 percentile of the daily averages is a more relevant PM_{10} indicator in the context of the Ambient Air Quality Directive (EC, 2008) than the formerly used 36th highest daily mean (Horálek et al., 2017a).

The maps of PM_{10} and $PM_{2.5}$ are based on the improved mapping methodology developed and tested in Horálek et al. (2019). The map layers are created for the rural, urban background and urban traffic areas separately on a grid at 1x1 km^2 resolution. Subsequently, the urban background and urban traffic map layers are merged together using the gridded GRIP road data (Meijer et al., 2018) into one urban map layer. This urban map layer is further combined with the rural map layer into the final PM_{10} or $PM_{2.5}$ map using a population density grid at 1x1 km^2 resolution. For details, see Annex 1, Section A1.1. The supplementary data used are chemical transport model (CTM) output, altitude, wind speed and land cover for rural areas, CTM output for urban background areas and CTM output and wind speed for urban traffic areas (Annex 3, Sections A3.1 and A3.2). For all PM_{10} and $PM_{2.5}$ indicators, the final combined map is presented in the 1x1 km^2 grid resolution. Be it noted that this final map is representative for rural and urban background areas, but not for urban traffic areas (which are smoothed in this 1x1 km^2 spatial resolution).

The current number of $PM_{2.5}$ measurement stations is still somewhat limited and its spatial distribution is irregular over Europe. Therefore, in this paper the mapping of the health-related indicator $PM_{2.5}$ annual average is based on a mapping methodology developed in Denby et al. (2011). This methodology derives additional pseudo $PM_{2.5}$ annual mean concentrations from PM_{10} annual mean measurement concentrations. As such, it increases the number and spatial coverage of $PM_{2.5}$ 'data points' and these data are used to derive a European wide map of annual mean $PM_{2.5}$. Pseudo $PM_{2.5}$ stations data are estimated using PM_{10} measurement data, surface solar radiation, latitude and longitude.

The population exposure tables are calculated based on the concentration maps, according to the methodology described in Horálek et al. (2019), i.e. they are calculated separately for urban areas directly influenced by traffic and for the background (both rural and urban) areas, in order to better reflect the population exposed to traffic. For details, see Annex 1, Equation A1.6.

Annex 3, Sections A3.1 and A3.2 provide details on the regression and kriging parameters applied for deriving the PM_{10} and $PM_{2.5}$ maps, as well as the uncertainty analysis of these maps. Annex 4, Sections A4.1 and A4.2 discuss briefly the concentration and population exposure change in 2020 in comparison to the five-year average 2015-2019.

2.1 PM_{10} annual average

2.1.1 Concentration map

Map 2.1 presents the final combined concentration map for the 2020 PM_{10} annual average. Red and purple areas indicate concentrations above the limit value (LV) of 40 µg/m^3.

The stations are not presented in the map, in order to better visualise the urban areas. However, concentration values from the station measurements used in the kriging interpolation methodology (Annex 3, Section A3.1) are considered to provide relevant information to the concentration map. In Map A5.1 of Annex 5 these point values are presented on top of Map 2.1 and illustrate the smoothing effect the interpolation methodology can have on the gridded concentration fields.

Map 2.1 shows annual mean concentrations above the LV in urban areas of south-eastern Europe states (Bosnia and Herzegovina, North Macedonia, Serbia, Türkiye). In general, the south-eastern, the south and the central parts of Europe appear with higher concentrations and population-weighted concentrations than the western and the northern parts.

Map 2.1: Concentration map of PM_{10} annual average, 2020

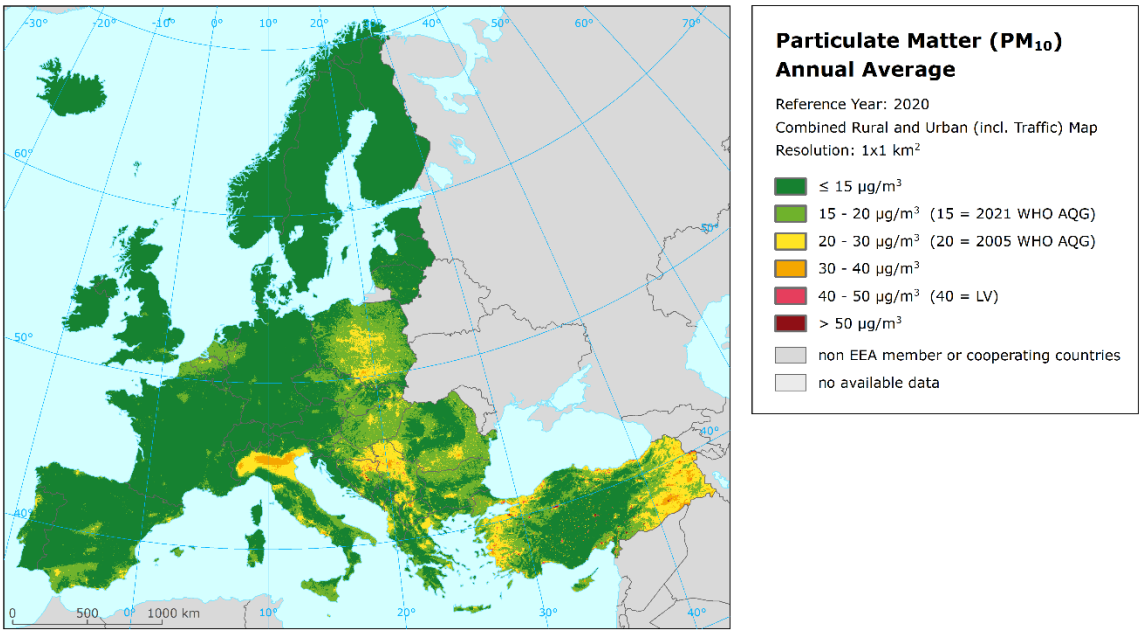

The uncertainty of the concentration map can be expressed in relative terms of the absolute Root Mean Square Error (RMSE) uncertainty related to the mean air pollution indicator value for all stations (see Annex 1, Section A1.4). This relative mean uncertainty (RRMSE) of the final combined map of PM_{10} annual average is 23 % for rural areas and 27 % for urban background areas including Turkish stations (i.e. quite similar to the last years), and respectively 22 % for rural areas and 20 % for urban background areas without Turkish stations (Annex 3, Section A3.1). This means quite good mapping uncertainty, compared to the data quality objective for models of PM_{10} annual average (i.e. 50 %) as set in the Air

Quality Directive (EC, 2008). The main reason for presenting the results without Turkish stations is to enable the comparison with previous years.

For the comparison with five-year average 2015-2019 values, see Annex 4, Section A4.2. The highest increases are observed in parts of southern and south-eastern Europe (especially in west Balkan and Po Valley in northern Italy). Contrary to that, main decreases occur in central Europe, in large areas of south-eastern Europe and in southern Spain and Portugal.

2.1.2 Population exposure

Table 2.1 and Figure 2.1 give the population frequency distribution for a limited number of exposure classes to PM_{10} concentrations. Table 2.1 also presents the population-weighted concentration for individual countries, for five European regions, for EU-27, and for the total mapping area according to Equation A1.7.

About 65 % and 35 % of the considered European population([3]), including Türkiye ([4]), has been exposed to annual average concentrations above the current 2021 and the 2005 WHO Air Quality Guideline levels of 15 µg/m^3 (WHO, 2021a) and 20 µg/m^3 (WHO, 2005), respectively. The same is true for 62 % and 29 % for the considered European population excluding Türkiye and for 67 % and 31 % of the EU-27 population.

Approximately 6 % of population of the considered European area (including Türkiye) has been exposed to concentrations above the EU annual limit value (ALV) of 40 µg/m^3; the same is the case for 0.6 % for the considered European population excluding Türkiye and for less than 0.05 % of the EU-27 population.

No population has been exposed to concentrations above the ALV in 33 countries out of 41 assessed countries. A limited fraction of the population (> 0.04-14 %) has been exposed to concentrations above the ALV in Bulgaria, Croatia, Greece, Cyprus and Serbia (in ascending order). More than 37 % and 22 % of the population has been exposed to concentrations above the ALV in Bosnia and Herzegovina and North Macedonia, respectively. Almost 43 % of the population has been exposed to concentrations above the ALV in Türkiye. However, as the current mapping methodology tends to underestimate high values (see Annex 3, Section A3.1), the percentage of population exposed to concentrations above the ALV will most likely be underestimated. Additional population exposure above the ALV could therefore be expected in countries like Italy, Cyprus, Serbia, Bulgaria, Bosnia and Herzegovina, Türkiye, Montenegro and North Macedonia where a relatively large fraction (ca 20-60 %) of the population lives in areas with concentration levels 30-40 µg/m^3.

The population-weighted concentration of the annual average for 2020 for the considered European population is estimated to be about 20 µg/m^3 including Türkiye and about 18 µg/m^3 both for the considered European population without Türkiye and for EU-27 only. The value for EU-27 and considered European population without Türkiye decreased by about 3 µg/m^3 compared to the previous five-year mean (for more details, see Annex 4, Section A4.1). The value for the whole area without Türkiye is the lowest value in the sixteen years' time series (see Table 6.1).

([3]) We consider Europe apart from Belarus, Moldova, Ukraine and the European parts of Russia and Kazakhstan, due to the lack of the measurement air quality data for these countries.

([4]) The whole Turkish population, both European and Asian.

Table 2.1: Population exposure and population-weighted concentration, PM_{10} annual average, 2020

Country	ISO	Population [inhbs·1000]	PM_{10} – annual average, exposed population, 2020 [%]						PM_{10} ann. avg.
			< 15	15-20	20-30	30-40	40-50	> 50	Pop. weighted
Albania	AL	2 797	2.8	15.7	76.3	5.2			24.2
Andorra	AD	84	3.4	96.6					16.6
Austria	AT	8 381	48.2	49.9	2.0				14.6
Belgium	BE	10 944	14.4	70.4	15.2				17.4
Bosnia and Herzegovina	BA	3 802	2.1	8.4	24.5	27.7	20.7	16.6	36.2
Bulgaria	BG	7 363	2.5	14.0	52.2	31.2	0.0		26.0
Croatia	HR	4 288	7.5	27.7	55.1	9.7	0.1		22.7
Cyprus	CY	1 018	1.1	10.2	16.7	62.5	9.4		32.3
Czechia	CZ	10 423	16.8	70.3	12.9				17.5
Denmark (incl. Faroe Islands)	DK	5 577	92.5	7.5					14.1
Estonia	EE	1 291	94.5	5.5					10.9
Finland	FI	5 339	100.0	0.0					8.7
France (metropolitan)	FR	62 744	51.3	45.9	2.8				15.0
Germany	DE	80 174	73.0	26.6	0.3				14.2
Greece	GR	10 634	1.7	18.1	70.7	9.0	0.5		23.9
Hungary	HU	9 937	0.3	30.2	69.6				21.5
Iceland	IS	318	100.0						9.1
Ireland	IE	4 574	98.0	2.0					11.4
Italy	IT	59 409	4.8	26.9	47.8	20.5			23.8
Latvia	LV	2 080	33.9	39.3	25.1	1.7			17.0
Liechtenstein	LI	34	100.0						11.3
Lithuania	LT	3 028	19.0	53.0	28.0				18.5
Luxembourg	LU	511	36.1	63.9					14.9
Malta	MT	417		1.3	92.9	5.7			25.2
Monaco	MC	33		100.0					18.7
Montenegro	ME	620	8.3	12.0	53.6	26.0			25.1
Netherlands	NL	16 600	15.6	84.3	0.1				16.5
North Macedonia	MK	2 061	0.3	6.2	48.2	23.3	19.5	2.5	31.6
Norway	NO	4 906	97.6	2.4					9.3
Poland	PL	38 494	2.2	28.0	60.9	8.9			22.7
Portugal (excl. Azores, Madeira)	PT	10 047	24.7	50.9	24.5				17.7
Romania	RO	20 138	6.0	25.3	54.2	14.5			23.2
San Marino	SM	32		16.1	83.9				20.8
Serbia (incl. Kosovo*)	RS	8 896	0.7	3.8	37.3	44.4	13.5	0.1	31.4
Slovakia	SK	5 399	1.7	55.2	43.0				20.1
Slovenia	SI	2 042	18.8	52.5	28.7				18.0
Spain (excl. Canarias)	ES	44 722	15.3	49.7	35.0				18.7
Sweden	SE	9 539	97.5	2.4	0.1				10.3
Switzerland	CH	7 893	88.3	11.1	0.6				12.6
Türkiye	TR	71 920	6.8	8.5	15.4	26.3	24.1	18.9	36.9
United Kingdom (& Crown dep.)	UK	63 415	75.2	23.2	1.7				13.9
Total		**601 926**	**34.6**	**30.0**	**21.8**	**7.9**	**3.3**	**2.4**	**20.3**
			64.6				**5.7**		
Total without Türkiye		**530 007**	**38.3**	**32.9**	**22.7**	**5.4**	**0.5**	**0.1**	**18.0**
			71.3				**0.6**		
EU-27		**498 253**	**32.9**	**36.2**	**25.6**	**5.3**	**0.0**		**18.3**
			69.1				**0.0**		
Northern Europe		**32 080**	**85.4**	**10.2**	**4.3**	**0.1**			**11.7**
Western Europe		**144 566**	**56.5**	**40.6**	**2.8**				**14.8**
Central Europe		**162 777**	**44.7**	**31.7**	**21.6**	**2.1**			**17.0**
Southern Europe		**140 620**	**13.7**	**37.2**	**39.1**	**9.8**	**0.1**		**20.9**
South-Eastern Europe		**121 885**	**5.6**	**12.1**	**29.5**	**24.9**	**16.2**	**11.7**	**32.6**
Kosovo*	KS	1 748	0.4	5.8	73.1	20.6	0.2		26.7
Serbia (excl. Kosovo*)	RS	7 148	0.8	3.4	28.6	50.3	16.8	0.2	32.6

(*) Under the UN Security Council Resolution 1244/99.

Note: The percentage value "0.0" indicates that an exposed population exists, but it is small and estimated to be less than 0.05 %. Empty cells mean no population in exposure.

Figure 2.1: Percentage of the population (%) exposed to different PM_{10} annual averages (µg/m³) at country level, 2020

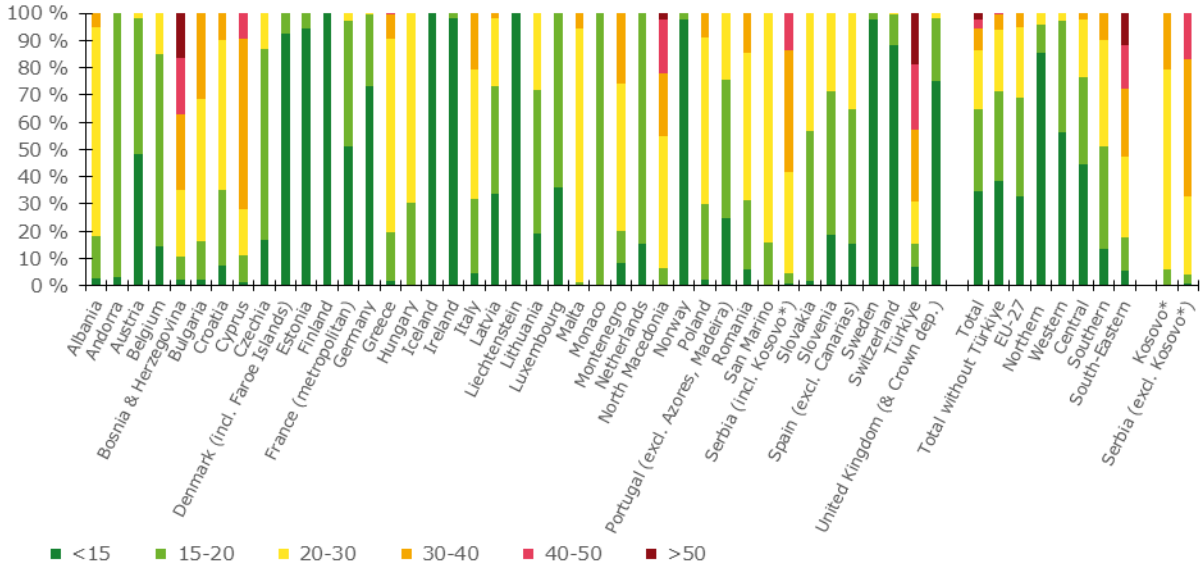

(*) Under the UN Security Council Resolution 1244/99.

Figure 2.2 shows, for the whole mapped area (that is, all considered countries including Türkiye), the population frequency distribution for exposure classes of 1 µg/m³. The highest population frequency can be seen for classes between 13 and 20 µg/m³. One can see a quite continuous strong decline of population frequency for classes between 20 and 35 µg/m³ and a mild decline for classes beyond 40 µg/m³.

Figure 2.2: Population frequency distribution, PM_{10} annual average, 2020. The 2021 WHO AQG level (15 µg/m³) is marked by the green line, the 2005 WHO AQG level (20 µg/m³) is marked by the yellow line, the EU annual limit value (40 µg/m³) is marked by the red line.

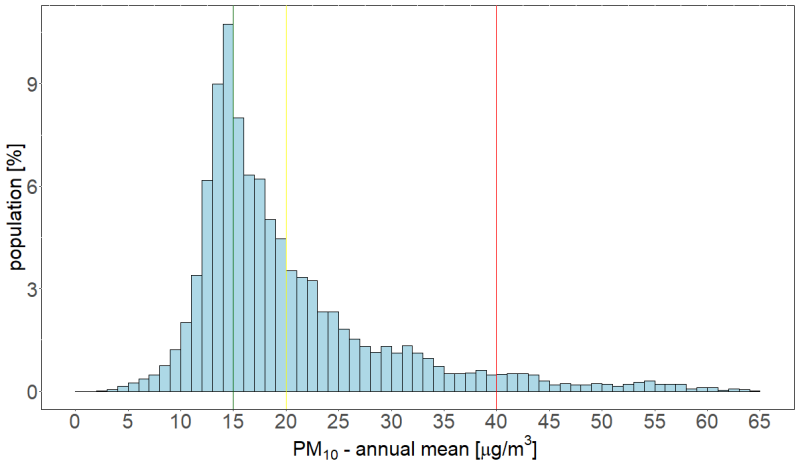

Note: Apart from the population distribution shown in graph, it was estimated that 0.02 % of population lived in areas with PM_{10} annual average concentration in between 65 and 91 µg/m³.

The boxplot showing for individual countries the PM_{10} annual average concentrations to which the population per country was exposed in 2020 is presented in Summary, Figure S.1.

2.2 PM_{10} – 90.4 percentile of daily means

The Ambient Air Quality Directive (EC, 2008) describes the PM_{10} daily limit value (DLV) as "a daily average of 50 µg/m^3 not to be exceeded more than 35 times a calendar year". This requirement can be evaluated by the indicator 36th highest daily mean, which is in principle equivalent to the indicator 90.4 percentile of daily mean. However, for measurement data these two indicators are equivalent only if no data is missing, which is in general not the case. As shown in de Leeuw (2012), the additional uncertainty related to incomplete time series is substantially smaller when using percentile values instead of the x-th highest value. Furthermore, the Air Quality Directive requires the use of the 90.4 percentile when random measurements are used to assess the requirements of the PM_{10} DLV. As in the previous reports since the maps for 2014 (Horálek et al., 2017a), the PM_{10} daily means are expressed as the 90.4 percentile instead of the formerly used 36th highest daily mean.

2.2.1 Concentration map

Map 2.2 presents the final combined map, where red and purple marked areas indicate values of the 90.4 percentile of daily means above 50 µg/m^3 (i.e. values of this indicator above the DLV of 50 µg/m^3 on more than 35 measurement days). The similar mapping procedure as in the case of the annual average is used. The mapping details and the uncertainty analysis are presented in Annex 3. Large areas with concentrations above the DLV are observed in northern Italy (i.e. the Po Valley), in the industrial region Ostrava (Czechia) – Katowice (Poland) – Krakow (Poland) and in eastern parts of Türkiye. Urban and surrounding areas with concentrations above the DLV are observed in Albania, Bosnia and Herzegovina, Bulgaria, Croatia, Cyprus, Greece, Italy, Montenegro, North Macedonia, Poland, Romania, Serbia and Türkiye.

In general, the south-eastern, the south and the central parts of Europe appear with higher concentrations and population-weighted concentrations than the western and the northern parts.

Map 2.2: Concentration map of PM_{10} indicator 90.4 percentile of daily means, 2020

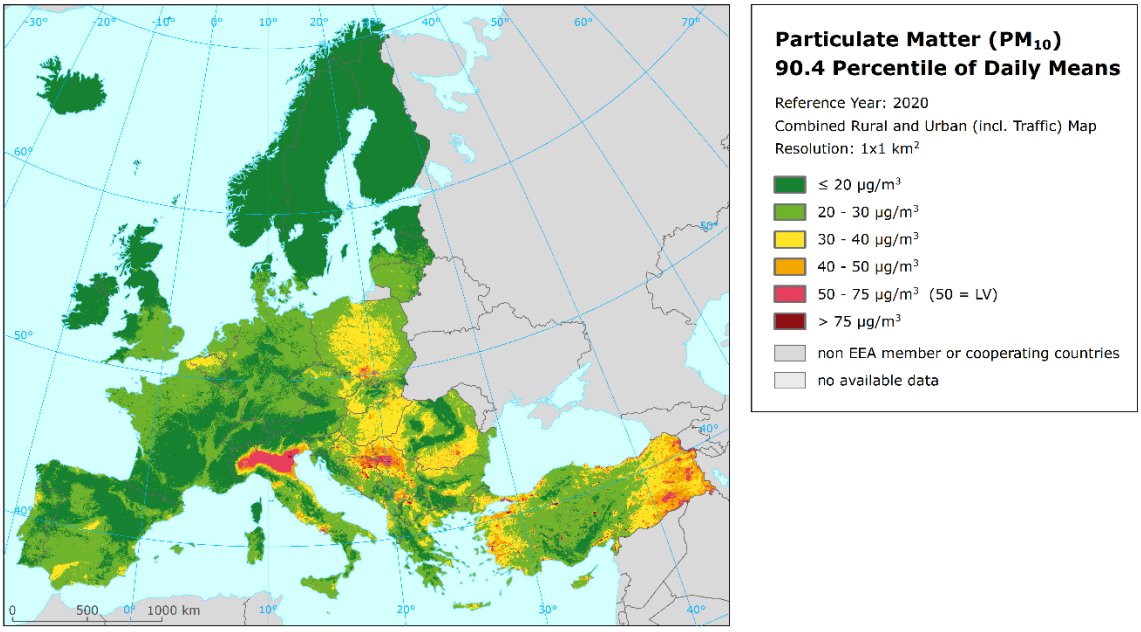

The relative mean uncertainty (relative RMSE) of the final combined map of the 90.4 percentile of PM_{10} daily means is 25 % for rural areas and 31 % for urban background areas including Turkish stations. The mean uncertainty for the map without Türkiye is 22 % for rural areas and 24 % for urban background areas (Annex 3, Section A3.1). Thus, the mapping uncertainty of this is at the similar level as in the case of the PM_{10} annual average.

For the comparison with five-year average 2015-2019 values, see Annex 4, Section A4.1. The highest increases and decreases can be seen in similar parts of Europe as in the case of the PM_{10} annual average.

2.2.2 Population exposure

Figure 2.3 and Table 2.2 give the population frequency distribution for a limited number of exposure classes calculated at 1x1 km^2 grid resolution. Table 2.2 also presents the population-weighted concentration for individual countries, large regions, EU-27 and for the total mapping area.

In 2020 about 17 % of the considered European population including Türkiye, 9 % of the considered European population excluding Türkiye and 8 % of the EU-27 population are estimated to live in areas where the 90.4 percentile of the PM_{10} daily means was above the EU limit value of 50 $\mu g/m^3$.

No population has been exposed to concentrations above the DLV in 24 countries out of 41 assessed countries. A limited fraction of the population (0.1-13 %) has been exposed to concentrations above the DLV in San Marino, Slovakia, Latvia, Hungary, Greece and Poland (in ascending order). More than 20 % but less than 50 % of the population has been exposed to concentrations above the DLV in Albania, Romania, Italy, Croatia, Montenegro and Bulgaria. More than half of the population has been estimated to be exposed to concentrations above the DLV in North Macedonia, Cyprus, Türkiye, Bosnia and Herzegovina and Serbia.

Figure 2.3: Percentage of the population (%) exposed to different values of PM_{10} indicator 90.4 percentile of daily means, 2020

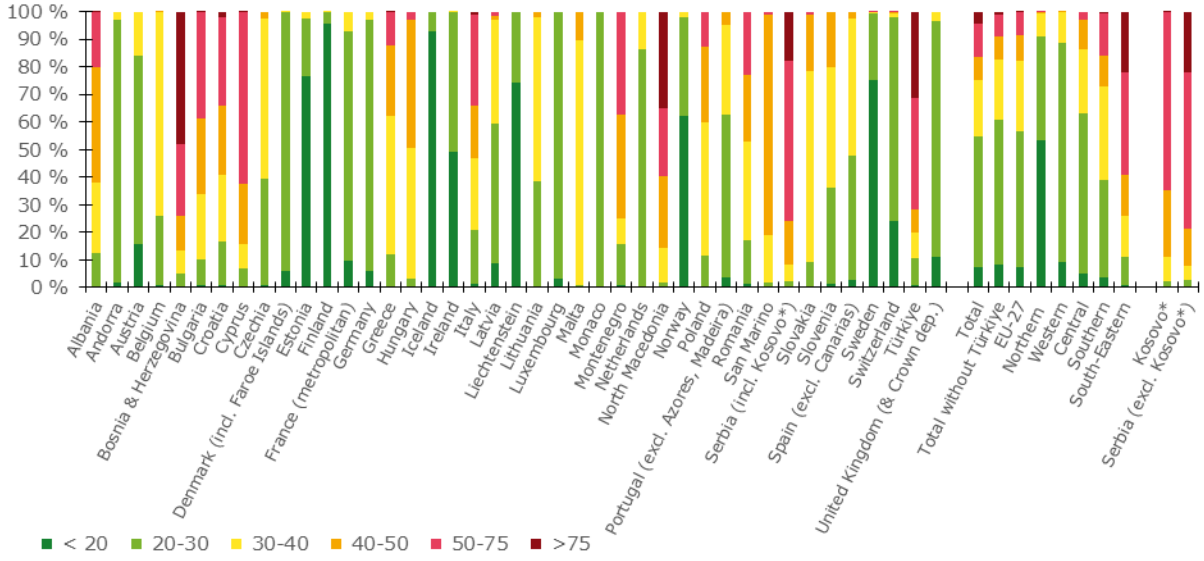

.

(*) Under the UN Security Council Resolution 1244/99.

Table 2.2: Population exposure and population-weighted concentrations, PM_{10} indicator 90.4 percentile of daily means, 2020

Country	ISO	Population [inhbs·1000]	PM_{10} - perc90.4, exposed population, 2020 [%]						PM_{10} - perc90.4
			< 20	20-30	30-40	40-50	50-75	> 75	Pop. Weighted
Albania	AL	2 797	0.1	12.2	25.6	41.8	20.4	0.0	42.2
Andorra	AD	84	1.9	95.1	2.9				28.5
Austria	AT	8 381	15.7	68.3	16.1				25.4
Belgium	BE	10 944	0.8	24.9	74.2	0.1			31.6
Bosnia and Herzegovina	BA	3 802	0.0	4.7	8.5	12.8	25.9	48.0	74.8
Bulgaria	BG	7 364	0.6	9.6	23.6	27.3	38.7	0.0	46.5
Croatia	HR	4 288	0.9	15.7	24.0	25.2	32.0	2.3	43.6
Cyprus	CY	1 018		6.9	8.5	22.0	62.6	0.0	53.5
Czechia	CZ	10 423	0.9	38.4	58.1	2.6			30.7
Denmark (incl. Faroe Islands)	DK	5 577	5.9	93.9	0.2				23.3
Estonia	EE	1 291	76.6	20.7	2.6				18.8
Finland	FI	5 339	95.8	4.2	0.0				15.6
France (metropolitan)	FR	62 744	9.6	83.4	7.0				25.0
Germany	DE	80 174	6.1	91.1	2.8				24.1
Greece	GR	10 635	0.3	11.6	50.3	25.3	12.4	0.0	38.8
Hungary	HU	9 937	0.0	3.3	47.4	46.2	3.1		39.6
Iceland	IS	318	93.1	6.9					15.7
Ireland	IE	4 574	49.1	50.9	0.0				19.7
Italy	IT	59 409	1.1	19.7	26.1	19.1	33.0	1.1	44.3
Latvia	LV	2 080	8.7	50.9	37.2	1.7	1.5		28.2
Liechtenstein	LI	34	74.3	25.7					19.1
Lithuania	LT	3 028	0.3	38.1	59.6	2.0			30.4
Luxembourg	LU	511	3.1	96.9					24.8
Malta	MT	417		0.9	88.9	10.2			37.7
Monaco	MC	33		100.0					27.9
Montenegro	ME	620	1.0	14.7	9.4	37.8	37.2		46.6
Netherlands	NL	16 600	0.0	86.5	13.5				27.3
North Macedonia	MK	2 061	0.0	1.6	12.4	26.2	24.8	35.0	63.7
Norway	NO	4 906	61.9	35.9	2.2				17.2
Poland	PL	38 494	0.0	11.6	48.0	27.7	12.7		39.5
Portugal (excl. Azores, Madeira)	PT	10 047	3.5	59.2	32.2	5.1			28.9
Romania	RO	20 138	1.3	15.6	35.9	24.0	23.1		41.2
San Marino	SM	32		1.7	17.2	80.1	1.0		40.4
Serbia (incl. Kosovo*)	RS	8 896	0.1	2.3	5.8	15.9	57.9	18.0	59.6
Slovakia	SK	5 399	0.2	9.1	68.9	20.6	1.2		36.2
Slovenia	SI	2 042	1.3	34.9	43.7	20.1			32.9
Spain (excl. Canarias)	ES	44 722	2.8	44.9	49.9	2.4			29.9
Sweden	SE	9 539	75.1	24.0	0.7	0.2	0.0		17.4
Switzerland	CH	7 893	23.9	73.9	1.6	0.6	0.0		21.9
Türkiye	TR	71 920	0.9	9.7	9.1	8.6	40.2	31.5	64.4
United Kingdom (& Crown dep.)	UK	63 415	11.0	85.7	3.3				24.8
Total		**601 927**	**7.3** / **54.6**	**47.3**	**20.3**	**8.5**	**12.0** / **16.6**	**4.6**	**35.4**
Total without Türkiye		**530 007**	**8.2** / **60.6**	**52.4**	**21.9**	**8.5**	**8.1** / **9.1**	**0.9**	**31.5**
EU-27		**435 073**	**7.1** / **56.5**	**49.4**	**25.7**	**9.4**	**8.2** / **8.4**	**0.2**	**31.6**
Northern Europe		**32 080**	**53.4**	**37.4**	**8.7**	**0.3**	**0.1**		**20.1**
Western Europe		**144 566**	**8.9**	**79.9**	**11.2**	**0.0**			**25.6**
Central Europe		**162 777**	**5.1**	**58.2**	**23.1**	**10.5**	**3.2**		**29.6**
Southern Europe		**140 620**	**3.3**	**35.8**	**33.8**	**11.3**	**15.3**	**0.4**	**36.2**
South-Eastern Europe		**121 885**	**0.8**	**10.2**	**15.1**	**14.7**	**37.1**	**22.1**	**58.1**
Kosovo*	KS	1 748	0.0	2.2	8.7	24.1	64.6	0.4	53.2
Serbia (excl. Kosovo*)	RS	7 148	0.1	2.3	5.1	13.9	56.3	22.3	61.2

(*) Under the UN Security Council Resolution 1244/99.

Note: The percentage value "0.0" indicates that an exposed population exists, but it is small and estimated to be less than 0.05 %. Empty cells mean no population in exposure.

The European-wide population-weighted concentration of the 90.4 percentile of PM_{10} daily means is estimated for 2020 at about 35 µg/m^3 for the total mapped area (including Türkiye), 32 µg/m^3 (without Türkiye), and 32 µg/m^3 for the EU-27. The population-weighted concentration of this PM_{10} indicator decreased by about 5 µg/m^3 for EU-27 and for the considered European population without Türkiye compared to the previous five-year mean (for more details, see Annex 4, Section A4.1).

As in previous years, the daily limit value was more widely exceeded than the annual limit value in 2020.

Figure 2.4 shows, for the whole mapped area, the population frequency distribution for exposure classes of 2 µg/m^3. One can see the highest population frequency for classes between 24 and 32 µg/m^3, continuous decline of population frequency for classes between 32 and 38 µg/m^3 and continuous mild decline of population frequency for classes between 38 and 70 µg/m^3.

Figure 2.4: Population frequency distribution, PM_{10} indicator 90.4 percentile of daily means, 2020. The EU daily limit value (50 µg/m^3) is marked by the red line

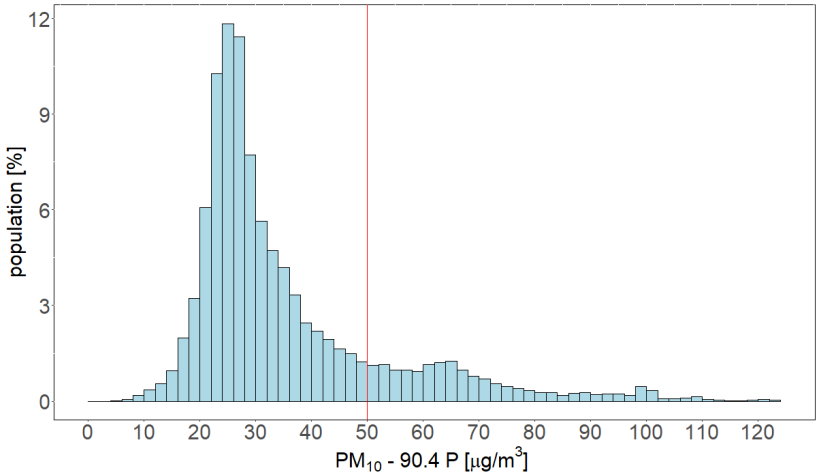

Note: Apart from the population distribution shown in graph, it was estimated that 0.07 % of population lived in areas with values of PM_{10} indicator 90.4 percentile of daily means in between 125 and 175 µg/m^3.

Figure 2.5 shows for individual countries the PM_{10} daily concentrations to which the population per country was exposed in 2020. It can be seen that the countries with the highest values of PM_{10} indicator 90.4 percentile of daily means are located in the central and south-eastern parts of Europe.

Figure 2.5: PM_{10} expressed as indicator 90.4 percentile of daily means to which the population per country was exposed in 2020. The EU daily limit value (50 µg/m³) is marked by the red line

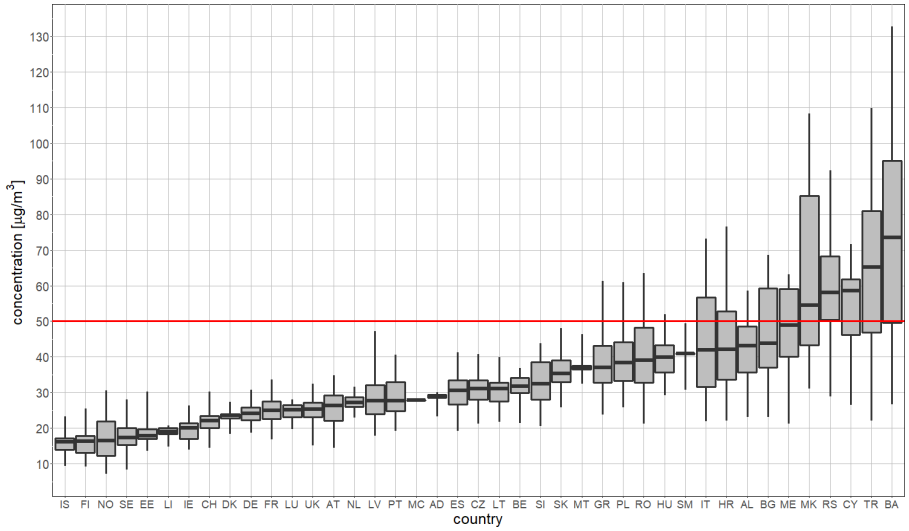

Note: For each country, the box plot shows the concentration to which a percentage of the population was exposed: 50 % in the case of the black marker, 25 % and 75 % in the cases of the box's edges, 2 % and 98 % in the cases of the whiskers' edges.

2.3 $PM_{2.5}$ annual average

2.3.1 Concentration map

Map 2.3 presents the final combined map for the 2020 $PM_{2.5}$ annual average. The dark red areas show concentrations above the ALV of 25 µg/m³. Red areas show concentrations above the indicative LV of 20 µg/m³ defined as Stage 2 (ILV).

Due to the lack of rural $PM_{2.5}$ stations in Türkiye, no proper interpolation results could be estimated for this country in a rural map. Therefore, the estimated $PM_{2.5}$ values for Türkiye are not presented in the final map.

According to Map 2.3, the areas with the highest $PM_{2.5}$ concentrations appear to be the Po Valley in northern Italy and in areas of Bosnia and Herzegovina, Serbia and Romania. The concentrations above the ALV appear around the Balkan cities of Belgrade, Sarajevo, Sofia, Bucharest, the Krakow – Katowice (Poland) – Ostrava (Czechia) industrial region and the area around Warsaw. Different other cities in Bosnia and Herzegovina, Bulgaria, Greece, North Macedonia, Poland and Serbia including Kosovo also show elevated $PM_{2.5}$ annual average concentrations. Like in the case of PM_{10}, the central and the south and south-eastern parts of Europe show higher concentrations than the western and the northern parts.

The relative mean uncertainty of the 2020 map of $PM_{2.5}$ annual average is 27 % for rural and 21 % for urban background areas and it is determined exclusively on the actual $PM_{2.5}$ measurement data points, i.e. not on the pseudo stations (Annex 3, Section A3.2). Similarly as in the case of PM_{10}, this uncertainty is satisfactory, compared to the data quality objective for models of $PM_{2.5}$ annual average (i.e. 50 %) as set in the Air Quality Directive (EC, 2008).

Map 2.3: Concentration map of $PM_{2.5}$ annual average, 2020

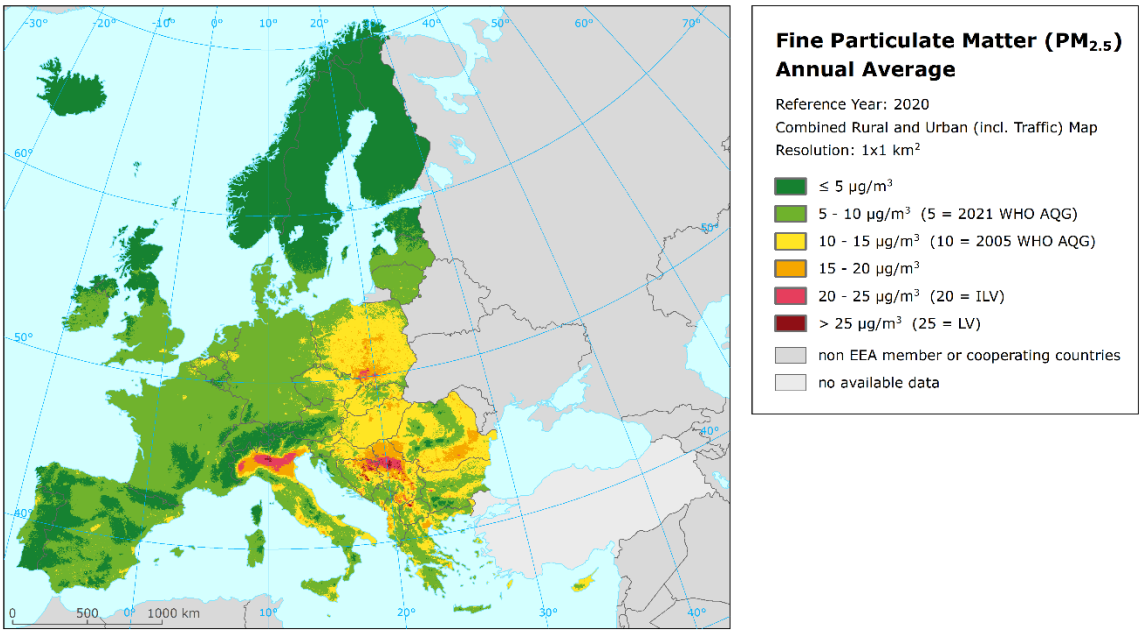

Similarly to the PM_{10}, the final map in 1x1 km^2 resolution is representative for the rural and the urban background areas, but not for the urban traffic areas (which are smoothed in the 1x1 km^2 resolution).

In order to provide more complete information of the air quality across Europe, the final combined map including the measurement data at stations is presented in Map A5.3 of Annex 5.

For the comparison with five-year average 2015-2019 values, see Annex 4, Section A4.2.

2.3.2 Population exposure

Figure 2.6 and Table 2.3 give the population frequency distribution for a limited number of exposure classes to $PM_{2.5}$ concentrations calculated on a grid of 1x1 km^2 resolution. Table 2.2 also presents the population-weighted concentration for individual countries, large regions, EU-27 and for the total mapping area.

About 97 % and 46 % of the considered European population (excluding Türkiye) has been exposed to annual average concentrations above the current 2021 and the 2005 WHO Air Quality Guideline levels of 5 µg/m^3 (WHO, 2021a) and 10 µg/m^3 (WHO, 2005), respectively. The same is true for 97 % and 52 % of the EU-27 population.

The total considered and EU-27 population exposure above the EU annual limit value (ALV) of 25 µg/m^3 has been 1 % and <1 %, respectively.

No population has been exposed to concentrations above the ALV in 32 countries out of 40 assessed countries. In Romania, Poland, Italy, Bulgaria and Croatia (in ascending order) between <0.1 and 2.3 % of population has been exposed to concentrations above the limit valure. In North Macedonia and Serbia, 27 % of the population suffers from exposures above this limit value; in Bosnia and Herzegovina, more than 50 % of the population suffers from exposures above this limit value.

Concentrations above the indicative limit value (ILV) of 20 µg/m^3 have happened in areas with 6 % of the considered European population and with 5 % of the EU-27 population. No population has been exposed to concentrations above the ILV in 27 countries out of 40 assessed countries. In Slovakia, Greece, Albania, Romania, Cyprus, Croatia and Poland (in ascending order) between <0.1 and 14 % of population has been exposed to concentrations above the ILV. In Italy, Bulgaria, Montenegro and

North Macedonia, 21-40 % of the population suffers from exposures above this indicative limit value; in Serbia and Bosnia and Herzegovina, 66 % and 72 % of the population suffers from exposures above this ILV, respectively.

Since $PM_{2.5}$ is one of the most relevant pollutants linked to health problems and premature mortality (EEA, 2019) it should be mentioned that in each country at least some part of the population was exposed to $PM_{2.5}$ annual mean concentrations above the 2021 WHO AQG (minimum of 11 % in Iceland). More than 90 % of the population has been exposed to concentrations above the 2021 WHO AQG level in 35 out of 40 assessed countries. The same is true for 14 out of 40 countries in case of the 2005 WHO AQG level. The only countries, where the $PM_{2.5}$ annual mean concentrations did not exceed the 2005 WHO AQG level, were Andorra, Denmark, Estonia, Finland, Iceland, Liechtenstein, Luxembourg, Norway and Sweden.

As the current mapping methodology tends to underestimate high values (Annex 3, Section A3.2), the percentages and/or the number of countries with population exposed to concentrations above both the current ALV and the indicative ILV will most likely be higher.

The population-weighted concentration of the $PM_{2.5}$ annual means has been estimated for 2020 at about 11 µg/m^3 for both total mapped area and for the EU-27, which means a decrease about 2 µg/m^3 compared to five-year mean for both characteristics (Annex 4, Section A4.1).

Figure 2.6: Percentage of the population (%) exposed to different values of $PM_{2.5}$ annual average (µg/m^3), 2020

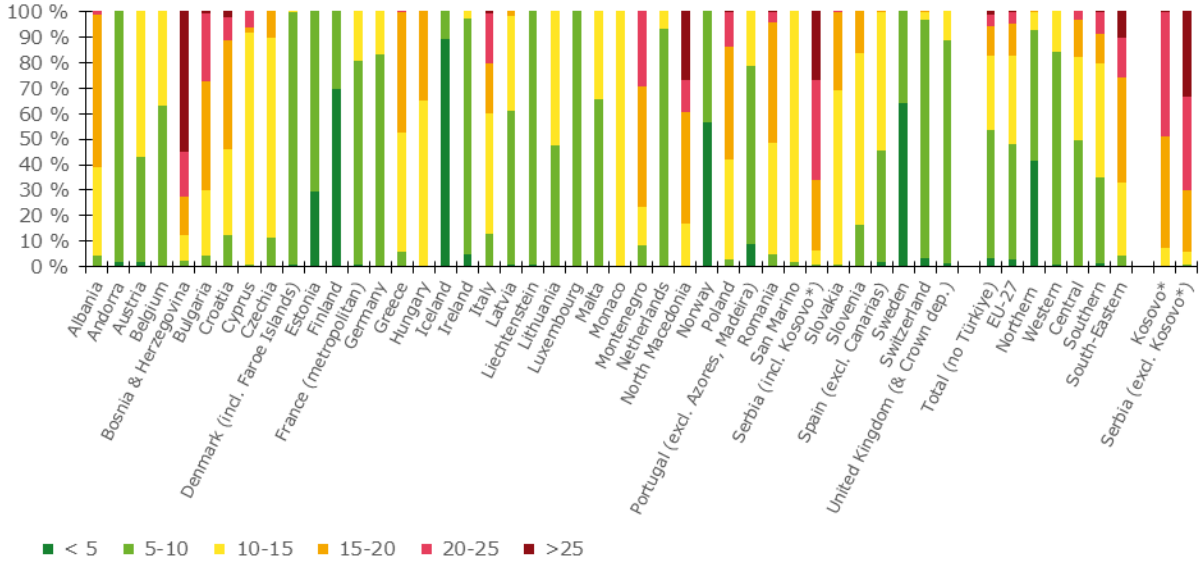

(*) Under the UN Security Council Resolution 1244/99.

Table 2.3: Population exposure and population-weighted concentration, $PM_{2.5}$ annual average 2020

Country	ISO	Population [inhbs·1000]	$PM_{2.5}$ – annual average, exposed population, 2020 [%]						$PM_{2.5}$ ann. avg.
			< 5	5-10	10-15	15-20	20-25	> 25	Pop. weighted
Albania	AL	2 797		4.4	34.6	59.7	1.3		15.6
Andorra	AD	84	1.7	98.3					8.5
Austria	AT	8 381	1.7	41.3	57.1				9.9
Belgium	BE	10 944	0.1	62.8	37.1				9.4
Bosnia and Herzegovina	BA	3 802		2.5	9.7	15.5	17.3	54.9	25.8
Bulgaria	BG	7 364	0.0	4.2	25.6	43.1	26.4	0.7	17.0
Croatia	HR	4 288	0.0	12.6	33.4	42.6	9.2	2.3	15.3
Cyprus	CY	1 018		0.8	90.8	2.0	6.4		14.0
Czechia	CZ	10 423	0.0	11.6	78.2	10.3			12.5
Denmark (incl. Faroe Islands)	DK	5 577	0.7	98.9	0.4				7.6
Estonia	EE	1 291	29.4	70.6					5.4
Finland	FI	5 339	69.7	30.3					4.5
France (metropolitan)	FR	62 744	1.1	79.5	19.4				8.6
Germany	DE	80 174	0.1	83.2	16.7				9.1
Greece	GR	10 635		5.9	46.8	47.1	0.2		14.4
Hungary	HU	9 937		0.1	65.2	34.7			14.5
Iceland	IS	318	89.3	10.7					4.2
Ireland	IE	4 574	4.7	92.3	3.0				7.1
Italy	IT	59 409	0.2	12.7	47.4	19.3	19.8	0.6	14.9
Latvia	LV	2 080	0.7	60.3	37.1	1.9			9.1
Liechtenstein	LI	34	1.2	98.8					8.1
Lithuania	LT	3 028		47.7	52.3				9.8
Luxembourg	LU	511	0.1	99.9					7.3
Malta	MT	417		65.6	34.4				10.1
Monaco	MC	33			100.0				10.5
Montenegro	ME	620		8.3	15.2	47.1	29.3		17.3
Netherlands	NL	16 600		93.1	6.9				9.2
North Macedonia	MK	2 061		0.5	16.5	43.4	12.6	26.9	20.3
Norway	NO	4 906	56.8	43.2					4.6
Poland	PL	38 494		2.9	39.1	44.3	13.5	0.2	16.0
Portugal (excl. Azores, Madeira)	PT	10 047	8.7	69.9	21.3				8.1
Romania	RO	20 138	0.0	4.9	43.4	47.3	4.2	0.1	15.2
San Marino	SM	32		2.0	98.0				12.8
Serbia (incl. Kosovo*)	RS	8 896		0.7	5.5	27.7	39.4	26.7	22.1
Slovakia	SK	5 399	0.0	0.8	68.2	30.9	0.1		14.5
Slovenia	SI	2 042	0.0	16.4	67.2	16.4			12.5
Spain (excl. Canarias)	ES	44 722	1.8	44.0	53.8	0.4			10.0
Sweden	SE	9 539	64.3	35.7					4.9
Switzerland	CH	7 893	3.4	93.1	3.0	0.5			8.1
United Kingdom (& Crown dep.)	UK	63 415	1.5	87.1	11.4				8.6
Total (no Türkiye) [a]		**530 007**	**3.3** / **53.5**	**50.2**	**29.3**	**11.5**	**4.7** / **5.8**	**1.1**	**11.1**
EU-27		**435 073**	**3.0** / **48.0**	**44.9**	**34.6**	**12.6**	**4.7** / **4.8**	**0.1**	**11.2**
Northern Europe		**32 080**	**41.7**	**50.8**	**7.4**	**0.1**			**6.0**
Western Europe		**144 566**	**1.0**	**83.0**	**16.0**				**8.7**
Central Europe		**162 777**	**0.3**	**49.3**	**32.6**	**14.5**	**3.2**	**0.0**	**11.5**
Southern Europe		**140 620**	**1.5**	**33.7**	**44.2**	**11.8**	**8.4**	**0.3**	**12.1**
South-Eastern Europe		**49 965**	0.0	4.4	28.7	40.9	15.7	10.4	17.8
Kosovo*	KS	1 748		0.3	7.3	43.3	49.1	0.1	19.4
Serbia (excl. Kosovo*)	RS	7 148		0.8	5.1	23.8	37.0	33.2	22.7

(*) Under the UN Security Council Resolution 1244/99.
(a) Türkiye not included due to the lack of the rural stations.

Note: The percentage value "0.0" indicates that an exposed population exists, but it is small and estimated to be less than 0.05 %. Empty cells mean no population in exposure.

Figure 2.7 shows, for the whole mapped area, the population frequency distribution for exposure classes of 1 µg/m^3. The highest population frequency is found for classes between 7 and 13 µg/m^3.

Figure 2.7: Population frequency distribution, $PM_{2.5}$ annual average, 2020. The 2021 WHO AQG level (5 µg/m^3) is marked by the green line, the 2005 WHO AQG level (10 µg/m^3) is marked by the yellow line, the EU annual indicative limit value (20 µg/m^3) is marked by the orange line and the EU annual limit value (25 µg/m^3) is marked by the red line

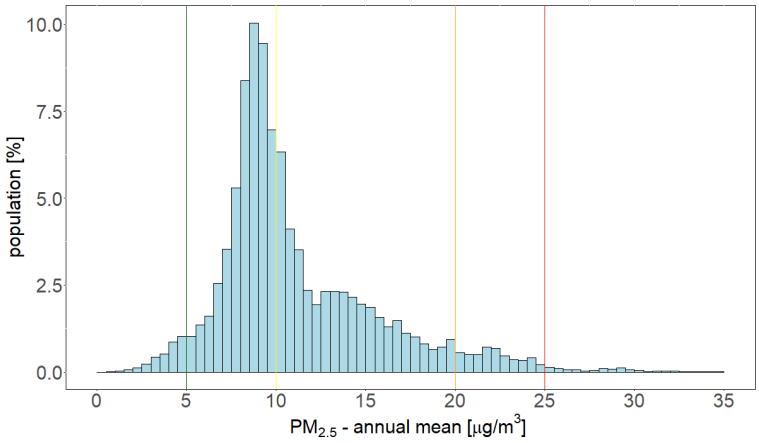

The boxplot showing for individual countries the $PM_{2.5}$ annual average concentrations to which the population per country was exposed in 2020 is presented in Summary, Figure S.2.

3 Ozone

For ozone, three health-related indicators, i.e. 93.2 percentile of maximum daily 8-hour means (see below), SOMO35 and SOMO10, and five vegetation-related indicators, i.e. AOT40 for vegetation, AOT40 for forests, POD_6 for wheat, potato and tomato are considered. For the definition of the SOMO35, SOMO10 and AOT40 and POD indicators, see following sections and Annex 2.

The separate rural and urban background health-related indicator map layers are calculated at a resolution of 10x10 km^2. Subsequently, the final health-related indicator maps are created by combining rural and urban areas based on the 1x1 km^2 gridded population density map, following the procedure as described in Annex 1, Section A1.1. The supplementary data used are chemical transport model (CTM) output, altitude and surface solar radiation for rural areas and CTM output, wind speed and surface solar radiation for urban areas (Annex 3). The final concentration maps are presented on the 1x1 km^2 grid resolution. The population exposure tables are calculated on the basis of these health-related indicator maps.

The vegetation-related indicator maps are created for rural areas only, as urban areas are considered not to represent areas covered by vegetation (although the vegetation located in the outskirts of agglomerations might be omitted by this approach). These maps are calculated from observations at rural background stations and are representative for rural areas only. The supplementary data used are CTM output, altitude and surface solar radiation. These supplementary data sources are the same as those used for the human health related ozone indicators in the rural areas. The maps have a resolution of 2x2 km^2. This resolution serves the needs of the EEA´s AIR004 indicator on ecosystem exposure to ozone (EEA, 2022b), earlier known as the Core Set Indicator 005.

Annex 3, Section A3.3 provides details on the regression and kriging parameters applied for deriving the maps of the ozone indicators, as well as the uncertainty analysis of the maps. Annex 4, Section A4.2 discusses briefly the inter-annual changes observed in the concentration maps and the relevant population and vegetation exposure.

3.1 Ozone – 93.2 percentile of maximum daily 8-hour means

The Ambient Air Quality Directive (EC, 2008) describes the ozone target value (TV) for the protection of human health as “a maximum daily 8-hour mean of 120 µg/m^3 not to be exceeded on more than 25 times a calendar year, averaged over three years”. On an annual basis, it can be evaluated by the indicator 26th highest maximum daily 8-hour mean, which is in principle equivalent to the indicator 93.2 percentile of maximum daily 8-hour means. However, for measurement data these two indicators are equivalent only if no data is missing, which is in general not the case. As shown in de Leeuw (2012), the additional uncertainty related to incomplete time series is substantially smaller when using percentile values instead of the x-th highest value. As in the previous reports since 2014 maps, this ozone indicator is expressed as the 93.2 percentile of maximum daily 8-hour means instead of the formerly used 26th highest maximum daily 8-hour mean. Only 2020 data are considered, and not the three-years average.

2.3.1 Concentration map

Map 3.1 presents the final combined map for 93.2 percentile of maximum daily 8-hour means. In the map, the red and dark red areas show values of the 93.2 percentile of maximum daily 8-hour means above 120 µg/m^3 in 2020, i.e. above the TV threshold of 120 µg/m^3 on more than 25 days in 2020. Note that in the Ambient Air Quality Directive (EC, 2008) the TV is actually defined as 120 µg/m^3 not to be exceeded on more than 25 days per calendar year averaged over three years. Here only 2020 data are presented, and no three-year average has been calculated.

The map shows that in 2020 percentile values above 120 µg/m^3 occur in some areas of Europe, namely in Belgium, France, Germany, Italy, Luxembourg, Netherlands, Portugal, San Marino, Spain, Switzerland and Türkiye. In general, the southern, the south-eastern and central parts of Europe show higher ozone concentrations than the northern parts, which is caused mainly by higher solar radiation and temperature in these areas. Nevertheless, concentrations above the TV threshold can occur even in northern Europe during warm year as it was presented for 2018 (Horálek et al., 2021).

For the comparison with five-year average 2015-2019 values, see Annex 4, Section A4.3. The highest increases have been observed in large areas of the western Europe (United Kingdom, Belgium, the Netherlands and parts of northern France), while the steepest decreases occur in most of the central, southern and south-eastern Europe.

The relative mean uncertainty of the 2020 map of the 93.2 percentile of maximum daily 8-h ozone means is about 7 % for rural and 9 % for urban areas (Annex 3, Section A3.2). The low uncertainty values are influenced by the character of this ozone indicator. Note that the Air Quality Directive (EC, 2008) sets no modelling uncertainty for ozone annual indicators.

In order to provide more complete information of the air quality across Europe, the final combined map including the measurement data at stations is presented in Map A5.4 of Annex 5.

Map 3.1: Concentration map of ozone indicator 93.2 percentile of maximum daily 8-hour means, 2020

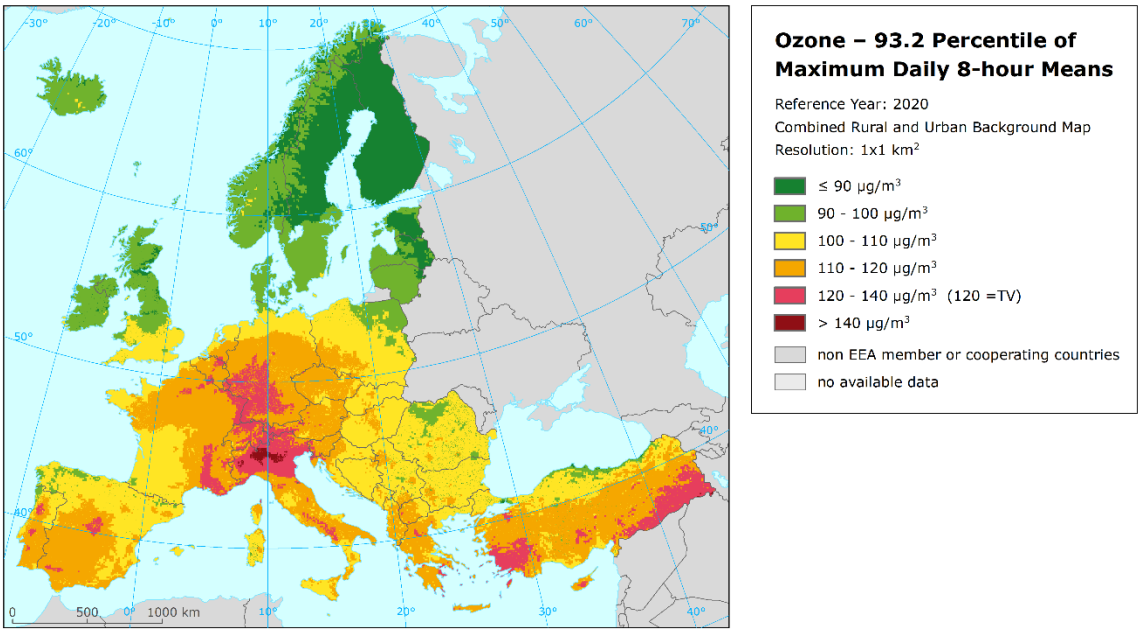

2.3.2 Population exposure

Table 3.1 and Figure 3.1 give, for the 93.2 percentile of maximum daily 8-hour means, the population frequency distribution for a limited number of exposure classes. Table 3.1 also presents the population-weighted concentration for individual countries, large regions, EU-27 and for the total mapping area.

Table 3.1: Population exposure and population-weighted concentrations, ozone indicator 93.2 percentile of maximum daily 8-hour means, 2020

Country	ISO	Population [inhbs·1000]	Ozone - perc93.2, exposed population, 2020 [%]						Ozone - perc93.2
			< 90	90-100	100-110	110-120	120-140	> 140	Pop. weighted
Albania	AL	2 797		1.3	69.0	29.7			108.2
Andorra	AD	84		98.7	1.3				95.1
Austria	AT	8 381			40.5	58.6	0.9		111.0
Belgium	BE	10 944			17.5	76.5	6.0		113.3
Bosnia and Herzegovina	BA	3 802		2.1	96.8	1.1			104.7
Bulgaria	BG	7 364	9.9	75.7	13.8	0.6			95.3
Croatia	HR	4 288			53.1	46.3	0.6		109.4
Cyprus	CY	1 018		0.4	80.5	17.5	1.6		108.1
Czechia	CZ	10 423			50.5	49.5	0.0		110.2
Denmark (incl. Faroe Islands)	DK	5 577	4.0	95.7	0.3				93.0
Estonia	EE	1 291	92.1	7.9					88.1
Finland	FI	5 339	99.1	0.9					86.3
France (metropolitan)	FR	62 744		0.9	29.7	63.2	6.3		112.8
Germany	DE	80 174		2.6	17.0	71.6	8.8		113.1
Greece	GR	10 635		3.6	20.4	74.4	1.6		113.2
Hungary	HU	9 937		0.0	98.1	1.9			106.3
Iceland	IS	318	94.5	5.5					85.8
Ireland	IE	4 574	55.9	43.4	0.6				90.6
Italy	IT	59 409	0.3	2.3	26.2	32.3	27.7	11.2	119.3
Latvia	LV	2 080	67.5	32.5	0.0				90.0
Liechtenstein	LI	34				99.6	0.4		114.7
Lithuania	LT	3 028	2.4	97.6	0.0				92.8
Luxembourg	LU	511				90.5	9.5		116.1
Malta	MT	417			97.4	2.6			105.3
Monaco	MC	33				100.0			118.7
Montenegro	ME	620		25.2	72.7	2.1			103.4
Netherlands	NL	16 600		1.5	55.2	40.4	2.9		108.7
North Macedonia	MK	2 061		25.3	71.6	3.1	0.0		102.6
Norway	NO	4 906	35.0	65.0					90.3
Poland	PL	38 494		24.3	71.2	4.6			103.4
Portugal (excl. Azores, Madeira)	PT	10 047		26.5	59.3	13.1	1.1		103.9
Romania	RO	20 138	2.6	76.5	20.7	0.2			97.5
San Marino	SM	32				96.8	3.2		116.1
Serbia (incl. Kosovo*)	RS	8 896	0.0	40.9	55.9	3.3			100.8
Slovakia	SK	5 399		0.0	99.2	0.8			105.0
Slovenia	SI	2 042			32.0	65.8	2.2		111.8
Spain (excl. Canarias)	ES	44 722	0.1	17.7	43.1	38.8	0.2		107.8
Sweden	SE	9 539	19.5	80.3	0.1				91.9
Switzerland	CH	7 893			4.2	54.1	41.6	0.1	118.8
Türkiye	TR	71 920	15.0	26.0	28.7	24.2	6.1	0.0	103.5
United Kingdom (& Crown dep.)	UK	63 415	18.4	46.7	34.9	0.0			96.2
Total		**601 927**	**6.4**	**20.0**	**33.6**	**32.7**	**6.1**	**1.1**	**106.8**
			26.4				**7.2**		
Total without Türkiye		**530 007**	**5.2**	**19.2**	**34.3**	**33.9**	**6.1**	**1.3**	**107.3**
			24.4				**7.4**		
EU-27		**435 073**	**3.2**	**14.8**	**33.7**	**40.0**	**6.7**	**1.5**	**109.1**
			18.0				**8.2**		
Northern Europe		**32 080**	**37.6**	**62.3**	**0.1**				**90.7**
Western Europe		**144 566**	**9.8**	**22.2**	**31.3**	**34.2**	**2.5**		**104.5**
Central Europe		**162 777**		**7.0**	**40.4**	**46.1**	**6.4**	**0.0**	**110.1**
Southern Europe		**140 620**	**0.2**	**9.1**	**36.2**	**36.8**	**13.0**	**4.7**	**113.1**
South-Eastern Europe		**121 885**	**9.9**	**36.2**	**33.3**	**17.0**	**3.6**	**0.0**	**102.2**
Kosovo*	KS	1 748		32.9	57.7	9.5			102.6
Serbia (excl. Kosovo*)	RS	7 148	0.0	42.8	55.4	1.8			100.3

(*) Under the UN Security Council Resolution 1244/99.

Note: The percentage value "0.0" indicates that an exposed population exists, but it is small and estimated to be less than 0.05 %. Empty cells mean no population in exposure.

It has been estimated that in 2020 more than 7 % of the considered European population including Türkiye, 7 % of the considered European population excluding Türkiye and 8 % of the EU-27 population lived in areas where the ozone concentration was above the health-related target value threshold (TV of 120 µg/m^3).

No population has been exposed to concentrations above the TV threshold in 24 countries out of 41 assessed countries. In Spain, Liechtenstein, Croatia, Austria, Portugal, Greece, Cyprus, Slovenia, Netherlands, San Marino, Belgium, Türkiye, France, Germany and Luxembourg (in ascending order) between < 0.2 and 9.5 % of population has been exposed to concentrations above the TV threshold. In Italy and Switzerland, 39 % and 42 % of the population suffers from exposures above this value, respectively.

As the current mapping methodology tends to underestimate high values due to interpolation smoothing (Annex 3, Section A3.3), the percentage of population exposed to values above the TV threshold is most likely somewhat underestimated; additional population exposure above the TV threshold might be expected in additional countries: Monaco, Liechtenstein, San Marino, Luxembourg, Belgium, Greece, Germany, Slovenia, France, Austria, Switzerland and Czechia. The reason is that in these countries the estimated percentage population exposed to the concentrations above 110 µg/m^3 is considerable (more than 50 %).

The overall population-weighted ozone concentrations in terms of the 93.2 percentile of maximum daily 8-hour means has been estimated for 2020 as being 107 µg/m^3 for both the considered European area with and without Türkiye. For the EU-27 area population-weighted ozone concentrations has been estimated as being 109 µg/m^3, i.e. of about 3 µg/m^3 less than five-year 2015-2019 mean concentration (Annex 4, Section A4.3).

Figure 3.1: Percentage of the population (%) exposed to different values of the ozone indicator 93.2 percentile of maximum daily 8-hour means (µg/m^3), 2020

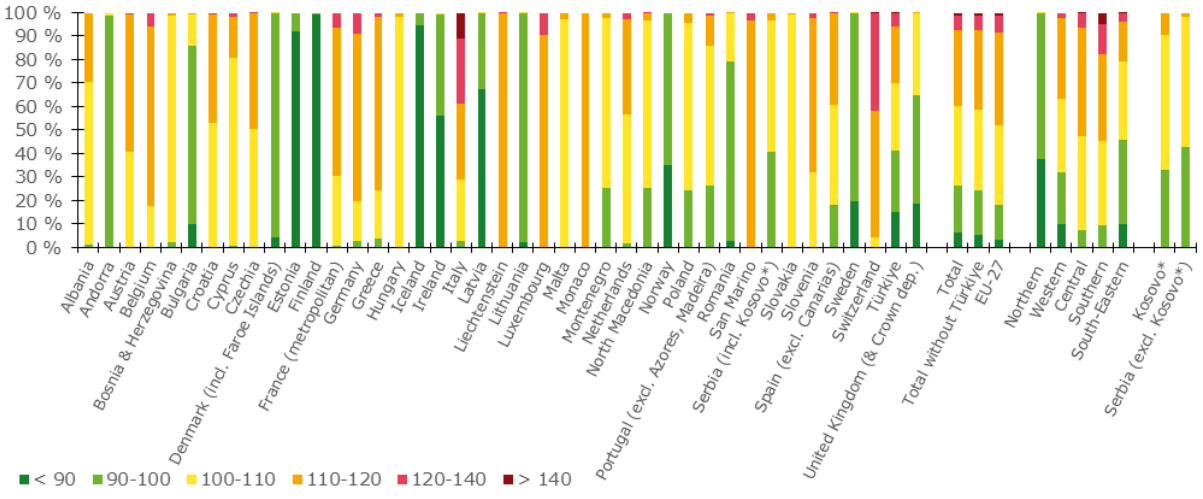

(*) Under the UN Security Council Resolution 1244/99.

Figure 3.2 shows, for the whole mapped area, the population frequency distribution for exposure classes of 2 µg/m^3. The highest population frequency is found for classes between 96 and 116 µg/m^3. For classes above 116 µg/m^3, a sharp decline of population frequency can be seen.

Figure 3.2: Population frequency distribution, O_3 indicator 93.2 percentile of maximum daily 8-hour means, 2020. The EU target value (120 µg/m^3) is marked by the red line

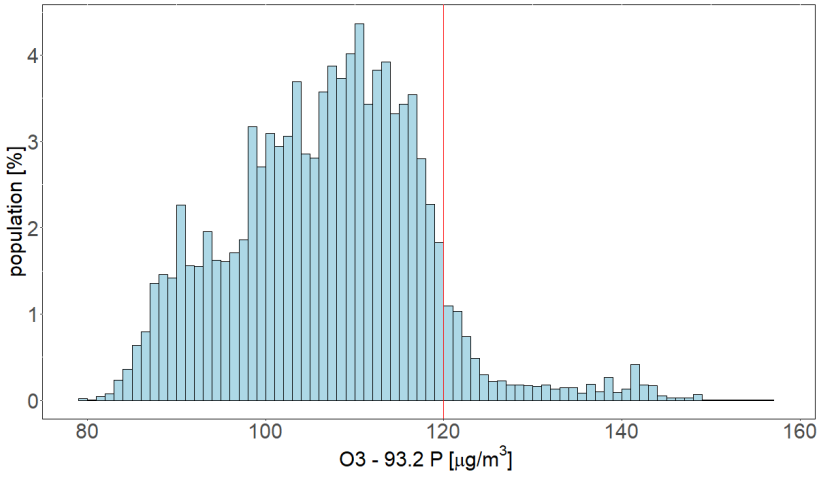

Figure 3.3 shows for individual countries the ozone concentrations to which the population per country was exposed to in 2020. It can be seen that the countries with the highest ozone concentrations are located in the southern and central parts of Europe.

Figure 3.3: Ozone concentrations expressed as indicator 93.2 percentile of maximum daily 8-hour means to which the population per country was exposed in 2020. The EU target value (120 µg/m^3) is marked by the red line

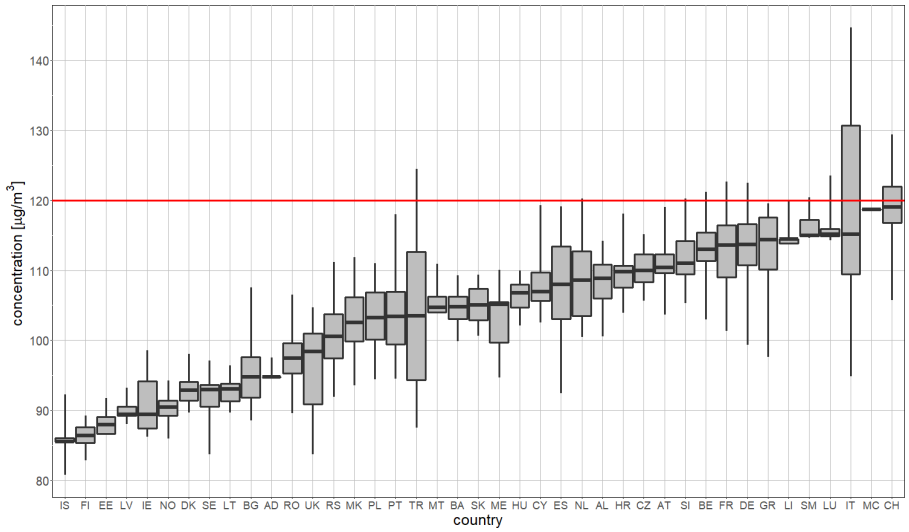

Note: For each country, the box plot shows the concentration to which a percentage of the population was exposed: 50 % in the case of the black marker, 25 % and 75 % in the cases of the box's edges, 2 % and 98 % in the cases of the whiskers' edges.

3.2 Ozone – SOMO35 and SOMO10

SOMO35 is the annually accumulated ozone maximum daily 8-hourly means in excess of 35 ppb (i.e. 70 µg/m^3). It is not regulated in any of the EU air quality directives and there are no limit or target values defined. Nevertheless, it is considered by the WHO as a good indicator of human exposure to ozone (WHO, 2013). Comparing the 93.2 percentile of maximum daily 8-hour means versus the SOMO35 for all background stations shows no simple relationship between the two indicators. However, it seems that the TV of the 93.2 percentile of maximum daily 8-hour means (being 120 µg/m^3) is related approximately with a SOMO35 value in the range of 6 000-8 000 µg/m^3·d. This comparison motivates a somewhat arbitrarily chosen threshold of 6 000 µg/m^3·d, in order to facilitate the discussion of the observed distributions of SOMO35 levels in their spatial and temporal context. This threshold is used in this and previous papers (Horálek et al., 2022a, and the references cited therein) when dealing with the population exposure estimates.

SOMO10 is the annually accumulated ozone maximum daily 8-hourly means in excess of 10 ppb (i.e. 20 µg/m^3). This indicator was introduced due to its link to the health impact assessment, since the WHO recommended using the SOMO10 as an alternative to the SOMO35 when estimating the health impact of ozone (WHO, 2013).

2.3.1 Concentration maps

Maps 3.2 and 3.3 presents the final combined map for SOMO35 and SOMO10. In the final combined map of SOMO35, the red and dark red areas show values above 8 000 µg/m^3·d, while the orange areas show values above 6 000 µg/m^3·d. In the case of SOMO10, the boundaries of concentration classes have been chosen quite arbitrary, in order to reflect the concentration distribution of this indicator. In the final combined map of SOMO10, the red and dark red areas show values above 24 000 µg/m^3·d.

Map 3.2: Concentration map of ozone indicator SOMO35, 2020

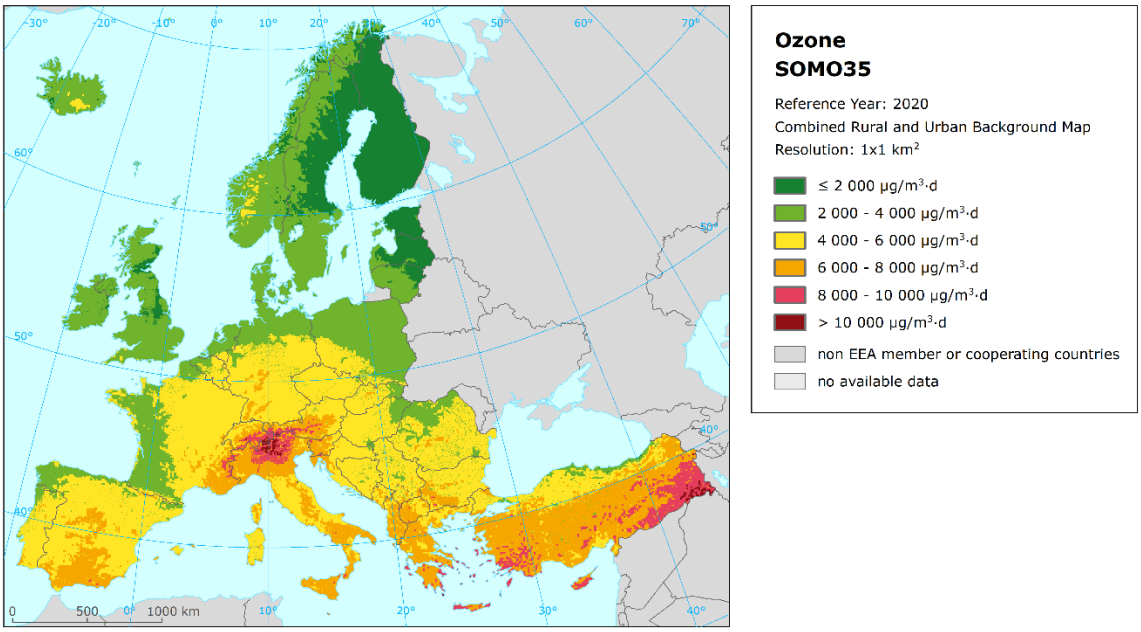

Map 3.3: Concentration map of ozone indicator SOMO10, 2020

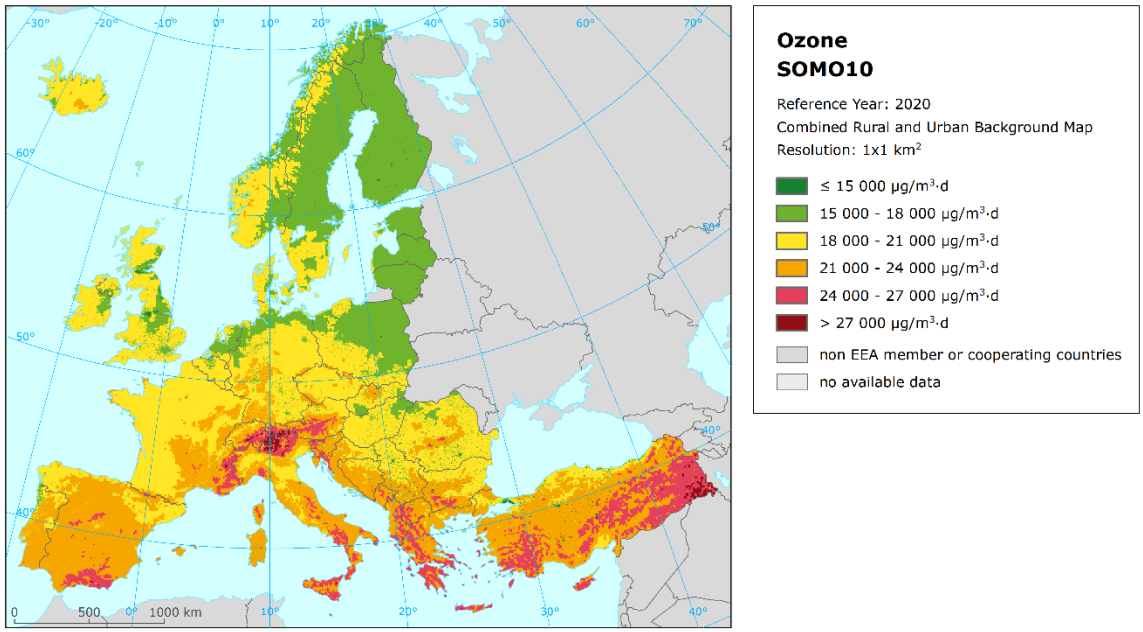

Like in the case of the 93.2 percentile of the maximum daily 8-hour means, generally the southern and south-eastern parts of Europe show higher ozone SOMO35 and SOMO10 concentrations than the northern parts. Higher levels of ozone also occur more frequently in mountainous areas south of 50 degrees latitude than in lowlands. The relative mean uncertainty of the 2020 maps of the SOMO35 and SOMO10 is about 30 % and 12 %, respectively, for rural areas and 32 % and 14 %, respectively, for urban areas (see Annex 3).

Compared to the five-year average 2015-2019, highest increase has (in terms of SOMO35) been observed in western Europe (United Kingdom, Ireland and northern France) and in some areas in south and south-eastern Europe (Portugal and Romania). Contrary to that, one can see a decline in most of the rest of Europe. For details, see Annex 4, Section A4.2.

2.3.2 Population exposure

Table 3.2 and Figure 3.4 give for SOMO35 the population frequency distribution for a limited number of exposure classes. Table 3.2 also presents the population-weighted concentration for individual countries, large regions, EU-27 and for the total mapping area.

It has been estimated that in 2020 about 10 % of the considered European population (including Türkiye), about 9 % both of the considered European population without Türkiye and of the EU-27 population, lived in areas with SOMO35 values above 6 000 µg/m^3·d (see above on the motivation of this criterion).

In 2020, like in the previous several years, the northern and western European countries have had almost no inhabitants exposed to SOMO35 concentrations above 6 000 µg/m^3·d. No population has been exposed to concentrations SOMO35 concentrations above 6 000 µg/m^3·d in 19 countries out of 41 assessed countries. In Slovakia, Portugal, Germany, Serbia, Bulgaria, North Macedonia, Liechtenstein, San Marino, Montenegro, France, Croatia, Austria, Switzerland, Spain and Slovenia (in ascending order) between < 0.1 and 16.5 % of population has been exposed to SOMO35 concentrations above 6 000 µg/m^3·d. In Albania, Türkiye, Italy, Cyprus, Greece, Malta and Monaco, between 23 and 100 % of population has been exposed to SOMO35 concentrations above 6 000 µg/m^3·d.

Table 3.2: Population exposure and population-weighted concentrations, ozone indicator SOMO35, 2020

Country	ISO	Population [inhbs·1000]	Ozone - SOMO35, exposed population, 2020 [%]						Ozone - SOMO35
			< 2000	2000-4000	4000-6000	6000-8000	8000-10000	> 10000	Pop, weighted
Albania	AL	2 797		0.2	76.8	23.0	0.0		5 679
Andorra	AD	84		98.7	1.3				2 813
Austria	AT	8 381		21.9	72.1	5.8	0.2	0.0	4 584
Belgium	BE	10 944		74.0	26.0				3 798
Bosnia and Herzegovina	BA	3 802		50.9	49.0	0.0			4 045
Bulgaria	BG	7 364	2.3	81.9	14.5	1.4	0.0		2 967
Croatia	HR	4 288		7.7	88.0	4.3	0.0		4 775
Cyprus	CY	1 018			43.4	49.6	7.0		6 300
Czechia	CZ	10 423		23.8	76.2	0.0			4 252
Denmark (incl. Faroe Islands)	DK	5 577	21.6	78.4	0.0				2 284
Estonia	EE	1 291	97.6	2.4					1 469
Finland	FI	5 339	99.4	0.6					1 362
France (metropolitan)	FR	62 744		46.6	50.1	3.3	0.0		4 274
Germany	DE	80 174	0.0	41.9	57.8	0.3			4 194
Greece	GR	10 635		1.2	35.2	57.9	5.6	0.1	6 181
Hungary	HU	9 937		40.4	59.6	0.0			4 044
Iceland	IS	318	93.3	6.7					1 582
Ireland	IE	4 574	55.0	44.8	0.2				1 911
Italy	IT	59 409	0.7	1.8	51.0	39.7	6.8	0.1	6 059
Latvia	LV	2 080	95.7	4.3					1 700
Liechtenstein	LI	34			98.0	1.9	0.1		4 971
Lithuania	LT	3 028	40.3	59.7					2 044
Luxembourg	LU	511			100.0				4 272
Malta	MT	417				98.3	1.7		6 590
Monaco	MC	33				100.0			6 445
Montenegro	ME	620		25.6	71.2	3.2			4 360
Netherlands	NL	16 600		85.9	14.1				3 426
North Macedonia	MK	2 061		20.9	77.2	2.0	0.0		4 345
Norway	NO	4 906	40.9	59.1	0.0				2 041
Poland	PL	38 494	1.7	87.8	10.6	0.0			3 216
Portugal (excl. Azores, Madeira)	PT	10 047		72.5	27.2	0.3			3 585
Romania	RO	20 138	1.3	87.1	11.6	0.0			2 955
San Marino	SM	32			97.9	2.1			5 387
Serbia (incl. Kosovo*)	RS	8 896	0.9	78.7	19.9	0.5			3 256
Slovakia	SK	5 399		56.7	43.2	0.1			3 867
Slovenia	SI	2 042		4.3	79.2	16.5	0.0		5 011
Spain (excl. Canarias)	ES	44 722	0.4	27.9	60.0	11.7	0.0		4 525
Sweden	SE	9 539	26.5	73.5					2 182
Switzerland	CH	7 893			91.5	7.4	1.1	0.0	5 388
Türkiye	TR	71 920	3.9	37.5	34.8	20.1	3.6	0.1	4 547
United Kingdom (& Crown dep.)	UK	63 415	35.6	64.2	0.2				2 300
Total		**601 927**	**7.6**	**45.0**	**37.0**	**9.2**	**1.2**	**0.0**	**4 017**
			52.6			**10.4**			
Total without Türkiye		**530 007**	**8.0**	**46.0**	**37.3**	**7.7**	**0.9**	**0.0**	**3 945**
			54.1			**8.6**			
EU-27		**530 007**	**8.0**	**46.0**	**37.3**	**7.7**	**0.9**	**0.0**	**3 945**
			54.1			**8.6**			
Northern Europe		**32 080**	**49.3**	**50.7**	**0.0**				**1 963**
Western Europe		**144 566**	**17.4**	**61.3**	**21.3**	**0.1**	**0.0**		**3 158**
Central Europe		**162 777**	**0.4**	**48.4**	**50.1**	**1.0**	**0.1**	**0.0**	**4 035**
Southern Europe		**140 620**	**0.4**	**19.1**	**50.2**	**27.0**	**3.3**	**0.0**	**5 267**
South-Eastern Europe		**121 885**	**2.7**	**49.6**	**32.8**	**12.7**	**2.1**	**0.1**	**4 108**
Kosovo*	KS	1 748		55.0	43.0	2.0			3 900
Serbia (excl. Kosovo*)	RS-	7 148	1.2	84.5	14.3	0.1			3 098

(*) Under the UN Security Council Resolution 1244/99.

Note: The percentage value "0.0" indicates that an exposed population exists, but it is small and estimated to be less than 0.05 %. Empty cells mean no population in exposure.

In 2020, the population-weighted ozone concentration in terms of SOMO35 for the total mapping area was estimated to be slightly above 4 000 µg/m^3·d. For both total area without Türkiye and the EU-27, it was almost 4 000 µg/m^3·d, which is the fifth lowest value in the sixteen years period 2005-2020 (Table 6.3). Compared to the five-year average 2015-2019, notably lower values have occurred in the most of Europe, while in the Benelux, the United Kingdom, Ireland and Iceland notably higher values occurred (Annex 4, Section A4.2).

Figure 3.4: Percentage of the population (%) exposed to different values of the ozone indicator SOMO35 (µg/m^3·d), 2020

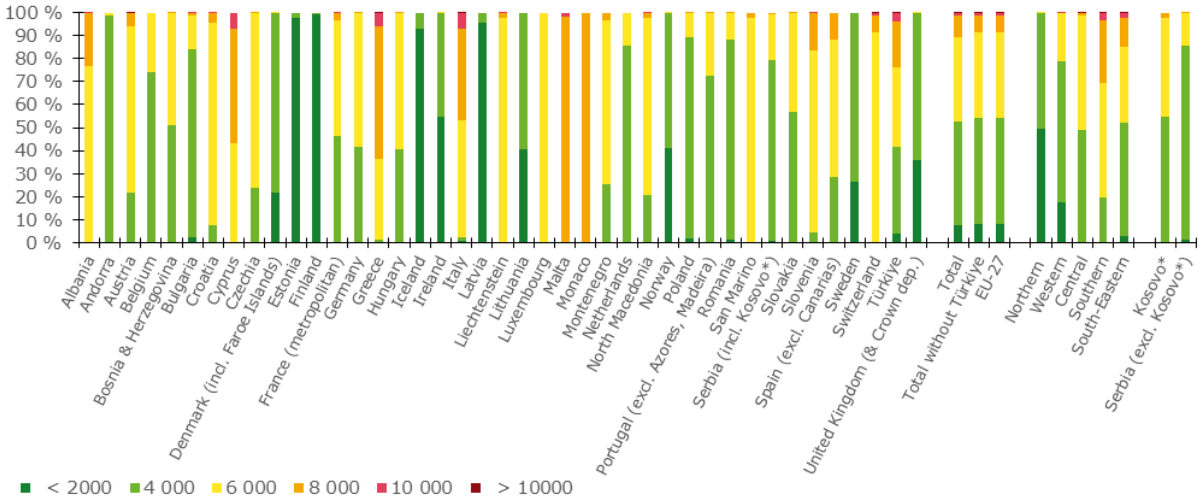

(*) Under the UN Security Council Resolution 1244/99.

Figure 3.5 and Table 3.3 give for SOMO10 the population frequency distribution for a limited number of exposure classes. Table 3.3 also presents the population-weighted concentration for individual countries, large regions, EU-27 and for the total mapping area.

Figure 3.5: Percentage of the population (%) exposed to different values of the ozone indicator SOMO10 (µg/m^3·d), 2020

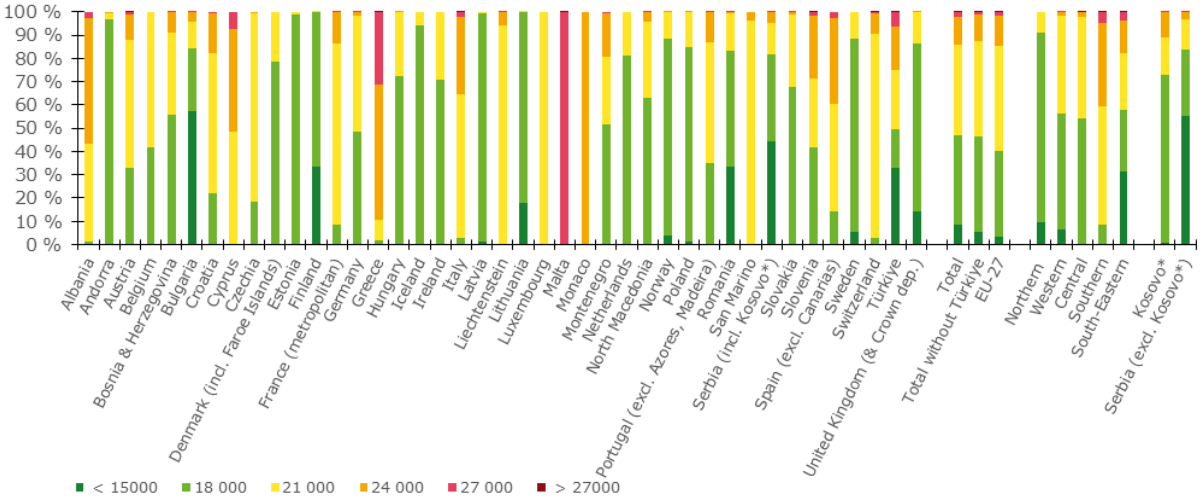

(*) Under the UN Security Council Resolution 1244/99.

Table 3.3: Population exposure and population-weighted concentrations, ozone indicator SOMO10, 2020

Country	ISO	Population [inhbs·1000]	Ozone – SOMO10, exposed population, 2020 [%]						Ozone – SOMO10
			< 15000	15000-18000	18000-21000	21000-24000	14000-27000	> 27000	Pop, weighted
Albania	AL	2 797	0.0	1.2	41.9	54.0	2.9	0.0	21 441
Andorra	AD	84	0.0	96.6	2.6	0.8	0.0	0.0	17 329
Austria	AT	8 381	0.0	33.1	54.7	10.9	1.4	0.0	18 738
Belgium	BE	10 944	0.0	41.5	58.5	0.0	0.0	0.0	18 046
Bosnia and Herzegovina	BA	3 802	0.4	55.4	35.2	9.1	0.0	0.0	18 056
Bulgaria	BG	7 364	57.5	26.9	11.4	4.0	0.1	0.0	15 630
Croatia	HR	4 288	0.0	21.9	60.5	17.2	0.4	0.0	19 359
Cyprus	CY	1 018	0.0	0.0	48.5	44.2	7.3	0.0	21 484
Czechia	CZ	10 423	0.0	18.5	80.6	0.9	0.0	0.0	18 561
Denmark (incl. Faroe Islands)	DK	5 577	0.0	78.6	21.4	0.0	0.0	0.0	17 563
Estonia	EE	1 291	0.0	98.9	1.1	0.0	0.0	0.0	15 863
Finland	FI	5 339	33.6	66.3	0.1	0.0	0.0	0.0	15 425
France (metropolitan)	FR	62 744	0.0	8.4	78.1	13.2	0.2	0.0	19 598
Germany	DE	80 174	0.0	48.7	49.9	1.4	0.0	0.0	18 214
Greece	GR	10 635	0.0	1.7	8.8	58.3	31.2	0.0	22 987
Hungary	HU	9 937	0.0	72.5	27.5	0.0	0.0	0.0	17 504
Iceland	IS	318	0.0	94.2	5.8	0.0	0.0	0.0	16 979
Ireland	IE	4 574	0.0	70.7	29.3	0.0	0.0	0.0	16 979
Italy	IT	59 409	0.0	2.7	61.6	33.3	2.4	0.0	20 655
Latvia	LV	2 080	1.1	98.4	0.5	0.0	0.0	0.0	15 714
Liechtenstein	LI	34	0.0	0.0	94.4	5.5	0.1	0.0	18 542
Lithuania	LT	3 028	17.9	81.7	0.3	0.0	0.0	0.0	15 871
Luxembourg	LU	511	0.0	0.0	100.0	0.0	0.0	0.0	18 787
Malta	MT	417	0.0	0.0	0.0	0.0	99.9	0.1	24 516
Monaco	MC	33	0.0	0.0	0.0	100.0	0.0	0.0	22 679
Montenegro	ME	620	0.0	51.8	28.8	18.7	0.7	0.0	18 639
Netherlands	NL	16 600	0.0	81.1	18.9	0.0	0.0	0.0	17 493
North Macedonia	MK	2 061	0.0	62.8	32.7	4.1	0.4	0.0	17 838
Norway	NO	4 906	4.1	84.6	11.3	0.0	0.0	0.0	16 538
Poland	PL	38 494	1.4	83.4	15.1	0.1	0.0	0.0	16 865
Portugal (excl. Azores, Madeira)	PT	10 047	0.0	35.0	51.8	13.1	0.0	0.0	18 701
Romania	RO	20 138	33.5	49.9	16.0	0.7	0.0	0.0	16 090
San Marino	SM	32	0.0	0.0	96.2	3.8	0.0	0.0	19 858
Serbia (incl. Kosovo*)	RS	8 896	44.5	37.4	13.5	4.6	0.0	0.0	15 959
Slovakia	SK	5 399	0.0	67.7	31.2	1.0	0.0	0.0	17 676
Slovenia	SI	2 042	0.0	41.7	29.5	27.0	1.8	0.0	19 459
Spain (excl. Canarias)	ES	44 722	0.0	14.5	46.1	36.5	3.0	0.0	20 426
Sweden	SE	9 539	5.4	83.1	11.4	0.0	0.0	0.0	16 929
Switzerland	CH	7 893	0.0	2.6	87.7	8.8	0.8	0.1	19 417
Türkiye	TR	71 920	32.8	16.6	25.5	18.6	6.3	0.2	17 635
United Kingdom (& Crown dep.)	UK	63 415	14.1	72.5	13.3	0.1	0.0	0.0	16 541
Total		**601 927**	**8.5**	**38.2**	**39.2**	**12.1**	**1.9**	**0.0**	**18 314**
			46.7				**1.9**		
Total without Türkiye		**530 007**	**5.2**	**41.2**	**41.1**	**11.2**	**1.3**	**0.0**	**18 406**
			46.4				**1.3**		
EU-27		**435 073**	**3.3**	**36.9**	**45.3**	**12.9**	**1.6**	**0.0**	**18 717**
			40.2				**1.6**		
Northern Europe		**32 080**	**9.6**	**81.4**	**9.0**	**0.0**			**16 508**
Western Europe		**144 566**	**6.2**	**50.1**	**42.2**	**1.5**	**0.0**		**17 705**
Central Europe		**162 777**	**0.3**	**53.9**	**43.5**	**2.1**	**0.1**	**0.0**	**17 957**
Southern Europe		**140 620**		**8.5**	**51.0**	**35.8**	**4.7**	**0.0**	**20 638**
South-Eastern Europe		**121 885**	**31.6**	**26.2**	**24.2**	**14.0**	**3.8**	**0.1**	**17 306**
Kosovo*	KS	1 748		50.6	29.1	15.4	4.9	0.0	17 364
Serbia (excl. Kosovo*)	RS-	7 148	4.5	64.2	20.6	9.4	1.3		21 910

(*) Under the UN Security Council Resolution 1244/99.

Note: The percentage value "0.0" indicates that an exposed population exists, but it is small and estimated to be less than 0.05 %. Empty cells mean no population in exposure.

The population-weighted ozone concentrations, in terms of SOMO10, were estimated to be above 18 000 µg/m^3·d for the total mapping area with and without Türkiye. For the EU-27, it was almost 19 000 µg/m^3·d.

Figure 3.6 shows, for the whole mapped area, the frequency distribution of SOMO35 for population exposure classes of 250 µg/m^3·d. The highest frequencies are found for classes between 2 250 and 5 600 µg/m^3·d. One can see a steep decline of population frequency for exposure classes between 5 600 and 8 500 µg/m^3·d and a continuous mild decline of population frequency for classes above 8 500 µg/m^3·d.

Figure 3.6: Population frequency distribution, ozone indicator SOMO35, 2020

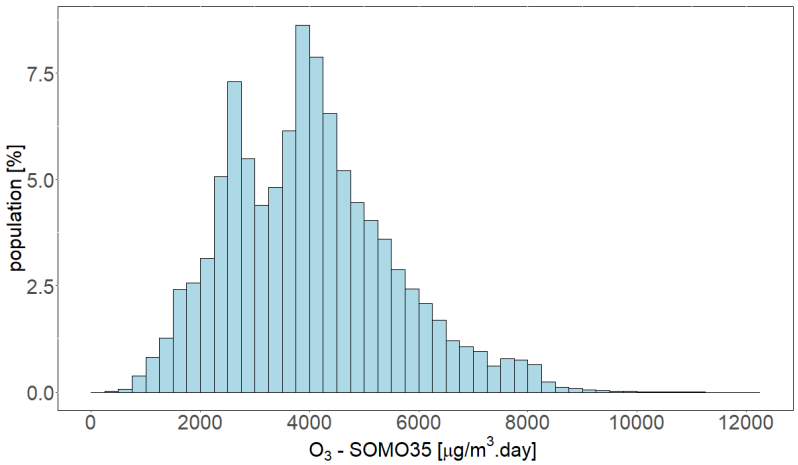

Figure 3.7 shows the population frequency distribution of SOMO10 for population exposure classes of 500 µg/m^3·d. The graph shows the highest frequencies for classes between 16 000 and 20 500 µg/m^3·d.

Figure 3.8 shows for individual countries the ozone indicator SOMO10 to which the population per country was exposed in 2020 (for similar figure for SOMO35, see Figure S.4.). It can be seen that the countries with the highest ozone concentrations are located in the southern and south-eastern parts of Europe.

Figure 3.7: Population frequency distribution, ozone indicator SOMO10, 2020

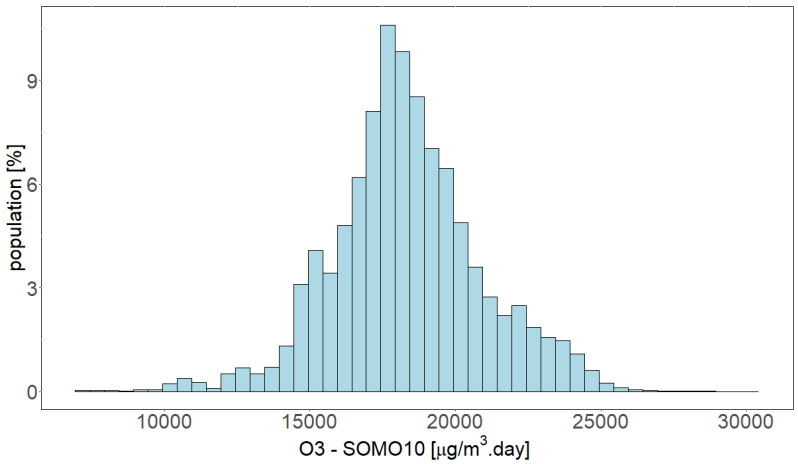

Figure 3.8: Ozone concentrations expressed as indicator SOMO10 to which the population per country was exposed in 2020

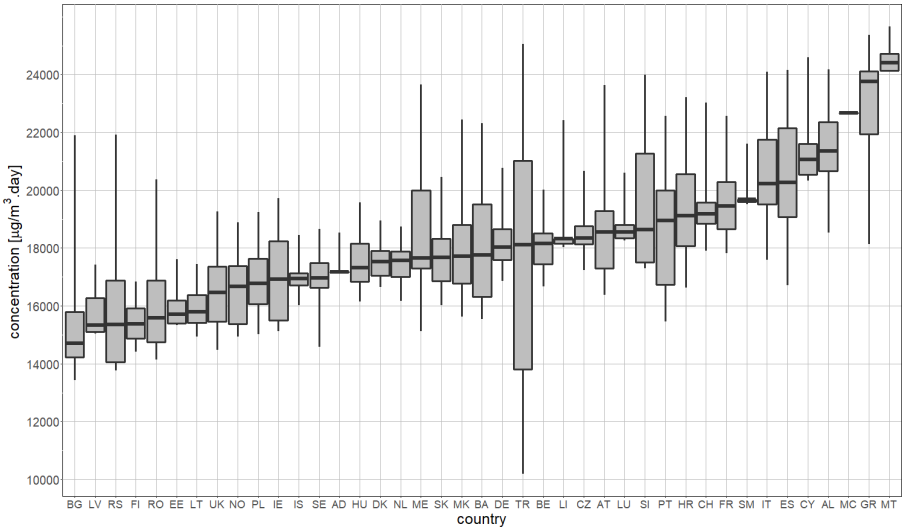

Note: For each country, the box plot shows the concentration to which a percentage of the population was exposed: 50 % in the case of the black marker, 25 % and 75 % in the cases of the box's edges, 2 % and 98 % in the cases of the whiskers' edges.

3.3 Ozone – AOT40 vegetation and AOT40 forests

In the Ambient Air Quality Directive (EC, 2008) a target value (TV) and a long-term objective (LTO) for the protection of vegetation from high ozone concentrations accumulated during the growing season have been defined. TV and LTO are specified using "accumulated ozone exposure over a threshold of 40 parts per billion" (AOT40). This is calculated as a sum of the difference between hourly concentrations greater than 40 ppb (i.e. 80 µg/m^3) and 40 ppb, using only observations between 08:00 and 20:00 Central European Time (CET) each day, calculated over three months from 1 May to 31 July. The TV is 18 000 µg/m^3·h (averaged over five years) and the LTO is 6 000 µg/m^3·h.

Note that the term "vegetation" as used in the Ambient Air Quality Directive (EC, 2008) is not further defined. Nevertheless, the TV used in the directive is quite similar as the critical level used in the Mapping Manual (CLRTAP, 2017a) for "agricultural crops" (although the definitions of AOT40 by the EU and the CLRTAP are slightly different), so the term vegetation in the Air Quality Directive has been interpreted as primarily agricultural crops. Therefore, the exposure of agricultural crops has been evaluated here based on the AOT40 for vegetation as defined in the Air Quality Directive and the agricultural areas, defined as the CORINE Land Cover level-1 class 2 Agricultural areas (encompassing the level-2 classes 2.1 Arable land, 2.2 Permanent crops, 2.3 Pastures and 2.4 Heterogeneous agricultural areas), see Section 3.3.2. Note that in addition to these agricultural areas there are several other CLC classes that could be considered "vegetation", namely level-2 classes 1.4 Artificial, non-agricultural vegetated areas (encompassing the level-3 classes 1.4.1 Green urban areas and 1.4.2 Sport and leisure facilities), 3.1 Forests (see below) and 3.2 Scrub and/or herbaceous vegetation associations.

Next to the AOT40 for vegetation protection, the Ambient Air Quality Directive (EC, 2008) defines also the AOT40 for forest protection, which is calculated similarly as the AOT40 for vegetation, but is summed over six months from 1 April to 30 September. For AOT40 for forests there is no TV defined in the Air Quality Directive. However, there is a critical level (CL) established by the CLRTAP, see CLRTAP (2017a). This critical level is set at 10 000 µg/m^3·h. Although CLRTAP (2017a) calculates the AOT40 indicators somewhat differently (e.g. it uses the ozone concentration corrected at canopy height), we further use this CL level for the AOT40 for forests calculated according to the EC (2008).

For the exposure of forests evaluation, the CLC level-2 class 3.1 Forests has been used.

The ecosystem based accumulative ozone indicators described in this section are specifically prepared for calculation of the EEA indicator on ecosystem exposure to ozone (EEA, 2022b). For the estimation of the vegetation and forested area exposure to accumulated ozone, the maps in this section are created on a grid of 2x2 km^2 resolution. The exposure frequency distribution outcomes are based on the overlay with the 100x100 m^2 grid resolution of the CLC2018 land cover classes.

2.3.1 Concentration maps

The interpolated maps of AOT40 for vegetation and AOT40 for forests are applicable for rural areas only. Map 3.4 presents the final map of AOT40 for vegetation in 2020. Note that in the Ambient Air Quality Directive (EC, 2008) the TV is actually defined as 18 000 µg/m^3·h averaged over five years. Here only 2020 data are presented, and no five-year average has been calculated.

Map 3.4: Concentration map of ozone indicator AOT40 for vegetation, rural map, 2020

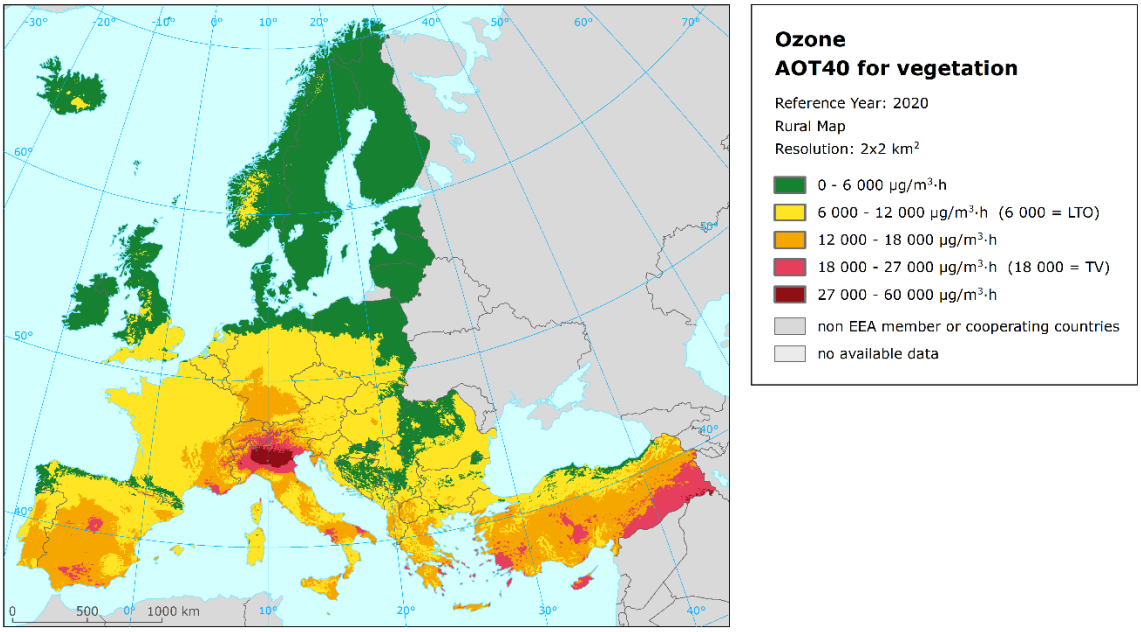

The areas in the map with concentrations above the TV threshold of 18 000 µg/m^3·h are marked in red and dark red. The areas below the long-term objective (LTO) are marked in green. The high and very high AOT40 levels for vegetation occur specifically in southern of Europe (Italy, relatively smaller parts of Spain, France and Greece) and in Türkiye. Highest levels (dark red) were estimated in the north of Italy. The relative mean uncertainty of the 2020 map of the AOT40 for vegetation is about 38 % (Annex 3, Section A3.3).

Map 3.5 presents the final map of AOT40 for forests in 2020. The areas in the map with concentrations above the critical level (CL) defined by CLRTAP (2017a) are marked in yellow, orange, red and dark red. One can see large European forested areas exceeding this level.

Like for the AOT40 for vegetation indicator, the highest levels of the AOT40 for forests are found in the southern and south-eastern European region and Türkiye. Nevertheless, values above the CL are found everywhere in Europe except larger parts of the United Kingdom, northern Europe, northern part of Poland, the Atlantic areas in the north-west of Spain and even a few parts of south-eastern Europe (mainly in Romania and Bosnia and Herzegovina). The relative mean uncertainty of the 2020 map of the AOT40 for forests is about 32 % (Annex 3, Section A3.3).

For the comparison with five-year average 2015-2019 values, see Annex 4, Section A4.3.

In order to provide more complete information of the air quality across Europe, the AOT40 maps including the AOT40 values based on the actual rural background measurement data at stations are presented in Maps A5.7 and A5.8 of Annex 5.

Map 3.5: Concentration map of ozone indicator AOT40 for forests, rural map, 2020

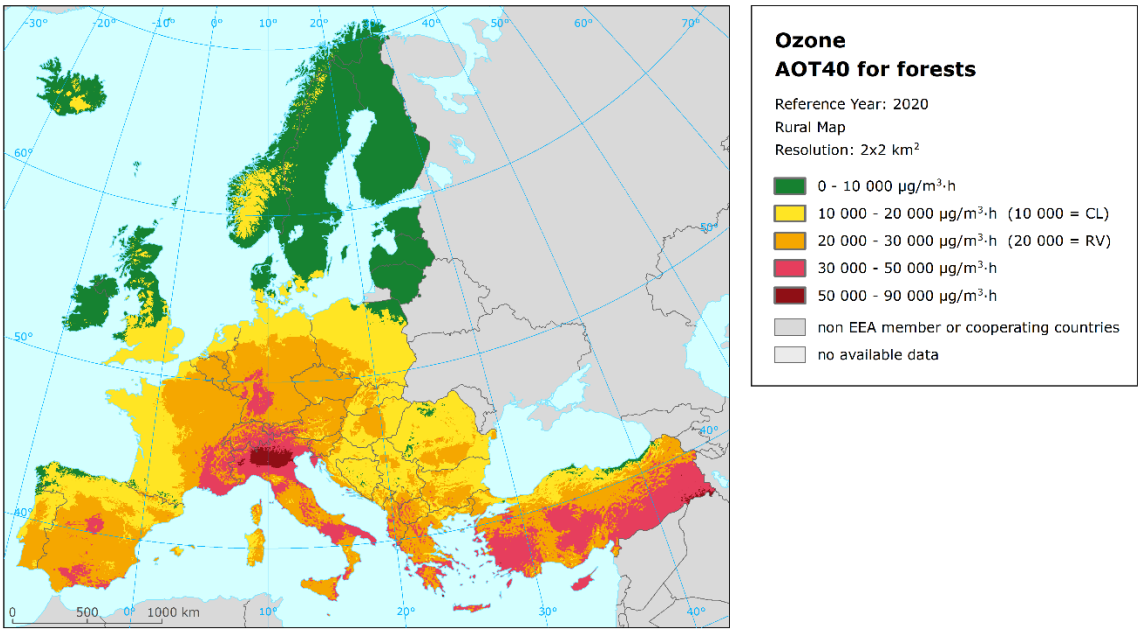

3.3.2 Vegetation exposure

Agricultural crops

The rural map with the ozone indicator AOT40 for vegetation has been combined with the land cover CLC2018 map. Following a similar procedure as described in Horálek et al. (2007), the exposure of agricultural areas (as defined above) has been calculated at the country-level.

Table 3.4 gives the absolute and relative agricultural area for each country and for five European regions where ozone concentrations are above the target value (TV) threshold and the long-term objective (LTO) for protection of vegetation as defined in the Ambient Air Quality Directive (EC, 2008). The frequency distribution of the agricultural area over some exposure classes per country is presented as well. The table presents the country grouping of the following regions: northern Europe, western Europe, central Europe, southern Europe and south-eastern Europe (for more details see Chapter 1).

Table 3.4 illustrates that in 2020, 5 % of all European agricultural land including Türkiye has been exposed to ozone concentrations above the TV threshold of 18 000 µg/m^3·h. For the areas excluding Türkiye and for the EU-27, it has been about 3 %, which is the lowest number of the sixteen-year period 2005-2020, see Table 6.4. None of the agricultural area presents ozone levels in excess of the TV in 29 out of 40 countries (excluding Monaco with no agricultural area). Agricultural areas with ozone concentrations above TV threshold covered less than 17 % in Portugal, Austria, Albania, Slovenia, France, Croatia, Switzerland, Spain, Greece and Türkiye (in ascending order). In Italy and Cyprus, 28 % and 76 % of agricultural area has been exposed to ozone concentrations above the TV threshold, respectively.

Considering the LTO of 6 000 µg/m^3·h, the total European area including Türkiye in excess has been about 75 %. For the areas excluding Türkiye and for the EU-27, it has been 71 % and 74 %, respectively. In 2020, values of the AOT40 for vegetation above the LTO have occurred in all countries with the exception of a few countries situated in northern and western Europe (Estonia, Finland, Iceland, Ireland, Latvia, Lithuania and Sweden). Very small areas (< 0.01 %) with the values above LTO have also occurred in Norway and Denmark. Only in a few of the remaining countries (Bosnia and Herzegovina, Poland and United Kingdom), the agricultural area exposed above the LTO in 2020 has been lower than 50 %, since in most of them between 58 % and 100 % of the agricultural area has been exposed to ozone levels in excess of the LTO.

Forests

The rural map with ozone indicator AOT40 for forests was combined with the land cover CLC2018 map. Following a similar procedure as described in Horálek et al. (2007), the exposure of forest areas (as defined above) has been calculated for each country, for the same five European regions as for crops and for Europe as a whole. Table 3.5 gives the absolute and relative forest area where the critical level (CL) set at 10 000 µg/m^3·h, the same level as defined in CLRTAP (2017a), and the value 20 000 µg/m^3·h (which is equal to the earlier used reporting value, RV, as was defined in the repealed ozone directive 2002/3/EC) are exceeded. Next to the forest area in exceedance, the table presents the frequency distribution of the forest area over some exposure classes.

The CL was exceeded in 2020 at about 61 % of all European forested area including Türkiye. For the area excluding Türkiye and for the EU-27 it was exceeded at about 58 % and 59 %, respectively, which is the second lowest exceedance observed for the sixteen-year period 2005-2020 (Table 6.4). As in previous years, most countries continue to have in 2020 the whole or considerable forest areas in excess of the CL. The CL was not exceeded only in the Baltic states, Finland and Iceland, in large parts of Scandinavia, the United Kingdom and Ireland, and in small parts of Poland, Spain, Türkiye and Romania.

Table 3.4: Agricultural area exposure and agricultural-weighted concentrations, ozone indicator AOT40 for vegetation, 2020

Country	Agricultural area, 2020					Percentage of agricultural area, 2020 [%]					Agricult.-weighted conc.
	Total area	> LTO (6 000 µg/m³·h)		> TV (18 000 µg/m³·h)		< 6 000	6 000 - 12 000	12 000 - 18 000	18 000 - 27 000	> 27 000	
	[km²]	[km²]	[%]	[km²]	[%]	µg/m³·h	µg/m³·h	µg/m³·h	µg/m³·h	µg/m³·h	[µg/m³·h]
Albania	8 017	7 929	98.9	2	0.0	1.1	51.4	47.5	0.0		11 585.0
Andorra	13	11	79.9			20.1	77.5	2.4			8 437.0
Austria	26 827	26 729	99.6	6	0.0	0.4	94.6	5.0	0.0		10 032.3
Belgium	17 473	17 473	100.0				98.7	1.3			9 953.1
Bosnia and Herzegovina	17 023	4 873	28.6			71.4	28.6				5 277.1
Bulgaria	57 390	50 729	88.4			11.6	88.3	0.1			7 646.5
Croatia	22 168	15 526	70.0	285	1.3	30.0	61.4	7.3	1.3		7 650.5
Cyprus	4 291	4 291	100.0	3 275	76.3			23.7	76.3		19 649.3
Czechia	44 784	44 784	100.0				99.9	0.1			9 328.7
Denmark (incl. Faroe Is.)	31 235	3	0.0			100.0	0.0				3 217.8
Estonia	14 252					100.0					2 089.8
Finland	27 504					100.0					1 217.4
France (metropolitan)	323 377	314 462	97.2	1 195	0.4	2.8	89.3	7.5	0.4		9 185.5
Germany	204 463	160 912	78.7			21.3	58.1	20.6			8 895.3
Greece	50 052	49 593	99.1	3 636	7.3	0.9	40.1	51.8	7.3		12 929.4
Hungary	60 390	54 116	89.6			10.4	88.4	1.2			7 838.9
Iceland	2 518					100.0					892.3
Ireland	46 756					100.0					3 242.8
Italy	155 718	155 457	99.8	43 616	28.0	0.2	34.4	37.4	17.2	10.8	15 966.4
Latvia	25 532					100.0					1 981.9
Liechtenstein	37	37	100.0				89.1	10.9			11 490.9
Lithuania	38 155					100.0					2 832.1
Luxembourg	1 351	1 351	100.0				100.0				10 774.4
Malta	125	125	100.0					100.0			14 601.0
Monaco											
Montenegro	2 242	1 608	71.7			28.3	70.5	1.2			7 118.5
Netherlands	23 644	18 224	77.1			22.9	77.1				7 283.5
North Macedonia	9 146	9 078	99.3			0.7	70.2	29.0			10 553.5
Norway	15 637	1	0.0			100.0	0.0				1 661.9
Poland	183 268	74 257	40.5			59.5	40.5				5 852.8
Portugal (excl. Az., Mad.)	42 566	41 393	97.2	8	0.0	2.8	45.1	52.2	0.0		10 885.7
Romania	135 279	79 252	58.6			41.4	58.6				6 508.1
San Marino	42	42	100.0					100.0			15 103.8
Serbia (incl. Kosovo*)	46 768	30 769	100.0			34.2	65.4	0.4			6 548.6
Slovakia	23 100	17 664	76.5			23.5	76.5				7 208.7
Slovenia	6 986	6 986	100.0	22	0.3		90.8	8.9	0.3		9 451.7
Spain (excl. Canarias)	241 014	230 519	95.6	10 803	4.5	4.4	36.0	55.1	4.5		12 552.7
Sweden	39 035					100.0					2 470.8
Switzerland	11 359	11 359	100.0	191	1.7		14.4	83.9	1.6	0.1	13 325.4
Türkiye	339 984	325 701	95.8	58 703	17.3	4.2	23.1	55.5	17.2	0.0	14 256.8
United Kingdom (& dep.)	135 760	58 000	42.7			57.3	42.7				5 359.9
Total	**2 435 285**	**1 813 256**	**74.5**	**121 742**	**5.0**	**25.5**	**48.3**	**21.2**	**4.3**	**0.7**	**9 340.3**
Total without Türkiye	**2 095 301**	**1 487 555**	**71.0**	**63 039**	**3.0**	**29.0**	**52.3**	**15.6**	**2.2**	**0.8**	**8 543.6**
EU-27	**1 846 681**	**1 363 848**	**73.9**	**62 845**	**3.4**	**26.1**	**53.6**	**16.9**	**2.5**	**0.9**	**8 875.7**
Northern Europe	**193 869**	**4**	**0.0**			**100.0**	**0.0**				**2 306.3**
Western Europe	**481 770**	**351 426**	**72.9**	**0**	**0.0**	**27.1**	**70.2**	**2.8**	**0.0**		**7 493.1**
Central Europe	**561 215**	**396 846**	**70.7**	**219**	**0.0**	**29.3**	**61.0**	**9.7**	**0.0**	**0.0**	**7 904.3**
Southern Europe	**560 414**	**539 515**	**96.3**	**62 532**	**11.2**	**3.7**	**40.2**	**44.9**	**8.2**	**3.0**	**13 036.9**
South-Eastern Europe	**638 018**	**525 465**	**82.4**	**58 990**	**9.2**	**17.6**	**42.2**	**30.9**	**9.2**	**0.0**	**10 873.4**
Kosovo	4 167	3 570	85.7			14.3	81.7	3.9			8 773.3
Serbia (without Kosovo*)	42 601	27 199	63.8			36.2	63.8				6 330.9

(*) Under the UN Security Council Resolution 1244/99.

Note: The percentage value "0.0" indicates that an exposed vegetation exists, but it is small and estimated to be less than 0.05 %. Empty cells mean no vegetation in exposure.

Table 3.5: Forested area exposure and forest-weighted concentrations, ozone indicator AOT40 for forests, 2020

Country	Forested area, 2020					Percentage of forested area, 2020 [%]					Forest - weighted conc.
	Total area	> CL (10 000 µg/m³·h)		> RV (20 000 µg/m³·h)		< 10 000	10 000 - 20 000	20 000 - 30 000	30 000 - 50 000	> 50 000	
	[km²]	[km²]	[%]	[km²]	[%]	µg/m³·h	µg/m³·h	µg/m³·h	µg/m³·h	µg/m³·h	[µg/m³·h]
Albania	7 104	7 104	100.0	6 746	95.0		5.0	75.9	19.0		26 361.1
Andorra	128	128	100.0	18	13.7		86.3	13.7			16 529.7
Austria	36 667	36 667	100.0	32 984	90.0		10.0	85.0	5.0		23 846.3
Belgium	6 089	6 089	100.0	6 039	99.2		0.8	99.2			25 074.2
Bosnia-Herzegovina	23 911	23 522	98.4	1 281	5.4	1.6	93.0	5.4			15 763.1
Bulgaria	34 675	34 675	100.0	17 120	49.4		50.6	48.6	0.7		20 370.5
Croatia	19 734	19 734	100.0	9 119	46.2		53.8	34.7	11.5		21 504.4
Cyprus	1 458	1 458	100.0	1 458	100.0			0.4	99.6		38 364.9
Czechia	25 867	25 867	100.0	24 972	96.5		3.5	96.5	0.0		23 993.1
Denmark (incl. Faroe Is.)	3 747	1 386	37.0			63.0	37.0				9 711.1
Estonia	21 080					100.0					4 119.9
Finland	211 668					100.0					2 126.3
France	143 376	142 492	99.4	95 175	66.4	0.6	33.0	52.5	13.9		22 953.3
Germany	108 031	108 030	100.0	91 313	84.5	0.0	15.5	69.1	15.4		24 988.0
Greece	26 122	26 122	100.0	23 572	90.2		9.8	66.9	23.4	0.0	26 499.7
Hungary	17 407	17 407	100.0	8 037	46.2		53.8	46.2			19 935.4
Iceland	537					100.0					3 025.8
Ireland	4 510	65	1.4			98.6	1.4				7 036.2
Italy	79 052	79 052	100.0	77 171	97.6		2.4	45.5	45.0	7.1	32 673.5
Latvia	24 261					100.0					4 660.6
Liechtenstein	79	79	100.0	79	100.0			34.4	65.6		31 425.3
Lithuania	19 455	34	0.2			99.8	0.2				6 561.5
Luxembourg	937	937	100.0	937	100.0			100.0			27 795.1
Malta	2	2	100.0	2	100.0				100.0		36 304.5
Monaco	1	1	100.0	1	100.0				100.0		42 316.4
Montenegro	5 777	5 777	100.0	3 166	54.8		45.2	54.1	0.7		20 480.0
Netherlands	3 118	3 118	100.0	1 021	32.7		67.3	32.7			19 508.7
North Macedonia	8 144	8 144	100.0	7 183	88.2		11.8	71.6	16.6		25 583.7
Norway	103 494	10 698	10.3			89.7	10.3				5 931.1
Poland	96 966	90 003	92.8	19 419	20.0	7.2	72.8	20.0			15 596.6
Portugal	16 512	16 052	97.2	10 446	63.3	2.8	34.0	63.2	0.0		19 626.5
Romania	71 273	69 627	97.7	10 228	14.4	2.3	83.3	14.3	0.0		16 187.0
San Marino	6	6	100.0	6	100.0				100.0		34 113.7
Serbia (including Kosovo)	27 211	27 152	99.8	8 583	31.5	0.2	68.2	30.4	1.2		18 827.5
Slovakia	20 484	20 484	100.0	9 714	47.4		52.6	47.4	0.0		19 485.5
Slovenia	11 441	11 441	100.0	10 658	93.2		6.8	82.1	11.1		24 704.5
Spain	107 927	99 814	92.5	55 868	51.8	7.5	40.7	48.2	3.6		19 638.5
Sweden	261 757	5 444	2.1			97.9	2.1				4 986.6
Switzerland	11 850	11 850	100.0	11 814	99.7		0.3	42.3	56.0	1.4	31 492.3
Türkiye	114 886	110 006	95.8	77 042	67.1	4.2	28.7	39.6	27.2	0.3	24 592.7
United Kingdom (including Crown dep.)	20 247	7 934	39.2			60.8	39.2				9 478.5
Total	**1 696 989**	**1 028 402**	**60.6**	**621 173**	**36.6**	**39.4**	**24.0**	**28.6**	**7.7**	**0.4**	**15 260.7**
Total without Türkiye	**1 582 104**	**918 396**	**58.0**	**544 131**	**34.4**	**42.0**	**23.7**	**27.8**	**6.3**	**0.4**	**14 583.8**
EU-27	**1 373 615**	**816 000**	**59.4**	**505 254**	**36.8**	**40.6**	**22.6**	**29.9**	**6.5**	**0.4**	**14 912.5**
Kosovo	4 316	4 316	100.0	3 131	72.5		27.5	65.2	7.4		22 967.5
Serbia (without Kosovo)	22 894	22 836	99.7	5 452	23.8	0.3	75.9	23.8			18 047.3
Northern Europe	**645 997**	**17 561**	**2.7**			**97.3**	**2.7**				**4 233.4**
Western Europe	**124 907**	**108 150**	**86.6**	**75 742**	**60.6**	**13.4**	**25.9**	**54.8**	**5.8**		**20 448.3**
Central Europe	**328 793**	**321 829**	**97.9**	**208 991**	**63.6**	**2.1**	**34.3**	**55.5**	**8.0**	**0.1**	**21 628.5**
Southern Europe	**284 577**	**275 120**	**96.7**	**195 971**	**68.9**	**3.3**	**27.8**	**45.9**	**21.0**	**2.0**	**24 489.5**
South-Eastern Europe	**312 715**	**305 742**	**97.8**	**140 469**	**44.9**	**2.2**	**52.9**	**33.0**	**11.8**	**0.1**	**20 826.9**
Kosovo	4 316	4 316	100.0	3 131	72.5		27.5	65.2	7.4		22 967.5
Serbia (without Kosovo)	22 894	22 836	99.7	5 452	23.8	0.3	75.9	23.8			18 047.3

(*) Under the UN Security Council Resolution 1244/99.

Note: The percentage value "0.0" indicates that an exposed vegetation exists, but it is small and estimated to be less than 0.05 %. Empty cells mean no vegetation in exposure.

In this context, it should be mentioned that the AOT40 indicator is probably not the best proxy for vegetation damage assessment. AOT40 does not take into account plant physiological control of ozone absorbed doses, which is taken into account in the POD (i.e. Phytotoxic Ozone Dose) indicators, as discussed in Section 3.4. POD indicators are known to be more related with ozone effects on plant

growth than ambient air ozone concentrations alone. The AOT40 does not take into account either the influence of meteorological conditions on growing season timing. Growing season´s start and end dates can change across Europe, and between years for a given site, depending on factors such as air temperature, solar radiation, photoperiod or rainfall. High temperature and dry weather favouring ozone pollution cause a reduction of ozone absorbed doses by plants due to plant physiological response to drought (i.e. the vegetation closes its stomata protecting itself from the exposure to ozone). However, plants may still be sensitive to ozone in such weather conditions, as illustrated by foliar injury records in Aleppo pine stands growing in southern France (CLRTAP, 2016) or controlled experimental results (e.g. Alonso et al., 2014).

3.4 Ozone – Phytotoxic Ozone Dose (POD) for crops

Ozone is generally recognized to be the most relevant pollutant for plants. Visible injury, reduction in growth, changes in biomass partitioning, or a higher susceptibility to pathogen attack can be the effect of ozone influence (Krupa et al., 2000). Scientific evidence suggests that observed effects of ozone on vegetation are more strongly related to the uptake of ozone through the stomatal leaf pores into the leaf interior (stomatal flux) than to the concentration in the atmosphere around the plants (Mills et al., 2011; Reich, 1987; Ashmore et al., 2004).

The cumulative stomatal ozone fluxes (F_{sto}) through the stomata of leaves found at the top of the canopy are calculated over the course of the growing season based on ambient ozone concentration and stomatal conductance (g_{sto}) to ozone. The stomatal conductance has been calculated using a multiplicative stomatal conductance model (Emberson et al., 2000) based on Jarvis (1976) as a function of species-specific maximum g_{sto} (expressed on a single leaf-area basis), phenology, and prevailing environmental conditions (photosynthetic photon flux density, PPFD), air temperature, vapour pressure deficit (VPD), and soil moisture.

POD_Y (Phytotoxic Ozone Dose) is the accumulated plant uptake (flux) of ozone above a threshold of Y during a specified time or growth period. The flux-based POD_Y metrics are preferred in risk assessment over the concentration-based AOT40 exposure index. AOT40 accounts for the atmospheric ozone concentration above the leaf surface and is therefore biologically less relevant for ozone impact assessment than POD_Y as it does not take into account how ozone uptake is affected by climate, soil and plant factors.

Several POD_Y indicators are described in CLRTAP (2017a). POD_YSPEC is a species or group of species-specific POD_Y that requires comprehensive input data and is suitable for detailed risk assessment. POD_YIAM is a vegetation-type specific POD_Y that requires less input data and is suitable for large-scale modelling, including integrated assessment modelling. POD_YSPEC is further used in this report.

For the wheat as for other crop species including potato and tomato, the Y value is taken equal to 6 nmol/m^2 PLA s^{-1} (i.e. per unit projected leaf area). For the details of POD_Y (and specifically POD_6SPEC as used in this report) calculation, see Annex 1, Section A1.3.

The species-specific flux models and associated response functions and critical levels for ozone-sensitive crops and cultivars can be used to quantify the potential negative impacts of O_3 on the security of food supplies at the local and regional scale. They can be used to estimate yield losses, including economic losses. A flux-threshold Y of 6 (POD_6SPEC) provides the strongest flux-effect relationships for crops (Pleijel et al., 2007). O_3 effects proved to be significant at a 5 % reduction of the effect parameter (Mills et al., 2011), hence critical levels (CL) were determined for this 5 % reduction of the effect parameter (i.e. yield, weight or quality of grain, tuber or fruit), based on the slope of the relationship. The POD_6SPEC CLs for crops were determined based on this reduction of relevant yield or weight, as shown in Table 3.6.

Wheat, potato and tomato are considered as representative species of crops in Europe (tomato can be regarded as representative horticultural crop for the Mediterranean and Black Sea regions, while

potato for other regions). Therefore, POD_6SPEC for these crops (labelled further simply as POD_6 for wheat, potato and tomato, respectively) are recommended for regular map construction. This report presents maps of POD_6 for wheat (*Triticum aestivum*), potato (*Solanum tuberosum*) and tomato (*Solanum lycopersicum*).

Table 3.6: POD_6SPEC critical levels for crops as determined by CLRTAP

Crop	Effect parameter	POD_6SPEC critical level
Wheat	grain yield	1.3 mmol/m^2 PLA
Wheat	1000-grain weight	1.5 mmol/m^2 PLA
Wheat	protein yield	2.0 mmol/m^2 PLA
Potato	tuber yield	3.8 mmol/m^2 PLA
Tomato	fruit yield	2 mmol/m^2 PLA
Tomato	fruit quality	3.8 mmol/m^2 PLA

Source: CLRTAP, 2017a.

The POD maps have been calculated based on the hourly ozone concentration maps, together with the meteorological and soil hydraulic properties data, based on the methodology described in Annex 1, Section A1.3. The calculation has been executed in 0.1° x 0.1° resolution. The hourly ozone maps are created for rural areas only, based on rural background stations. The POD maps are therefore applicable to rural areas only. Next to this, it should be noted that in the POD calculations for wheat and potato, all growing areas are considered rain-fed (i.e. without irrigation), see Colette et al. (2018). Thus, the maps are directly applicable only for areas without irrigation. If applied for irrigated areas, the POD values for wheat and potato might be somewhat underestimated. On the other hand, no limitation of stomatal conductance due to soil moisture can be assumed for tomato, since it is an irrigated horticultural crop (see Annex 1, Section A1.3).

The hourly ozone maps needed for POD calculation have been calculated at the 2x2 km^2 resolution, based on rural background measurements. The maps for each hour of the year 2020 have been constructed using the same methodology as the annual maps, i.e. the multiple linear regression followed by the kriging of its residuals (see Annex 1, Section A1.1) based on the measurement data, chemical transport model (CAMS-Ensemble forecast) output, altitude and the surface solar radiation. For details, see Annex 3, Section A3.3.

3.4.1 Phytotoxic Ozone Dose maps

Maps 3.6 to 3.8 present the final maps of Phytotoxic Ozone Dose (POD_6) for wheat, potato and tomato in 2020. High values of the POD_6 can be found in different parts of Europe since the POD_6 is dependent not only on ozone levels but also on the environmental conditions and plant phenology. On the other hand, the lowest levels of the POD_6 usually occur in areas with lower ozone concentrations (e.g. northern European regions) and/or in areas where environmental conditions limit the ozone stomatal conductance (dry and warm areas, including parts of the southern, south-western and south-eastern Europe).

The areas in the Map 3.6 with POD_6 values below the CL for grain yield of wheat (i.e. 1.3 mmol/m^2 PLA) are marked in dark green and green. The areas with POD_6 values in between CLs for grain yield and 1 000-grain weight (i.e. 1.5 mmol/m^2 PLA) and in between CLs for 1 000-grain weight and protein yield (i.e. 2 mmol/m^2 PLA) are marked in yellow and dark yellow, respectively. The areas with POD_6 values above the CL for protein yield of wheat (i.e. 2 mmol/m^2 PLA) are marked in orange, red and dark red.

In 2020, the exceedance of CLs values for wheat is most noticeable over large parts of France, the United Kingdom, Poland and Czechia. However, exceedances of the CLs for wheat have also occurred in other areas of varying size in many other countries from the north to the south of the whole mapped area (namely in Estonia, Denmark, Sweden, Germany, Hungary, Austria, Benelux, Spain, Italy, Slovenia, Croatia, Albania, Serbia, Greece, Türkiye and Cyprus).

POD_6 values above the highest CL for wheat (i.e. for protein yield) are found in northern Europe (parts of Denmark and small area in the south of Sweden), western Europe (parts of France and the United Kingdom) and in southern and south-eastern Europe (parts of Spain, Italy, Croatia, Greece and Türkiye).

Map 3.6: Phytotoxic Ozone Dose (POD_6) for wheat, rural map, 2020

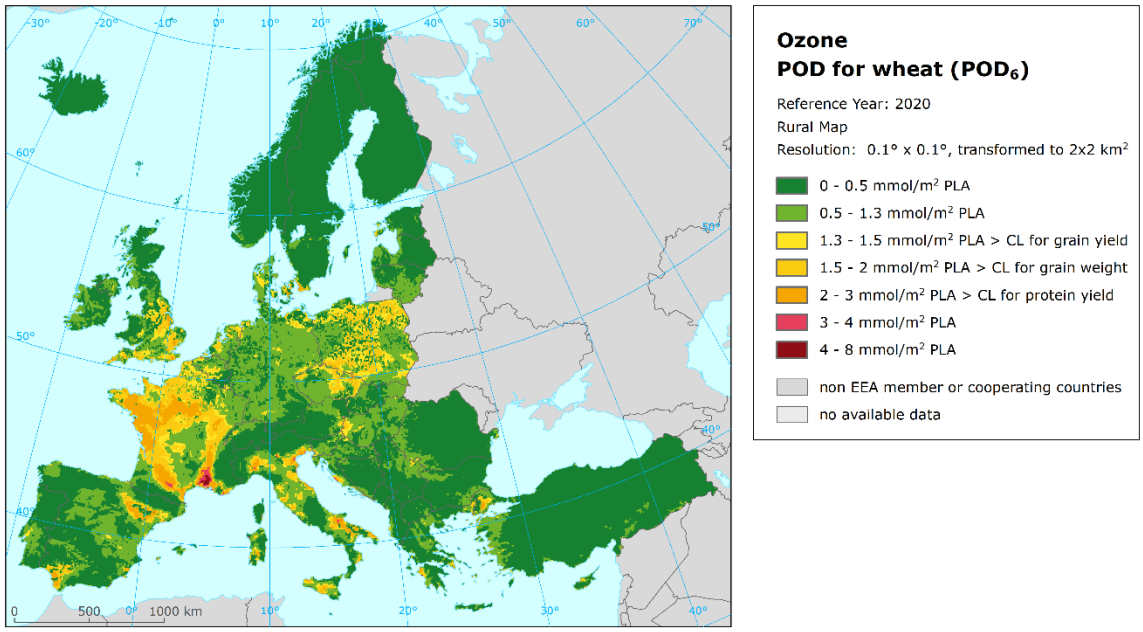

Map 3.7 presents the final map of POD_6 for potato in 2020. The areas with POD_6 values above the CL for tuber yield of potato (i.e. 3.8 mmol/m^2 PLA) are marked in yellow, dark yellow, orange, red and dark red. Most of France and the Benelux showed values of POD_6 for potato above this CL in 2020 as well as parts of the United Kingdom, Germany, Poland, Hungary, Italy, Portugal and Spain. The lowest levels of the POD_6 for potato in 2020 are found in northern Europe but also in parts of central, southern and south-eastern Europe. The highest levels of the POD_6 for potato in 2020 are found in the United Kingdom and parts of Portugal, Spain and France.

Map 3.8 presents the final map of POD_6 for tomato in 2020. The areas with POD_6 values above the CL for fruit yield are marked in red and dark red, the areas with POD_6 values above the CL for fruit quality in dark red. The Modelling and Mapping Manual (CLRTAP, 2017a) defines the parameterization for tomato for the Mediterranean area. EU-27 agriculture statistics show that ca 70 % of tomato in 2020 was produced in Italy, Spain, Portugal and Greece (EC, 2021). In the colder regions of Europe, tomato would be mostly grown in greenhouses. Most of the Mediterranean areas showed the values of POD_6 for tomato below the CLs for tomato in 2020. POD_6 values above the CLs have occurred only in small parts of the coastal Mediterranean areas, similarly as in the previous years.

For the purpose of completeness, the POD_6 has been modelled even for non-Mediterranean areas using the same parameterization (lighter colours in the Map 4.8).

Map 3.7: Phytotoxic Ozone Dose (POD_6) for potato, rural map, 2020

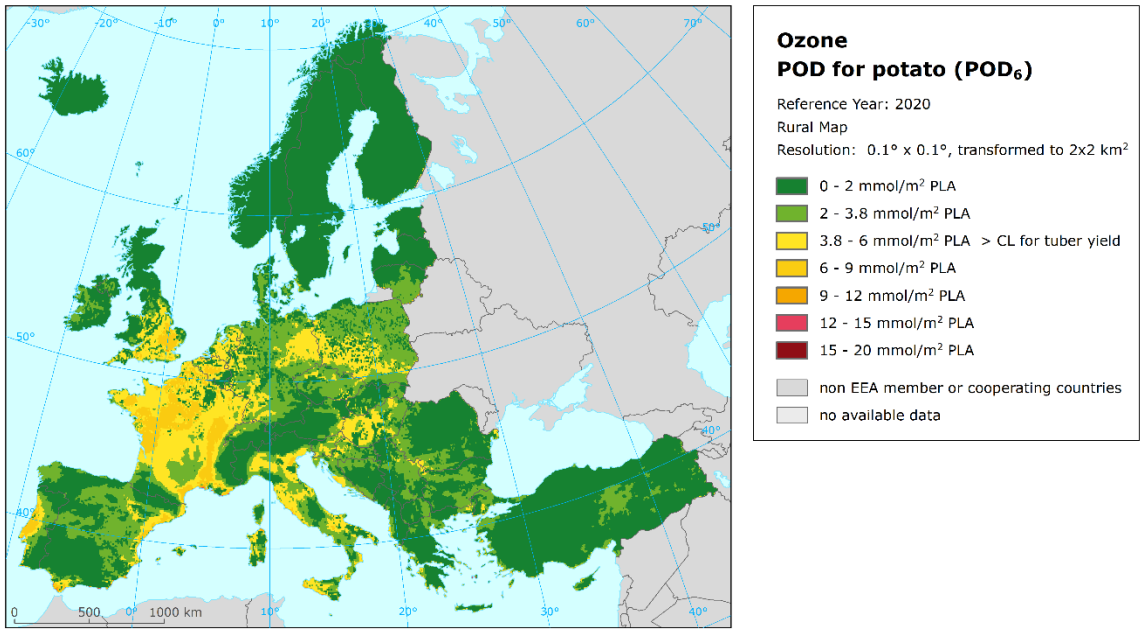

Map 3.8: Phytotoxic Ozone Dose (POD_6) for tomato, rural map, 2020

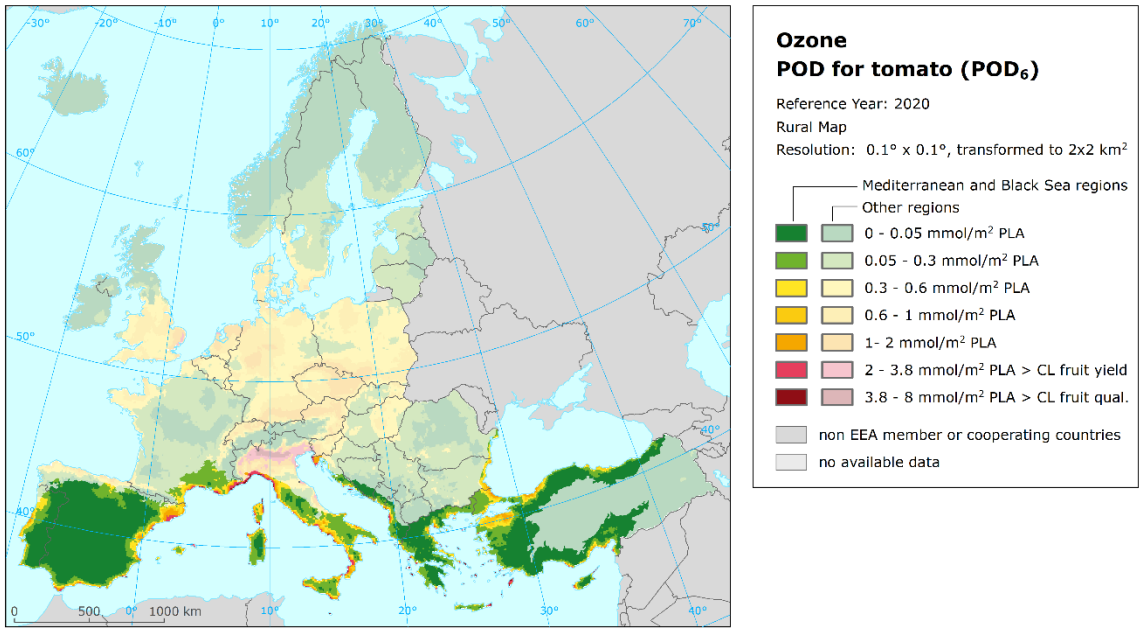

4 NO_2 and NO_x

Annual average maps for NO_2 (related to protection of human health) and for NO_x (related to protection of vegetation) have been produced and presented in the regular mapping report since the maps for year 2014.

The methodology for creating the concentration maps follows the same principle as for the rest of pollutants: a linear regression model on the basis of European wide station measurement data, followed by kriging of the residuals produced from that regression model (residual kriging).

The map on NO_2 is based on an improved mapping methodology developed in Horálek et al. (2017b, 2018). The map layers are created for the rural, urban background and urban traffic areas separately on a grid at 1x1 km^2 resolution. Subsequently, the urban background and urban traffic map layers are merged using the gridded road data into one urban map layer. This urban map layer is further combined with the rural map layer into the final NO_2 map using a population density grid at 1x1 km^2 resolution. For details, see Annex 1, Section A1.1. Supplementary data used consist of chemical transport model (CTM) output, altitude, Sentinel-5P satellite data, wind speed, population density and land cover indicators for rural areas; for urban background areas these are CTM output and temperature, altitude, Sentinel-5P satellite data, wind speed, population density and land cover indicators; for traffic areas the CTM output, altitude, and Sentinel-5P satellite data are used (Annex 3, Section A3.4). The final concentration map is presented in the 1x1 km^2 grid resolution. Be it noted that this final map is representative for rural and urban background areas, but not for urban traffic areas (which are smoothed in this 1x1 km^2 spatial resolution).

The map of the vegetation-related indicator NO_x annual average is created on a grid at 2x2 km^2 resolution, based on rural background measurements only, as vegetation is considered not to be extensively present at urban and suburban areas. Hence, this map is applicable to rural areas only. The resolution is chosen equally to the one of the vegetation indicator for ozone.

The population exposure to NO_2 has been calculated based on the methodology described in Horálek et al. (2017b), i.e. according to Equation A1.6 of Annex 1. It has been calculated separately for urban areas directly influenced by traffic and for the background (both rural and urban) areas, in order to better reflect the population exposed to traffic. Based on this, the different concentration levels in urban background and traffic areas inside the 1x1 km^2 grid cells are taken into account. Thus – like for PM_{10} and $PM_{2.5}$ – the population exposure refers not only to the rural and urban background areas, but to the urban traffic locations as well. However, it should be mentioned that only population density data at 1x1 km^2 resolution has been used. This means that contrary to the concentration levels, the population density is constant within each 1x1 km^2 grid cell. This shortcoming can increase the uncertainty of the population exposure results.

Annex 3 provides details on the regression and kriging parameters applied for deriving the maps, as well as the uncertainty analysis of the maps.

4.1 NO_2 – Annual mean

The Ambient Air Quality Directive (EC, 2008) sets two limit values (LV) for NO_2 for the human health protection. The first one is an annual LV (ALV) at the level of 40 µg/m^3. This is the same concentration level as recommended by the World Health Organization for the NO_2 annual average as the 2005 Air Quality Guideline level (WHO, 2005). Nevertheless, the current WHO Air Quality Guideline level for the NO_2 annual average is set to 10 µg/m^3, as introduced in 2021 (WHO, 2021a). The second one is an hourly LV (HLV, 200 µg/m^3 not to be exceeded on more than 18 hours per year). Concentrations above the HLV were observed in 0.3 % (10 stations) of all reporting stations only in 2020, mostly at urban traffic stations, see Targa et al. (2022). In view of this low number of exceedances, the short-term LV has not been included in the mapping procedures.

4.1.1 Concentration map

Map 4.1 presents the final combined concentration 1x1 km^2 gridded map for the 2020 NO_2 annual average. According to Map 4.1, the areas where NO_2 concentrations were above the ALV of 40 µg/m^3 include urbanized parts of some large cities, particularly Milan, Ankara and Istanbul, and some other smaller cities in Türkiye. Some other cities show NO_2 levels above 30 µg/m^3, e.g. in France, Greece, Italy, Romania, Spain and Türkiye. Most of the European area shows NO_2 levels below 20 µg/m^3, with most of the rural areas below 10 µg/m^3. Some larger areas above 20 µg/m^3 can be found in the Po Valley, the Benelux, the German Ruhr region, in central and southern England, in the Île de France region and around Rome and Naples and in the Krakow – Katowice (PL) – Ostrava (CZ) industrial region.

It should be noted that the interpolated map is created at 1x1 km^2 only. Although the urban traffic map layer is used in the map creation, the traffic locations are smoothed in the 1x1 km^2 resolution. Thus, the maps as such refers to the rural and urban background situations only, while the concentrations above the NO_2 limit values occur mostly at local hotspots such as dense traffic locations and densely urbanised and industrialised areas. Such concentrations are mostly not visible in the 1x1 km^2 map.

The relative mean uncertainty of the NO_2 annual average map is 32 % for rural and 34 % for urban background areas (Annex 3, Section A3.4). This means slightly worse mapping uncertainty compared to the quality objective for models of NO_2 annual average (i.e. 30 %) as set in the Air Quality Directive (EC, 2008).

Map 4.1: Concentration map of NO_2 annual average, 2020

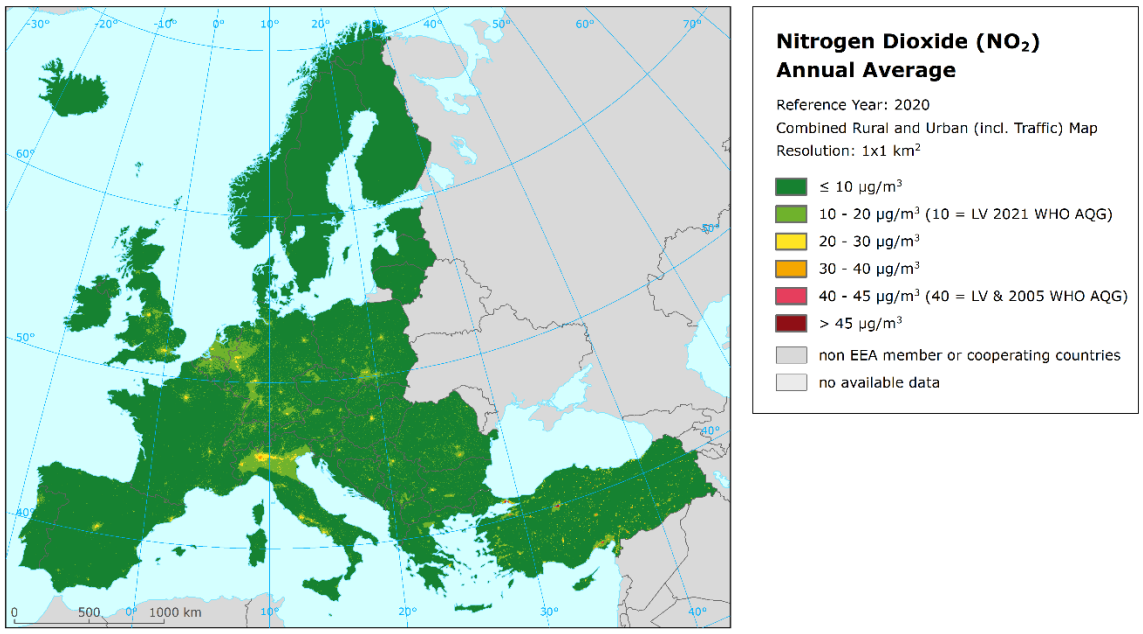

For the comparison with five-year average 2015-2019 values, see Annex 4, Section A4.4. Compared to five-year mean, general decrease in NO_2 annual concentration is shown. The steepest decreases are observed in areas of London, Paris, Rome, Napoli, Milano, Madrid, and Barcelona. The decreases have been also observed in some areas of the United Kingdom, Benelux, parts of Spain, France, Italy and countries in central Europe. The main reason for this is the lockdown measures connected with the COVID-19 pandemic.

In order to provide more complete information of the air quality across Europe, the final combined map including the measurement data at stations is presented in Map A5.9 of Annex 5.

4.1.2 Population exposure

Figure 4.1 and Table 4.1 give the population frequency distribution for a limited number of exposure classes calculated on a grid of 1x1 km^2 resolution. Table 5.1 also presents the population-weighted concentration for individual countries, large regions, EU-27 and for the whole mapping area.

It has been estimated that in 2020 about 2 % of the considered European population including Türkiye and less than 0.2 % of both the considered European population without Türkiye and the EU-27 population lived in areas with NO_2 annual average concentrations above the EU limit value of 40 µg/m^3 (i.e. also 2005 WHO AQG).

About 72 % of the considered European population (both including and excluding Türkiye) and 71 % of the EU-27 population has been exposed to annual average concentrations above the current 2021 WHO AQG level of 10 µg/m^3 (WHO, 2021a).

No population has been exposed to concentrations above the ALV in 36 countries out of 41 assessed countries. In Romania, Italy, France and Greece (ascending order) between 0.4 and 1.5 % of population has been exposed to concentrations above the limit value. In Türkiye, 19 % of the population suffers from exposures above this limit value.

The population-weighted concentration of the NO_2 annual average for 2020 has been estimated to be about 15 µg/m^3 for the total considered European population and 14 µg/m^3 for EU-27 only population and for the total considered European population without Türkiye. In the last case, this means a decrease of almost 4 µg/m^3 compared to the previous five-year mean (Annex 4, Section A4.3). The value for the whole area without Türkiye is the lowest value in the sixteen years' time series (see Table 6.5). The main reason for this probably is the lockdown measures connected with the COVID-19 pandemic.

Figure 4.1: Percentage of the population (%) exposed to different values of NO_2 annual average (µg/m^3), 2020

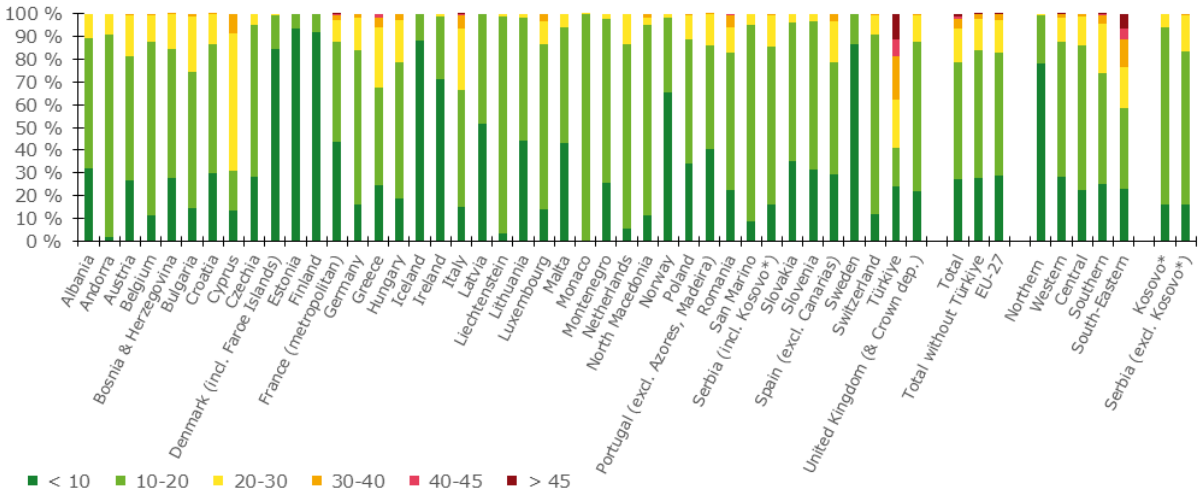

(*) Under the UN Security Council Resolution 1244/99.

Table 4.1: Population exposure and population-weighted concentration, NO_2 annual average 2020

Country	ISO	Population [inhbs·1000]	NO_2 – annual average, exposed population, 2020 [%]						NO_2 ann. avg.
			< 10	10-20	20-30	30-40	40-45	> 45	Pop. weighted
Albania	AL	2 797	31.9	57.6	10.5				12.8
Andorra	AD	84	1.9	89.0	9.0				17.6
Austria	AT	8 381	26.7	54.5	18.3	0.5			14.3
Belgium	BE	10 944	11.2	76.6	11.7	0.5			14.3
Bosnia and Herzegovina	BA	3 802	28.0	56.3	15.5	0.2			14.1
Bulgaria	BG	7 364	14.4	60.2	24.4	1.1			16.7
Croatia	HR	4 288	29.9	56.6	13.2	0.3			13.1
Cyprus	CY	1 018	13.2	17.6	60.8	8.4			20.8
Czechia	CZ	10 423	28.2	66.9	4.9				12.5
Denmark (incl. Faroe Islands)	DK	5 577	84.7	14.9	0.4				7.4
Estonia	EE	1 291	93.5	6.5					5.8
Finland	FI	5 339	92.1	7.9					6.2
France (metropolitan)	FR	62 744	43.7	43.9	9.6	2.2	0.6	0.0	12.2
Germany	DE	80 174	16.1	68.0	14.1	1.9			15.2
Greece	GR	10 635	24.6	42.9	26.8	4.1	1.5		16.8
Hungary	HU	9 937	18.9	59.9	18.6	2.6			14.9
Iceland	IS	318	88.0	12.0					7.1
Ireland	IE	4 574	71.4	27.7	1.0				7.4
Italy	IT	59 409	15.2	51.1	27.0	6.1	0.5	0.0	17.6
Latvia	LV	2 080	51.7	48.3	0.0				9.6
Liechtenstein	LI	34	3.5	95.4	1.1				15.3
Lithuania	LT	3 028	44.3	53.9	1.8				10.1
Luxembourg	LU	511	14.2	72.7	9.7	3.3			15.8
Malta	MT	417	43.2	51.0	5.9				11.0
Monaco	MC	33		99.9	0.1				18.0
Montenegro	ME	620	25.4	72.5	2.1				13.7
Netherlands	NL	16 600	5.7	80.7	13.6				15.8
North Macedonia	MK	2 061	11.6	83.7	3.0	1.8			14.2
Norway	NO	4 906	65.5	32.8	1.7				8.0
Poland	PL	38 494	34.1	54.7	10.5	0.7			13.0
Portugal (excl. Azores, Madeira)	PT	10 047	40.6	45.5	13.7	0.2			12.5
Romania	RO	20 138	22.4	60.5	11.2	5.5	0.4		15.1
San Marino	SM	32	8.6	86.8	4.6				13.2
Serbia (incl. Kosovo*)	RS	8 896	16.2	69.2	14.2	0.4			14.8
Slovakia	SK	5 399	35.1	61.4	3.5				11.3
Slovenia	SI	2 042	31.5	65.3	3.2				12.8
Spain (excl. Canarias)	ES	44 722	29.4	49.3	18.1	3.2			14.6
Sweden	SE	9 539	86.6	13.4					6.5
Switzerland	CH	7 893	11.7	79.3	8.3	0.7			14.5
Türkiye	TR	71 920	24.1	17.1	21.1	19.0	7.8	11.0	24.9
United Kingdom (& Crown dep.)	UK	63 415	22.0	66.0	11.4	0.7			13.9
Total		**601 927**	**27.5**	**51.4**	**14.7**	**4.1**	**1.1**	**1.3**	
			78.9				**2.4**		**15.3**
Total without Türkiye		**530 007**	**28.0**	**56.0**	**13.8**	**2.1**	**0.2**	**0.0**	
			84.0				**0.2**		**14.0**
EU-27		**435 073**	**29.0**	**54.0**	**14.4**	**2.4**	**0.2**	**0.0**	
			83.0				**0.2**		**14.1**
Northern Europe		**32 080**	**78.0**	**21.5**	**0.5**				**7.4**
Western Europe		**144 566**	**28.2**	**59.5**	**10.7**	**1.3**	**0.2**	**0.0**	**13.4**
Central Europe		**162 777**	**22.4**	**63.9**	**12.4**	**1.3**			**14.2**
Southern Europe		**140 620**	**25.1**	**48.9**	**21.6**	**4.0**	**0.3**	**0.0**	**15.6**
South-Eastern Europe		**121 885**	**22.9**	**35.6**	**18.0**	**12.2**	**4.7**	**6.5**	**20.8**
Kosovo*	KS	1 748	15.9	78.0	6.1				14.4
Serbia (excl. Kosovo*)	RS-	7 148	16.3	67.0	16.1	0.5			14.9

(*) Under the UN Security Council Resolution 1244/99.

Note: The percentage value "0.0" indicates that an exposed population exists, but it is small and estimated to be less than 0.05 %. Empty cells mean no population in exposure.

Figure 4.2 shows, for the whole mapped area, the population frequency distribution for exposure classes of 1 µg/m^3. One can see the highest population frequency for classes between 7 and 17 µg/m^3, continuous decline of population frequency for classes between 18 and 30 µg/m^3 and continuous mild decline of population frequency for classes between 31 and 60 µg/m^3.

Figure 4.2: Population frequency distribution, NO_2 annual average, 2020. NO_2 annual mean concentrations to which the population per country was exposed in 2020. The 2021 WHO AQG level (10 µg/m^3) is marked by the green line, the EU annual limit value and 2005 WHO AQG level (40 µg/m^3 in both cases) are marked by the red line

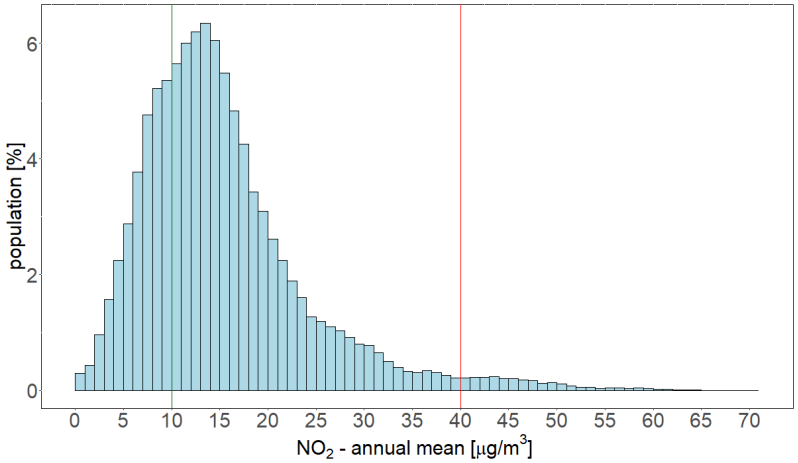

The boxplot showing for individual countries the NO_2 annual average concentrations to which the population per country was exposed in 2020 is presented in Summary, Figure S.1.

4.2 NO_x – Annual mean

4.2.1 Concentration map

The Ambient Air Quality Directive (EC, 2008) sets a critical level (CL) for the protection of vegetation for the NO_x annual mean at 30 µg·m^{-3}. According to this directive, the sampling points targeted at the protection of vegetation and natural ecosystems shall be in general sited more than 20 km away from agglomerations or more than 5 km away from other built-up areas. Thus, only the observations at rural background stations are used for the NO_x mapping and the resulting map is representative for rural areas only.

The number of NO_x measurement stations is limited. The mapping of the NO_x annual average has been therefore performed on the basis of an approach presented in Horálek et al. (2007). This approach derives additional pseudo NO_x annual mean concentrations from NO_2 annual mean measurement concentrations and increases as such the number and spatial coverage of NO_x 'data points', and applies these data to the NO_x mapping. Section A1.1 of Annex 1 provides some details.

Map 4.2 presents the concentration map of NO_x annual average. It concerns rural areas only, representing an indicator for vegetation exposure to NO_x.

Most of the European area shows NO_x levels below 20 µg/m^3. However, in the Po Valley, southern part of the Netherlands, northern Belgium, the German Ruhr region and around some larger European

cities (typically being the national capitals) elevated NO_x concentrations above the CL are observed. Furthermore, around many larger European cities concentrations just below the CL are observed. These concentrations are expected to be the result of large emissions from transport in and around the cities, as well as energy production and industrial facilities taking place at these areas. This is relevant only for the so the called peri-urban vegetation where patches of agricultural land and of natural or planted vegetation can be found. On the contrary, low concentrations (below 10 µg/m^3) are observed in large areas of Spain, France, Italy, Croatia, Bosnia and Herzegovina, Montenegro, Hungary, Germany, Poland, Czechia, Scandinavia, Iceland, Ireland and the Baltic States.

Map 4.2: Concentration map of NO_x annual average, rural map, 2020

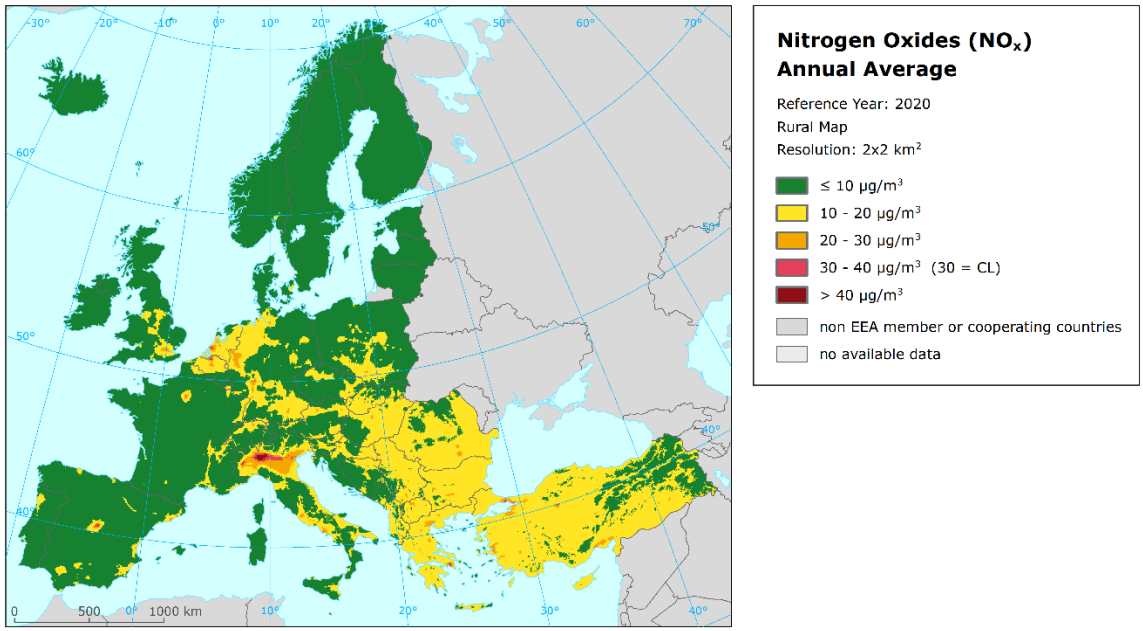

For the comparison with five-year average 2015-2019 values, see Annex 4, Section A4.4.

The relative mean uncertainty of this rural map is 46 %. This means worse mapping uncertainty compared to the quality objective for models of NO_x annual average (i.e. 30 %) as set in the Air Quality Directive (EC, 2008). This higher relative uncertainty is highly influenced by the low concentration values of NO_x in the most areas. The NO_x annual average rural map including the data measured at rural background stations is presented in Map A5.10 of Annex 5. The map illustrates the lack of the NO_x rural stations in the Balkan area.

Vegetation exposure has not been calculated for NO_x, as the CL applies actually to vegetation only, which is by nature mostly allocated in rural areas where there has been limited CL exceedance observed. Therefore, values above the CL for protection of the vegetation would occur in limited vegetation areas only and, as such, is considered not to provide essential information from the European scale perspective. Furthermore, contrary to vegetation exposure to high ozone concentrations in Europe that leads to considerable damage, vegetation exposure to NO_x pollution is of minor importance in terms of actual impacts. On the other hand, NO_x concentrations contribute in part to the total N-deposition, which leads to acidifying and eutrophying effects on vegetation. These effects, especially eutrophication, are still very important in Europe (e.g. EMEP, 2020). However, these effects on vegetation cannot be expressed by an exposure to NO_x as many oxidized and reduced nitrogen compounds contribute to total atmospheric nitrogen deposition.

Concerning the potential exposure estimate of vegetation and natural ecosystems to NO_x there is an additional dilemma: which receptor types should be selected to estimate the exposure and CL exceedance of vegetation and natural ecosystems? An option would be the use of CLC classes (e.g. like in Horálek et al., 2008); nevertheless this classification is too general. Another option would be the NATURA 2000 database. However, that data source contains a wide series of receptor types, species and classes. Serious additional efforts would be needed to conclude on the most relevant set of receptors from the NATURA 2000 geographical database.

Currently, the ICP Vegetation Coordination Centre is performing a review of NO_x CLs in relation to vegetation. The existing NO_x CLs were first proposed in 1988 and set at an unchanged annual level (30 µg/m^3) since 1993. Therefore, it was deemed timely to review evidence around NO_x CLs (CLRTAP, 2022).

5 Benzo(a)pyrene

An annual average map for benzo(a)pyrene (BaP) has been produced and is presented in the regular mapping report for the first time. In agreement with the conclusions of Horálek et al. (2022b), it is labelled as experimental map to indicate that it does not yet meet the same accuracy standards as the regularly produced maps of other pollutants.

The map of BaP is based on the mapping methodology developed and tested in Horálek et al. (2022b). The methodology for creating the concentration maps follows the same principle as for the rest of pollutants: a linear regression model on the basis of European wide station measurement data, followed by kriging of the residuals produced from that regression model (residual kriging). The map layers are created for the rural and urban background areas separately on a grid at 1x1 km^2 resolution. For details, see Annex 1, Section A1.1. Supplementary data used in the linear regression consist of chemical transport model (CTM) output, altitude, temperature, wind speed and land cover for rural areas; for urban background areas these are CTM output and temperature (Annex 3, Section A3.5). The final concentration map is presented in the 1x1 km^2 grid resolution.

Due to the poor spatial coverage of the BaP measurement stations, so-called pseudo BaP stations have been also used in addition. Pseudo BaP data in locations with $PM_{2.5}$ measurements (or with pseudo $PM_{2.5}$ data based on PM_{10} measurements) and with no BaP measurements have been estimated based on the exponential regression of the observed BaP concentrations with the $PM_{2.5}$ data, geographical coordinates and the land cover. Due to quite high uncertainty of the pseudo data estimates, the pseudo data are used only in areas with a lack of BaP measurements. Due to the serious lack of Turkish data, Türkiye is not included in the mapping area. Annex 3, Section A3.5 provides details on the regression and kriging parameters applied for deriving the BaP map, as well as the uncertainty analysis of this map.

The 2004 Ambient Air Quality Directive (EC, 2004) sets a target value for ambient air concentration of BaP, as a marker for the carcinogenic risk of PAHs in ambient air. The target value (TV) for BaP (measured in PM_{10}) is set to 1 ng/m^3 as an annual mean.

An estimated reference level (RL) of 0.12 ng/m^3 was calculated assuming WHO unit risk (WHO, 2010) for lung cancer for polycyclic aromatic hydrocarbon (PAH) mixtures and an acceptable risk of additional lifetime cancer risk of approximately 1 in 100 000 (WHO, 2010; de Leeuw and Ruyssenaars, 2011).

Both the EU target value (1 ng/m^3) and the estimated WHO RL (0.12) are based on the WHO lung cancer unit risk for PAH mixtures (8.7×10^{-5} per ng/m3 B[a]P), and correspond to an additional lifetime cancer risk of approximately 9 cases and 1 case in 100 000 exposed individual (WHO, 2021b).

5.1 Benzo(a)pyrene – Annual mean

5.1.1 Concentration map

Map 5.1 presents the final combined concentration 1x1 km^2 gridded map for the 2020 BaP annual average. Red and purple areas indicate concentrations above the target value (TV) of 1.0([5]) ng/m^3.

The highest BaP concentrations are shown in Poland, north-eastern Czechia and some populated locations in the central and south-eastern Europe and the eastern Po Valley in northern Italy. Contrary to that, western Europe shows low BaP values. In the maps, generally lower levels of BaP concentrations in natural areas can be seen, compared to the other land cover area types.

([5]) As stated earlier (see Section 1), maps presented in this report do not allow for formal compliance checking with the limit or target values as set by EC (2004, 2008). So, as for other maps, no rounding is executed in the results and all values above 1 ng/m^3 (without rounding) are shown in red. Whereas according to the formal compliance checking, values above 1.5 ng/m^3 (rounded to 2) are considered as TV exceedances.

The relative mean uncertainty of the 2020 map of BaP annual average is 136 % for rural and 84 % for urban areas and determined exclusively on the actual BaP measurement data points, i.e. not on the pseudo stations (Annex 3, Section A3.5). This uncertainty is at the considerably higher level (especially in the rural areas) compared to the quality objective for models of BaP annual average (i.e. 60 %) as set in the European directive (EC, 2004).

The high uncertainty in the rural areas is probably highly affected (besides the low density of the rural stations) by the fact that stations classified as “rural background” comprise both regional stations with low BaP values and stations located in villages, which are often highly influenced by the local heating leading to high BaP concentrations.

Map 5.1: Concentration map of benzo(a)pyrene annual average, 2020, experimental map

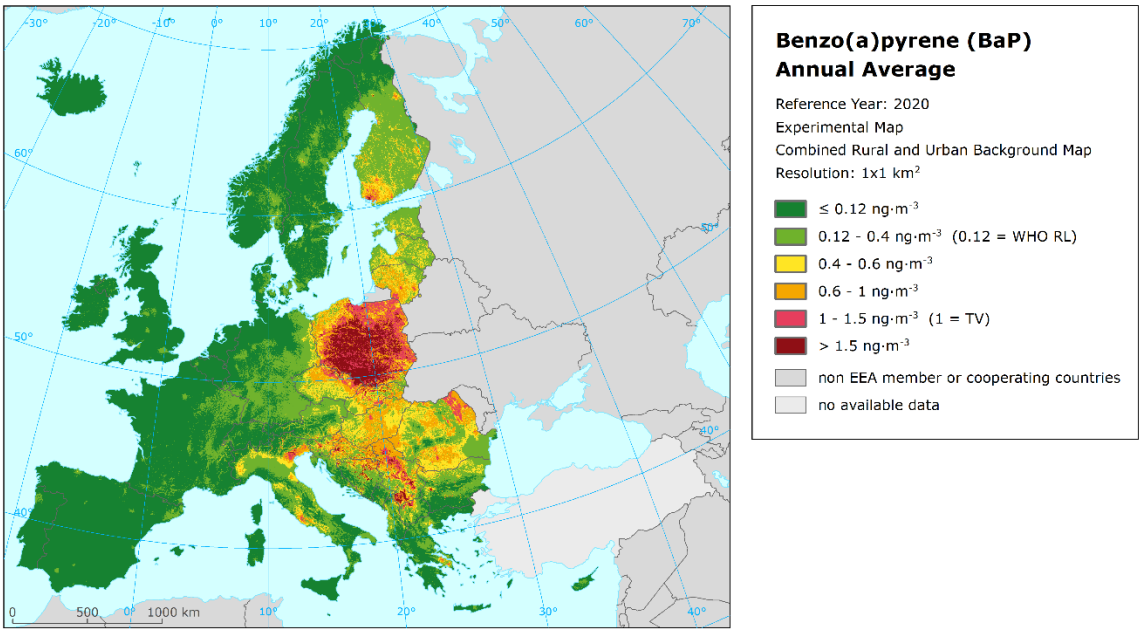

5.1.2 Population exposure

Table 5.1 gives the population frequency distribution for a limited number of exposure classes to BaP concentrations, as well as the population-weighted concentration. Due to the experimental character of the benzo(a)pyrene map and its high uncertainty, the population exposure is presented only for EU-27, for five European regions and for the total mapping area, not for individual countries.

Based on the experimental map, it is estimated that 14 % of population living in the considered (i.e. mapped) European area has been exposed to concentrations above the EU target value (TV) of 1.0 ng/m^3. Further, it is estimated that more than 70 % population living in the considered (i.e. mapped) European area has been exposed to concentrations above the WHO RL of 0.12 ng/m^3. The population-weighted concentration of the BaP annual average for 2020 for the considered European countries is estimated to be about 0.5 ng/m^3.

Table 5.1: Population exposure and population-weighted concentration, benzo(a)pyrene annual average, 2020, based on experimental map

Area	Population [inhbs·1000]	BaP – annual average, exposed population, 2020 [%]						BaP ann. avg.
		< 0.12	0.12-0.4	0.4-0.6	0.6-1.0	1.0-1.5	> 1.5	Pop. weighted
Northern Europe	32 080	8.4	51.1	18.5	15.1	5.6	1.3	0.44
Western Europe	144 566	57.0	42.6	0.4	0.1	0.0		0.13
Central Europe	162 777	8.7	45.5	8.8	8.8	6.4	21.7	0.92
Southern Europe	140 620	33.5	45.3	11.5	6.2	2.9	0.5	0.27
South-Eastern Europe	49 965	0.5	11.7	20.2	25.3	14.3	27.9	1.32
Total	**530 007**	**27.7**	**41.8**	**8.9**	**7.7**	**4.4**	**9.5**	**0.54**
EU-27	**435 073**							

Note: The percentage value "0.0" indicates that an exposed population exists, but it is small and estimated to be less than 0.05 %. Empty cells mean no population in exposure.

Figure 5.1 shows, for the whole mapped area, the population frequency distribution for exposure classes of 0.05 ng/m^3. The highest population frequency is found for classes between 0.05 and 0.30 ng/m^3. A quite continuous decline of population frequency is visible for classes beyond 0.30 ng/m^3.

Figure 5.1: Population frequency distribution, benzo(a)pyrene annual average, 2020. The EU target value (1.0 ng/m^3) is marked by the red line

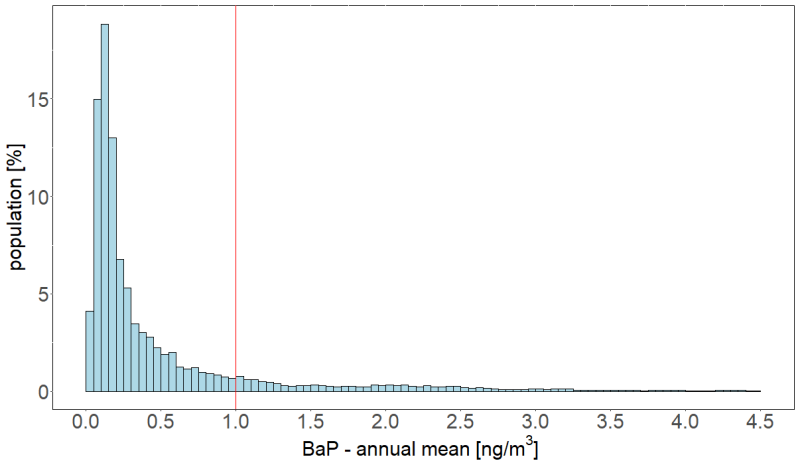

Note: Apart from the population distribution shown in graph, it was estimated that 1.24 % of population lived in areas with BaP annual average concentration in between 4.5 and 11.5 ng/m^3.

6 Exposure trend estimates

This report has presented the interpolated maps for 2020 on the PM_{10}, $PM_{2.5}$, ozone and NO_2 human health related air pollution indicators (annual average and the 90.4 percentile of PM_{10} daily means, annual average for $PM_{2.5}$, the 93.2 percentile of maximum daily 8-hour means, SOMO35 and SOMO10 for ozone, and the annual average for NO_2), as well as the BaP annual average experimental map, together with tables showing the frequency distribution of the estimated population exposures and the population-weighted concentration per country (apart from BaP), large European region, EU-27 and the total mapping area.

Furthermore, interpolated maps of ozone and NO_x vegetation related air pollution indicators have been produced. More specifically, these include a map of the ozone indicator AOT40 for vegetation and AOT40 for forests, and tables with the frequency distribution of estimated land area exposures and vegetation-weighted concentration per country, large region, EU-27 and the total mapping area. In addition, the maps of the Phytotoxic Ozone Dose (POD) for wheat, potato and tomato, and the NO_x annual average map have been produced, but without exposure estimates.

A mapping approach similar to previous years (Horálek et al., 2021 and references therein) based primarily on observational data has been used. With the interpolated air pollution maps and exposure estimates for the year 2020 completed, a sixteen-year overview of comparable exposure estimates has been obtained (with full time series coverage for PM_{10} and ozone, except SOMO10 and POD indicators, with one year missing for $PM_{2.5}$ and with four years missing for NO_2). In this chapter these multi-annual overviews of exposure estimates are provided for each of the indicators of PM_{10}, $PM_{2.5}$ and ozone (except SOMO10 and POD), including a trend analysis.

For the previous years, mapping results as presented in Horálek et al. (2022a) and previous mapping reports have been used. Since 2017 results, PM_{10} and $PM_{2.5}$ maps have been prepared based on the updated method (Horálek et al., 2019). For comparability reasons, results for 2015-2019 (and partly also for 2005 and 2009) are presented in two variants for these pollutants, i.e. based on the old and the updated methodologies. Ozone maps based on the 1x1 km^2 merging resolution as tested in Horálek et al. (2010) and routinely applied since 2008 results are used for the whole period, due to consistency.

For the human health indicators, the exposure estimates are expressed, on one hand, as population-weighted concentration and, on the other hand, as percentage of population exposed to concentrations above the limit/target value. For the vegetation related indicators, the exposure estimates are expressed as the agricultural- and forest-weighted concentrations, as well as the agricultural or forest areas exposed to concentrations above defined thresholds.

It should be noted that the percentage of population, agricultural area, or forest area exposed is a less robust indicator compared to the population-weighted, agricultural-weighted, or forest-weighted concentration, as a small concentration increase (or decrease) may lead to a major increase (or decrease) of population, agricultural or forest area exposed. This is not the case when taking the population-weighted or agricultural/forest-weighted concentration as indicator. Therefore, the trend analysis is done based on the population-weighted, agricultural-weighted and forest-weighted concentrations only.

When thinking about a trend, the following should be taken into account: (i) the meteorologically induced variations, (ii) the uncertainties involved in the interpolation (Annex 3), and (iii) the year-to-year variation of the station density and their spatial distribution, which induce a variation in interpolated maps from year to year. In addition, one should be aware of the fact that different trends in various parts of Europe may occur. However, bearing in mind these limitations here a trend analysis is provided for the period 2005-2020 on the population-, agricultural- and forest-weighted concentrations for the total mapping area.

For comparability reasons, in this chapter the results for the total mapped area do not include Türkiye, because 2016 was the first year for which the area of Türkiye was mapped.

6.1 Human health PM_{10} indicators

Table 6.1 summarises the average concentration to which the considered European population has been exposed to over the sixteen-year period 2005-2020 for both human health PM_{10} indicators, expressed as the population-weighted concentration, and the percentage of population exposed to PM_{10} concentrations above limit values (LV), i.e. the annual (ALV) and daily (DLV) limit value, respectively.

For the years 2012 and 2013 both the 36th highest value and the 90.4 percentile of daily mean(s) have been calculated. Their results demonstrate an underestimation of almost 1 µg/m^3 at the 36th highest daily mean. One may conclude that this underestimation is caused by the fact that when calculating the 36th highest daily mean value there is no correction for the missing values at incomplete time series. Whereas the 90.4 percentile of daily means adjusts for such missing data.

As the PM_{10} maps for 2020 (as presented in Chapter 2) have been constructed using the updated methodology as developed and tested in Horálek et al. (2019), the table presents the results for 2015-2019 (and 2005 and 2009, for annual average) both based on the updated and the old methodologies, for comparability reasons.

Table 6.1: Population-weighted concentration and percentage of the considered European population (without Türkiye) exposed to concentrations above the PM_{10} limit values (LV) for the protection of health for 2005 to 2020

PM_{10}		method	2005	2006	2007	2008	2009	2010	2011	2012	2013	2014	2015	2016	2017	2018	2019	2020
Annual average																		
Popul.-weighted concentration	[µg.m^{-3}]	old	28.0	28.9	26.6	25.1	24.6	24.5	25.3	22.9	22.2	21.1	21.2	20.2	20.2	20.1	18.3	
		new	28.6				25.3						21.6	20.5	20.8	20.8	18.7	18.0
Population exposed > ALV (40 µg.m^{-3})	[%]	old	13.3	10.9	7.1	5.9	6.0	5.2	7.2	3.4	2.6	2.0	0.6	1.7	2.9	2.1	0.3	
		new	11.5				6.2						0.7	1.7	3.3	2.4	0.5	0.6
36th highest daily mean / 90.4 percentile of daily means																		
Popul.-weighted conc. [µg.m^{-3}]	36th high.	old	47.4	48.3	44.7	41.9	41.6	42.0	44.9	40.0	38.6							
	90.4 perc.	old								40.8	39.4	37.1	36.9	35.7	36.1	34.5	32.1	
	90.4 perc.	new											37.5	36.1	37.0	35.4	32.8	31.5
Popul. exposed > DLV (50 µg.m^{-3}) [%]	36th high.	old	35.9	37.2	27.6	20.3	17.0	20.8	24.8	16.9	16.4							
	90.4 perc.	old								18.1	17.3	13.3	14.7	14.0	15.8	12.0	7.2	
	90.4 perc.	new											16.2	14.6	17.0	13.2	8.1	9.1

In 2020 the population exposed to annual mean concentrations of PM_{10} above the limit value of 40 µg/m^3 has been 0.6 % of the total population (calculated using the new methodology), which is the second lowest percentage in the sixteen years' time series. Furthermore, it is estimated that the considered European inhabitants have been exposed on average to an annual mean PM_{10} concentration of 18 µg/m^3, the lowest value in the sixteen years' time series. The comparison of results for 2015-2018 illustrates well that a clear decrease in the population-weighted concentration does not lead necessarily to a similar decrease in the percentage of population exposed to concentrations above a certain standard.

In the sixteen-year time series, the percentage of people living in areas with concentrations above the annual LV is lower in the latest eight years (2013-2019) than in the first eight years. The overall picture of the population-weighted annual mean concentration of the whole mapping area (i.e. totals of 40 European countries considered) demonstrates a downward trend of about -0.6 µg/m^3 per year for the years 2005-2020, based on the old mapping method results for 2005-2019 and the new methodology for 2020 (for trend estimation methodology, see Annex 1, Section A1.2). This trend is statistically significant (at the strongest level ***, i.e. 0.001) and expresses a mean decrease of 0.6 µg/m^3 per year.

In 2020 about 9 % of the considered European population have lived in areas where concentrations have been above the PM_{10} daily limit value (calculated using the 90.4 percentile and the new methodology), being the second lowest of the sixteen-year period. The overall population-weighted concentration of the 90.4 percentile of the PM_{10} daily means (formerly the 36th highest daily mean) for the background areas is estimated to be about 32 µg/m^3 in 2020 for the whole mapping area, which is the lowest of the sixteen years considered. This is the case even though the 36th highest daily means (i.e. possibly underestimated data if applied instead of the 90.4 percentiles, see above) have been used in the 2005-2011 calculations. The population-weighted concentrations of the whole mapping area (i.e. total of 40 European countries considered) show a statistically significant (at the strongest level ***, i.e. 0.001) downward trend of about -1.0 µg/m^3 per year for the years 2005-2020, for the daily LV related indicator 90.4 percentile of daily means (formerly the 36th highest daily mean), as calculated based on the old mapping method results for 2005-2019 and the new methodology for 2020.

6.2 Human health $PM_{2.5}$ indicators

Table 6.2 summarises for human health $PM_{2.5}$ indicator (annual average) the population-weighted concentration and the percentage of the considered European population exposed to $PM_{2.5}$ concentrations above the EU LV for the years 2005 to 2020 (without 2006, for which neither a map nor a population exposure was prepared).

As in the case of PM_{10}, the $PM_{2.5}$ maps for 2020 (as presented in Chapter 3) has been constructed using the updated methodology. The table presents the results for 2005, 2009 and 2015-2019 (all the years for which maps using both methods are available) both based on the updated and the old methodology, for comparability reasons.

Table 6.2: Population-weighted concentration and percentage of the considered European population (without Türkiye) exposed to concentrations above the $PM_{2.5}$ limit value (LV) for the protection of health for 2005 to 2020

$PM_{2.5}$		method	###	2006	###	###	###	###	###	###	###	###	###	###	###	###	###	###
Annual average																		
Popul.-weighted concentration	[µg.m^{-3}]	old	18.8	not mapped	16.2	16.4	16.2	16.9	17.8	15.7	15.3	14.1	14.2	13.4	13.6	13.2	11.6	
		new	19.0				16.6						14.3	13.6	13.8	13.5	11.8	11.1
Population exposed > LV (25 µg.m^{-3})	[%]	old			8.2	7.9	7.6	8.3	13.3	9.1	5.8	4.2	6.3	5.4	7.0	4.1	0.9	
		new	16.8				7.6						6.5	5.4	7.2	4.5	1.2	1.1

The percentage of population exposed in 2020 to annual mean concentrations of $PM_{2.5}$ above the LV of 25 µg/m^3 has been 1.1 %, which is the lowest value in the sixteen years' time series. Furthermore, it is estimated that the considered European inhabitants have been exposed on average to an annual mean $PM_{2.5}$ concentration of 11 µg/m^3 in 2020, being again the lowest value in the time series.

The trend analysis of the population-weighted concentrations across the period 2005-2020 for the total mapping area has been executed, based on the old mapping method results for the period 2005-2019 and the new method for 2020. At European scale a statistical significant (at the level ***, i.e. 0.001) downward trend can be observed, estimated to be -0.5 µg/m^3 per year.

6.3 Human health ozone indicators

Table 6.3 summarises the exposure levels of the considered European inhabitants in terms of population-weighted concentrations for both human health ozone indicators. Furthermore, it presents the percentage of considered European population exposed to concentrations above the target value (TV) and above a level of 6 000 µg/m^3·d for the SOMO35 for the years 2005 to 2020.

Table 6.3: Population-weighted concentration and percentage of the considered European population (without Türkiye) exposed to concentrations above the target value (TV) threshold for the protection of health and a SOMO35 threshold of 6 000 µg/m^3·d for 2005 to 2020

Ozone		2005	2006	2007	2008	2009	2010	2011	2012	2013	2014	2015	2016	2017	2018	2019	2020
26th highest daily max. 8-h mean / 93.2 percentile of daily max. 8-h means																	
Pop.-weighted conc. [µg.m^{-3}]	26th high.	111.4	117.6	110.0	109.4	107.7	106.5	108.4	107.3	108.3							
Pop.-weighted conc. [µg.m^{-3}]	93.2 perc.								107.9	108.9	102.9	110.4	104.8	105.0	114.4	109.9	107.3
Pop. exp. > TV (120 µg.m^{-3})	26th high.	29.5	49.8	24.9	13.6	14.9	15.8	15.0	19.0	15.0							
Pop. exp. > TV (120 µg.m^{-3})	93.2 perc.								20.2	15.9	5.6	34.0	8.4	12.9	34.8	20.3	7.4
SOMO35																	
Pop.-weighted concentration	[µg.m^{-3}.d]	4622	5045	4291	4164	4233	3850	4318	4174	4089	3500	4312	3619	3890	4962	4478	3945
Pop. exposed > 6000 µg.m^{-}	[%]	26.8	27.1	26.3	17.0	23.2	15.9	22.0	23.2	18.8	9.4	22.2	11.7	19.1	31.3	20.0	8.6

For 2012 and 2013, both the 26th highest value and the 93.2nd percentile of maximum daily 8-hour mean(s) have been calculated. It demonstrates an underestimation of about 0.6 µg/m^3 at the 26th maximum daily 8-hour mean, which is caused by the fact that when calculating this indicator there is no correction for the missing values in the incomplete measurement time series.

Using the 93.2 percentile of ozone maximum daily 8-hour means it is estimated that 7 % of the population have lived in 2020 in areas where concentrations were above the ozone target value (TV) threshold of 120 µg/m^3, which is the second lowest number of the sixteen-year period. The overall population-weighted ozone concentration in terms of the 93.2 percentile maximum daily 8-hour means in the background areas is estimated at about 107 µg/m^3 for the total mapping area, which is the fifth lowest value of the whole sixteen-year period (it should be noted that for 2005-2011 the 26th highest value of the maximum daily eight-hour mean was considered instead).

Examining the time series for 2005-2020, it can be concluded that 2006, but also 2005, 2015 and 2018 are exceptional years with high ozone concentrations, leading to increased exposure levels compared to the other twelve years. The years 2014, 2016, 2017 and 2020 show the lowest exposure levels in the sixteen years' time series for the 93.2 percentile of the maximum daily 8-hour means.

The trend analysis of the population-weighted concentrations for the 93.2 percentile of the maximum daily 8-hour means across the period 2005-2020 for the total mapping area (i.e. totals of 40 European countries considered) does not estimate a statistically significant trend. The reason is in the ozone variability, which correlates with warm and dry summers.

A similar tendency is observed for SOMO35. In 2005-2007, a bit more than one-fourth of the population has lived in areas where a level of 6 000 µg/m^3·d ([6]) has been exceeded, with the highest level in 2006. In the period of 2008-2019, it fluctuated from about 16 % to 23 % of the population, except 2014 with about 9 %, 2016 with about 12 %, and 2018 with about one-third of the population.

([6]) Note that the 6 000 µg/m^3·d does not represent a health-related legally binding 'threshold'. In this and previous papers it represents a somewhat arbitrarily chosen threshold to facilitate the discussion of the observed distributions of SOMO35 levels in their spatial and temporal context. For motivation of this choice, see Section 4.2.

The population-weighted SOMO35 concentrations show the lowest value in 2020. Trend analysis on the population-weighted concentration for the total mapping area shows no trend for the period 2005-2020. The reason is the same as in the case of the 93.2 percentile of the maximum daily 8-hour means.

6.4 Vegetation related ozone indicators

Exposure indicators describing the agricultural and forest areas exposed to accumulated ozone concentrations above defined thresholds are summarised in Table 6.4. Those thresholds are the target value (TV) threshold of 18 000 µg/m^3·h and the long-term objective (LTO) of 6 000 µg/m^3·h for the AOT40 for vegetation, and the former reporting value (RV) of 20 000 µg/m^3·h and the critical level (CL) of 10 000 µg/m^3·h for the AOT40 for forests.

Table 6.4: Percentages of the considered European agricultural and forest area (without Türkiye) exposed to ozone concentrations above the target value (TV) threshold and the long-term objective (LTO) for AOT40 for vegetation, and above critical level (CL) and reporting value (RV) for AOT40 for forests and agricultural- and forest-weighted concentrations for 2005 to 2020

Ozone	2005	2006	2007	2008	2009	2010	2011	2012	2013	2014	2015	2016	2017	2018	2019	2020
AOT40 for vegetation																
Agricult. area exp. > TV (18 000 µg/m^3·h [%]	48.5	69.1	35.7	37.8	26.0	21.3	19.2	30.0	22.1	17.8	31.4	14.7	23.8	39.7	29.7	3.0
Agricult. area exp. > LTO (6 000 µg/m^3·h [%]	88.8	97.6	77.5	95.5	81.0	85.4	87.9	86.4	81.0	85.5	79.7	74.1	73.4	95.1	84.0	71.0
Agricultural-weighted concentr. [µg/m^3·h]	17481	22344	14597	15214	13157	13310	13255	14041	12838	12427	14223	10942	11750	16311	13735	8544
AOT40 for forests																
Forest area exp. > RV (20 000 µg/m^3·h [%]	59.1	69.4	48.4	50.2	49.2	49.3	53.0	47.2	44.1	37.7	52.4	41.9	38.9	56.1	51.4	34.4
Forest area exp. > CL (10 000 µg/m^3·h [%]	76.4	99.8	62.1	79.6	67.4	63.4	68.6	65.0	67.2	68.2	59.8	60.0	55.4	86.7	84.0	58.0
Forest-weighted concentration [µg/m^3·h]	25900	31154	23744	21951	23532	19625	21892	21580	21753	17124	21150	17573	16798	25397	22343	14584

In 2020, some 3 % of all agricultural land (crops) has been exposed to accumulated ozone concentrations (AOT40 for vegetation) above the target value (TV) threshold, which is the lowest value in the sixteen-year time series. About 71 % of all agricultural land has been exposed to levels in excess of the long-term objective (LTO), which is also the lowest values in the sixteen-year period.

The trend analysis of the agricultural-weighted concentrations for the AOT40 for vegetation across the period 2005-2020 for the total mapping area (i.e. totals of 40 European countries considered) does not estimate any statistically significant trend, even though the 2020 value (8544 µg/m^3.h) is the lowest in the sixteen-years period.

For the ozone indicator AOT40 for forests, the level of 20 000 µg/m^3·h (earlier used reporting value, RV) has been exceeded in about 34 % of the considered European forest area in 2020, which is the lowest value of the whole time series. The forest area exceeding the CL has been in 2020 about 58 %, which is the second lowest percentage of the sixteen-year period. The temporal pattern of the concentrations above the AOT40 for forests CL shows some similarity with those of the AOT40 for vegetation, despite their different definitions and receptors and their natural difference in area type characteristics and occurrence. Their annual variability is, however, heavily dependent on meteorological variability.

The trend analysis of the forest-weighted concentrations for the AOT40 for forests across the period 2005-2020 for the total mapping area (i.e. totals of 40 European countries considered) shows no statistically significant trend, although again the 2020 value is the lowest in the series. The reason again is in the ozone variability correlated with the variability of meteorology,

6.5 Human health NO_2 indicators

Table 6.5 summarises the development in exposure levels of the considered European population for the human health NO_2 indicator (annual average), in terms of population-weighted concentrations and percentage of population exposed to concentrations above the annual LV (40 µg/m^3), for the years 2005, 2009, 2010 and 2013 to 2020, for which the maps based on the current methodology are available. The population-weighted concentration is presented additionally also for 2007, although based on different mapping methodology than the other years. This 2007 value is probably slightly underestimated; based on Horálek et al. (2017b), one can suppose the true value would be of about 1 % higher (i.e. it would be about 23.5 µg/m^3).

Table 6.5: Population-weighted concentration and percentage of the considered European population (without Türkiye) exposed to concentrations above the NO_2 limit value (LV) of 40 µg/m^3 for the protection of health for 2005 to 2020

NO_2	2005	2006	2007	2008	2009	2010	2011	2012	2013	2014	2015	2016	2017	2018	2019	2020
Annual average																
Popul.-weighted concent[µg.m^{-3}	23.3	not mapped	23.3	not mapped	22.1	22.1	not mapped		19.4	18.6	18.8	18.6	18.4	17.6	16.8	14.0
Pop. exp. > LV (40 µg.m^{-3} [%]	7.9				5.6	4.9			3.2	2.8	3.2	2.8	3.0	1.8	1.3	0.2

In 2020 the population exposed to NO_2 annual mean concentrations above the limit value of 40 µg/m^3 has been 0.2 % of the total population, which is the lowest in the whole series. Furthermore, it is estimated that considered European inhabitants have been exposed on average to an annual mean NO_2 concentration of 14 µg/m^3, again the lowest in the whole series. The main reason for this probably is the lockdown measures connected with the COVID-19 pandemic.

Trend analysis on the population-weighted concentration for the total mapping area shows a slight downward trend of about -0.5 µg/m^3 per year, for the period 2005-2020, which is statistically significant (at the highest level ***, i.e. 0.001).

List of abbreviations

Abbreviation	Name	Reference
ALV	Annual Limit Value	
AOT40	Accumulated Ozone exposure over a Threshold of 40 ppb (i.e. 80 µg/m³) in a specific period	http://eur-lex.europa.eu/LexUriServ/LexUriServ.do?uri=OJ:L:2008:152:0001:0044:EN:PDF
AQ	Air Quality	
CL	Critical Level	https://icpvegetation.ceh.ac.uk/chapter-3-mapping-critical-levels-vegetation
CLC	CORINE Land Cover	https://land.copernicus.eu/pan-european/corine-land-cover
CLRTAP	Convention on Long-range Transboundary Air Pollution (Air Convention)	https://unece.org/environment-policy/air
CORINE	Co-ORdinated INformation on the Environment	https://land.copernicus.eu/pan-european/corine-land-cover
CTM	Chemical Transport Model	
CSI	Core Set of Indicators	https://www.eea.europa.eu/ims
Defra	UK Department for Environment Food & Rural Affairs	
DLV	Daily Limit Value	
ECMWF	European Centre for Medium-Range Weather Forecasts	https://www.ecmwf.int/
EBAS	EMEP dataBASe	https://ebas.nilu.no/
EEA	European Environment Agency	www.eea.europa.eu
EMEP	European Monitoring and Evaluation Programme	https://www.emep.int/
ETC/ACM	European Topic Centre on Air pollution and Climate change Mitigation	https://www.eionet.europa.eu/etcs
ETC/ATNI	European Topic Centre on Air pollution, Noise, Transport and Industrial pollution	https://www.eionet.europa.eu/etcs
ETC HE	European Topic Centre on Human Health and the Environment	https://www.eionet.europa.eu/etcs
EU	European Union	https://european-union.europa.eu
GMTED	Global Multi-resolution Terrain Elevation Data	
GRIP	Global Roads Inventory Dataset	
HLV	Hourly Limit Value	
ICP	International scientific Cooperative Programme	https://icpvegetation.ceh.ac.uk/
ILV	Indicative Limit Value	
JRC	Joint Research Centre	https://ec.europa.eu/info/departments/joint-research-centre_en

Abbreviation	Name	Reference
LV	Limit Value	http://eur-lex.europa.eu/LexUriServ/LexUriServ.do?uri=OJ:L:2008:152:0001:0044:EN:PDF
NILU	Norwegian Institute for Air Research	https://www.nilu.no/
NO_2	Nitrogen dioxide	
NO_x	Nitrogen oxides	
O_3	Ozone	
ORNL	Oak Ridge National Laboratory	https://www.ornl.gov/
PLA	Projected Leaf Area	https://icpvegetation.ceh.ac.uk/chapter-3-mapping-critical-levels-vegetation
PM_{10}	Particulate Matter with a diameter of 10 micrometres or less	
$PM_{2.5}$	Particulate Matter with a diameter of 2.5 micrometres or less	
POD_6	Phytotoxic Ozone Doze above a threshold of 6 nmol/m^2 PLA s^{-1}	https://icpvegetation.ceh.ac.uk/chapter-3-mapping-critical-levels-vegetation
R^2	Coefficient of determination	
RIMM	Regression – Interpolation – Merging Mapping	
RMSE	Root Mean Square Error	
SOMO10	Sum of Ozone Maximum daily 8-hour means Over 10 ppb (i.e. 20 µg/m^3)	
SOMO35	Sum of Ozone Maximum daily 8-hour means Over 35 ppb (i.e. 70 µg/m^3)	
TV	Target Value	http://eur-lex.europa.eu/LexUriServ/LexUriServ.do?uri=OJ:L:2008:152:0001:0044:EN:PDF
UN	United Nations	https://www.un.org
UNECE	United Nations Economic Commission for Europe	https://unece.org/
UTC	Coordinated Universal Time	
WHO	World Health Organization	https://www.who.int/

References

Alonso, R., et al., 2014, 'Drought stress does not protect Quercus ilex L. from ozone effects: results from a comparative study of two subspecies differing in ozone sensitivity', *Plant Biology 16*, pp. 375-384 (https://onlinelibrary.wiley.com/doi/10.1111/plb.12073) accessed 21 January 2021.

Ashmore, M., et al., H., 2004, 'New directions: a new generation of ozone critical levels for the protection of vegetation in Europe', *Atmospheric Environment* 38, pp. 2213-2214 (https://doi.org/10.1016/j.atmosenv.2004.02.029) accessed 20 November 2020.

Brancher, M., 2021, 'Increased ozone pollution alongside reduced nitrogen dioxide concentrations during Vienna's first COVID-19 lockdown: Significance for air quality management', *Environmental Pollution* 284, p. 117153 (https://doi.org/10.1016/j.envpol.2021.117153) accessed 16 February 2021.

CLRTAP, 2016, *Forest condition in Europe*, 2016 Technical Report of ICP Forests, UNECE Convention on Long-range Transboundary Air Pollution (https://www.icp-forests.org/pdf/TR2016.pdf) accessed 19 November 2020.

CLRTAP, 2017a, *Manual for modelling and mapping critical loads & levels. Chapter III: "Mapping Critical levels for Vegetation"*, UNECE Convention on Long-range Transboundary Air Pollution (https://icpvegetation.ceh.ac.uk/chapter-3-mapping-critical-levels-vegetation) accessed 7 May 2021.

CLRTAP, 2017b, *Scientific Background Document A of Chapter 3 of "Manual on methodologies and criteria for modelling and mapping critical loads and levels of air pollution effects, risks and trends"* (https://icpvegetation.ceh.ac.uk/sites/default/files/ScientificBackgroundDocumentAOct2018.pdf) accessed 11 December 2020.

CLRTAP, 2020, *Scientific Background Document B of Chapter 3 of "Manual on methodologies and criteria for modelling and mapping critical loads and levels of air pollution effects, risks and trends"* (https://icpvegetation.ceh.ac.uk/sites/default/files/Scientific%20Background%20document%20B%20June%202020.pdf) accessed 11 December 2020.

CLRTAP, 2022, *ICP Vegetation: Review of NOx critical levels, full workshop report* (https://icpvegetation.ceh.ac.uk/sites/default/files/NOx_critical_levels_workshop_REPORT.pdf) accessed 22 November 2022.

Colette, A., et al., 2018, *Long term evolution of the impacts of ozone air pollution on agricultural yields in Europe. A modelling analysis for the 1990-2010 period*, Eionet Report ETC/ACM 2018/15 (https://www.eionet.europa.eu/etcs/etc-atni/products/etc-atni-reports/eionet_rep_etcacm_2018_15_o3impacttrends) accessed 26 August 2020.

Cressie, N., 1993, *Statistics for spatial data,* Wiley series, New York.

Danielson, J. J. and Gesch, D. B., 2011, Global multi-resolution terrain elevation data 2010 (GMTED2010), *U.S. Geological Survey Open-File Report*, pp. 2011-1073 (https://pubs.er.usgs.gov/publication/ofr20111073) accessed 19 November 2020.

Defra, 2022, *UK Air information resource, Data archive*, UK Department for Environment Food & Rural Affairs (https://uk-air.defra.gov.uk/data/) assessed 26 August 2022.

de Leeuw, F., 2012, *AirBase: a valuable tool in air quality assessments at a European and local level,* ETC/ACM Technical Paper 2012/4 (http://www.eionet.europa.eu/etcs/etc-atni/products/etc-atni-reports/etcacm_tp_2012_4_airbase_aqassessment) accessed 26 August 2020.

de Leeuw, F. and Ruyssenaars, R., 2011, *Evaluation of current limit and target values as set in the EU Air Quality Directive*, ETC/ACM Technical Paper 2011/3 (https://www.eionet.europa.eu/etcs/etc-atni/products/etc-atni-reports/etcacm_tp_2011_3_evaluationaq_lv_lt) accessed 22 September 2022.

Denby, B., et al., 2008, 'Comparison of two data assimilation methods for assessing PM_{10} exceedances on the European scale', *Atmospheric Environment* 42, pp. 7122-7134 (https://doi.org/10.1016/j.atmosenv.2008.05.058) accessed 26 August 2020.

Denby, B., et al., 2011, *Mapping annual mean $PM_{2.5}$ concentrations in Europe: application of pseudo $PM_{2.5}$ station data*, ETC/ACM Technical Paper 2011/5 (http://www.eionet.europa.eu/etcs/etc-atni/products/etc-atni-reports/etcacm_tp_2011_5_spatialpm2-5mapping) accessed 26 August 2020.

de Smet, P., et al., 2011, *European air quality maps of ozone and PM_{10} for 2008 and their uncertainty analysis*, ETC/ACC Technical Paper 2010/10 (http://www.eionet.europa.eu/etcs/etc-atni/products/etc-atni-reports/etcacc_tp_2010_10_spataqmaps_2008) accessed 26 August 2020.

Deumier, J. M. and Hannon, C., 2010, 'La période d' initiation de la tubérisation: comment la repérer?' (in French), CNIPT (http://www.cnipt.fr/wp-content/uploads/2013/10/Irrigation-juin-2010.pdf) accessed 8 February 2021.

EC, 2004, *Directive 2004/107/EC of the European Parliament and of the Council of 15 December 2004 relating to arsenic, cadmium, mercury, nickel and polycyclic aromatic hydrocarbons in ambient air*, OJ L 23, 26.1.2005, 3-16 (https://eur-lex.europa.eu/legalcontent/EN/TXT/PDF/?uri=CELEX:32004L0107&from=EN) accessed 10 June 2022.

EC, 2008, *Directive 2008/50/EC of the European Parliament and of the Council of 21 May 2008 on ambient air quality and cleaner air for Europe,* OJ L 152, 11.06.2008, 1-44 (http://eur-lex.europa.eu/LexUriServ/LexUriServ.do?uri=OJ:L:2008:152:0001:0044:EN:PDF) accessed 26 May 2021.

EC, 2021, *The tomato market in the EU: Vol. 1: Production statistics* (https://agriculture.ec.europa.eu/data-and-analysis/markets/overviews/market-observatories/fruit-and-vegetables/tomatoes-statistics_en) accessed 6 December 2022.

ECMWF, 2020, *European State of the Climate 2020*, Copernicus Climate Change Service, Full report (https://climate.copernicus.eu/ESOTC/2020) accessed 13 October 2021.

EEA, 2010, *ORNL Landscan 2008 Global Population Data conversion into EEA ETRS89-LAEA5210 1km grid* (by Hermann Peifer of EEA) (https://sdi.eea.europa.eu/catalogue/geoss/api/records/1d68d314-d07c-4205-8852-f74b364cd699) accessed 26 August 2020.

EEA, 2018, *Guide for EEA map layout. EEA operational guidelines*, January 2015, version 5 (https://www.eionet.europa.eu/gis/docs/GISguide_v5_EEA_Layout_for_map_production.pdf) accessed 26 August 2020.

EEA, 2019, *Healthy environment, healthy lives: how the environment influences health and well-being in Europe*, EEA Report 21/2019 (https://www.eea.europa.eu/publications/healthy-environment-healthy-lives) accessed 2 June 2021.

EEA, 2020, *Air quality in Europe – 2020*, EEA Report 09/2020 (https://www.eea.europa.eu/publications/air-quality-in-europe-2020-report) accessed 16 June 2022.

EEA, 2022a, *Air Quality e-Reporting. Air quality database (*https://www.eea.europa.eu/data-and-maps/data/aqereporting-8). Data extracted in March 2022.

EEA, 2022b, *Exposure of Europe's ecosystems to ozone* (https://www.eea.europa.eu/ims/exposure-of-europes-ecosystems-to-ozone) accessed 13 September 2022.

Emberson, L. D., et al., 2000, 'Modelling stomatal ozone flux across Europe', *Environmental Pollution* 109, pp. 403-413 (https://doi.org/10.1016/S0269-7491(00)00043-9) accessed 26 May 2021.

EMEP, 2022, *Data of HMs and POPs for the EMEP region*, Meteorological Synthetizing Centre – East (MCS-E) (https://www.msceast.org/index.php/pollution-assessment/emep-domain-menu/data-hm-pop-menu) accessed 30 September 2022.

ESA, 2019, *Land cover classification gridded maps from 1992 to present derived from satellite observations* (https://cds.climate.copernicus.eu/cdsapp#!/dataset/satellite-land-cover) accessed 17 February 2021.

EU, 2020, *Corine land cover 2018 (CLC2018) raster data*, 100x100m^2 gridded version 2020_20 (https://land.copernicus.eu/pan-european/corine-land-cover/clc2018) accessed 19 November 2020.

Eurostat, 2014, *GEOSTAT 2011 grid dataset*, Population distribution dataset (http://ec.europa.eu/eurostat/web/gisco/geodata/reference-data/population-distribution-demography) accessed 26 August 2020.

Eurostat, 2021, *Total population for European states for 2020* (https://ec.europa.eu/eurostat/web/main/data/database) accessed 29 August 2022.

Gilbert, R. O., 1987, *Statistical Methods for Environmental Pollution Monitoring*, Van Nostrand Reinhold, New York.

Gusev, A., et al., 2005, *Regional Multicompartment Model MSCE-POP*, EMEP/MSC-E Technical Report 5/2005 (http://www.msceast.org/reports/5_2005.pdf) accessed 9 December 2021.

Gusev, A., et al., 2006, *Progress in further development of MSCE-HM and MSCE-POP models (implementation of the model review recommendations*, EMEP/MSC-E Technical Report 4/2006 (http://www.msceast.org/reports/4_2006.pdf) accessed 10 December 2021.

Haberle, J. and Svoboda, P., 2015, 'Calculation of available water supply in crop root zone and the water balance of crop's, *Contributions to Geophysics and Geodesy* 45, pp. 285-298 (https://www.researchgate.net/publication/293194127_Calculation_of_available_water_supply_in_crop_root_zone_and_the_water_balance_of_crops) accessed 21 January 2021.

Horálek, J., et. al., 2007, *Spatial mapping of air quality for European scale assessment*, ETC/ACC Technical paper 2006/6 (http://www.eionet.europa.eu/etcs/etc-atni/products/etc-atni-reports/etcacc_technpaper_2006_6_spat_aq) accessed 26 August 2020.

Horálek, J., et. al., 2008, *European air quality maps for 2005 including uncertainty analysis*, ETC/ACC Technical paper 2007/7 (http://www.eionet.europa.eu/etcs/etc-atni/products/etc-atni-reports/etcacc_tp_2007_7_spataqmaps_ann_interpol) accessed 26 August 2020.

Horálek, J., et. al., 2016, *Application of FAIRMODE Delta tool to evaluate interpolated European air quality maps for 2012*, ETC/ACM Technical Paper 2015/2 (http://www.eionet.europa.eu/etcs/etc-atni/products/etc-atni-reports/etcacm_tp_2015_2_delta_evaluation_aqmaps2012) accessed 26 August 2020.

Horálek, J., et. al., 2017a, *European air quality maps for 2014*, ETC/ACM Technical Paper 2016/6 (https://www.eionet.europa.eu/etcs/etc-atni/products/etc-atni-reports/etcacm_tp_2016_6_aqmaps2014) accessed 30 September 2022.

Horálek, J., et. al., 2017b, *Inclusion of land cover and traffic data in NO_2 mapping methodology*, ETC/ACM Technical Paper 2016/12 (http://www.eionet.europa.eu/etcs/etc-atni/products/etc-atni-reports/etcacm_tp_2016_12_lc_and_traffic_data_in_no2_mapping) accessed 27 May 2021.

Horálek, J., et. al., 2018, *Satellite data inclusion and kernel based potential improvements in NO_2 mapping*, ETC/ACM Technical Paper 2017/14 (http://www.eionet.europa.eu/etcs/etc-atni/products/etc-atni-reports/etcacm_tp_2017_14_improved_aq_no2mapping) accessed 27 May 2021.

Horálek, J., et. al., 2019, *Land cover and traffic data inclusion in PM mapping*, Eionet Report ETC/ACM 2018/18 (http://www.eionet.europa.eu/etcs/etc-atni/products/etc-atni-reports/etc-acm-report-18-2018-land-cover-and-traffic-data-inclusion-in-pm-mapping) accessed 27 May 2021.

Horálek, J., et al., 2021, *Potential use of CAMS modelling results in air quality mapping under ETC/ATNI*, Eionet Report ETC/ATNI 2019/17 (https://doi.org/10.5281/zenodo.4627762) accessed 15 June 2021.

Horálek, J., et. al., 2022a, *European air quality maps for 2019*, Eionet Report ETC/ATNI 2021/1 (https://doi.org/10.5281/zenodo.6241308) accessed 13 June 2022.

Horálek, J., et al., 2022b, *Benzo(a)pyrene (BaP) annual mapping*, Eionet Report ETC/ATNI 2021/18 (https://doi.org/10.5281/zenodo.5898376) accessed 26 August 2022.

Horálek, J., et al., 2022c, *Interim European air quality maps for 2020*, Eionet Report ETC/ATNI 2021/19 (https://doi.org/10.5281/zenodo.6397268) accessed 16 June 2022.

Jarvis, P. G., 1976, 'The interpretation of the variation in leaf water potential and stomatal conductance found in canopies in the field', Philosophical Transactions of the Royal Society of London, Series B: *Biological Sciences 273*, pp. 593-610 (https://doi.org/10.1098/rstb.1976.0035) accessed 26 May 2021.

JRC, 2009, *Population density disaggregated with Corine land cover 2000,* 100x100 m^2 grid resolution, EEA version (http://www.eea.europa.eu/data-and-maps/data/population-density-disaggregated-with-corine-land-cover-2000-2) accessed 26 August 2020.

JRC, 2016, *Maps of indicators of soil hydraulic properties for Europe*, dataset/maps downloaded from the European Soil Data Centre (http://esdac.jrc.ec.europa.eu/content/maps-indicators-soil-hydraulic-properties-europe) accessed 8 December 2020.

Krupa, S., et al., 2000, 'Ambient ozone and plant health', *Plant Disease* 85, pp. 4-12 (https://apsjournals.apsnet.org/doi/pdf/10.1094/pdis.2001.85.1.4) accessed 8 December 2020.

Kuenen, J. J. P., et al., 2014, 'TNO-MACC_II emission inventory; a multi-year (2003-2009) consistent high-resolution European emission inventory for air quality modelling', *Atmospheric Chemistry and Physics* 14, pp. 10963–10976 (https://doi.org/10.5194/acp-14-10963-2014) accessed 16 February 2021.

Marécal, V., et al., 2015, 'A regional air quality forecasting system over Europe: The MACC-II daily ensemble production', *Geoscientific Model Development* 8, pp. 2777–2813 (https://doi.org/10.5194/gmd-8-2777-2015) accesed 16 February 2021.

MDA, 2015, *World Land Cover at 30m resolution from MDAUS BaseVue 2013* (https://www.arcgis.com/home/item.html?id=1770449f11df418db482a14df4ac26eb) accessed 17 February 2021.

Meijer, J. R., et al., 2018, 'Global patterns of current and future road infrastructure', *Environmental Research Letters* 13, 0640 (https://doi.org/10.1088/1748-9326/aabd42) accessed 10 June 2019.

Mills, G., et al., 2011, 'New stomatal flux-based critical levels for ozone effects on vegetation', *Atmospheric Environment* 45, pp. 5064-5068 (https://doi.org/10.1016/j.atmosenv.2011.06.009) accessed 19 November 2020.

Musselman, R. C. and Massman, W. J., 1998, 'Ozone flux to vegetation and its relationship to plant response and ambient air quality standards', *Atmospheric Environment* 33, pp. 65-73 (https://doi.org/10.1016/S1352-2310(98)00127-7) accessed 26 May 2021.

NILU, 2022, *EBAS, database of atmospheric chemical composition and physical properties* (http://ebas.nilu.no) accessed 11 April 2022.

Nussbaum, S., et al., 2003, 'High-resolution spatial analysis of stomatal ozone uptake in arable crops and pastures', *Environmental International* 129, pp. 385-392 (https://www.ncbi.nlm.nih.gov/pubmed/12676231) accessed 26 May 2021.

Pedersen, S. M., et al., 2005, *Potato production in Europe - a gross margin analysis*, University of Copenhagen, FOI WorkingPaper Vol. 2005 No. 5, pp. 1-39 (https://curis.ku.dk/ws/files/135440168/5.pdf) accessed 26 May 2021.

Pleijel, H., et al., 2007, 'Ozone risk assessment for agricultural crops in Europe: Further development of stomatal flux and flux-response relationships for European wheat and potato', *Atmospheric Environment* 41, pp.3022-3040 (https://doi.org/10.1016/j.atmosenv.2006.12.002) accessed 8 December 2020.

Reich, P. B., 1987, 'Quantifying plant response to ozone: a unifying theory', *Tree Physiology* 3, pp. 63-91 (https://doi.org/10.1093/treephys/3.1.63) accessed 19 November 2020.

Sicard, P., et al., 2020, 'Amplified ozone pollution in cities during the COVID-19 lockdown', *Science of The Total Environment* 735, p. 139542 (https://doi.org/10.1016/j.scitotenv.2020.139542) accessed 19 August 2021.

Simpson, D., et al., 2012, 'The EMEP MSC-W chemical transport model – technical description', *Atmospheric Chemistry and Physics* 12, pp. 7825-7865 (https://doi.org/10.5194/acp-12-7825-2012) accessed 26 August 2020.

Targa, J., et al., 2022, *Status report of air quality in Europe for year 2020, using validated data*, Eionet Report ETC HE 2022/2 (https://www.eionet.europa.eu/etcs/etc-he/products/etc-he-products/etc-he-reports/etc-he-report-2022-2-status-report-of-air-quality-in-europe-for-year-2020-using-validated-data) accessed 22 November 2022.

Tobías, A., et al., 2020, 'Changes in air quality during the lockdown in Barcelona (Spain) one month into the SARS-CoV-2 epidemic', *Science of Total Environment* 726, 138540 (https://doi.org/10.1016/j.scitotenv.2020.138540) accessed 19 August 2021.

UN, 2020, *World Population Prospects 2019*, United Nations, Department of Economic and Social Affairs, Population Division (https://population.un.org/wpp/Download/Standard/Population/) accessed 19 May 2021.

van Geffen, J., et al., 2019, 'TROPOMI ATBD of the total and tropospheric NO_2 data products', KNMI (https://sentinel.esa.int/documents/247904/2476257/Sentinel-5P-TROPOMI-ATBD-NO2-data-products) accessed 30 August 2021.

van Geffen, J., et al., 2020, 'S5P TROPOMI NO_2 slant column retrieval: Method, stability, uncertainties and comparisons with OMI', *Atmospheric Measurement Techniques* 13, pp. 1315–1335 (https://doi.org/10.5194/amt-13-1315-2020) accessed 30 August 2021.

Veefkind, J. P., et al., 2012. 'TROPOMI on the ESA Sentinel-5 Precursor: A GMES mission for global observations of the atmospheric composition for climate, air quality and ozone layer applications', *Remote Sensing of Environment* 120, pp. 70–83 (https://doi.org/10.1016/j.rse.2011.09.027) accessed 30 August 2021.

WHO, 2005, *WHO Air quality guidelines for particulate matters, ozone, nitrogen dioxide and sulphur dioxide, Global update 2005,* World Health Organization (https://apps.who.int/iris/handle/10665/107823) accessed 16 November 2022.

WHO, 2010, *Human health effects of polycyclic aromatic hydrocarbons as ambient air pollutants* (https://apps.who.int/iris/handle/10665/260127) accessed 22 September 2022.

WHO, 2013, *Review of evidence on health aspects of air pollution: REVIHAAP project: technical report,* World Health Organization (https://apps.who.int/iris/handle/10665/341712) accessed 16 November 2022.

WHO, 2021a, *WHO global air quality guidelines: particulate matter ($PM_{2.5}$ and PM_{10}), ozone, nitrogen dioxide, sulfur dioxide and carbon monoxide*, World Health Organization (https://apps.who.int/iris/handle/10665/345329) accessed 10 December 2021.

WHO, 2021b, Human health effects of polycyclic aromatic hydrocarbons as ambient air pollutants (https://apps.who.int/iris/bitstream/handle/10665/350636/9789289056533-eng.pdf?sequence=1&isAllowed=y) accessed 22 September 2022.

Annex 1
Methodology

A1.1 Mapping methodology

Previous mapping reports like Horálek et al. (2007, 2010, 2017b, 2018, 2019, 2022c), de Smet et al. (2011) and Denby et al. (2011) discuss methodological developments and details on spatial interpolations and their uncertainties. No changes took place in the mapping methodology compared to the preceding report (Horálek et al., 2022a). The only change is an addition of the BaP mapping, in agreement with Horálek et al. (2022c). This annex summarizes the currently applied method for all the considered indicators. The mapping method has been evaluated with the FAIRMODE Delta tool in Horálek et al. (2016). The method is called the *Regression – Interpolation – Merging Mapping* (RIMM).

Pseudo $PM_{2.5}$, NO_x and BaP station data estimation

To supplement $PM_{2.5}$ measurement data, in the mapping procedure data from so-called pseudo $PM_{2.5}$ stations are also used. These data are the estimates of $PM_{2.5}$ concentrations at the locations of PM_{10} stations with no $PM_{2.5}$ measurement. These estimates are based on PM_{10} measurement data and different supplementary data, using linear regression:

$$\hat{Z}_{PM_{2.5}}(s) = c + b.Z_{PM_{10}}(s) + a_1X_1(s) + a_2X_2(s) + \cdots + a_nX_n(s) \qquad \text{(A1.1)}$$

where $\hat{Z}_{PM_{2.5}}(s)$ is the estimated value of $PM_{2.5}$ at the station *s*,
$Z_{PM_{10}}(s)$ is the measurement value of PM_{10} at the station *s*,
$c, b, a_1,\ldots, a_n$ are the parameters of the linear regression model calculated based on the data at the points of stations with both $PM_{2.5}$ and PM_{10} measurements,
$X_1(s),\ldots, X_n(s)$ are the values of other supplementary variables at the station *s*,
n is the number of other supplementary variables used in the linear regression.

When applying this estimation method, all background stations (either classified as rural, urban or suburban) are handled together for estimating $PM_{2.5}$ values at background pseudo stations. For details, see Denby et al. (2011). For estimating $PM_{2.5}$ values at urban traffic pseudo stations, Equation A1.1 is applied for the urban traffic stations. For details, see by Horálek et al. (2019).

To supplement NO_x measurement data, NO_x values are estimated at locations of NO_2 stations with no NO_x data. The estimates are calculated similarly as in Horálek et al. (2007), using regression:

$$\hat{Z}_{NO_x}(s) = a_1Z_{NO_2}(s)^2 + a_2Z_{NO_2}(s) + c \qquad \text{(A1.2)}$$

where $\hat{Z}_{NO_x}(s)$ is the estimated value of NO_x at the station s,
$Z_{NO_2}(s)$ is the measurement value of NO_2 at the station s,
a_1, a_2, c are the parameters of the regression calculated based on the data at the points of measuring stations with both NO_x and NO_2 measurements.

To supplement BaP measurement data, BaP concentrations are estimated at the locations with $PM_{2.5}$ data with no BaP measurement. These estimates are based on $PM_{2.5}$ measurement data (or $PM_{2.5}$ pseudo stations data) and different supplementary data, using exponential regression:

$$\hat{Z}_{BaP}(s) = \exp(c + b.Z_{PM_{2.5}}(s) + a_1X_1(s) + a_2X_2(s) + \cdots + a_{\mathrm{n}}X_{\mathrm{n}}(s)) \qquad \text{(A1.3)}$$

where $\hat{Z}_{BaP}(s)$ is the estimated value of BaP at the station *s*,
$Z_{PM_{2.5}}(s)$ is the measurement (or estimated) value of $PM_{2.5}$ at the station *s*,
$c, b, a_1,\ldots, a_n$ are the parameters of the linear regression model calculated based on the data at the points of stations with both BaP and $PM_{2.5}$ measurements,
$X_1(s),\ldots, X_n(s)$ are the values of other supplementary variables at the station *s*,
n is the number of other supplementary variables used in the linear regression.

When applying this estimation, all background stations (either classified as rural, urban or suburban) are handled together for estimating BaP values at background pseudo stations. The reason for introducing the exponential regression is the exponential relation between BaP and $PM_{2.5}$. In agreement with Horálek et al. (2022c), the pseudo BaP data are calculated in areas which the lack of BaP data only (see Annex 3, Section A3.5). The estimates are calculated primarily for the locations with $PM_{2.5}$ measurement with no BaP measurements. In the limited areas with lack of both BaP and $PM_{2.5}$ measurements, the pseudo $PM_{2.5}$ data (see Eq. A1.1) are used for locations with PM_{10} measurements.

Interpolation

The mapping method used is a linear regression model followed by kriging of the residuals produced from that model (residual kriging). Interpolation is therefore carried out according to the relation:

$$\hat{Z}(s_0) = c + a_1 X_1(s_0) + a_2 X_2(s_0) + \cdots + a_n X_n(s_0) + \hat{R}(s_i) \qquad \text{(A1.4)}$$

where $\hat{Z}(s_0)$ is the estimated value of the air pollution indicator at the point s_o,
$X_1(s_0), X_2(s_0),\ldots, X_n(s_0)$ are *n* number of individual supplementary variables at the point s_o
$c, a_1, a_2,,\ldots, a_n$ are the *n+1* parameters of the linear regression model calculated based on the data at the points of measurement,
$\hat{R}(s_i)$ is the spatial interpolation of the residuals of the linear regression model at the point s_o calculated based on the residuals at the points of measurement.

For different pollutants and area types (rural, urban background, and in the case of PM and NO_2, also urban traffic), different supplementary data are used, depending on their improvement to the fit of the regression. Ordinary kriging is used to interpolate the residuals:

$$\hat{R}(s_i) = \sum_{i=1}^{N} \lambda_i R(s_i) \,, \sum_{i=1}^{N} \lambda_i = 1 \qquad \text{(A1.4a)}$$

where $R(s_i)$ are the residuals in the points of the measuring stations s_i,
$\lambda_1, \ldots, \lambda_N$ are the weights estimated based on variogram,
N is the number of the stations used in the interpolation.

The variogram (as a measure of a spatial correlation) is estimated using a spherical function (with parameters nugget, sill, range). For details, see Horálek et al. (2007), Section 2.3.5 and Cressie (1993).

For $PM_{2.5}$, NO_x and BaP, both measurement data and the estimated data from the pseudo stations are used. For the PM_{10} and $PM_{2.5}$ indicators, prior to linear regression and interpolation, a logarithmic transformation is applied to measurement and modelling concentrations. After interpolation, a back-transformation is applied. For details, see de Smet et al. (2011) and Denby et al. (2008).

For the vegetation-related indicators (AOT40 for vegetation and forests, POD, and NO_x) only rural maps are constructed based on rural background stations, based on the assumption that no vegetation is located in urban areas. For the health-related indicators, the rural and urban background map layers (and for PM and NO_2 also urban traffic map layer) are constructed separately and then merged.

Merging of rural and urban background (and urban traffic) map layers

Health related indicator map layers are created for rural and urban background areas on a grid at resolution of 1x1 km^2 (for PM, NO_2 and BaP) and 10x10 km^2 (for ozone), and for urban traffic areas at 1x1 km^2 (for PM and NO_2). The rural background map layer is based on rural background stations, the urban background map layer on urban and suburban background stations and the potential urban traffic map layer is based on urban and suburban traffic stations. The separate dealing with the map layers is based on the assumption that the estimated rural values are lower (PM_{10}, $PM_{2.5}$, NO_2 and BaP) or higher (ozone) than the estimated urban background map value. In limited areas when this criterion does not hold, a joint urban/rural map layer (created using all background stations regardless of their type) is applied, as far as its value lies in between the rural and urban background map value. Thus,

the adjusted rural and urban background map layers are calculated and further used. For details, see de Smet et al. (2011).

Subsequently, the separate map layers are merged into one combined final map at 1x1 km^2 resolution, according to

$$\hat{Z}_F(s_0) = \left(1 - w_U(s_0)\right) \cdot \hat{Z}_R(s_0) + w_U(s_0)\left(1 - w_T(s_0)\right) \cdot \hat{Z}_{UB}(s_0) + w_T(s_0) \cdot \hat{Z}_{UT}(s_0) \quad \text{for } PM_{10}, PM_{2.5}, \text{ and } NO_2 \text{ and BaP}$$

$$= \left(1 - w_U(s_0)\right) \cdot \hat{Z}_R(s_0) + w_U(s_0) \cdot \hat{Z}_{UB}(s_0) \quad \text{for ozone} \qquad \text{(A1.5)}$$

where
- $\hat{Z}_F(s_0)$ is the resulting estimated concentration value in a grid cell s_o for the final map,
- $\hat{Z}_R(s_0)$ is the estimated value in a grid cell s_o for the rural background map layer,
- $\hat{Z}_{UB}(s_0)$ is the estimated value in a grid cell s_o for the urban background map layer,
- $\hat{Z}_{UT}(s_0)$ is the estimated value in a grid cell s_o for the urban traffic map layer,
- $w_U(s_0)$ is the weight representing the ratio of the urban character of the a grid cell s_o,
- $w_T(s_0)$ is the weight representing the ratio of areas exposed to traffic air quality in a grid cell s_o.

The weight $w_U(s_0)$ is based on the population density grid, while $w_T(s_0)$ is based on the buffers around the roads. For further details, see Horálek et al. (2017b).

In all calculations and map presentations the EEA standard projection ETRS89-LAEA5210 (also known as ETRS89 / LAEA Europe, see www.epsg-registry.org) is used. The interpolation and mapping domain consists of the areas of all EEA member and cooperating countries, and other microstates, as far as they fall into the EEA map extent Map_2c (EEA, 2018). The mapping area covers the whole Europe apart from Belarus, Moldova, Ukraine and the European parts of Russia and Kazakhstan.

A1.2 Calculation of population and vegetation exposure

Population and vegetation exposure estimates are based on the interpolated concentration maps, population density data and land cover data.

Population exposure

Population exposure for individual countries, for large regions, for EU-27 and for the whole mapping area is calculated for ozone (and apart from the individual countries also for BaP) from the air quality maps and population density data, both at 1x1 km^2 resolution. For each concentration class, the total population per country as well as the European-wide total is determined.

For PM and NO_2, the population exposure is calculated separately for the areas where the air quality is considered to be directly influenced by traffic and for the background (both rural and urban) areas. For each concentration class 'j', the percentage population per country as well as the European-wide total is determined according to:

$$P_j = \frac{\sum_{i=1}^{N} I_{Bij}\left(1 - w_U(\mathrm{i}) w_T(\mathrm{i})\right) p_i + \sum_{i=1}^{N} I_{Tij} w_U(\mathrm{i}) w_T(\mathrm{i}) p_i}{\sum_{i=1}^{N} p_i} . 100 \qquad \text{(A1.6)}$$

where
- P_j is the percentage population living in areas of the *j*-th concentration class in either the country or in Europe as a whole,
- p_i is the population in the *i*-th grid cell,
- I_{Bij} is the Boolean 0-1 indicator showing whether the background air quality concentration (estimated by the combined rural/urban background map layer) in the *i*-th grid cell is within the *j*-th concentration class (I_{Bij} = 1), or not (I_{Bij} = 0),

I_{Tij} is the Boolean 0-1 indicator showing whether the traffic air quality concentration in the *i*-th grid cell is within the *j*-th concentration class (I_{Tij} = 1), or not (I_{Tij} = 0),$w_U(s_0)$ is the weight representing ratio of the urban character of the a grid cell s_o,

$w_T(s_0)$ is the weight representing ratio of areas exposed to traffic air quality in a grid cell s_o.

N is the number of grid cells in the country, in the region or in the whole mapped area.

In addition, the exposure for individual countries, large regions, EU-27 and the whole area is expressed also as the population-weighted concentration, i.e. the average concentration weighted according to the population in a 1x1 km^2 grid cell:

$$\hat{c} = \frac{\sum_{i=1}^{N} c_i p_i}{\sum_{i=1}^{N} p_i} \quad \text{(A1.7)}$$

where $\hat{c}$ is the population-weighted average concentration in the country, large region, EU-27 or in the whole mapping area,

p_i is the population in the i^{th} grid cell,

c_i is the concentration in the i^{th} grid cell (based on the final merged map),

N is the number of grid cells in the country or in Europe as a whole.

Vegetation exposure

Vegetation exposure for individual countries, large regions, EU-27 and for the total mapping area is calculated based on the air quality maps and land cover data, both in 2x2 km^2 grid resolution. For each concentration class, the total agricultural and forest area per country as well as European-wide is determined.

Next to this, per-country and European-wide exposure are expressed as the agricultural- and forest-weighted concentration, i.e. the average concentration weighted according to the agricultural and forest area in a 1x1 km^2 grid cell, similarly like in Eq. A1.7.

Estimation of trends

For detecting and estimating the trends in time series of annual values of population exposure, the non-parametric Mann-Kendall's test for testing the presence of the monotonic increasing or decreasing trend is used. Next to that, the non-parametric Sen's method for estimating the slope of a linear trend is executed. For details, see Gilbert (1987). The significance of the Mann-Kendal test is shown by the usual way, i.e. + for 0.1, * for 0.05, ** for 0.01, and *** for 0.001.

Geographical distribution of countries to large regions for use in the assessment

The population and vegetation exposure is presented, apart from the individual countries, the EU-27 and the whole mapped area, also in five large European regions. For this purpose, the countries have been grouped into the large European regions as follows. See also Map A1.1.

1) Northern Europe (N): Denmark (including Faroes), Estonia, Finland, Iceland, Latvia, Lithuania, Norway, Sweden;

2) Western Europe (W): Belgium, France north of 45°, Ireland, Luxembourg, Netherlands, United Kingdom (including Crown dependencies);

3) Central Europe (C): Austria, Czechia, Germany, Hungary, Liechtenstein, Poland, Slovakia, Slovenia, Switzerland;

4) Southern Europe (S): Andorra, Cyprus, France south of 45°, Greece, Italy, Malta, Monaco, Portugal, San Marino, Spain;

5) South-eastern Europe (SE): Albania, Bosnia and Herzegovina, Bulgaria, Croatia, Montenegro, North Macedonia, Romania, Serbia (including Kosovo under the UN Security Council Resolution 1244/99), Türkiye.

Map A1.1: Five large European regions

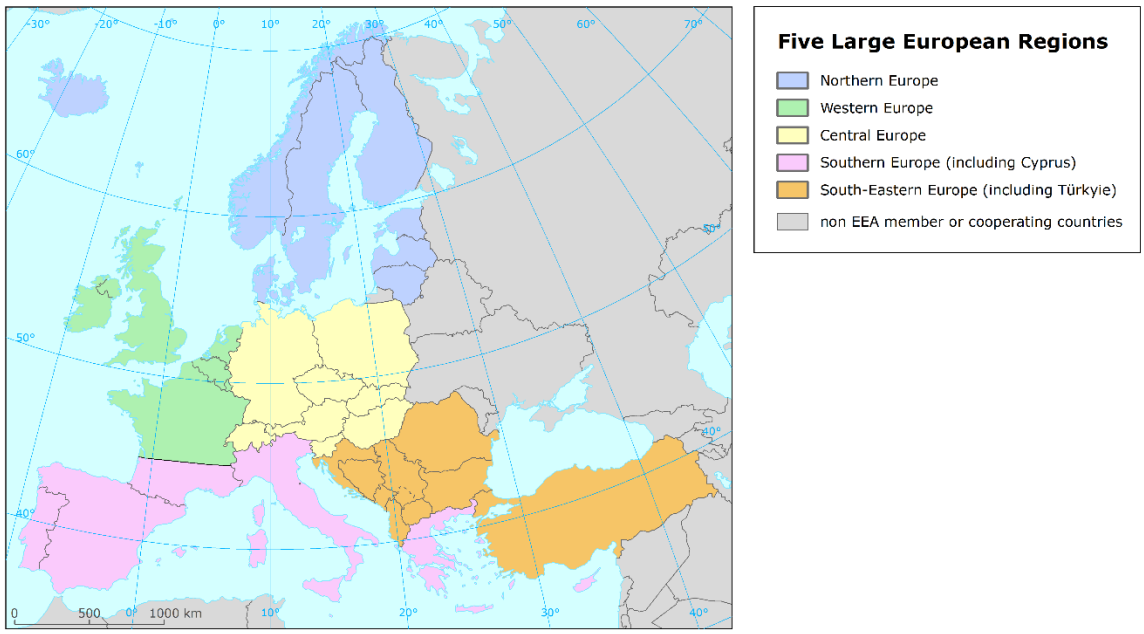

A1.3 Phytotoxic Ozone Dose above a threshold flux Y (POD_Y) calculation

The calculation of the phytotoxic ozone dose above a threshold *Y* (POD_Y) as described below follows the methodology described in the Manual for modelling and mapping critical loads & levels of the Long-Range Transboundary Air Pollution Convention (CLRTAP) in its most recent available revision (CLRTAP, 2017a), including some specifications presented in the Scientific background documents of this manual (CLRTAP, 2017b, 2020), as prepared by the International scientific Cooperative Programme on effects of air pollution on natural vegetation and crops of the Working Group on Effects of the CLRTAP (ICP Vegetation). The steps to be taken are presented in Table A1.1.

Table A1.1: Steps to calculate POD_Y of flux-based critical levels

1	Decide on the species and biogeographical region(s) to be included.
2	Obtain the ozone concentrations at the top of the canopy for the species or vegetation-specific accumulation period.
3	Calculate the hourly stomatal conductance of ozone (g_{sto}).
4	Model the hourly stomatal flux of ozone (F_{sto}).
5	Calculation of POD_Y from F_{sto}.

Source: CLRTAP, 2017a

The cumulative stomatal ozone fluxes (F_{sto}) are calculated over the course of the growing season based on ambient ozone concentration and stomatal conductance (g_{sto}) to ozone. g_{sto} is calculated using a

multiplicative stomatal conductance model proposed by Jarvis (1976) and modified by Emberson et al. (2000) as a function of species-specific maximum g_{sto} (expressed on a single leaf-area basis), phenology, and prevailing environmental conditions (photosynthetic photon flux density (PPFD)), air temperature, vapour pressure deficit (VPD), and soil moisture.

Hourly averaged stomatal ozone fluxes (F_{sto}) in excess of a threshold Y (expressed in mmol/m^2 PLA ([7])) are accumulated over a species or vegetation-specific accumulation period during daylight hours, in order to get the phytotoxic ozone dose above the threshold *Y* (POD_Y).

For the wheat as for other crop species, the Y value is taken equal to 6 nmol/m^2 PLA s^{-1}. Although several POD indicators are proposed in CLRTAP (2017a), POD_6 is recommended for wheat, as the hourly averaged stomatal ozone fluxes above a value of 6 are more relevant for that crop. For potato and tomato, POD_6 is also recommended. Two POD_6 versions are available in CLRTAP (2017a): POD_6IAM (which is a simplified version recommended for Integrated Assessment Modelling) and POD_6SPEC (which is specific to a given specie). Here, POD_6SPEC was preferred and used, in agreement with Colette et al. (2018).

Obtaining the ozone concentrations at the top of the canopy for the species or vegetation-specific accumulation period

The ozone concentration at the top of the canopy (nmol/m^3) in the given hour H is calculated according to

$$c(z_1) = c(z_{m,O3}) * \left[1 - \frac{R_a(z_{tgt},\ z_{m,O3})}{R_a\left(d+z_0,\ z_{m,O3}\right) + R_b + R_{surf}}\right] \quad \text{(A1.8)}$$

where
- $c(z_1)$ is ozone concentration at the top of the canopy;
- $c(z_{m,O3})$ is the ozone concentration measured at the height z_m;
- $R_a(x, y)$ is the aerodynamic resistance between the height of y and the height of x;
- R_b is the resistance to ozone diffusion in the laminar sub-layer;
- R_{surf} is the overall resistance to ozone deposition to the underlying surfaces;

while

$$R_a(z_{tgt},\ z_{m,O3}) = \frac{1}{k.u*}\left[ln\left(\frac{z_{m,O3}-d}{z_{tgt}-d}\right) - \Psi_H\left(\frac{z_{m,O3}-d}{L}\right) + \Psi_H\left(\frac{z_{tgt}-d}{L}\right)\right] \quad \text{(A1.8a)}$$

$$R_a(d+z_0,\ z_{m,O3}) = \frac{1}{k.u*}\left[ln\left(\frac{z_{m,O3}-d}{z_0}\right) - \Psi_H\left(\frac{z_{m,O3}-d}{L}\right) + \Psi_H\left(\frac{z_0}{L}\right)\right] \quad \text{(A1.8b)}$$

$$R_b = \frac{2}{k\ .u*}\left(\frac{Sc}{Pr}\right)^{2/3} \quad \text{(A1.8c)}$$

$$R_{surf} = \frac{1}{\frac{LAI}{R_{sto}} + \frac{SAI}{R_{ext}} + \frac{1}{R_{inc}+R_{soil}}} \quad \text{(A1.8d)}$$

where
- k is the von Kármán constant (equal to 0.41);
- z_{tgt} is the top canopy height (the target height);
- $z_{m,O3}$ is the height of the available ozone measurement above the canopy;
- z_0 is the roughness length, usually assumed as 1/10 of the canopy height;
- L is the Obukhov length;
- d is the displacement height, usually assumed as 2/3 of the canopy height;
- $u*$ is the friction velocity;
- Sc is the Schmidt number for ozone (equal to 0.41);
- Pr is the Prandtl number of air (equal to 0.71);
- LAI is the projected leaf area in [m^2/m^2];
- SAI is the surface area of the canopy in [m^2/m^2];

([7]) PLA, or the projected leaf area, is the total area of the sides of the leaves that are projected towards the sun. PLA is different to the total leaf area, which accounts for both sides of the leaves.

$\Psi_H(..) = \Psi_H(\zeta)$ is the similarity function for heat with ζ as the argument ([8]),

according to

$$(\zeta) = 2 \quad \text{when } \zeta < 0$$
$$= -5\zeta \quad \text{when } \zeta \geq 0 \qquad \text{(A1.8e)}$$

with $x = (1 - 16 * \zeta)^{1/4}$ (A1.8f)

and R_{ext} is the resistance to cuticular deposition of ozone (equal to 2 500 s/m);
R_{soil} is the soil resistance (equal to 200 s/m[1]),

while $R_{sto} = 1/g_{sto}$ (A1.8g)
$R_{inc} = b.SAI.h / u^*$ (A1.8h)

where g_{sto} is the actual stomatal conductance;
b is the empirical constant (equal to 14 m^{-1});
h is the height of the canopy.

Calculation of the hourly stomatal conductance of ozone (g_{sto})

The basis of the approach used for calculating phytotoxic ozone doses is the calculation of an instantaneous stomatal conductance g_{sto} in the given hour H, according to the equation

$$g_{sto} = g_{max} * [min(f_{phen}, f_{O3})] * f_{light} * max[f_{min}, (f_{temp} * f_{VPD} * f_{SW})] \qquad \text{(A1.9)}$$

where g_{sto} is the actual stomatal conductance in [mmol O_3 /m^2 PLA per second];
g_{max} is the species-specific maximum stomatal conductance in [mmol O_3 /m^2 PLA per second]; see Table A1.2;
f_{phen} is the relative proportion function for the phenology for the different stage of growing;
f_{O3} is the relative proportion function for the influence of ozone on stomatal flux by promoting premature senescence;
f_{min} is the species-specific relative minimum stomatal conductance that occurs during daylight hours, see Table A1.2;
f_{temp}, f_{VPD}, f_{SW}, f_{light} are relative proportion functions for leaf stomata respond to temperature, air humidity, soil moisture and light.

Parameters f_{phen}, f_{O3}, f_{light}, f_{temp}, f_{VPD}, f_{SW} and f_{min} are expressed as relative proportion functions, taking values between 0 and 1 as a proportion of g_{max}. These functions allow taking into account irradiance (f_{light}), temperature (f_{temp}), water vapour deficit at leaves level (f_{vpd}), soil moisture (f_{sw}), phenology for the different stage of growing (f_{phen}) and the influence of ozone on stomatal flux by promoting premature senescence (f_{O3}). f_{min} is the minimum relative value of stomatal conductance during the daylight.

The parameter f_{phen} is calculated based on the accumulation of thermal time over the growing season of the crop being considered (Colette, 2018), according to CLRTAP (2017a). For wheat and potato, the accumulation period is defined for each year using the effective temperature sum (*ETS*) in ˚C for days in excess of 0 ˚C, while for tomato for days in excess of 10 ˚C.

For wheat, the total accumulation period during which wheat is sensitive to ozone exposure is 200 °C days and 300 °C days before mid-anthesis (mid-point in flowering) to 700 °C days to 550 °C days after mid-anthesis for Atlantic, Boreal and Continental regions and Mediterranean region, respectively. The timing of mid-anthesis is estimated by starting at the first date after 1 January (or just 1 January) when the temperature exceeds 0 °C. The mean daily temperature is then accumulated (temperature sum),

([8]) For more details see CLRTAP (2017b).

and mid-anthesis is estimated to be a temperature sum of 1075 °C days for Atlantic, Boreal and Continental regions and 1250 °C days for Mediterranean region, which in general corresponds to bread wheat.

For potato, the accumulation period stands between 330 °C days before the tuber initiation date and 800 °C days after this date. The tuber initiation date is considered to be homogeneous throughout Europe. The reasons for its simplification are a) heterogeneous climatic conditions in the European countries naturally lead to different time of potato planting (Pedersen et al., 2005) followed by different time of the tuber initiation and b) lack of detailed local data availability for modelling and mapping.

As discussed ([9]) with the French national Chamber of agriculture (APCA, http://chambres-agriculture.fr), the tuber initiation starts 15 days after the transplantation in the field, which occurs in May. Therefore, the fixed date for the tuber initiation was set to June 1st.

For tomato, the accumulation period is from 250 ˚C days to 1500 ˚C days after transplantation in the field over a base temperature of 10 °C. The timing of the transplantation is set on the date June 1st.

The parameter f_{phen} is calculated according to following equations:

in the case of wheat:

$$\begin{aligned} f_{phen} &= 1 && \text{when} \quad (f_{phen\_2\_ETS} + f_{phen\_1\_ETS}) \le ETS \le (f_{phen\_2\_ETS} + f_{phen\_3\_ETS}) \\ &= 1 - \left(\frac{f_{phen\_a}}{f_{phen\_4\_ETS} - f_{phen\_3\_ETS}}\right) * (ETS - f_{phen\_3\_ETS}) \\ & && \text{when} \quad (f_{phen\_2\_ETS} + f_{phen\_3\_ETS}) < ETS \le (f_{phen\_2\_ETS} + f_{phen\_4\_ETS}) \\ &= f_{phen\_e} - \left(\frac{f_{phen\_e}}{f_{phen\_5\_ETS} - f_{phen\_4\_ETS}}\right) * (ETS - f_{phen\_4\_ETS}) \\ & && \text{when} \quad (f_{phen\_2\_ETS} + f_{phen\_4\_ETS}) < ETS \le f_{phen\_5\_ETS} \end{aligned} \qquad \text{(A1.9a)}$$

in the case of potato (formulated based on CLRTAP, 2017b):

$$\begin{aligned} f_{phen} &= 1 - \left(\frac{1 - f_{phen\_a}}{f_{phen\_1\_ETS}}\right) * ETS && \text{when} \quad f_{phen\_1\_ETS} \le ETS < 0 \\ &= 1 - \left(\frac{1 - f_{phen\_e}}{f_{phen\_2\_ETS}}\right) * ETS && \text{when} \quad 0 < ETS \le f_{phen\_2\_ETS} \end{aligned} \qquad \text{(A1.9b)}$$

in the case of tomato (formulated based on CLRTAP, 2017b):

$$f_{phen} = \frac{ETS - f_{phen\_2\_ETS}}{A_{start\_ETS} - f_{phen\_2\_ETS}} \quad \text{when } A_{start\_ETS} \le ETS < A_{end\_ETS} \qquad \text{(A1.9c)}$$

where *ETS* is the effective temperature sum in ˚C days using a base temperature of 0 ˚C for wheat and potato and a base temperature of 10 °C for tomato (see Table A1.2);
for wheat, ETS is set to 0 °C days at mid-anthesis day. Then A_{start_ETS} will be at 200 ˚C days before mid-anthesis, and A_{end_ETS} will be at 700 ˚C days after mid-anthesis over a base temperature of 0 °C;
for potato, ETS is set to 0 °C days at tuber initiation day. Then A_{start_ETS} will be at 330 ˚C days before tuber initiation and A_{end_ETS} at 800 ˚C days after tuber initiation over a base temperature of 0 °C;

([9]) There is a lack of information on a date of potato tuber initiation in Europe. It should ideally rely on existing models based on agricultural practices, local climatology, ground properties, and location. INERIS, while developing the POD script, relied on contents of discussions with the French National Chamber of Agriculture (consultation with APCA, March 2018; Deumier and Hannon, 2010). Based on the information given that the tuber initiation starts 15 days after the transplantation in the field, which occurs in May in France, a fixed date of June 1st has been chosen for France and applied also for the rest of Europe. This date should be revised according to the availability of more accurate information on potato plantations in Europe.

for tomato, ETS is set to 0 °C days at transplantation day in the field. Then A_{start_ETS} will be at 250 ˚C days after transplantation in the field and A_{end_ETS} at 1500 ˚C days after transplantation in the field over a base temperature of 10 °C,

f_{phen_a}, f_{phen_e} is the phenology function, which consists of terms describing rate changes of g_{max} expressed as fractions (see Table A1.2),

$f_{phen\_1\_ETS}$, $f_{phen\_2\_ETS}$, $f_{phen\_3\_ETS}$, $f_{phen\_4\_ETS}$, $f_{phen\_5\_ETS}$ are °C days (see Table A1.2; $f_{phen\_1\_ETS}$ and $f_{phen\_5\_ETS}$ define period crops to be sensitive to ozone exposure),

A_{start_ETS} and A_{end_ETS} are the effective temperature sums (counted from the day of the mid-anthesis for wheat, from the day of the tuber initiation for potato and from the day of the transplantation in the field for tomato) above a base temperature of 0 ˚C for wheat and potato and 10 ˚C for tomato at the start and end of the O_3 accumulation period respectively; see Table A1.2.

The parameter f_{O3} in the case of wheat is calculated according to equation

$$f_{O3} = [(1+(POD_0/14)^8]^{-1} \quad \text{(A1.9d)}$$

while $$POD_0 = \sum_{n=A_{start}}^{H-1} F_{sto}\,(n) \cdot \frac{3600}{10^6} \quad \text{(A1.9e)}$$

where POD_0 is the ozone flux already accumulated since the beginning of the vegetation period A_{start} up to the last hour *H-1*,

$F_{sto}(n)$ is the hourly ozone flux in the hour n, calculated in the previous steps based on Equation A1.10, while $F_{sto}(A_{start})$ is equal to 0.

The parameter (ozone function) f_{O3} in the case of potato is calculated according to equation

$$f_{O3} = [(1+(AOT0/40)^5]^{-1} \quad \text{(A1.9f)}$$

where *AOT0* is accumulated ozone concentration from the start of the vegetation period A_{start} up to the last hour *H-1*.

The parameter (ozone function) f_{O3} in the case of tomato is not determined.

The parameter f_{light} is calculated according to

$$f_{light} = 1 - EXP[(-light\_a)*PPFD] \quad \text{(A1.9g)}$$

while $$PPFD = SSRD * 0.5 * 4.5 \quad \text{(A1.9h)}$$

where *PPFD* represents the photosynthetic photon flux density [µmol/m^2 per second],
light_a is a light parameter (see Table A1.2),
SSRD represents the surface net solar radiation in [W/m^2].

The parameter f_{temp} is calculated according to:

$$f_{temp} = \max\{f_{min}, [(T - T_{min}) / (T_{opt} - T_{min})] * [(T_{max} - T) / (T_{max} - T_{opt})]^{bt}\} \quad \text{when } T_{min} < T < T_{max}$$
$$= f_{min} \quad \textit{when } T_{min} > T > T_{max} \quad \text{(A1.9i)}$$

while $$bt = (T_{max} - T_{opt}) / (T_{opt} - T_{min}) \quad \text{(A1.9j)}$$

where T_{min}, T_{max} and T_{opt} are minimum, maximum and optimum temperatures determining leaf stomata opening (see Table A1.2)

The parameter f_{VPD} is calculated according to:

$$f_{VPD} = \min\{1,\max\{f_{min}, [(1-f_{min})*(VPD_{min} - VPD) / (VPD_{min} - VPD_{max})] + f_{min}\}\} \quad \text{(A1.9k)}$$

while $$VPD = e_s(Ta) * (1-hr) \quad \text{(A1.9l)}$$
$$e_s(Ta) = a \exp[bT_a/(T_a+c)] \quad \text{(A1.9m)}$$

where VPD_{min} is the minimum vapour pressure deficit determining leaf stomata opening
VPD_{max} is the maximum vapour pressure deficit determining leaf stomata opening

T_a	is the air temperature [°C]
h_r	is the relative humidity [%]/100
$e_s(Ta)$	is the potential (saturation) water vapour pressure
a, b, c	are the empirical constants (a = 0.611 kPa, b = 17.502, c = 240.97 °C)

The ΣVPD (i.e. the function describing stomatal re-opening in the afternoon) is taken into account for maps POD_YSPEC for wheat and potato in 2020. ΣVPD (kPa) should be calculated for daylight hours until dawn of the next day. If ΣVPD ≥ ΣVPD_crit, g_{sto} calculated using Equation A1.9 is valid if smaller or equal to g_{sto} of the preceding hour. If g_{sto} is larger than g_{sto} of the preceding hour, given that ΣVPD is larger than or equal to ΣVPD_crit, it is replaced by the g_{sto} of the preceding hour.

Table A1.2: Parametrisation for POD_6SPEC for wheat flag leaves and the upper-canopy sunlit leaves of potato and tomato, for different biogeographical regions

Parameter	Units	(Bread) Wheat		Potato	Tomato
		Atlantic, Boreal, Continental *(Pannonia, Steppic)*	Mediterranean	Atlantic, Boreal, Continental *(Mediterranean Pannonia, Steppic)*	Mediterranean
g_{max}	mmol O_3 /m^2 PLA per second	500	430	750	330
f_{min}	fraction	0.01	0.01	0.01	0.06
light_a	-	0.0105	0.0105	0.005	0.0125
T_{min}	°C	12	12	13	18
T_{opt}	°C	26	28	28	28
T_{max}	°C	40	39	39	37
VPD_{max}	kPa	1.2	3.2	2.1	1
VPD_{min}	kPa	3.2	4.6	3.5	4
ΣVPD_crit	kPa	8	16	10	-
f_{O3}	POD0 mmol O_3/m^2 PLA per second	14	-	-	-
f_{O3}	AOT0, ppmh	-	-	40	-
f_{O3}	exponent	8	-	5	-
Astart_ETS	ºC day	-	-	-	250
Aend_ETS	ºC day	-	-	-	1500
Leaf dimension	cm	2	2	4	3
Canopy height	m	1	0.75	1	2
f_{phen_a}	fraction	0.3	0.5	0.4	1
f_{phen_b}	fraction	-	-	-	-
f_{phen_c}	fraction	-	-	-	-
f_{phen_d}	fraction	-	-	-	-
f_{phen_e}	fraction	0.7	0.5	0.2	0.0
$f_{phen\_1\_ETS}$	°C day	-200	-300	-330	0
$f_{phen\_2\_ETS}$	°C day	0	0	800	2770
$f_{phen\_3\_ETS}$	°C day	100	70	-	-
$f_{phen\_4\_ETS}$	°C day	525	312	-	-
$f_{phen\_5\_ETS}$	°C day	700	550	-	-
mid-anthesis	°C day	1075	1250	-	-

Source: CLRTAP, 2017a; González-Fernández et al., 2013; González-Fernández (personal communication, May 2021).

The parameter f_{SW} is replaced by f_{SMI} (where *SMI* represents Soil Moisture Index with maximum at field capacity), taking values between 0 and 1 as a proportion of g_{max} (with 0 for soil moisture at and below wilting point), following the parameterization given in Simpson et al. (2012), similar to the plant

available water (*PAW*) parameterization f_{PAW} as defined for wheat in CLRTAP (2017a). The basic equation used for f_{SW} resp. f_{SMI} is:

$$f_{SMI} = 0 \quad \text{for SMI} \le 0$$
$$= \frac{\text{SMI}}{\text{PAW}_t} \quad \text{for } 0 < \text{SMI} \le PAW_t$$
$$= 1 \quad \text{for SMI} > PAW_t \qquad \text{(A1.9n)}$$

while $$\text{SMI} = \frac{\text{SWLL} - \text{PWP}}{\text{FC} - \text{PWP}} \qquad \text{(A1.9o)}$$

where PAW_t is the threshold amount of water in the soil available to the plants, above which stomatal conductance is at a maximum, set to 0.5

SWLL is the soil moisture in [m^3/m^3]
PWP is the permanent wilting point in [cm^3/cm^3]
FC is the field capacity in [cm^3/cm^3]

The Soil Moisture Index using the EMEP methodology as described in Simpson et al. (2012) and CLRTAP (2020) is used. It is computed using the soil moisture variable available from a meteorological model, which represents the water content in m^3 of water per m^3 of ground [m^3/m^3] in a specific ground level, in dependence on the available dataset. For soil moisture, the ECWMF's ERA5-Land variable Volume of water in soil layer 3 (i.e. 28-100 cm) has been used, see Section 3.3. The level of soil layer was chosen based on recommendation of Haberle and Svoboda (2015). The soil moisture is quite a sensitive parameter in the calculation of the POD. Next to the soil moisture, the soil moisture index also takes into account the permanent wilting point and the field capacity; they are taken from JRC soil database (JRC, 2016), see Annex 2, Section A2.3.

No limitation of stomatal conductance due to soil moisture can be assumed for tomato, since it is an irrigated horticultural crop. Thus, f_{SMI} for this crop could be established to $f_{SMI} = 1$ over the whole range of SMI values to remove limitation due to soil moisture deficit.

Modelling the hourly stomatal flux of ozone (F_{sto})

Once the hourly stomatal conductance of ozone (g_{sto}) and all relevant variables are computed, the stomatal flux of ozone (F_{sto}) can be calculated, based on the assumption that the concentration of ozone at the top of the canopy represents a reasonable estimate of the concentration at the upper surface of the laminar layer for a sunlit upper canopy leaf. F_{sto} is calculated according to the CLRTAP (ICP Vegetation) methodology, thus the fraction of the ozone taken up by the stomata is given using a combination of the stomatal conductance, the external leaf, or cuticular, resistance and the leaf surface resistance. The hourly stomatal flux in the given hour H is calculated according to

$$F_{sto} = c(z_1) * g_{sto} * \frac{r_c}{r_b + r_c} \qquad \text{(A1.10)}$$

where F_{sto} is the hourly stomatal flux of ozone in [nmol/m^2 PLA per second]
$c(z_1)$ is the concentration of ozone at canopy top in [nmol/m^3]
r_b is the quasi-laminar resistance in [s/m]
r_c is the leaf surface resistance in [s/m]
g_{sto} is the actual stomatal conductance in [m/s],

while $r_c = 1/(g_{sto} + g_{ext})$ (A1.10a)

$$r_b = 1.3 * 150 * \sqrt{\frac{L}{u(z_1)}} \qquad \text{(A1.10b)}$$

where g_{ext} is the external leaf, or cuticular, resistance in [m/s], equal to 1/2500 m/s
$u(z_1)$ is the wind speed at height z_1 (z_1 is the canopy top)
L is the cross-wind leaf dimension (2 cm, see Table A1.2)

while $u_{(z1)} = \frac{u*}{k} * ln\ (\frac{z_1 - d}{z_0})$ (A1.10c)

where
- k is the von Kármán constant (equal to 0.41)
- d is the displacement height usually assumed as 2/3 of the canopy height,
- z_1 is the top of the canopy
- z_0 is the roughness length usually assumed as 1/10 of the canopy height
- $u*$ is the friction velocity.

Box A1.1 shows the conversion of stomatal conductance and ozone concentration to units demanded for POD_Y calculation.

Box A1.1: Conversion of stomatal conductance g_{sto} and ozone concentration to units demanded for POD_Y calculation

Stomatal conductance g_{sto} has to be converted from units mmol/m^2 per second to units m/s (since all the resistances are expressed in the unit of s/m). At standard temperature (20 °C) and air pressure (1.013 x 10^5 Pa), the conversion is made by dividing the conductance in mmol/m^2 per second by 41 000 to give conductance in m/s.

To convert the **ozone concentration (C)** at canopy height from µg/m^3 resp. ppb to nmol/m, the following equation should be used:

C [nmol·m^{-3}] = C [ppb] * $P/(R \cdot T)$ = C [µg/m^3] / 2 * $P/(R \cdot T)$ (A1.11)

where
- P is the atmospheric pressure in Pa,
- R is the universal gas constant of 8.31447 J/mol per Kelvin
- T is the air temperature in Kelvin.

At standard temperature (20 °C) and air pressure (1.013 x 10^5 Pa), the concentration in ppb should be multiplied by 41.56 to calculate the concentration in nmol/m^3.

Source: CLRTAP, 2017a

In the routine used in this report (Section 2.3), an alternative conversion of the ozone concentrations from µg/m^3 resp. ppb to nmol/m^3 is done, using the air density instead of the atmospheric pressure, according to

C [nmol·m^{-3}] = C [ppb] * $\rho / N_a * 10^6$ = C [µg/m^3] / 2 * $\rho / N_a * 10^6$ (A1.12)

where
- ρ is the air density showing the number of the molecules in cm^{-3},
- N_a is the Avogadro constant, which is equal to 6.022·10^{23} mol^{-1}.

Calculation of POD_Y from F_{sto}

Hourly averaged stomatal ozone fluxes (F_{sto}) in excess of a Y threshold are accumulated over a species or vegetation-specific accumulation period using the following equation:

$$POD_Y = \sum_n (F_{sto}(n) - Y) \cdot \frac{3600}{10^6} \quad \text{(A1.13)}$$

while Y (for wheat, potato or tomato) = 6 nmol/m^2 PLA per second

where
- POD_Y is the phytotoxic ozone dose related to the threshold Y, in [mmol/m^2 PLA]
- $F_{sto}(n)$ is the hourly ozone flux in the hour n of the accumulation period.

The value *Y* (in [nmol/m2PLA s^{-1}]) is subtracted from each hourly averaged F_{sto} (in [nmol/m^2 PLA s^{-1}]) value and the F_{sto} (after the subtracting of *Y*) is accumulated only when F_{sto}>Y, during daylight hours (when global radiation is more than 50 W/m^2). The value is then converted to hourly fluxes by multiplying by 3 600 and to mmol by dividing by 10^6 to get the stomatal ozone flux in mmol/m^2 PLA.

A1.4 Methods for uncertainty analysis

The uncertainty estimation of the European map is based on leave-one-out cross-validation. This cross-validation method computes the quality of the spatial interpolation for each point of measurement (i.e. monitoring station) from all available information except from the point in question, i.e. it withholds one data point and then makes a prediction at the spatial location of that point. This procedure is repeated for all measurement points in the available set. The predicted and measurement values at these points are plotted in the form of a scatter plot. With help of statistical indicators (see below), the quality of the predictions is demonstrated objectively. The advantage of the nature of this cross-validation technique is that it enables evaluation of the quality of the predicted values at locations without measurements, as long as they are within the area covered by the measurements.

In addition, a simple comparison is made between the point measurement data and the estimated values of the 1x1 km^2 grid cells (for PM and NO_2) or the 10x10 km^2 grid cells (for ozone) for the separate rural and urban background (and urban traffic, where relevant) map layers and the 1x1 km^2 grid cells for the final combined maps, for the health-related indicators, and the 2x2 km^2 grid cells in the case of AOT40 and NO_x. Note that the grid cell value is the mean estimated value of this grid cell area. The estimated value within a grid cell will only approximate the predicted value(s) at the station(s) lying within that cell. This additional analysis has not been performed for BaP.

Another method to estimate uncertainties is based on geostatistical theory: together with the prediction, the prediction standard error is computed at all the grid cells, which represents in fact the interpolation uncertainty map (see Cressie, 1993 for a detailed discussion). Based on the concentration and the uncertainty map, the exceedance probability map is created.

Cross-validation

The results of cross-validation are described by the statistical indicators and scatter plots. The main indicator used is root mean squared error (RMSE) and the additional ones are relative RMSE (RRMSE), which is expressed in relative terms(by relating the RMSE to the mean of the air pollution indicator value for all stations), and bias (mean prediction error, MPE):

$$RMSE = \sqrt{\frac{1}{N}\sum_{i=1}^{N}\left(\hat{Z}(s_i) - Z(s_i)\right)^2} \quad \text{(A1.14)}$$

$$RRMSE = \frac{RMSE}{\bar{Z}}.100 \quad \text{(A1.15)}$$

$$bias(MPE) = \frac{1}{N}\sum_{i=1}^{N}\left(\hat{Z}(s_i) - Z(s_i)\right) \quad \text{(A1.16)}$$

where $\hat{Z}(s_i)$ is the air quality indicator value derived from the measured concentration at the i^{th} point, i = 1, …, N,

$Z(s_i)$ is the air quality estimated indicator value at the i^{th} point using other information, without the indicator value derived from the measured concentration at the i^{th} point,

RRMSE is the relative RMSE, expressed in percent,

$\bar{Z}$ is the arithmetic average of the indicator values $Z(s_1), \ldots, Z(s_N)$, as derived from measurement concentrations at the stations $i = 1, \ldots, N$,

N is the number of the measuring points.

Other indicators are R^2 and the regression equation (y = a·x + c) parameters slope (a) and intercept (c), following from the scatter plot between the predicted (using cross-validation) and the observed concentrations. RMSE should be as small as possible, bias (MPE) should be as close to zero as possible, R^2 should be as close to 1 as possible, slope *a* should be as close to 1 as possible, and intercept *c* should be as close to zero as possible (in the regression equation $y = a \cdot x + c$).

In the cross-validation of $PM_{2.5}$, NO_x and BaP, only stations with $PM_{2.5}$, NO_x and BaP measurement data, respectively, are used (not the pseudo $PM_{2.5}$, NO_x and BaP stations, see Annex 1 Section A1.1).

Comparison of the point measurement and interpolated grid values

The comparison of point measurement and predicted grid values is described by the linear regression equation and its parameters and statistical values. The comparison is executed separately for rural and urban background (and urban traffic, where relevant) map layers and for the final combined map. In the case of of $PM_{2.5}$ and NO_x, only the stations with actual $PM_{2.5}$ and NO_x measurement data are used (not the pseudo $PM_{2.5}$ and NO_x stations). This analysis is done for PM, ozone, NO_2 and NO_x, not for BaP.

The point observation – point cross-validation prediction analysis (Annex 3, sections "Uncertainty estimated by cross-validation") describes interpolation performance at point locations when there is no observation (as it follows the leave-one-out approach). In this case, the smoothing effect of the interpolation is most prevalent.

The point observation – grid prediction approach indicates performance of the value for the grid cell (either in 1x1 km^2, 2x2 km^2 or 10x10 km^2 resolution) with respect to the observations that are located within that cell. As such, some variability is due to smoothing but it also includes smoothing due to spatial averaging into the grid cells. As such, the point-grid validation approach tells us how well our interpolated and aggregated grid values approximate the measurements at the actual station (point) locations. Whereas the point-point approach tells us how well our interpolated values estimate the indicator at a point where there is no actual measurement at that location, under the constraint that the point lies within the area covered by measurements.

Annex 2
Input data

The types of input data in this paper are similar as in Horálek et al. (2022a), apart from the modelling data: instead of the EMEP model results, the CAMS Ensemble Forecast model outputs have been used, see Section A2.2. The air quality, modelling, satellite and meteorological data as used in Horálek et al. (2022a) has been updated for 2020. For readability of this paper, the list of the input data is reproduced here. The key data is the air quality measurements at the monitoring stations extracted from the Air Quality e-Reporting database, including geographical coordinates (*latitude*, *longitude*).

The supplementary data cover the whole mapping domain and are converted into the EEA reference projection ETRS89-LAEA5210 on a 1 x 1 km^2 grid resolution (for health-related indicators apart from ozone) resp. a 10x10 km^2 grid resolution (ozone). The data for the maps of vegetation related indicators (particularly AOT40) were converted – like in the previous reports (Horálek et al., 2021, and references cited therein) – into a 2 x 2 km^2 resolution to allow accurate land cover exposure estimates to be prepared for use in the EEA indicator on ecosystem exposure to ozone (EEA, 2022b).

A2.1 Air quality monitoring data

Air quality station monitoring data for the relevant year as extracted from the official EEA Air Quality e-Reporting database, EEA (2022a) in March 2022 has been used. This data set has been supplemented with several EMEP stations from the databases EBAS (NILU, 2022) and Defra (2022) not reported to the Air Quality e-Reporting database ([10]). Specifically, 9 additional stations (including 4 British ones) for PM_{10}, 7 (including 2 British) for $PM_{2.5}$, 14 (including 7 British) for NO_2 and 14 (including 9 British) for NO_x from the EBAS database have been added and 24 BaP British stations from the data archive Defra (2022) have been added. Apart from this, for the mapping purposes, several British stations from the E2a UTD database have been added. Specifically, 15 additional British stations for PM_{10}, 15 for $PM_{2.5}$, 63 for ozone and 119 for NO_2 have been used, in order to supplement British stations from the EBAS and Defra databases. These stations with the non-validated data have been used in the mapping, but not in the uncertainty analysis (Annex 3) and are not shown in the maps of Annex 5.

The following pollutants and aggregations are considered:

PM_{10} – annual average [µg/m^3], year 2020
– 90.4 percentile of the daily average values [µg/m3], year 2020
$PM_{2.5}$ – annual average [µg/m^3], year 2020
Ozone – 93.2 percentile of the maximum daily 8-hour average values [µg/m3], year 2020
– SOMO35 [µg/m^3·day], year 2020
– SOMO10 [µg/m^3·day], year 2020
– AOT40 for vegetation [µg/m^3·hour], year 2020
– AOT40 for forests [µg/m^3·hour], year 2020
– hourly values [µg/m^3], all hours of the year 2020 (for the purpose of POD_6 mapping)
NO_2 – annual average [µg/m^3], year 2020
NO_x – annual average [µg/m^3], year 2020
NO – annual average [µg/m^3], year 2020 (for the purposes of NO_x mapping only)
BaP – annual average [ng/m^3], year 2020

[10] The United Kingdom exited the European Union in January 2020. Nevertheless, results in this report include this country. In this way, a comparison of the 2020 results with the previous years can be done. This is especially important because 2020 saw an exceptional decrease in the emission of certain pollutants, specifically NO_2, due to the lockdown measures adopted to prevent the spread of the COVID-19.

The exact values of percentiles are actually 90.41 in the case of PM_{10} daily means and 93.15 in the case of ozone maximum daily 8-hour means.

For a considerable number of stations NO_x is measured, but it is not reported as such but separately as NO and NO_2. For these stations reporting NO and NO_2 separately, the NO_x concentrations were derived according to the equation

$$NO_x = NO_2 + \frac{46}{30} \cdot NO \qquad \text{(A2.1)}$$

In this equation, all components are expressed in µg/m^3, with a molecular mass for NO of 30 g/mol and for NO_2 of 46 g/mol.

SOMO35 is the annual sum of the differences between maximum daily 8-hour concentrations above 70 µg/m^3 (i.e. 35 ppb) and 70 µg/m^3. SOMO10 is the annual sum of the differences between maximum daily 8-hour means above 20 µg/m^3 (i.e. 10 ppb) and 20 µg/m^3. AOT40 is the sum of the differences between hourly concentrations greater than 80 µg/m^3 (i.e. 40 ppb) and 80 µg/m^3, using only observations between 08:00 and 20:00 CET, calculated over the three months from May to July for AOT40 for vegetation and over the six months from April to September for AOT40 for forests.

Only the stations with annual data coverage of at least 75 percent are used. In the case of SOMO35, SOMO10 and AOT40 indicators, a correction for the missing data is applied according to the equation

$$I_{corr} = \mathrm{I} \cdot \frac{N_{max}}{N} \qquad \text{(A2.2)}$$

where I_{corr} is the corrected indicator (SOMO35, SOMO10 or AOT40 for vegetation or for forests),
I is the value of the given indicator without any correction,
N is the number of the available daily resp. hourly data in a year for the given station,
N_{max} is the maximum possible number of the days or hours applicable for the indicator.

For the indicators relevant to human health (i.e. for all PM_{10} and $PM_{2.5}$ indicators, ozone indicators 93.2 percentile of maximum daily 8-hour means, SOMO35 and SOMO10, and NO_2 and BaP annual averages), data from stations classified as *background* (for all the three types of area, *rural*, *urban* and *suburban*) are considered; for PM_{10} and $PM_{2.5}$ and NO_2, also *urban* and *suburban traffic* stations are considered. (Throughout the paper, the urban and suburban stations are handled together). *Industrial* stations are not considered, as they represent local concentration levels that cannot be easily generalized for the whole map. For the indicators relevant to vegetation damage (i.e. for ozone AOT40 and POD_6 parameters and NO_x annual average), only *rural background* stations are considered; the relevant maps are constructed (and applicable) for rural areas only. In case of existing data (with sufficient annual time coverage) from two or more different measurement devices in the same station location, the average of these data is used.

The stations from French overseas areas (departments), Svalbard, Azores, Madeira and Canary Islands were excluded. These areas outside the EEA map extent Map_2c (EEA, 2018) were excluded from the interpolation and mapping domain, as the interpolation should be performed across generally compact territory.

Table A2.1 shows the number of the measurement stations (not pseudo stations) selected for the individual pollutants and their respective indicators.

Table A2.1: Number of stations selected for each pollutant indicator and area type, 2020

Station type	PM_{10}		$PM_{2.5}$	Ozone				NO_2	NO_x	BaP
	Ann. avg.	90.4 perc.	Ann. avg.	Health related	AOT40 for veg.	AOT40 for for.	POD_6	Ann. avg.	Ann. avg.	Ann. avg.
Rural background	388	385	234	551	551	556	549	476	401	111
Urban/suburb. backgr.	1467	1462	806	1223	-	-	-	1400	-	460
Urban/suburb. traffic	737	737	396	-	-	-	-	1127	-	-

For the $PM_{2.5}$ mapping, in addition to the $PM_{2.5}$ stations, 171 rural background, 654 urban/suburban background and 362 urban/suburban traffic PM_{10} stations (at locations without $PM_{2.5}$ measurement) have been also used for the purpose of calculating the pseudo $PM_{2.5}$ station data.

In the case of NO_x, 343 stations with NO_x reported data have been used, while for 58 stations NO_x values are calculated from reported NO_2 and NO data using Eq. A2.1. Next to this, for the NO_x mapping 71 additional rural background NO_2 stations (at locations without NO_x measurement) were also used for the purpose of calculating the pseudo NO_x station data.

For the BaP mapping, in addition to the BaP stations, 60 rural and 46 urban background pseudo BaP stations calculated based on the $PM_{2.5}$ measurements and 3 rural pseudo BaP stations calculated based on the pseudo $PM_{2.5}$ data (as estimated based on the PM_{10} measurements).

A2.2 Chemical transport modelling outputs

In the previous years, EMEP MSC-W (formerly called Unified EMEP) model was used, specifically its model results for year Y based on meteorology for year Y and emissions for year Y-1. However, the EMEP model results for year 2020 based on the emissions for year 2019 was not prepared by the EMEP modelling team. The reason was that the emissions for 2019 were supposed not to be a good approximation of the 2020 emissions, as the year 2020 was a special year due to the COVID-19 situation.

Instead of the EMEP model results, the CAMS Ensemble Forecast model output has been used for all pollutants apart from the BaP, in agreement with Horálek et al. (2021), which recommended this modelling product as an alternative to the EMEP model. The CAMS modelled data are provided by the Copernicus Atmosphere Monitoring Service (CAMS) at a regional scale over Europe. The European regional production consists of an ensemble of nine air quality models run operationally. For further details of individual models, see Marécal et al. (2015). The models provide (together with other products) a 72-hour forecast made available at 07:00 UTC the day of the forecast. The forecast data product is available on an hourly time resolution and at a spatial resolution of 0.1° x 0.1°, i.e., ca. 10x10 km^2. All the models used in the CAMS ensemble products were run using the TNO-MACC emissions representative of 2011 (Kuenen et al-, 2014) and the meteorology (i.e., the weather forecast) provided by the European Centre for Medium Range Weather Forecasts (ECMWF) operationally. Each model forecast is combined into the Ensemble Forecast by taking the median of all nine models.

The CAMS Ensemble Forecast data were downloaded in the form of hourly means from the CAMS data archive (http://www.regional.atmosphere.copernicus.eu/?category=data_access). These primary data have been aggregated to the same set of parameters as for the air quality observations:

PM_{10} – annual average [µg/m^3], year 2020
– 90.4 percentile of the daily means [µg/m^3], year 2020 (aggregated from daily means)

$PM_{2.5}$ – annual average [µg/m^3], year 2020

Ozone – 93.2 percentile of the highest maximum daily 8-hour average value [µg/m^3], year 2020 (aggregated from hourly means)
– SOMO35 [µg/m^3·day], year 2020 (aggregated from hourly means)

– SOMO10 [µg/m^3·day], year 2020 (aggregated from hourly means)
– AOT40 for vegetation [µg/m^3·hour], year 2020 (aggregated from hourly means)
– AOT40 for forests [µg/m^3·hour], year 2020 (aggregated from hourly means)

NO_2 – annual average [µg/m^3], year 2020

NO_x – annual average [µg/m^3], year 2020

Due to the complete temporal data coverage available at the modelled data, the PM_{10} indicator 90.4 percentile of daily means is identical with the 36th highest daily mean and the ozone indicator 93.2 percentile of maximum daily 8-hour means is identical with the 26th highest maximum daily 8-hour mean.

The data were re-gridded into the reference EEA 10x10 km^2 grid (for ozone health related indicators), 1x1 km^2 grid (for PM and NO_2) and 2x2 km^2 grid (for vegetation related indicators).

For BaP, the chemical dispersion model used is the *EMEP MSC-E POP* model, EMEP (2022). It is a three-dimensional Eulerian multi-compartment chemistry transport model (Gusev et al., 2005, 2006). Its resolution is 0.1°x0.1°, i.e., circa 10x10 km^2. The model's output completely covers the mapping domain (i.e., the area of the EEA member and cooperating countries within the map extent Map_2c, EEA, 2018). The parameter used is

Benzo(a)pyrene – annual average [ng.m^{-3}], year 2020.

A2.3 Other supplementary data

Meteorological parameters

The meteorological data used are the ECWMF data extracted from the CDS (Climate Data Store, https://cds.climate.copernicus.eu/cdsapp#!/home). Hourly data for 2020 are used. Most of the data come from the reanalysed data set ERA5-Land in 0.1°x0.1° resolution (of CDS), namely the indicators:

Surface solar radiation [MWs/m^2] – variable "Surface solar radiation downwards"
Temperature [K] – variable "2m temperature"
Wind speed [m.s^{-1}] – calculated based on variables "10m u-component of wind" and "10m v-component of wind"
Relative humidity [%] – calculated based on variables "2m temperature" and "2m dewpoint temperature"
Soil water – variable "Volumetric soil water layer 3", i.e. layer of 28-100 cm (used for POD only)

Wind speed (WV) is derived from the "10m u-component of wind" (10U) and "10m v-component of wind" (10V) according to relation

$$WV = \sqrt{(10U)^2 + (10V)^2} \qquad \text{(A2.3)}$$

Relative humidity (RH) is derived by means of the saturated water vapour pressure (e_t) as a function of "2m temperature" (2T) and "2m dew point temperature" (2D) according to relation

$$RH = \frac{e_{2D}}{e_{2T}} \cdot 100, \text{ with} = e_t = 6.1365^{\frac{17.502 \cdot t}{24097+t}} \qquad \text{(A2.4)}$$

where t is 2T and 2D, respectively.

In the coastal areas (where the data from ERA5-Land are not available), the same parameters from the reanalysed data set ERA5 in 0.25°x0.25° resolution are applied. Next to this, the following data (not available in the ERA5-Land data set) from the ERA5 data set is also used:

Friction velocity [m.s^{-1}] – variable "Friction velocity". The friction velocity (also known as the shear-stress velocity) has the dimensions of velocity.

Next to the meteorological data of ERA5-Land and ERA5, the following indicators based on the meteorological ECWMF's IFS (Integrated Forecasting System) data and coming from the CHIMERE pre-processing are used, being the hourly data for 2020 in 0.1°x0.1° resolution:

Obukhov length [m] – the stability of the atmospheric surface layer expressed in terms of the Obukhov length L (1/L = 0 if the atmosphere is neutral, 1/L < 0 if the atmosphere is unstable, 1/L > 0 if the atmosphere is stable).

Air density [molec/cm^3] – expressed the number of the molecules in cm^{-3}.

Most of the meteorological parameters are used for POD_6 maps only. For other maps than POD_6, annual aggregations based on hourly data are used, namely for the parameters:

Wind speed	– annual average [m/s^1], year 2020
Relative humidity	– annual average [%], year 2020
Surface solar radiation	– annual average of daily sum [MWs/m^2], year 2020

All meteorological data were re-gridded and converted into the reference EEA 1x1 km^2 grid, 10x10 km^2 grid and 2x2 km^2 grid, in the ETRS89-LAEA5210 projection.

Altitude

The altitude data field (in meters) of Global Multi-resolution Terrain Elevation Data 2010 (GMTED2010) is used, with an original grid resolution of 15x15 arcseconds (some 463x463 m at 60N). Source: U.S. Geological Survey Earth Resources Observation and Science, see Danielson and Gesch (2011). The field is converted into the ETRS 1989 LAEA projection. (The resolution after projection was 449.2x449.2 m). In the following step, the raster dataset was resampled to 100x100 m^2 resolution and shifted to the extent of EEA reference grid. As a final step, the dataset was spatially aggregated into 1x1 km^2, 2x2 km^2 and 10x10 km^2 resolutions.

Population density and population totals

Population density (in inhbs/km^2, census 2011) is based on Geostat 2011 grid dataset, Eurostat (2014). The dataset is in 1x1 km^2 resolution, in the EEA reference grid.

For regions not included in the Geostat 2011, alternative sources were used. Primarily, JRC (Joint Research Centre) population data in resolution 100x100 m^2 were used (JRC, 2009). The JRC 100x100 m^2 population density data is spatially aggregated into the reference 1x1 km^2 EEA grid. For regions that are neither included in the Geostat 2011 nor in the JRC database, population density data from ORNL LandScan Global Population Datase, https://landscan.ornl.gov/ was used. This dataset in 30x30 arcsec resolution; based on the annual mid-year national population estimates for 2008 (from the Geographic Studies Branch, US Bureau of Census, http://www.census.gov) was earlier re-projected and converted from its original WGS1984 30x30 arcsecs grids into EEA's reference projection ETRS89-LAEA5210 at 1x1 km^2 resolution by the EEA (EEA, 2010). The areas lacking Geostat 2011 data, and supplemented with JRC or ORNL data were: Gibraltar (JRC); Faroe Islands, British crown dependencies (Jersey, Guernsey and Man) and northern Cyprus (ORNL). As such, the Geostat 2011 1x1 km^2 data and these supplements cover the entire mapping area.

To verify the consistency of merging Geostat 2011 with JRC and ORNL data, the Geostat 2011 data were compared to the JRC supplemented with ORNL data on the basis of the national population totals of the individual countries. Additionally, the national population totals for the Geostat 2011 gridded data were verified with the Eurostat national population data for 2020 (Eurostat, 2022). Figure A2.1 presents both comparisons. From these verifications, one can conclude a high correlation of the national population totals of each data source. Slight underestimation of the supplemented JRC and ORNL data in comparison with the Geostat 2011 data can be seen, which is caused by the fact that the Geostat 2011 data is more up-to-date than both the JRC and the ORNL data source. Geostat 2011 and

Eurostat 2020 data correlate even better and leads to a similar conclusion. Based on this, in the further calculations on national population totals the actual Eurostat data for 2020 (Eurostat, 2022) were used, as described further.

Figure A2.1: Correlation of national population totals for JRC supplemented with ORNL (left) and Eurostat 2020 (right) with Geostat 2011

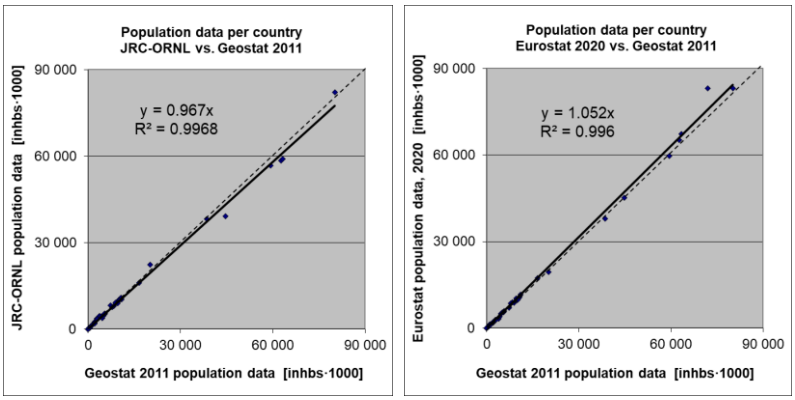

Population density data can be used to classify the spatial distribution of each type of area (rural, urban or mixed population density) in Europe. This information is used to select and weight the air quality values, grid cell by grid cell and merge them into a final combined map (Annex 1). Furthermore, it is used to estimate population health exposure and percentages above standards per country, large regions, EU-27 and for the total mapping area, including involved uncertainties. These activities take place on the 1x1 km^2 resolution grid in accordance with the recommendations of Horálek et al. (2010). The supplemented Geostat data (as described above) are used in all the calculations.

National population totals presented in the exposure tables of this paper are based on Eurostat national population data for 2020 (Eurostat, 2022). For France, Portugal and Spain, the population totals of areas outside the mapping area (i.e. French oversea departments Azores, Madeira and Canarias) are subtracted. For Andorra, Bosnia and Herzegovina, Monaco, San Marino, Faroe Islands and Crown dependencies with no data for 2020 in the Eurostat database, the population totals are based on UN (2021). For Cyprus, population of the northern part of Cyprus (based on http://www.devplan.org) is added to the population total based on Eurostat.

Land cover

CORINE Land Cover 2018 (CLC2018) – grid 100 x 100 m^2, Version 2020_20 is used (EU, 2020). For Andorra that is missing is this database, World Land Cover at 30m resolution from MDAUS BaseVue 2013 (MDA, 2015) resampled to 100m resolution is used. For areas that are neither included in the CLC2018 nor in the World Land Cover database (i.e. Jan Mayen and some border areas), ESA Climate Change Initiative Global Land Cover for 2018 (ESA, 2019) is used, resampled to 100m resolution.
In agreement with Horálek et al. (2017b), the 44 CLC classes have been re-grouped into the 8 more general classes. In this paper four of these general classes are used, see Table A2.2.

Two aggregations are used, i.e. into 1x1 km^2 grid and into the circle with radius of 5 km. For each general CLC class, the high land use resolution is spatially aggregated into the 1x1 km^2 EEA standard grid resolution. The aggregated grid square value represents for each general class the total area of this class as percentage of the total 1x1 km^2 square area. For details, see Horálek et al. (2017b).

Table A2.2: General land cover classes, based on CLC2018 classes, used in mapping

Label	General class description	CLC classes grid codes	CLC classes codes	CLC classes description
HDR	High density residential areas	1	111	Continuous urban fabric
LDR	Low density residential areas	2	112	Discontinuous urban fabric
AGR	Agricultural areas	12-22	211-244	Agricultural areas
NAT	Natural areas	23-34	311-335	Forest and semi natural areas

Road type vector data

GRIP (Meijer et al., 2018) vector road type data provided by the Netherlands Environmental Assessment Agency (PBL) are used for the weighting procedure of the urban background and the urban traffic map layers (Annex 1, Section A1.1). The road types are distributed into 5 classes, from highways to local roads and streets. In agreement with Horálek et al. (2017b), road classes No. 1 “Highways”, No. 2 “Primary roads” and No. 3 “Secondary roads” are used.

Percentage of the area influenced by traffic is represented by buffers around the roads: for the individual classes 1-3 and for classes 1-3 together, at all 1x1 km^2 grid cells; a buffer of 75 metres distance at each side from each road vector is taken for the roads of classes 1 and 2, while a buffer of 50 metres is taken for the roads of class 3. For details, see Horálek et al. (2017b).

Satellite data

The annual average NO_2 dataset was constructed based on data from the TROPOspheric Monitoring Instrument (TROPOMI) onboard of the Sentinel-5 Precursor satellite (Veefkind et al., 2012). All available swath-based Level-2 data with an irregular pixel geometry was acquired for the year 2020. The spatial resolution of the product was 5.5 km by 3.5 km. The product used is the S5P_OFFL_L2__NO2 product (van Geffen et al., 2019, 2020) and it provides the tropospheric vertical column density of NO_2, i.e. a vertically integrated value over the entire troposphere. All overpasses for a specific day were then mosaicked using HARP (https://stcorp.github.io/harp/doc/html/index.html) and retrievals with a quality assurance values greater than 0.75 (indicating high quality and cloud-free conditions) were gridded to a regular projected grid for all area with a 1x1 km^2 spatial resolution in a ETRS89 / ETRS-LAEA (EPSG 3035) projection. The daily gridded files were subsequently averaged to an annual mean. I.e. the parameter used is

NO_2 – annual average tropospheric vertical column density (VCD) [number of NO_2 molecules per cm^2 of earth surface], year 2020 (aggregated from cloud-free high-quality daily data).

Soil hydraulic properties data

JRC data called "Maps of indicators of soil hydraulic properties for Europe" in 1x1 km^2 resolution are used for POD_6 calculations, JRC (2016). Namely the following indicators are used:

Wilting Point – water content at wilting point [cm^3/cm^3]
Field Capacity – water content at field capacity [cm^3/cm^3]

Annex 3 Technical details and mapping uncertainties

This annex contains technical details on the linear regression models and the residual kriging, including the performance. Furthermore, uncertainty estimates for the maps of the indicators are given.

A3.1 PM_{10}

Technical details on the mapping and uncertainty estimates for both PM_{10} indicators maps annual average (Map 2.1) and 90.4 percentile of daily means (Map 2.2) are presented in this section.

Technical details on the mapping

Table A3.1 presents the estimated parameters of the linear regression models (c, a_1, a_2, …) and of the residual kriging (nugget, sill, range) and includes the statistical indicators of both the regression and the kriging, for both PM_{10} indicators. The linear regression and ordinary kriging of its residuals are applied on the logarithmically transformed data of both measurement and modelled PM_{10} values. In Table A3.1 the standard error and variogram parameters (nugget, sill and range) refer to these transformed data, whereas RMSE and bias refer to the interpolation after a back-transformation. Since 2017 maps, an updated methodology as developed and tested under Horálek et al. (2019) has been used, i.e. including land cover among the supplementary data and using the traffic urban map layer.

The adjusted R^2 and standard error are indicators for the fit of the regression relationship, where the adjusted R^2 should be as close to 1 as possible and the standard error should be as small as possible. The adjusted R^2 for the rural areas was 0.62 at the annual average and 0.64 at the 90.4 percentile of daily means (P90.4); for the urban background areas 0.45 at both the annual average and the P90.4; for the urban traffic areas 0.50 at the annual average and 0.45 at the P90.4.

Table A3.1: Parameters and statistics of linear regression model and ordinary kriging of PM_{10} indicators annual average and 90.4 percentile of daily means for 2020 in rural, urban background and urban traffic areas for the final combined map

		Annual average			90.4 percentile of daily means		
		Rural areas	Urb. b. ar.	Urb. tr. ar.	Rur. ar.	Urb. b. ar.	Urb. tr. ar.
Linear regresion model (LRM, Eq. A1.3)	c (constant)	0.98	0.80	1.66	1.20	0.88	2.12
	a1 (log. CAMS model)	0.812	0.883	0.61	0.764	0.880	0.55
	a2 (altitude GMTED)	-0.00021			-0.00016		
	a3 (wind speed)	-0.053		-0.049	-0.045		-0.075
	a4 (relative humidity)	*non signif.*			*non signif.*		
	a5 (land cover NAT)	-0.002			-0.002		
	Adjusted R^2	**0.62**	**0.45**	**0.50**	**0.64**	**0.45**	**0.45**
	Stand. Error [µg/m^3]	**0.25**	**0.30**	**0.25**	**0.23**	**0.33**	**0.29**
Ordinary kriging (OK) of LRM residuals	Nugget	0.018	0.020	0.015	0.018	0.024	0.028
	Sill	0.053	0.055	0.038	0.049	0.072	0.068
	Range [km]	1000	130	450	1000	130	450
LRM + OK of its residuals	**RMSE [µg/m^3]**	**3.4**	**5.9**	**3.9**	**6.3**	**11.9**	**8.2**
	Relative RMSE [%]	**23.5**	**27.0**	**18.5**	**25.1**	**30.8**	**22.0**
	Bias (MPE) [µg/m^3]	**-0.1**	**0.0**	**-0.1**	**-0.2**	**0.1**	**-0.3**

RMSE (the smaller the better) and bias (the closer to zero the better), highlighted by orange, are the cross-validation indicators, showing the quality of the resulting map. The bias indicates to what extent the predictions are under- or overestimated on average. Further in this section, more detailed uncertainty analysis is presented.

Uncertainty estimated by cross-validation

Using RMSE as the most common indicator, the absolute mean uncertainty of the final combined map at areas 'in between' the station measurements (i.e. at locations without measurements, as long as they are within the area covered by the measurements) can be expressed in µg/m^3. Table A3.1 shows that the absolute mean uncertainty of the final combined map of PM_{10} annual average and 90.4 percentile of daily means expressed by RMSE is 3.4 µg/m^3 and 6.3 µg/m^3 for the rural areas, 5.9 µg/m^3 and 11.9 µg/m^3 for the urban background areas, and 3.9 µg/m^3 and 8.2 µg/m^3 for the urban traffic areas, respectively. Alternatively, one can express this uncertainty in relative terms by relating the absolute RMSE uncertainty to the mean air pollution indicator value for all stations. This relative mean uncertainty (Relative RMSE) of the final combined map of PM_{10} annual average and 90.4 percentile of daily means is 23.5 % and 25.1 % for rural areas, 27.0 % and 30.8 % for urban background areas, and 18.5 % and 22.0 % for urban traffic areas, respectively. These quite high numbers in urban background areas compared to previous years up to 2015 are caused by inclusion of Türkiye since 2016 mapping. For the mapping results without Türkiye, the relative mean uncertainty is 20.0 % and 22.4 % for rural areas, 19.8 % and 23.7 % for urban background areas and 18.4 % and 21.9 % for urban traffic areas, respectively. Nevertheless, the relative uncertainty values including Türkiye fulfil the data quality objectives for models as set in Annex I of the Air Quality Directive (EC, 2008).

Figure A3.1 shows the cross-validation scatter plots, obtained according to Annex 1, Section A1.4 for rural, urban background and urban traffic areas, for both PM_{10} indicators. The R^2 indicates that the variability is attributable to the interpolation for about 70 % at the rural areas for both indicators, for about 71 % and 70 % at the urban background areas, and for about 79 % and 77 % at the urban traffic areas, for the annual average and the 90.4 percentile of daily means, respectively.

Figure A3.1: Correlation between cross-validated predicted (y-axis) and measurement values for PM_{10} indicators annual average (top) and 90.4 percentile of daily means (bottom) for 2020 for rural (left), urban background (middle) and urban traffic (right) areas

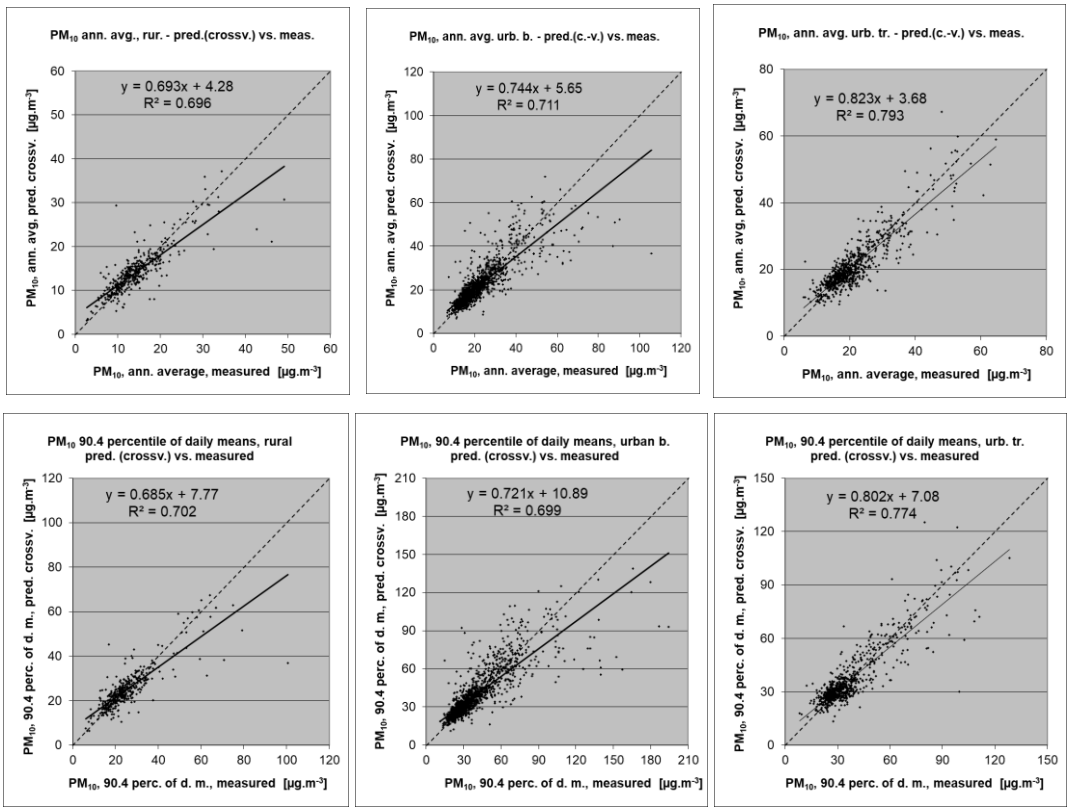

The trend line in the scatter-plots deviates at the lowest values somewhat above, and at higher values below the symmetry axis, indicating that the interpolation methods tend to underestimate the high concentrations and overestimate the low concentrations. For example, in urban background areas for annual average an observed value of 40 µg/m^3 is estimated in the interpolations to be about 35 µg/m^3, about 11 % lower. This underestimation at high values is common to all spatial interpolation methods. It could be reduced by either using a higher number of stations with an improved spatial distribution, or by introducing an improved regression that uses either other supplementary data or more advanced chemical transport model (resp. model in finer resolution).

Comparison of point measurement values with the predicted grid value

In addition to the above point observation – point prediction cross-validation, a simple comparison has been made between the point observation values and interpolated prediction values spatially averaged at grid cells. This point observation – grid averaged prediction comparison indicates to what extent the predicted value of a grid cell represents the corresponding measurement values at stations located in that cell. The comparison has been made primarily for the separate rural, urban background and urban traffic map layers at 1x1 km^2 resolution. (One can directly relate this comparison result to the cross-validation results of Figure A3.1). Apart from this, the comparison has been done also for the final combined maps at the same 1x1 km^2 resolution. Figure A3.2 shows the scatterplots for these comparisons, for PM_{10} annual average only as an illustration. The results of the point observation – point prediction cross-validation of Figure A3.1 and those of the point observation – grid averaged prediction validation for separate rural, urban background and urban traffic map layers, and for the final combined maps are summarised in Table A3.2 for both PM_{10} indicators.

Figure A3.2: Correlation between predicted grid values from rural (upper left), urban background (upper middle) and urban traffic (upper right) map layer and final combined map (all bottom) (y-axis) versus measurements from rural (left), urban/suburban background (middle) and urban/suburban traffic stations (right) (x-axis) for PM_{10} annual average 2020

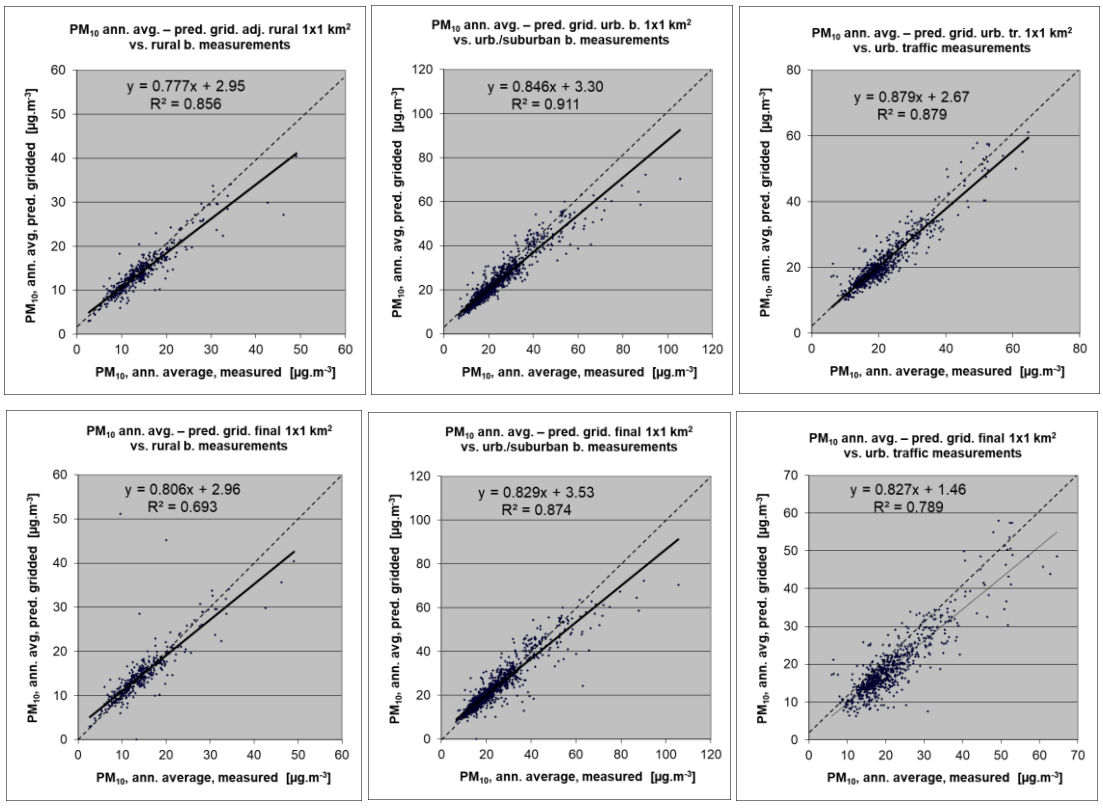

Table A3.2: Statistical indicators from the scatter plots for the predicted grid values from separate (rural, urban background or urban traffic) map layers and final combined map versus the measurement point values for rural (upper left), urban background (upper right) and urban traffic (bottom left) stations for PM_{10} indicators annual average (top) and 90.4 percentile of daily means (bottom) for 2020

PM_{10}	rural backgr. stations				urban/suburban backgr. stations			
	RMSE	bias	R^2	lin. r. equation	RMSE	bias	R^2	lin r. equation
Annual average								
cross-val. prediction, separate (r or ub) map layer	3.0	0.0	0.696	y = 0.693x + 4.28	5.9	0.0	0.711	y = 0.744x + 5.65
grid prediction, 1x1 km^2 separ. (r or ub) map layer	2.4	-0.2	0.856	y = 0.777x + 2.95	3.4	-0.1	0.911	y = 0.846x + 3.30
grid prediction, 1x1 km^2 final combined map	3.5	0.2	0.693	y = 0.806x + 2.96	4.0	-0.2	0.827	y = 0.829x + 3.53
90.4 percentile of daily means								
cross-val. prediction, separate (r or ub) map layer	6.3	-0.2	0.702	y = 0.685x + 7.77	12.5	0.1	0.699	y = 0.721x + 10.89
grid prediction, 1x1 km^2 separ. (r or ub) map layer	4.8	-0.4	0.843	y = 0.758x + 5.65	6.8	-0.2	0.909	y = 0.830x + 6.38
grid prediction, 1x1 km^2 final combined map	6.4	0.3	0.711	y = 0.804x + 5.28	8.1	-0.6	0.867	y = 0.805x + 6.95

PM_{10}	urban/suburban traffic stations			
	RMSE	bias	R^2	lin. r. equation
Annual average				
cross-valid. prediction, urban traffic map layer	3.9	-0.1	0.793	y = 0.823 + 3.68
grid prediction, 1x1km^2 urban traffic map layer	3.0	0.1	0.879	y = 0.879x + 2.67
grid prediction, 1x1 km^2 final combined map	4.6	-2.2	0.789	y = 0.827x + 1.46
90.4 percentile of daily means				
cross-valid. prediction, urban traffic map layer	8.2	-0.3	0.774	y = 0.802x + 7.08
grid prediction, 1x1km^2 urban traffic map layer	5.3	0.2	0.905	y = 0.886x + 4.43
grid prediction, 1x1 km^2 final combined map	9.1	-3.8	0.767	y = 0.794x + 3.83

By comparing the scatterplots and the statistical indicators for the separate rural, urban background and urban traffic map layers with the final combined map, one can evaluate the level of representation of the rural, urban background and urban traffic areas in the final combined map. Both the rural and the urban air quality are fairly well represented in the 1x1 km^2 final combined map, while the traffic air quality is underestimated in this spatial resolution. One can conclude that the final combined map in 1x1 km^2 resolution is representative for rural and urban background areas, but not for urban traffic areas.

The Table A3.2 shows a better relation (i.e. lower RMSE, higher R^2, smaller intercept and slope closer to 1) between station measurements and the interpolated values of the corresponding grid cells at either rural, urban background or urban traffic areas than it does at the point cross-validation predictions. That is because the simple comparison between point measurements and the gridded interpolated values shows the uncertainty at the actual station locations (points), while the point cross-validation prediction simulates the behaviour of the interpolation at point positions assuming no actual measurement would exist at that point. The uncertainty at measurement locations is introduced partly by the smoothing effect of the interpolation and partly by the spatial averaging of the values in the 1x1 km^2 grid cells. The level of the smoothing effect leading to underestimation at areas with high values is there smaller than in situations where no measurement is represented in such areas. For example, in rural areas the predicted interpolation gridded annual average value in the separate rural map will be about 37 µg/m^3 at the corresponding station with the measurement value of 40 µg/m^3. This means an underestimation of about 7 %. It is a slightly less than the prediction underestimation of 11 % at the same point location, when leaving out this one actual measurement point and the interpolation is done without this station (see the previous subsection).

A3.2 $PM_{2.5}$

Technical details and uncertainty estimates for Map 2.3 with the $PM_{2.5}$ annual average are presented in this section.

Technical details on the mapping

Like for PM_{10}, an updated methodology as developed and tested under Horálek et al. (2019) has been used, i.e. including the land cover among supplementary data and using the traffic urban map layer.

Table A3.3 presents the regression coefficients determined for pseudo $PM_{2.5}$ stations data estimation, based on the 869 rural and urban/suburban background and 341 urban/suburban traffic stations that have both $PM_{2.5}$ and PM_{10} measurements available (see Section 2.1.1).

Table A3.3: Parameters and statistics of linear regression model for generating pseudo $PM_{2.5}$ annual average data for 2020 in rural and urban background (left) and urban traffic (right) areas

		Rural and urban background areas	Urban traffic areas
Linear regresion model (LRM, Eq. A1.1)	c (constant)	31.1	41.8
	b (PM_{10} measurement data)	0.680	0.488
	a1 (surface solar radiation)	-0.004	-0.004
	a2 (latitude)	-0.384	-0.557
	a3 (longitude)	0.078	0.107
	Adjusted R^2	**0.84**	**2.14**
	Standard Error [$\mu g.m^{-3}$]	**2.0**	**2.3**

Table A3.4 presents the estimated parameters of the linear regression models (c, a_1, a_2,…) and of the residual kriging (nugget, sill, range) and includes the statistical indicators of both the regression and the kriging of its residuals. The same supplementary data as in Horálek et al. (2019) has been used. Like in the case of PM_{10}, the linear regression is applied on the logarithmically transformed data of both measurement and modelled $PM_{2.5}$ values. Thus, the standard error and variogram parameters refer to these transformed data, whereas RMSE and bias refer to the interpolation after the back-transformation.

Table A3.4: Parameters and statistics of linear regression model and ordinary kriging of $PM_{2.5}$ annual average 2020 in rural, urban background and urban traffic areas for final combined map

$PM_{2.5}$		Annual average		
		Rural areas	Urban b. areas	Urban tr.. areas
Linear regresion model (LRM, Eq. A1.3)	c (constant)	0.52	0.76	0.78
	a1 (log. CAMS model)	0.907	0.794	0.778
	a2 (altitude GMTED)	-0.00027		
	a3 (wind speed)	-0.036		
	a4 (land cover NAT1)	-0.0017		
	Adjusted R^2	**0.67**	**0.47**	**0.64**
	Standard Error [µg.m^{-3}]	**0.29**	**0.30**	**0.26**
Ordinary kriging (OK) of LRM residuals	nugget	0.028	0.014	0.015
	sill	0.066	0.069	0.041
	range [km]	673	490	190
LRM + OK of its residuals	**RMSE [µg.m^{-3}]**	**2.4**	**2.5**	**2.2**
	Relative RMSE [%]	**27.5**	**20.9**	**19.3**
	Bias (MPE) [µg.m^{-3}]	**-0.1**	**0.0**	**0.0**

The adjusted R^2 and standard error are indicators for the quality of the fit of the regression relation. The adjusted R^2 is 0.67 for the rural areas, 0.47 for urban background areas and 0.64 for urban traffic areas. Quite weaker regression relation in the urban background areas causes a higher impact of the interpolation part of the interpolation-regression-merging mapping methodology in these areas.

RMSE and bias – highlighted in orange – are the cross-validation indicators, showing the quality of the resulting map; the bias indicates to what extent the predictions are under- or overestimated on average. Only stations with $PM_{2.5}$ measurement data are used for calculating the RMSE and the bias (i.e. the pseudo $PM_{2.5}$ stations are not used). These statistical indicators are calculated excluding the pseudo stations because they are estimated values only, not actual measurement values. According to Denby et al (2011), the pseudo $PM_{2.5}$ data does not satisfy the quality objectives for fixed monitoring alone. The pseudo stations are used as they improve the mapping estimate, whereas the actual measurements can be used for evaluating the quality of the map. For the future, it will be considered to quit the application of the $PM_{2.5}$ pseudo stations as the current number of the actual $PM_{2.5}$ measurement stations has increased over time such that the use of pseudo $PM_{2.5}$ stations may not contribute enough any longer to improve the mapping estimates.

Due to the lack of rural stations in Türkiye for $PM_{2.5}$, no proper interpolation results could be presented for this country in a rural map, so the estimated $PM_{2.5}$ values for Türkiye are not presented in the final map. Thus, the stations located in Türkiye have not been used in the uncertainty estimates (although used in the mapping process), as they lie outside the mapping area.

Uncertainty estimated by cross-validation

Table A3.4 shows that the absolute mean uncertainty of the final combined map of $PM_{2.5}$ annual average expressed as RMSE is 2.4 µg/m^3 for the rural areas, 2.5 µg/m^3 for the urban background areas and 2.2 µg/m^3 for the urban traffic areas. On the other hand, the relative mean uncertainty (Relative RMSE) of the final combined map of $PM_{2.5}$ annual average is 27.5 % for rural areas, 20.9 % for urban background areas and 19.3 % for urban traffic areas. These relative uncertainty values fulfil the data quality objectives for models as set in Annex I of the Air Quality Directive (EC, 2008).

Figure A3.3 shows the cross-validation scatter plots, obtained according to Section A1.3, for different area types. The R^2 indicates that about 74 % of the variability is attributable to the interpolation for the rural areas, 73 % for the urban background areas and 82 % for the urban traffic areas.

Figure A3.3: Correlation between cross-validated predicted and measurement values for $PM_{2.5}$ annual average 2020 for rural (left), urban background (middle) and urban traffic (right) areas

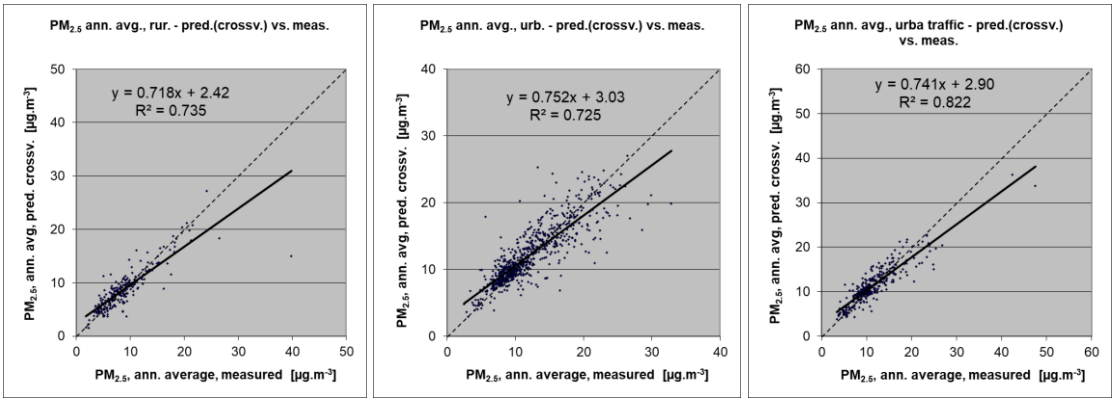

The scatter plots indicate that in areas with high concentrations the interpolation methods tend to underestimate the levels. For example, in rural areas an observed value of 25 µg/m^3 is estimated in the interpolations to be about 20 µg/m^3, which is an underestimated prediction of about 20 %. This underestimation at high values is an inherent feature of all spatial interpolations. It could be reduced by either using a higher number of the stations at improved spatial distribution, or by introducing a closer regression that uses either other supplementary data or more improved CTM output.

Comparison of point measurement values with the predicted grid value

Like for PM_{10}, a simple comparison has been made between the point observation values and interpolated prediction values spatially averaged in grid cells, in addition to the cross-validation. The comparison has been made primarily for the separate rural, urban background and urban traffic map layers at 1x1 km^2 resolution. Next to this, the comparison has been done also for the final combined maps at the same 1x1 km^2 resolution. Figure A3.4 shows the scatterplots for these comparisons.

The results of the point observation – point prediction cross-validation of Figure A3.3 and those of the point observation – grid averaged prediction validation Figure A3.4 for separate map layers and for the final combined map are summarised in Table A3.5.

Figure A3.4: Correlation between predicted grid values from rural (upper left), urban background (upper middle) and urban traffic (upper right) map layer and final combined map (all bottom) (y-axis) versus measurements from rural (left), urban/suburban background (middle) and urban/suburban traffic stations (right) (x-axis) for $PM_{2.5}$ annual average 2020

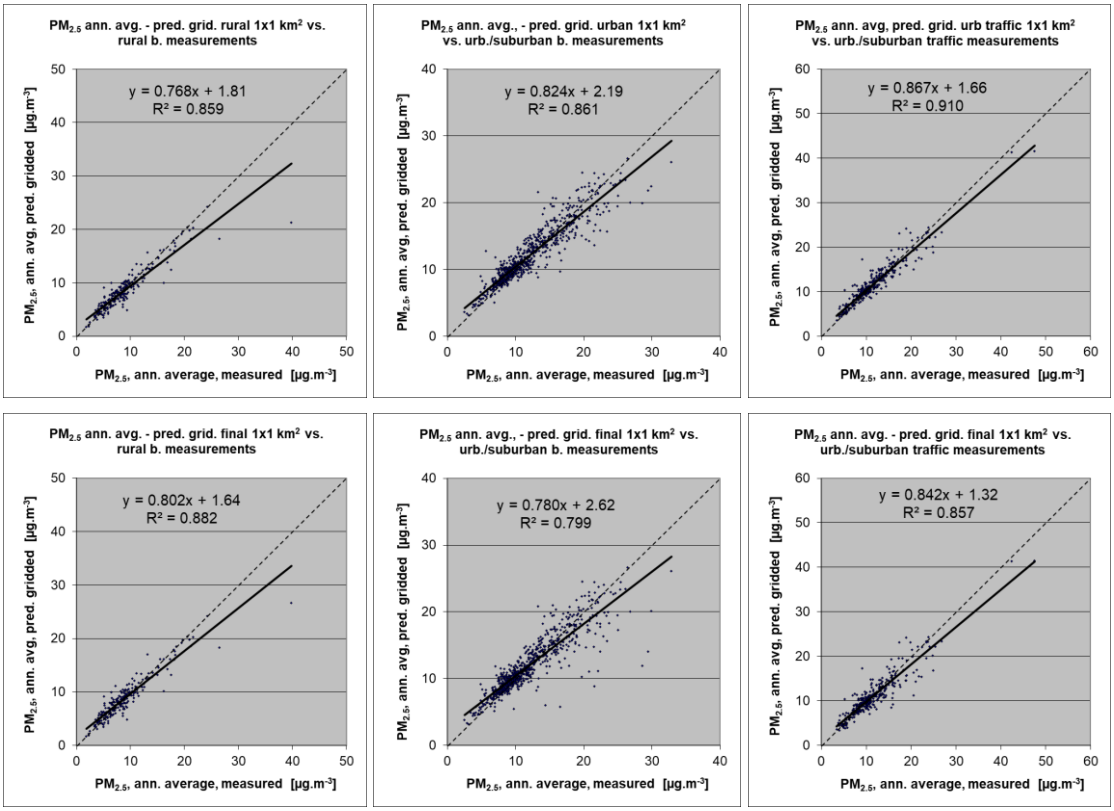

By comparing the scatterplots and the statistical indicators for separate rural, urban background and urban traffic map layers with the final combined maps, one can evaluate the level of representation of the rural, urban background and urban traffic areas in the final combined map. Similar results as for PM_{10} can be observed: the final combined map in 1x1 km^2 resolution is fairly well representative for rural and urban background areas, but not for urban traffic areas.

Like in the case of PM_{10}, Table A3.5 shows a better correlated relation with the station measurements (i.e. lower RMSE, higher R^2, smaller intercept and slope closer to 1) for the simply interpolated gridded values than for the point cross-validation predictions, at rural, urban background and urban traffic map areas. That is because the simple comparison shows the uncertainty at the actual station locations, while the cross-validation prediction simulates the behaviour of the interpolation (within the area covered by measurements) at point positions assuming no actual measurements would exist at these points.

The uncertainty at measurement locations is introduced partly by the smoothing effect of the interpolation and partly by the spatial averaging of the values in the 1x1 km^2 grid cells. For example, in urban background areas the predicted interpolation gridded value in the final map will be about 26 µg/m^3 at the corresponding station with the measurement value of 30 µg/m^3 (calculated based on the linear regression equation), which coincides with an underestimation of about 13 %.

Table A3.5: Statistical indicators from the scatter plots for the predicted grid values from separate (rural, urban background or urban traffic) map layers and final combined map versus the measurement point values for rural (upper left), urban background (upper right) and urban traffic (bottom left) stations for $PM_{2.5}$ annual average 2020

$PM_{2.5}$	rural backgr. stations				urban/suburban backgr. stations			
	RMSE	bias	R^2	lin. r. equation	RMSE	bias	R^2	lin r. equation
cross-val. prediction, separate (r or ub) map layer	2.4	-0.1	0.735	y = 0.718x + 2.42	2.5	0.0	0.725	y = 0.752x + 3.03
grid prediction, 1x1 km^2 separ. (r or ub) map layer	1.8	-0.2	0.859	y = 0.768x + 1.81	1.8	0.1	0.861	y = 0.824x + 2.19
grid prediction, 1x1 km^2 final merged map	1.7	-0.1	0.882	y = 0.802x + 1.64	2.2	0.0	0.799	y = 0.780x + 2.62

$PM_{2.5}$	urban/suburban traffic stations			
	RMSE	bias	R^2	lin. r. equation
cross-val. prediction, urban traffic map layer	2.2	0.0	0.822	y = 0.741x + 2.90
grid prediction, 1x1 km^2 urban traffic map layer	1.5	0.2	0.910	y = 0.867x + 1.66
grid prediction, 1x1 km^2 final merged map	2.0	-0.5	0.857	y = 0.842x + 1.32

A3.3 Ozone

In this section, the technical details and the uncertainty estimates are presented for the maps of ozone health-related indicators 93.2 percentile of maximum daily 8-hour means, SOMO35 and SOMO10 (Maps 3.1-3.3), as well as for the maps of ozone vegetation-related indicators AOT40 for vegetation and AOT40 for forests (Maps 3.4 and 3.5). Next to this, the details of POD_6 maps are presented.

Technical details on the mapping

Table A3.6 presents the estimated parameters of the linear regression models and of the residual kriging, including the statistical indicators of both the regression and the kriging.

The adjusted R^2 and standard error show the quality of the fit of the regression relation. For the rural areas, all indicators show the value of the adjusted R^2 between 0.4 and 0.6. For the urban areas, the adjusted R^2 is 0.37 for 93.2 percentile of daily 8-hour maximums, 0.34 for SOMO35 and 0.14 for SOMO10. For the vegetation-related indicators the urban maps are not constructed. RMSE and bias – highlighted by orange – are the cross-validation indicators, showing the quality of the resulting map.

Table A3.6: Parameters and statistics of linear regression model and ordinary kriging for ozone indicators 93.2 percentile of maximum daily 8-hourly means, SOMO35 and SOMO10 in rural and urban areas for the final combined map and for O_3 indicators AOT40 for vegetation and for forests in rural areas for 2020

		93.2 perc. of dmax 8h		SOMO35		SOMO10		AOT40v	AOT40f
		Rur. areas	Urb. ar.	Rur. ar.	Urb.ar.	Rur. ar.	Urb.ar.	Rur. ar.	Rur. ar.
Linear regresion model (LRM, Eq. A1.3)	c (constant)	-13.6	14.5	256	428	1990	5654	1271	3373
	a1 (CAMS model)	1.19	0.96	0.85	0.62	0.82	0.48	0.89	0.89
	a2 (altitude GMTED)	0.0096		2.06		2.81		5.01	10.12
	a3 (wind speed)		-1.87		-389.5		*n. sign.*		
	a4 (s. solar radiation)	*n.sign.*	*n.sign.*	*n.sign.*	*n.sign.*	*n.sign.*	*n. sign.*	*n. sign.*	*n. sign.*
	Adjusted R^2	**0.54**	**0.37**	**0.46**	**0.34**	**0.41**	**0.14**	**0.57**	**0.58**
	Stand. Err. [µg/m³·x]*	**8.7**	**11.4**	**1550**	**1553**	**2450**	**3204**	**4173**	**7877**
Ord. krig. (OK) of LRM	Nugget	12	54	1.3E+06	1.0E+06	3.3E+06	2.8E+06	7.2E+06	2.7E+07
	Sill	49	65	1.9E+06	1.4E+06	5.0E+06	4.6E+06	1.4E+07	4.5E+07
	Range [km]	60	550	147	540	120	550	120	110
LRM + OK of its residuals	**RMSE [µg/m³·x]***	**7.7**	**10.0**	**1485**	**1347**	**2450**	**2675**	**3923**	**7266**
	Relative RMSE [%]	**6.9**	**9.2**	**29.8**	**31.8**	**11.8**	**14.5**	**37.7**	**31.6**
	Bias (MPE) [µg/m³·x]*	**0.4**	**0.1**	**45**	**3**	**25**	**-14**	**118**	**284**

* Units: 93.2 percentile of daily 8-h maximums: [µg/m³], SOMO35 and SOMO10: [µg/m³·d], AOT40v and AOT40f: [µg/m³·h].

Uncertainty estimated by cross-validation

The basic uncertainty analysis is provided by cross-validation. Table A3.6 shows both absolute and relative mean uncertainty, expressed by RMSE and Relative RMSE. The relative mean uncertainty of the 2020 ozone map is around 7-9 % for the 93.2 percentile of daily 8-h maximums, around 30-32 % for SOMO35, around 12-15 % for SOMO10 and around 32-38 % at AOT40 indicators. The small levels of the relative uncertainty for the 93.2 percentile of maximum daily 8-h means and SOMO10 are highly influenced by the low ratio between the relevant standard error and mean calculated based on all annual station concentration data: for these two indicators the ratio is at the level of about 0.13- 0.19, while for SOMO35 and for both AOT40 indicators it is at the level of about 0.46-0.61.

Figure A3.5 shows the cross-validation scatter plots for both the rural and urban areas of the 2020 map for the health-related ozone indicators.

The R^2, an indicator for the interpolation correlation with the observations, shows that for the health-related ozone indicators, about 42-63 % is attributable to the interpolation in the rural areas, while in the urban areas it is about 41-51 %.

The scatter plots indicate that the higher values are underestimated and the lower values somewhat overestimated by the interpolation method; a typical smoothing effect inherent to the interpolation method with the linear regression and its residuals kriging. For example, in the case of the 93.2 percentile of daily 8-h maximums, in urban areas (Figure A3.5, upper right panel) an observed value of 150 µg/m^3 is estimated in the interpolation as 131 µg/m^3, which is 13 % lower. Or, in the case of SOMO35, in rural areas (Figure A3.5, middle left panel) an observed value of 9 000 µg/m^3·d is estimated in the interpolation as about 7 100 µg/m^3·d, which is 21 % lower.

Figure A3.5: Correlation between cross-validated predicted (y-axis) and measurement values for ozone indicators 93.2 percentile of max. daily 8-hourly means (top), SOMO35 (middle) and SOMO10 (bottom) for 2020 for rural (left) and urban (right) areas

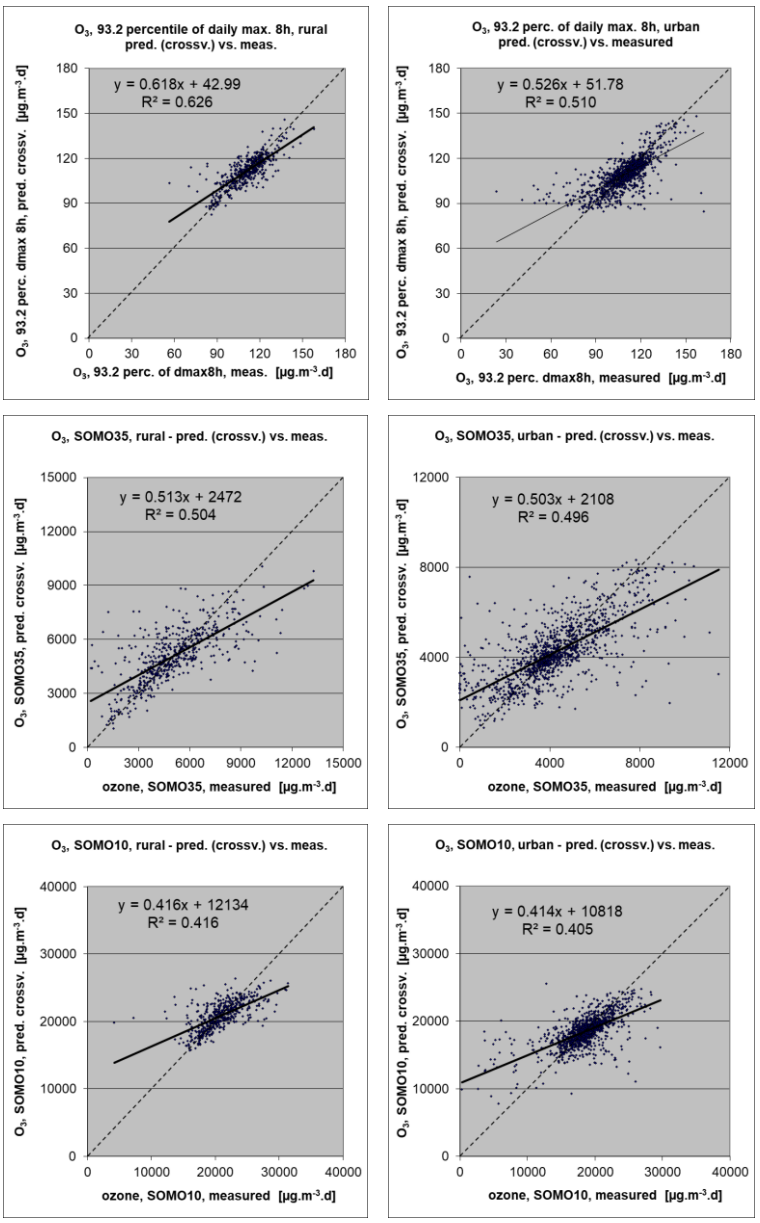

Figure A3.6 shows the cross-validation scatter plots of the AOT40 for both vegetation and forests. R^2 indicates that about 62 % of the variability is attributable to the interpolation in the case of AOT40 for vegetation, while for AOT40 for forests it is about 64 %.

The cross-validation scatter plots show again that in areas with higher accumulated ozone concentrations the interpolation methods tend to deliver underestimated predicted values. For example, in agricultural areas (Figure A3.6, left panel) an observed value of 25 000 µg/m^3·h is estimated in the interpolation as about 20 000 µg/m^3·h, i.e. an underestimation of about 20 %. In addition, an overestimation at the lower end of predicted values occurred. One could reduce this under- and overestimation by extending the number of measurement stations and by optimising the spatial distribution of those stations, specifically in areas with elevated values over years.

Figure A3.6: Correlation between cross-validated predicted (y-axis) and measurement values for ozone indicators AOT40 for vegetation (left) and AOT40 for forests (right) for 2020 for rural areas

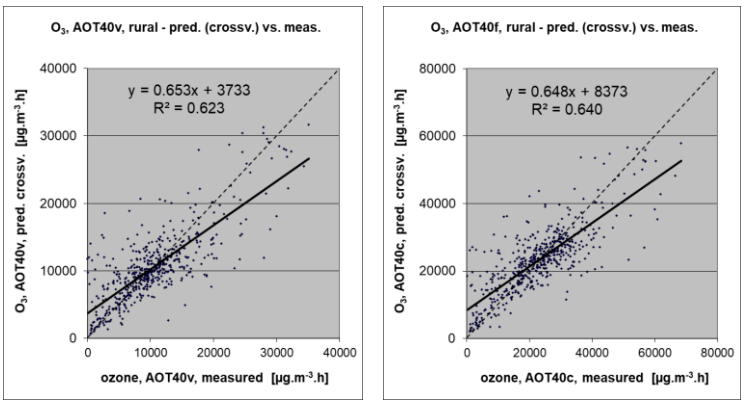

Comparison of point measurement values with the predicted grid value

In addition to the above point observation – point prediction cross-validation, a simple comparison has been made between the point observation values and interpolated predicted grid values.

For health-related indicators, the comparison has been made primarily for the separate rural and separate urban background maps at 10x10 km^2 resolution. (One can directly relate this comparison result to the cross-validation of the previous section.) Next to this, the comparison has been done also for the final combined maps at 1x1 km^2 resolution.

Figure A3.7 shows the scatterplots for these comparisons, for ozone indicator 93.2 percentile of maximum daily 8-hour means only, as an illustration.

The results of the point observation – point prediction cross-validation of Figure A3.5 and those of the point observation – grid averaged prediction validation for the separate rural and the separate urban background map, and for the final combined maps are summarised in Table A3.7. By comparing the scatterplots and the statistical indicators for the separate rural and separate urban background map with the final combined maps, one can evaluate the level of representation of the rural resp. urban background areas in the final combined maps. Both the rural and the urban air quality are fairly well represented in the 1x1 km^2 final combined map.

The uncertainty of the map layers at measurement locations is caused partly by the smoothing effect of interpolation and partly by the spatial averaging of the values in the 10x10 km^2 grid cells. The level of smoothing, which leads to underestimation in areas with high values, is weaker in areas where measurements exist than in areas where a measurement point is not available. For example, in the case of the 93.2 percentile of daily 8-h maximums, in urban areas an observed value of 150 µg/m^3 is estimated in the interpolation as about 142 µg/m^3, which is about 5 % lower. It is less than the cross-validation underestimation of 13 % at the same point location, when leaving out this one actual measurement point and the interpolation without this station is done (see the previous subsection).

Figure A3.7: Correlation between predicted grid values from rural 10x10 km² (upper left), urban 10x10 km² (bottom left) and final combined 1x1 km² (both right) map (y-axis) versus measurements from rural (top), resp. urban/suburban (bottom) background stations (x-axis) for ozone indicator 93.2 percentile of daily max. 8-hourly means for 2020

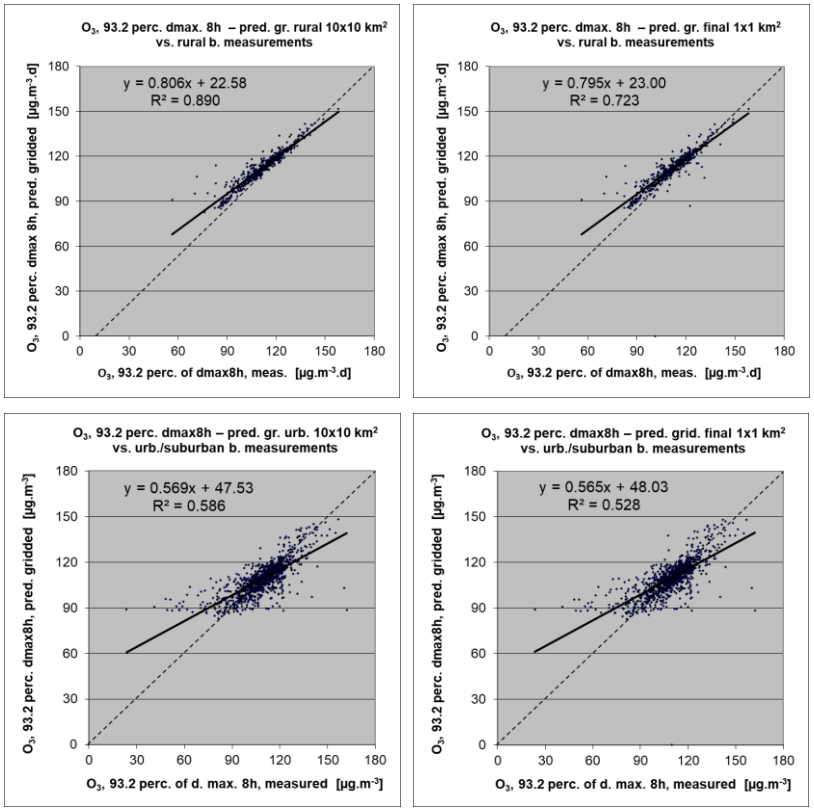

Table A3.7: Statistical indicators from the scatter plots for the predicted point values based on cross-validation and the predicted grid values from separate (rural resp. urban) 10x10 km² and final combined 1x1 km² map versus the measurement point values for rural (left) and urban (right) background stations for ozone indicators 93.2 percentile of daily max 8h means (top), SOMO35 (middle) and SOMO10 (bottom) for 2020

Ozone	rural backgr. stations				urban/suburban backgr. stations			
	RMSE	Bias	R^2	lin. r. equation	RMSE	Bias	R^2	lin r. equation
93.2 percentile of daily max. 8-hour means								
cross-val. prediction, separate (r or ub) map layer	7.7	0.4	0.626	y = 0.618x + 42.99	10.0	0.1	0.510	y = 0.526x + 51.78
grid prediction, 10x10 km² separate (r or ub) map layer	4.4	0.9	0.890	y = 0.806x + 22.58	9.2	0.1	0.586	y = 0.569x + 44.53
grid prediction, 1x1 km² final merged map	6.7	0.1	0.723	y = 0.795x + 23.00	9.9	0.6	0.528	y = 0.565x + 48.03
SOMO35								
cross-val. prediction, separate (r or ub) map layer	1485	45	0.504	y = 0.513x + 2472	1347	3	0.496	y = 0.503x + 2108
grid prediction, 10x10 km² separate (r or ub) map layer	1073	50	0.757	y = 0.644x + 1823	1197	-11	0.607	y = 0.554x + 1879
grid prediction, 1x1 km² final merged map	1140	-78	0.717	y = 0.634x + 1744	1248	90	0.570	y = 0.559x + 1961
SOMO10								
cross-val. prediction, separate (r or ub) map layer	2450	25	0.416	y = 0.416x + 12134	2675	-14	0.405	y = 0.414x + 10818
grid prediction, 10x10 km² separate (r or ub) map layer	1707	23	0.748	y = 0.594x + 8440	3860	6	0.021	y = 0.095x + 16739
grid prediction, 1x1 km² final merged map	2257	-301	0.525	y = 0.603x + 7948	4080	212	0.010	y = 0.073x + 17353

Table A3.8 presents the results of the point observation – point prediction cross-validation of Figure A3.6 and those of the point-grid validation for the rural map, for vegetation related indicators AOT40 for vegetation and AOT40 for forests. Again, one can see for both indicators a better correlation

between the station measurements and the averaged interpolated predicted values of the corresponding grid cells, than at the point cross-validation predictions, of Figure A3.6.

Table A3.8: Statistical indicators from the scatter plots for predicted point values based on cross-validation and predicted grid values from rural 2x2 km^2 map versus measurement point values for rural background stations for ozone indicators AOT40 for vegetation (top) and forests (bottom) for 2020

Ozone	rural backgr. stations			
	RMSE	bias	R^2	linear regression equation
AOT40 for vegetation				
cross-valid. prediction, rural map	3923	118	0.623	y = 0.653x + 3733
grid prediction, 2x2 km^2 rural map	2207	53	0.887	y = 0.808x + 2053
AOT40 for forests				
cross-valid. prediction, rural map	7266	284	0.64	y = 0.618x + 8373
grid prediction, 2x2 km^2 rural map	4455	144	0.873	y = 0.787x + 5047

Details of POD_6 maps

POD_6 maps have been calculated using the ozone based on the hourly ozone rural maps, hourly meteorological data and soil hydraulic properties data, according to the methodology described in Annex 1, Section A1.3.

The hourly ozone maps needed for POD_6 calculation have been calculated at the 2x2 km^2 resolution, based on rural background measurements. The maps for each hour of the year 2020 have been constructed using the same methodology as for the annual maps, i.e. the multiple linear regression followed by the kriging of its residuals (see Annex 1, Section A1.1) based on the measurement data, CAMS-ENS Forecast model output, altitude and the surface solar radiation. Table A3.9 presents the summary results of the RMSE, RRMSE and bias for the whole year, based on the annual average and percentiles of these three statistics. For bias, annual sum is also shown in addition.

Table A3.9: Annual statistics average, 2nd percentile, 25th percentile, 50th percentile (median), 75th percentile, 98th percentile and sum (where relevant) for average ozone concentration, number of stations considered, and cross-validation parameters RMSE, RRMSE and Bias of hourly ozone maps, 1.1.2020-31.12.2020. Units: µg/m^3 apart from N and RRMSE.

	Rural background areas						
	avg	p2	p25	p50	p75	p98	Sum
N	529	505	523	531	536	544	
avg	60.5	34.2	47.6	58.3	71.7	100.0	
RMSE	**14.5**	9.1	11.9	**14.0**	16.6	22.7	
RRMSE	**26.3%**	11.2%	17.0%	**25.7%**	33.8%	48.0%	
Bias	**-0.02**	-0.58	-0.15	**-0.02**	0.11	0.55	**-157**

Figure A3.8 and A3.9 presents the averages of the cross-validation indicators Bias and RMSE in the individual hours of the year 2020.

Figure A3.8: Cross-validation statistical indicator Bias of hourly ozone maps, average at rural background stations, 1.1.2020-31.12.2020

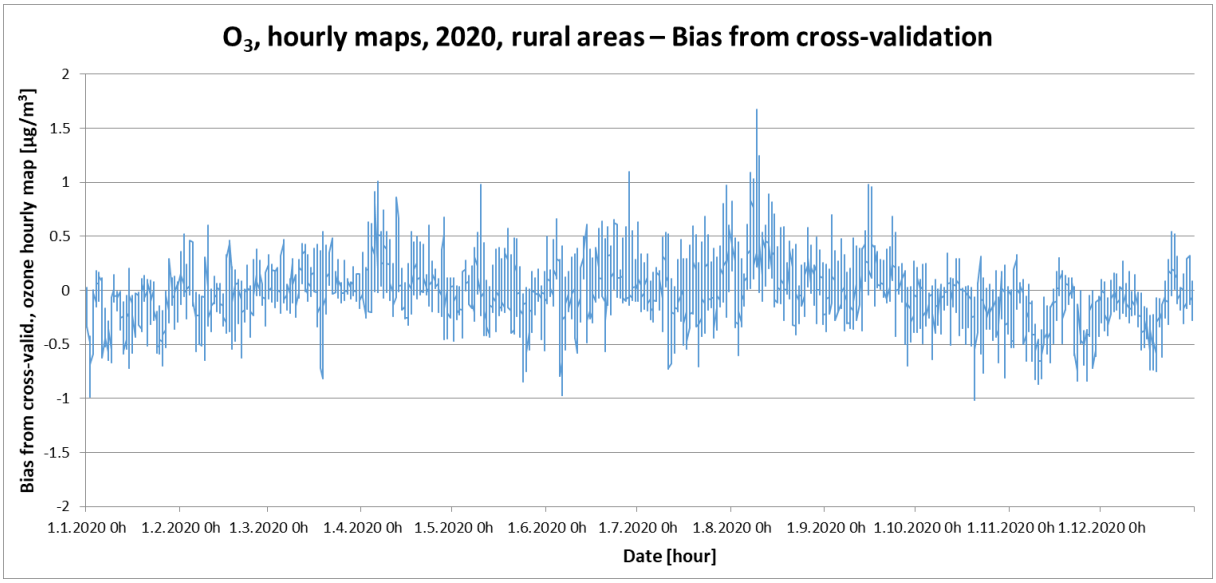

Figure A3.9: Cross-validation statistical indictor RMSE of hourly ozone maps, average at rural background stations, 1.1.2020-31.12.2020

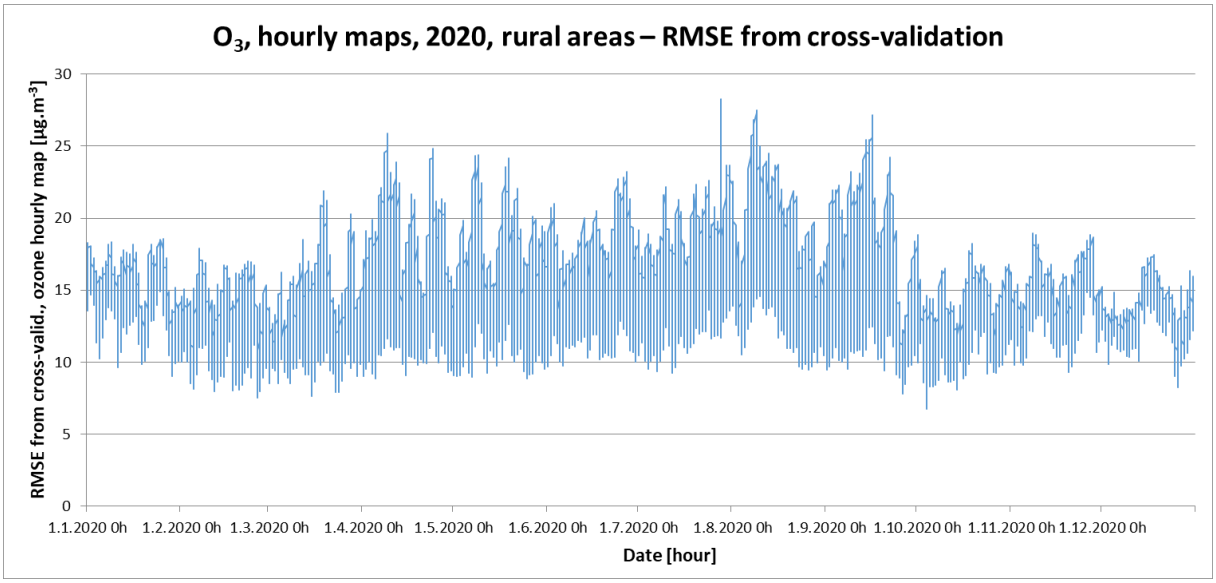

In the POD_6 calculations, the module to estimate phytotoxic ozone doses from a given atmospheric ozone exposure developed by INERIS and adapted by CHMI has been used.

During the POD_6 maps calculation, different biogeographical regions were considered. Plant stomatal functioning varies per plant species and can vary by biogeographical region, reflecting different adaptations of plants to climate and soil water in these regions. Parametrization for POD_6 (i.e. for wheat, potato and tomato) is currently available for all different biogeographic regions of Europe apart from Alpine region, i.e. for Atlantic, Boreal, Continental, Pannonian, Steppic, and Mediterranean regions (CLRTAP, 2017a). In the case of wheat, the parametrization is the same for most of these regions (namely Atlantic, Boreal, Continental, Pannonian, and Steppic), while for Mediterranean regions is different. Thus, these areas are calculated separately. For Alpine region, the parametrisation

of the Continental and several other regions are used. For potato and tomato, only one parametrisation exists – in the case of potato, the parametrisation is set for all regions apart from the Alpine one, while for tomato for the Mediterranean region only (see Table 1.2). In the calculations, the existing parametrisation has been applied for the entire mapping area.

The values calculated in 0.1° x 0.1° resolution were converted into the standard ETRS89-LAEA5210 projection and transferred into the EEA 2x2 km^2 grid.

A3.4 NO_2 and NO_x

In this section, the technical details and the uncertainty estimates for the maps of NO_2 annual average and NO_x annual average, for Maps 4.1 and 4.2, are presented.

Technical details on the mapping

In agreement with Horálek et al. (2007) and Annex 1, the NO_x measurements are supplemented by the so-called pseudo NO_x stations. The pseudo NO_x data are calculated based on the NO_2 data, using quadratic regression Eq. A1.2a. The regression coefficients were estimated based on 380 rural background stations with both NO_x and NO_2 measurements (see Section 2.1.1). The estimated coefficients of Eq. A1.2 are: a = 0.0381, b = 0.846, c = 1.25. Adjusted R^2 is 0.92, the standard error is 0.9 µg/m^3.

Table A3.10 presents the estimated parameters of the linear regression models and of the residual kriging and includes the statistical indicators of both the regression and the kriging.

Table A3.10: Parameters and statistics of linear regression model and ordinary kriging of NO_2 annual average for 2020 in rural, urban background and urban traffic areas for the final combined map (left) and NO_x annual average for 2020 in rural areas (right)

		NO_2 Annual average			NO_x Annual average
		Rural areas	Urb. b. areas	Urb. tr. areas	Rural areas
Linear regresion model (LRM, Eq. A1.3)	c (constant)	4.7	13.2	2.35	2.8
	a1 (CAMS model)	0.419	*non signif.*	*non signif.*	0.927
	a2 (altitude)	-0.0063		*non signif.*	-0.0041
	a3 (altitude_5km_radius)	0.0061		*non signif.*	
	a4 (wind speed)	-0.77	-1.79	-1.79	-1.56
	a5 (solar radiation)				0.002
	a6 (satellite TROPOMI)	1.40	2.33	2.35	
	a7 (population*1000)	0.00073	0.00015		
	a8 (NAT_1km)		-0.0429		
	a9 (AGR_1km)		-0.0255		
	a10 (TRAF_1km)		0.0827		
	a11 (LDR_5km_radius)	*non signif.*	*non signif.*	0.0650	
	a12 (HDR_5km_radius)		0.1443	0.2075	
	a13 (NAT_5km_radius)	-0.0305			
	Adjusted R^2	**0.77**	**0.45**	**0.32**	**0.59**
	Standard Error [µg.m^{-3}]	**2.1**	**5.3**	**8.0**	**4.6**
Ordinary kriging (OK) of LRM residuals	nugget	3	7	19	13
	sill	4	16	40	16
	range [km]	180	100	190	230
LRM + OK of its residuals	**RMSE [µg.m^{-3}]**	**2.2**	**4.2**	**6.3**	**4.2**
	Relative RMSE [%]	**34.4**	**26.4**	**24.3**	**46.1**
	Bias (MPE) [µg.m^{-3}]	**0.0**	**0.0**	**0.0**	**0.0**

Only stations with actual measurement data of the relevant pollutant (i.e. not the pseudo stations) have been used for calculating the cross-validation parameters RMSE and bias.

Uncertainty estimated by cross-validation

Table A3.10 shows both absolute and relative mean uncertainty, expressed by RMSE and Relative RMSE. The absolute mean uncertainty of the final combined map of NO_2 annual average expressed as RMSE is 2.2 µg/m^3 for the rural areas, 4.2 µg/m^3 for the urban background areas and 6.3 µg/m^3 for the urban traffic areas. For the NO_x rural map it is 4.2 µg/m^3.

The relative mean uncertainty of the NO_2 annual average map is 34 % for rural areas, 26 % for urban background areas and 24 % for the urban traffic areas. The NO_x annual average rural map has a relative mean uncertainty of 46 %.

Figure A3.10 shows the point observation – point prediction cross-validation scatter plots for NO_2 annual average. The R^2 indicates that about 75 % of the variability is attributable to the interpolation for the rural areas, while for the urban background areas it is 67 % and for the urban traffic 58 %.

Figure A3.10: Correlation between cross-validated predicted and measurement values for NO_2 annual average 2020 for rural (left), urban background (middle) and urban traffic (right) areas

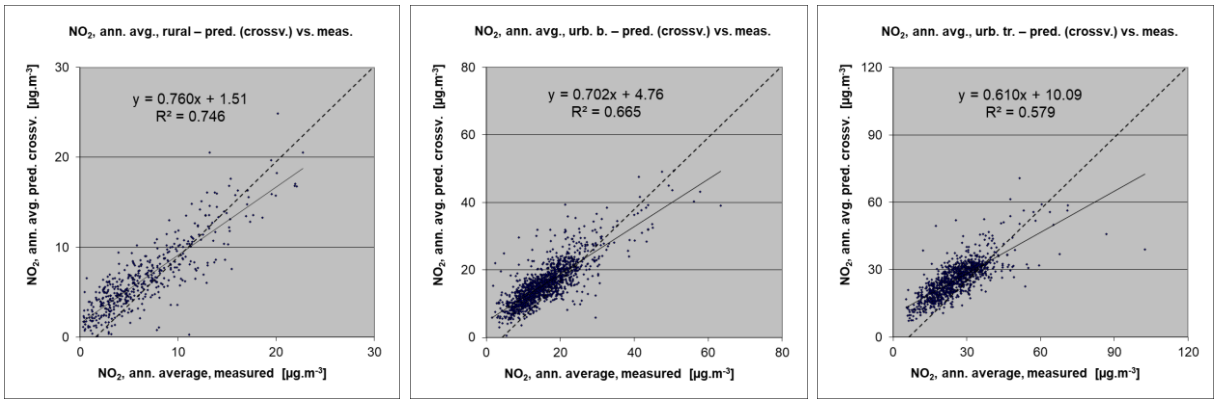

Like in the case of other pollutants, the cross-validation scatter plots show the underestimation of predictions at high concentrations at locations with no measurements. For example, in urban background areas an observed value of 40 µg/m^3 is estimated in the interpolations to be about 33 µg/m^3, which is an underestimated prediction of about 18 %.

Figure A3.11 shows the cross-validation scatter plot for NO_x annual average rural map. The R^2 indicates that about 61 % of the variability is attributable to the interpolation.

Figure A3.11: Correlation between cross-validated predicted and measurement values for NO_x annual average 2020 for rural areas

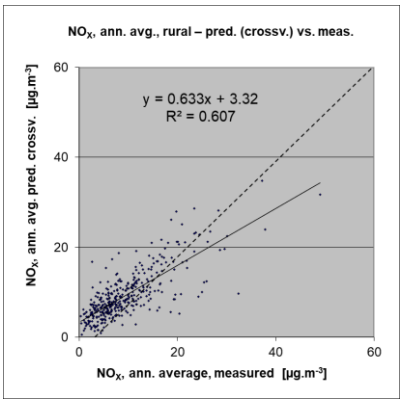

Comparison of point measurement values with the predicted grid value

Next to the above presented cross-validation, a simple comparison was made between the point observation values and interpolated predicted 1x1 km^2 resp. 2x2 km^2 grid values.

For NO_2 annual average, the comparison has been made primarily for the separate rural, separate urban background and separate urban traffic map layers at 1x1 km^2 resolution. Besides, the comparison has been done also for the final combined map. Table A3.11 presents the results of this comparison, together with the results of cross-validation prediction of Figure A3.10. One can conclude that the final combined map in 1x1 km^2 resolution is representative for rural and urban background areas, but not for urban traffic areas.

Table A3.11: Statistical indicators from the scatter plots for the predicted grid values from separate (rural, urban background or urban traffic) map layers and final combined map versus the measurement point values for rural (upper left), urban background (upper right) and urban traffic (bottom left) stations for NO_2 annual average 2020

NO_2	rural backgr. stations				urban/suburban backgr. stations			
	RMSE	Bias	R^2	lin. r. equation	RMSE	Bias	R^2	lin r. equation
cross-val. prediction, separate (r or ub) map layer	2.2	0.0	0.746	y = 0.760x + 1.51	4.2	0.0	0.665	y = 0.702x + 4.76
grid prediction, 1x1 km^2 separate (r or ub) map layer	1.8	-0.2	0.845	y = 0.815x + 1.05	2.7	0.1	0.858	y = 0.815x + 3.05
grid prediction, 1x1 km^2 final merged map	2.2	0.4	0.776	y = 0.910x + 0.94	3.3	0.4	0.792	y = 0.830x + 3.09

NO_2	urban/suburban traffic stations			
	RMSE	Bias	R^2	lin. r. equation
cross-valid. prediction, urban traffic map layer	6.3	0.0	0.579	y = 0.610x + 10.1
grid prediction, 1x1 km^2 urban traffic map layer	4.6	0.0	0.782	y = 0.721x + 7.25
grid prediction, 1x1 km^2 final merged map	10.1	-7.5	0.527	y = 0.485x + 5.80

Table A3.12 presents the cross-validation results of Figure A3.11 and those of the point observation – grid averaged prediction validation for the rural map of NO_x annual average.

Table A3.12: Statistical indicators from the scatter plots for predicted point values based on cross-validation and predicted grid values from rural 2x2 km^2 map versus measurement point values for rural background stations for NO_x annual average 2020

NO_x	rural background stations			
	RMSE	Bias	R^2	linear regression equation
cross-valid. prediction, rural map	4.2	0.0	0.607	y = 0.633x + 3.32
grid prediction, 2x2 km^2 rural map	3.5	0.0	0.730	y = 0.695x + 2.77

A3.5 BaP

In this section, the technical details and the uncertainty estimates for Map 5.1 of BaP annual average are presented.

Technical details on the mapping

The methodology as developed and tested under Horálek et al. (2022c) has been used. Table A3.13 presents the regression coefficients determined for pseudo BaP stations data estimation, based on the 299 rural and urban/suburban background that have both BaP and $PM_{2.5}$ and measurements available (see Section 2.1.1).

Looking at the parameters of the regression, one can note that the R^2 of 0.75 is a relatively poor correlation. Based on this and in agreement with Horálek et al. (2022c), the pseudo stations have been used only in areas with a significant lack of the BaP measurements. The pseudo stations have been applied for countries and areas, as follows. For the rural areas: All the mapping area, apart from Austria, Benelux, Czechia, Germany, Poland, Slovakia and Switzerland. For the urban background areas: Iceland, Ireland, Portugal, Scandinavia (including Denmark), Italy south of 45 degrees latitude, and most of the Balkan countries (namely, Albania, Bosnia and Herzegovina, Greece, Montenegro, Northern Macedonia, Romania, and Serbia including Kosovo).

Table A3.13: Parameters and statistics of linear regression model for generating pseudo BaP annual average data for 2020 in rural and urban background areas

		Rural and urban background areas
Nonlinear regresion model (NLRM, Eq. A1.2b)	c (constant)	-7.39
	a1 ($PM_{2.5}$ annual average)	0.160
	a2 (latitude)	0.074
	a3 (longitude)	0.075
	a4 (land cover NAT_1km)	-0.002
	a5 (land cover NAT_5km_r)	0.000
	Adjusted R^2	**0.75**
	Standard Error [ng/m^3]	**0.70**

Table A3.14 presents the estimated parameters of the linear regression models (c, a_1, a_2,…) and of the residual kriging (nugget, sill, range) and includes the statistical indicators of both the regression and the kriging of its residuals. The same supplementary data as in Horálek et al. (2022c) has been used.

Table A3.14: Parameters and statistics of linear regression model and ordinary kriging of BaP annual average 2020 in rural, urban background and urban traffic areas for final combined map

BaP		Annual average	
		Rural areas	Urban b. areas
Linear regresion model (LRM, Eq. A1.3)	c (constant)	2.11	2.40
	a1 (log. EMEP model)	0.564	0.672
	a2 (altitude GMTED)	-0.00078	
	a3 (wind speed)	-0.26215	
	a4 (temperature)	-0.124	-0.19
	a5 (land cover NAT_1km)	-0.0074	
	Adjusted R^2	**0.45**	**0.57**
	Standard Error [ng/m^3]	**1.04**	**0.93**
Ordinary kriging (OK) of LRM residuals	nugget	0.386	0.140
	sill	0.732	0.814
	range [km]	350	730
LRM + OK of its residuals	**RMSE [ng/m^3]**	**0.72**	**1.12**
	Relative RMSE [%]	**136.3**	**84.4**
	Bias (MPE) [ng/m^3]	**0.02**	**0.01**

The adjusted R^2 is 0.45 for the rural areas and 0.57 for urban background areas. One can see quite weaker regression relation compared to the other pollutants.

Uncertainty estimated by cross-validation

Table A3.14 shows that the absolute mean uncertainty of the final combined map of BaP annual average expressed by RMSE is 0.7 ng/m^3 for the rural areas and 1.1 ng/m^3 for the urban background areas. The RRMSE of this map is 136.3 % for rural areas and 84.4 % for urban background areas. The cross-validation relative uncertainty RRMSE is still at the considerably higher level (especially in the rural areas) compared to the 60%, being the data quality objective for the modelling uncertainty in the European directive (EC, 2004).

Annex 4
Concentration change in 2020 in comparison to the five-year mean 2015-2019

In this annex, air concentration changes in 2020 in comparison to the five-year mean 2015-2019 are presented, both for the mapped concentrations and for the population-weighted and vegetation-weighted concentrations. In all cases, the maps for 2015-2019 presented in Horálek et al. (2018, 2019, 2020, 2021 and 2022a) have been used. In the case of PM_{10} and $PM_{2.5}$, the maps constructed using the updated methodology have been used since 2015 maps.

A4.1 Particulate matter PM_{10} and $PM_{2.5}$

Concentration maps

Map A4.1 presents the difference between 2020 and five-year mean 2015-2019 for annual average and the 90.4 percentile of daily means for PM_{10}. Orange to red areas show an increase of PM_{10} concentration in 2020, while blue areas show a decrease.

Map A4.1: Difference concentrations between 2020 and five-year mean 2015-2019 for PM_{10} indicators annual average (left) and 90.4 percentile (right)

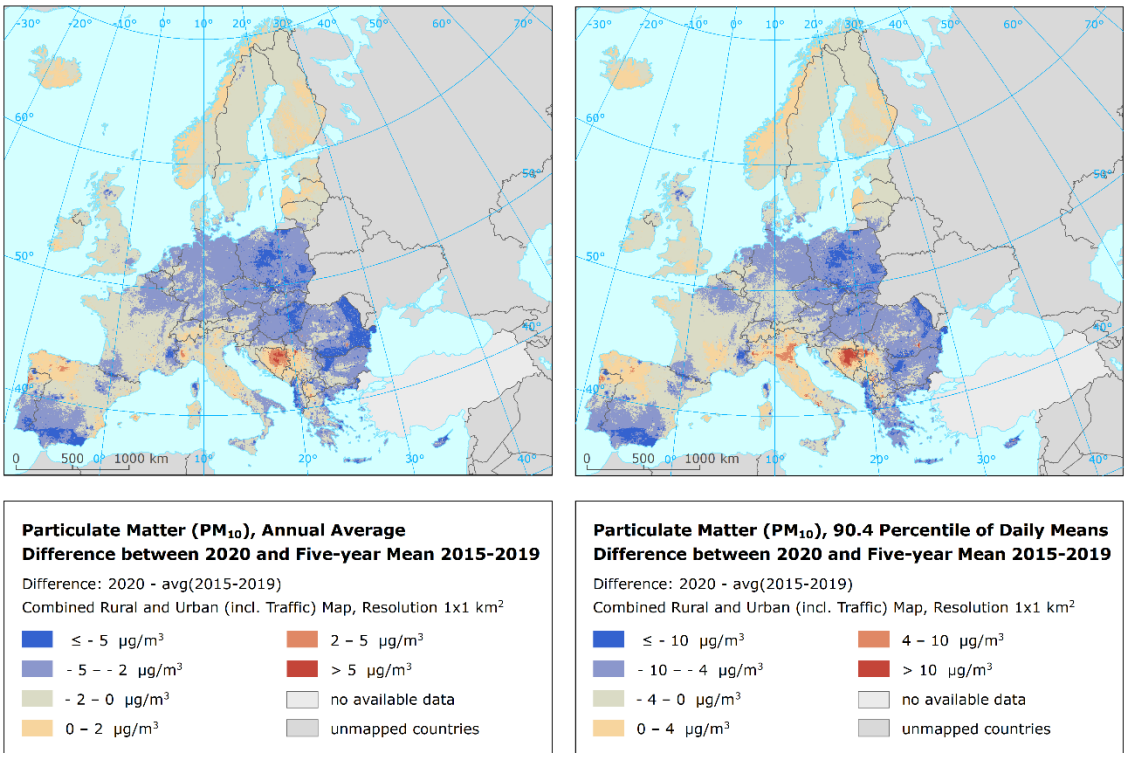

At the annual average PM_{10} difference map the highest increases are observed in parts of southern and south-eastern Europe (Bosnia and Herzegovina, parts of Italy, Spain and Portugal) and in parts of northern Europe. Contrary to that, decreases occur in the rest of countries, mainly central Europe, parts of some countries in south-eastern Europe and parts of France, Spain and Portugal. At the 90.4 percentile of daily means for PM_{10} the highest increases and decreases are seen in similar parts of Europe.

Be it noted that besides the actual changes in the concentrations, the variability of the linear regression model and variogram parameters, changes in the measurement network and changes in the dispersion model may cause minor differences in the concentration levels estimated.

Map A4.2 presents the difference between 2020 and five-year mean 2015-2019 for annual average $PM_{2.5}$.

At the annual average $PM_{2.5}$ difference map the highest increases is observed in parts of southern and south-eastern Europe (Bosnia and Herzegovina, Sebia, parts of Italy and Spain) and in parts of northern Europe (very similarly to PM_{10}). Contrary to that, decreases occur in the rest of countries, mainly central Europe, parts of some countries in south-eastern Europe and parts of France, Spain and Portugal.

Map A4.2: Difference $PM_{2.5}$ annual average concentrations between 2020 and five-year average 2015-2019

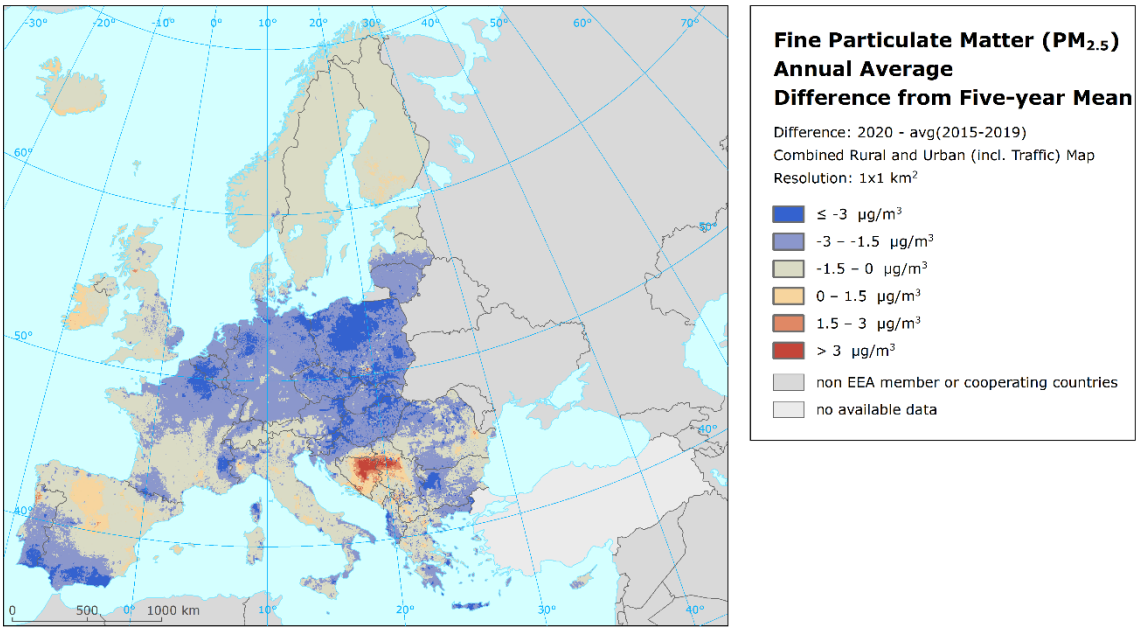

Population exposure

Table A4.1 shows the difference of the population-weighted concentrations between 2020 and five-year mean 2015-2019 for PM_{10} annual average and the 90.4 percentile of daily PM_{10} means, for individual countries, large regions, EU-27 and for the total mapping area (without Türkiye).

In 2020, the overall average population-weighted annual mean PM_{10} concentration for the total mapping area was 18.0 µg/m^3, i.e. its value decreased by about 2.5 µg/m^3 compared to the previous five-year mean. The steepest decreases per country were detected in North Macedonia (9 µg.m^{-3}), the highest increases were estimated in Bosnia and Herzegoniva (5 µg/m^3).

In the case of the 90.4 percentile of daily means, the overall average population-weighted concentration for 2020 is estimated at 31.5 µg/m^3, which is of about 4.2 µg/m^3 less than five-year mean. The steepest decreases were estimated in North Macedonia (20 µg/m^3), while the highest increases in Bosnia and Herzegovina (11 µg/m^3).

Table A4.1: Population-weighted concentration in 2020 and five-year mean 2015-2019 and its difference between 2020 and five-year mean for PM_{10} indicators annual average (left) and 90.4 percentile of daily means (right)

Country	ISO	Population-weighted concentration [µg/m³]						Country	ISO	Population-weighted concentration [µg/m³]					
		Annual average			90.4 percentile of daily means					Annual average			90.4 percentile of daily means		
		2020	5-year mean	Diff.	2020	5-year mean	Diff.			2020	5-year mean	Diff.	2020	5-year mean	Diff.
Albania	AL	24.2	31.9	-7.7	42.2	59.1	-16.8	Luxembourg	LU	14.9	16.8	-1.9	24.8	28.1	-3.3
Andorra	AD	16.6	22.6	-6.0	28.5	41.9	-13.4	Malta	MT	25.2	28.0	-2.8	37.7	42.9	-5.2
Austria	AT	14.6	17.7	-3.1	25.4	31.3	-5.8	Monaco	MC	18.7	22.0	-3.3	27.9	34.2	-6.3
Belgium	BE	17.4	19.8	-2.4	31.6	34.2	-2.6	Montenegro	ME	25.1	26.9	-1.8	46.6	53.3	-6.8
Bosnia & Herzegovina	BA	36.2	30.9	5.3	74.8	63.6	11.2	Netherlands	NL	16.5	18.5	-2.0	27.3	30.6	-3.4
Bulgaria	BG	26.0	31.7	-5.7	46.5	58.0	-11.6	North Macedonia	MK	31.6	40.6	-9.0	63.7	83.9	-20.2
Croatia	HR	22.7	24.2	-1.5	43.6	46.7	-3.1	Norway	NO	9.3	10.5	-1.3	17.2	19.4	-2.1
Cyprus	CY	32.3	33.5	-1.2	53.5	51.4	2.2	Poland	PL	22.7	28.3	-5.7	39.5	51.9	-12.4
Czechia	CZ	17.5	22.5	-5.0	30.7	40.6	-9.9	Portugal (excl. Az., Mad.)	PT	17.7	18.4	-0.8	28.9	30.8	-1.9
Denmark (incl. Faroes)	DK	14.1	16.1	-2.1	23.3	27.6	-4.3	Romania	RO	23.2	24.7	-1.6	41.2	42.2	-1.1
Estonia	EE	10.9	11.7	-0.8	18.8	20.6	-1.9	San Marino	SM	20.8	22.1	-1.3	40.4	39.7	0.7
Finland	FI	8.7	9.5	-0.8	15.6	16.9	-1.2	Serbia (incl. Kosovo*)	RS	31.4	34.3	-2.8	59.6	66.4	-6.7
France (metropolitan)	FR	15.0	17.2	-2.2	25.0	29.0	-4.0	Slovakia	SK	20.1	24.2	-4.1	36.2	44.4	-8.2
Germany	DE	14.2	17.1	-2.9	24.1	29.1	-5.0	Slovenia	SI	18.0	21.9	-3.9	32.9	40.4	-7.5
Greece	GR	23.9	30.2	-6.4	38.8	51.0	-12.2	Spain (excl. Canarias)	ES	18.7	20.6	-2.0	29.9	33.7	-3.7
Hungary	HU	21.5	25.4	-3.9	39.6	45.8	-6.2	Sweden	SE	10.3	11.8	-1.5	17.4	21.1	-3.6
Iceland	IS	9.1	9.9	-0.8	15.7	17.4	-1.7	Switzerland	CH	12.6	15.1	-2.5	21.9	26.9	-5.0
Ireland	IE	11.4	12.1	-0.7	19.7	21.5	-1.8	United Kingdom (& Cr. d.)	UK	13.9	15.2	-1.2	24.8	26.1	-1.3
Italy	IT	23.8	25.1	-1.2	44.3	44.1	0.2	**Total without Türkiye**		**18.0**	**20.5**	**-2.5**	**31.5**	**35.7**	**-4.2**
Latvia	LV	17.0	17.2	-0.1	28.2	29.9	-1.7	**EU-27**		**18.3**	**20.9**	**-2.6**	**31.6**	**36.2**	**-4.6**
Liechtenstein	LI	11.3	13.7	-2.4	19.1	25.2	-6.0	Kosovo*	KS	26.7	35.2	-8.5	53.2	72.0	-18.8
Lithuania	LT	18.5	18.8	-0.3	30.4	33.1	-2.8	Serbia (excl. Kosovo*)	RS-	32.6	34.0	-1.5	61.2	65.0	-3.8

(*) under the UN Security Council Resolution 1244/99
Notes: 5-year mean, i.e. five-year mean 2015-2019. Diff., i.e. difference concentrations between 2020 and five-year mean 2015-2019.

Table A4.2: Population-weighted concentration in 2020 and five-year mean 2015-2019 and its difference between 2020 and five-year mean for $PM_{2.5}$ annual average

Country	ISO	Population-weighted concentration [µg/m³]			Country	ISO	Population-weighted concentration [µg/m³]		
		Annual average					Annual average		
		2020	5-year mean	Diff.			2020	5-year mean	Diff.
Albania	AL	15.6	21.3	-5.6	Luxembourg	LU	7.3	10.4	-3.1
Andorra	AD	8.5	11.3	-2.8	Malta	MT	10.1	12.2	-2.1
Austria	AT	9.9	12.5	-2.6	Monaco	MC	10.5	13.4	-3.0
Belgium	BE	9.4	12.4	-3.0	Montenegro	ME	17.3	19.4	-2.0
Bosnia & Herzegovina	BA	25.8	23.3	2.5	Netherlands	NL	9.2	11.6	-2.4
Bulgaria	BG	17.0	21.8	-4.9	North Macedonia	MK	20.3	30.6	-10.3
Croatia	HR	15.3	17.4	-2.1	Norway	NO	4.6	5.8	-1.2
Cyprus	CY	14.0	15.6	-1.5	Poland	PL	16.0	20.6	-4.7
Czechia	CZ	12.5	16.6	-4.1	Portugal (excl. Az., Mad.)	PT	8.1	9.0	-0.9
Denmark (incl. Faroes)	DK	7.6	9.5	-1.9	Romania	RO	15.2	17.2	-1.9
Estonia	EE	5.4	6.2	-0.8	San Marino	SM	12.8	14.1	-1.3
Finland	FI	4.5	5.2	-0.8	Serbia (incl. Kosovo*)	RS	22.1	25.1	-3.0
France (metropolitan)	FR	8.6	10.8	-2.2	Slovakia	SK	14.5	17.6	-3.1
Germany	DE	9.1	11.7	-2.6	Slovenia	SI	12.5	15.7	-3.2
Greece	GR	14.4	20.7	-6.3	Spain (excl. Canarias)	ES	10.0	11.3	-1.3
Hungary	HU	14.5	17.8	-3.3	Sweden	SE	4.9	5.7	-0.8
Iceland	IS	4.2	4.9	-0.8	Switzerland	CH	8.1	10.1	-2.0
Ireland	IE	7.1	7.1	0.0	United Kingdom (& Cr. dep.)	UK	8.6	9.6	-1.0
Italy	IT	14.9	16.4	-1.5	**Total without Türkiye**		**11.1**	**13.4**	**-2.3**
Latvia	LV	9.1	10.9	-1.8	**EU-27**		**11.2**	**13.7**	**-2.5**
Liechtenstein	LI	8.1	9.5	-1.4	Kosovo*	KS	19.4	26.6	-7.2
Lithuania	LT	9.8	12.0	-2.2	Serbia (excl. Kosovo*)	RS-	22.7	24.7	-2.0

(*) Under the UN Security Council Resolution 1244/99.
Notes: 5-year mean, i.e. five-year mean 2015-2019. Diff., i.e. difference concentrations between 2020 and five-year mean 2015-2019.

Table A4.2 presents the difference of the population-weighted concentrations between 2020 and five-year mean 2015-2019 for $PM_{2.5}$ annual average, for individual countries and for Europe as a whole (without Türkiye, which is not mapped for this pollutant).

In 2020, the average overall population-weighted concentration is estimated at 11.1 µg/m^3, which means a decrease of 2.3 µg/m^3 compared to five-year mean. The decrease in concentrations in 2020 compared to five-year mean has been observed in all countries except Bosnia and Herzegovina (increase of 2.5 µg/m^3) and Ireland (no change). The steepest decrease was estimated in North Macedonia (10 µg/m^3).

Regarding year 2020, it should be mentioned the potential impact of lockdown measures connected with the SARS-CoV-2 (severe acute respiratory virus coronavirus 2) pandemic from mid-March 2020 on the air quality. Nevertheless, change of PM concentration as a result of these measures is quite complicated to assess. The reason is the different composition of PM and PM gaseous precursor emission sources (local heating, industry and transport as main emission sources) and strong dependency of PM concentrations on dispersion and meteorological conditions.

A4.2 Ozone

Concentration maps

In Map 4.3, the difference concentrations between 2020 and five-year average 2015-2019 for both the health-related ozone indicators (i.e. for 93.2 percentile of maximum daily 8-hour means and SOMO35) and the vegetation-related ozone indicators (i.e. for AOT40 for vegetation and AOT40 for forests) are presented. In all the maps, orange and red areas show an increase of ozone concentrations, while blue areas show a decrease.

In general, both increases and decreases are shown for the two health-related indicators. The increases for 93.2 percentile of maximum daily 8-hour means have been observed in the most of western Europe (United Kingdom, Ireland, Belgium and northern France) and in areas in south and south-eastern Europe (Portugal and Romania). Contrary to that, one can see a decline in most of the rest of Europe. The difference pattern for SOMO35 is quite similar to that of the percentile indicator.

In the case of both AOT40 indicators, the state is very similar to the health-related indicators, apart from some large area in Scandinavia, where increase is found.

To conclude, most of Europe show a quite high decrease in 2020 compared to five-year average, probably as a result of less favourable meteorological conditions for the formation of ozone (e.g. the heatwaves of 2020 were not as intense, widespread or long-lived as others in recent years or relatively wet June, July to September had near-average precipitation amounts (ECMWF, 2020)).

However, there has been an increase in ozone for all indicators in the United Kingdom, the Benelux, the Île de France and the Po Valley. In these mentioned areas, the steep decrease in NO_X concentrations has been showed (see Map A4.4). It has been stated by a few authors that decrease in NO_X concentrations due to lockdown measures can result in ozone concentrations increase, especially in cities and urban areas (e.g. Brancher, 2021, Sicard et al., 2020, Tobías et al., 2020). More details can be found in Horálek et al. (2022c).

Map A4.3: Difference concentrations between 2020 and five-year average 2015-2019 for ozone indicators 93.2 percentile of daily 8-hour maxima (top left), SOMO35 (top right), AOT40 for vegetation (bottom left) and AOT40 for forests (bottom right)

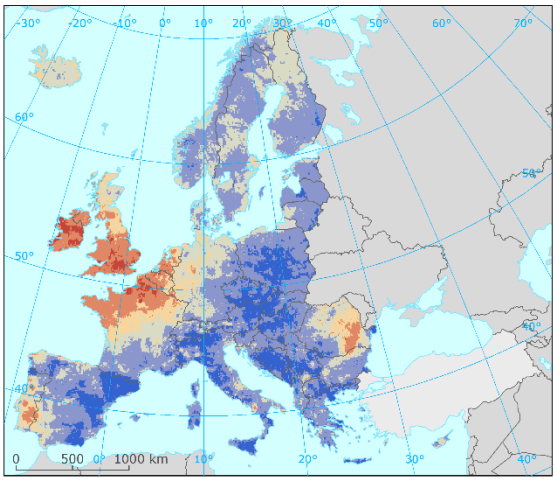

Ozone, 93.2 Percentile of Maximum daily 8-hour Means
Difference between 2020 and Five-year Mean 2015-2019

Difference: 2020 - avg(2015-2019)
Combined Rural and Urban Background Map, Resolution 1x1 km²

≤ - 10 µg/m³	4 – 10 µg/m³
- 10 – - 4 µg/m³	> 10 µg/m³
- 4 – 0 µg/m³	no available data
0 – 4 µg/m³	unmapped countries

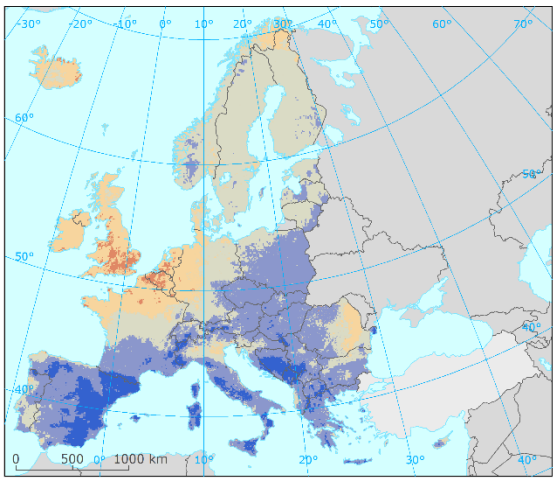

Ozone, SOMO35
Difference between 2020 and Five-year Mean 2015-2019

Difference: 2020 - avg(2015-2019)
Combined Rural and Urban Background Map, Resolution 1x1 km²

≤ - 2000 µg/m³·d	800 – 2000 µg/m³·d
- 2000 – - 800 µg/m³·d	> 2000 µg/m³·d
- 800 – 0 µg/m³·d	no available data
0 – 800 µg/m³·d	unmapped countries

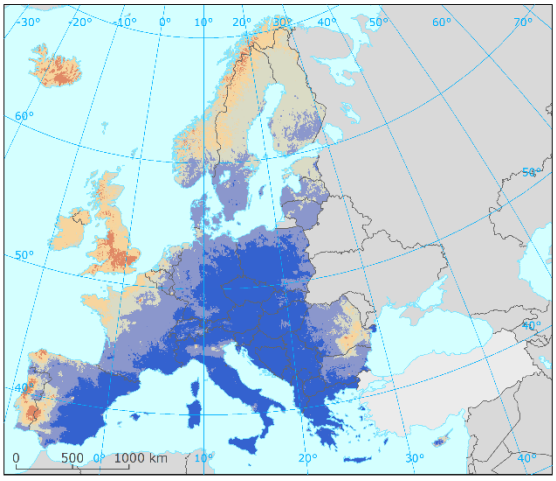

Ozone, AOT40 for Vegetation
Difference between 2020 and Five-year Mean 2015-2019

Difference: 2020 - avg(2015-2019)
Rural Map, Resolution 2x2 km²

≤ - 6000 µg/m³·h	2000 – 6000 µg/m³·h
- 6000 – - 2000 µg/m³·h	> 6000 µg/m³·h
- 2000 – 0 µg/m³·h	no available data
0 – 2000 µg/m³·h	unmapped countries

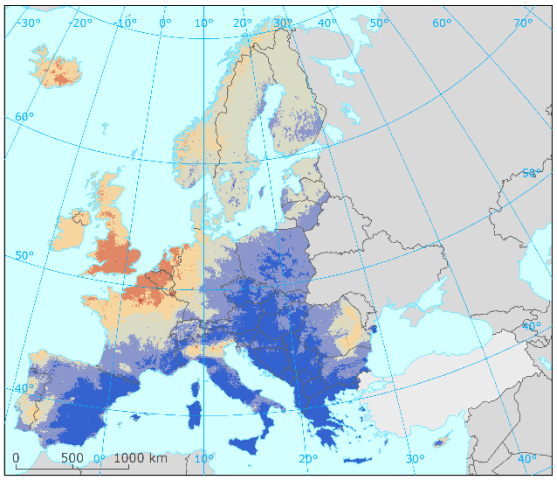

Ozone, AOT40 for Forests
Difference between 2020 and Five-year Mean 2015-2019

Difference: 2020 - avg(2015-2019)
Rural Map, Resolution 2x2 km²

≤ - 10000 µg/m³·h	4000 – 10000 µg/m³·h
- 10000 – - 4000 µg/m³·h	> 10000 µg/m³·h
- 4000 – 0 µg/m³·h	no available data
0 – 4000 µg/m³·h	unmapped countries

Population exposure

Table A4.3 provides the difference of the population-weighted concentrations between 2020 and five-year mean 2015-2019 for ozone health related indicators 93.2 percentile of 8-houry daily maximums and SOMO35, for individual countries, large regions, EU-27 and for the total mapping area (without Türkiye). Additionally, the difference of the population-weighted concentrations between 2020 and four-year mean is presented for SOMO10, for which the five-year time series is not available.

Table A4.3: Population-weighted concentration in 2020 and five-year mean 2015-2019 and its difference between 2020 and five-year mean for ozone indicators 93.2 percentile of 8-h daily maxima (left) and SOMO35 (middle) and population-weighted concentration in 2020 and four-year mean 2016-2019 and its difference between 2020 and four-year mean for ozone indicator SOMO10 (right)

Country	ISO	Population-weighted concentration								
		93.2 perc. of 8-h d. max [µg/m³]			SOMO35 [µg/m³·d]			SOMO10 [µg/m³·d]		
		2020	5-year mean	Diff.	2020	5-year mean	Diff.	2020	4-year mean	Diff.
Albania	AL	108.2	113.5	-5.3	5 679	6 183	-504	21 441	21 851	-410
Andorra	AD	95.1	112.7	-17.6	2 813	5 957	-3 144	17 329	21 603	-4 274
Austria	AT	111.0	120.9	-9.9	4 584	5 707	-1 123	18 738	20 736	-1 998
Belgium	BE	113.3	107.7	5.6	3 798	3 037	761	18 046	16 982	1 063
Bosnia & Herzegovina	BA	104.7	115.4	-10.7	4 045	5 942	-1 897	18 056	21 457	-3 401
Bulgaria	BG	95.3	101.4	-6.1	2 967	3 749	-782	15 630	17 428	-1 798
Croatia	HR	109.4	117.0	-7.6	4 775	6 176	-1 401	19 359	21 798	-2 440
Cyprus	CY	108.1	108.1	0.0	6 300	6 105	195	21 484	20 150	1 334
Czechia	CZ	110.2	120.3	-10.1	4 252	5 312	-1 060	18 561	20 624	-2 063
Denmark (incl. Faroe Islands)	DK	93.0	96.8	-3.9	2 284	2 709	-425	17 563	18 530	-967
Estonia	EE	88.1	93.1	-5.0	1 469	2 144	-675	15 863	17 061	-1 198
Finland	FI	86.3	90.1	-3.8	1 362	1 734	-371	15 425	16 495	-1 070
France (metropolitan)	FR	112.8	110.2	2.6	4 274	4 308	-34	19 598	19 860	-263
Germany	DE	113.1	115.8	-2.7	4 194	4 227	-33	18 214	18 713	-499
Greece	GR	113.2	113.0	0.2	6 181	6 578	-397	22 987	20 855	2 131
Hungary	HU	106.3	113.9	-7.6	4 044	4 976	-932	17 504	19 427	-1 923
Iceland	IS	85.8	82.1	3.8	1 582	1 040	542	16 979	16 223	756
Ireland	IE	90.6	82.7	7.9	1 911	1 656	255	16 979	17 296	-317
Italy	IT	119.3	125.6	-6.3	6 059	6 694	-634	20 655	21 873	-1 218
Latvia	LV	90.0	96.5	-6.5	1 700	2 435	-736	15 714	16 556	-841
Liechtenstein	LI	114.7	124.1	-9.4	4 971	5 711	-740	18 542	20 356	-1 813
Lithuania	LT	92.8	98.2	-5.4	2 044	2 599	-555	15 871	16 903	-1 031
Luxembourg	LU	116.1	109.9	6.1	4 272	3 417	855	18 787	18 051	736
Malta	MT	105.3	105.4	-0.1	6 590	5 864	726	24 516	23 559	957
Monaco	MC	118.7	122.1	-3.5	6 445	7 608	-1 163	22 679	23 791	-1 112
Montenegro	ME	103.4	112.7	-9.3	4 360	6 099	-1 739	18 639	21 672	-3 033
Netherlands	NL	108.7	104.0	4.6	3 426	2 868	559	17 493	17 079	414
North Macedonia	MK	102.6	103.6	-1.0	4 345	4 490	-145	17 838	17 878	-39
Norway	NO	90.3	91.1	-0.8	2 041	2 110	-69	16 538	17 408	-869
Poland	PL	103.4	111.8	-8.4	3 216	4 165	-949	16 865	18 504	-1 640
Portugal (excl. Azores, Madeira)	PT	103.9	104.1	-0.2	3 585	3 996	-411	18 701	19 461	-760
Romania	RO	97.5	96.4	1.1	2 955	3 245	-290	16 090	17 411	-1 321
San Marino	SM	116.1	123.7	-7.6	5 387	6 538	-1 152	19 858	21 783	-1 926
Serbia (incl. Kosovo*)	RS	100.8	104.3	-3.5	3 256	4 270	-1 014	15 959	17 664	-1 705
Slovakia	SK	105.0	114.4	-9.4	3 867	5 091	-1 224	17 676	20 080	-2 404
Slovenia	SI	111.8	119.6	-7.8	5 011	6 189	-1 178	19 459	21 576	-2 117
Spain (excl. Canarias)	ES	107.8	111.9	-4.1	4 525	5 658	-1 133	20 426	21 756	-1 330
Sweden	SE	91.9	94.7	-2.8	2 182	2 432	-250	16 929	18 023	-1 094
Switzerland	CH	118.8	124.3	-5.5	5 388	5 872	-483	19 417	20 755	-1 338
United Kingdom (& Crown dep.)	UK	96.2	87.9	8.3	2 300	1 576	724	16 541	15 542	999
Total without Türkiye		**107.3**	**108.9**	**-1.6**	**3 945**	**4 252**	**-307**	**18 406**	**19 072**	**-666**
EU-27		**109.1**	**111.9**	**-2.9**	**4 181**	**4 607**	**-426**	**18 717**	**19 568**	**-851**
Kosovo*	KS	102.6	103.4	-0.8	3 900	4 827	-927	17 393	18 592	-1 199
Serbia (excl. Kosovo*)	RS-	100.3	104.5	-4.2	3 098	4 134	-1 036	15 608	17 438	-1 830

(*) Under the UN Security Council Resolution 1244/99.

Notes: 5-year mean, i.e. five-year mean 2015-2019. Diff., i.e. difference concentrations between 2020 and five-year mean 2015-2019 for 93.2 percentile of 8-h daily maximums and SOMO35; difference concentrations between 2020 and four-year mean 2016-2019 for SOMO10

In 2020 the overall population-weighted concentration for ozone indicator 93.2 percentile of maximum daily 8-hour means was about 107.3 µg/m^3, i.e. of about 1.6 µg/m^3 lower than five-year mean concentration. The highest decreases are shown in countries of south-eastern and central Europe (Bosnia and Herzegovina, Czechia, Austria). The highest increases are found in countries of western Europe (United Kingdom, Ireland, Luxembourg).

In the case of SOMO35, the average overall population-weighted concentration for 2020 is estimated at about 3 945 µg/m^3·d, which is of about 307 µg/m^3·d lower than five-year mean SOMO35 value. The highest increases are found in Luxembourg (855 µg/m^3·d) and Belgium (761 µg/m^3·d), the steepest decreases are found in Bosnia and Herzegovina (almost 1 900 µg/m^3·d) and Montenegro (1 739 µg/m^3·d).

Vegetation exposure

Table A4.4 provides the difference of the agricultural-weighted concentrations for AOT40 for vegetation and the forest-weighted concentrations for AOT40 for forests between 2020 and five-year mean of AOT40.

Table A4.4: Agricultural-weighted (left) and forest-weighted (right) concentration in 2020 and five-year mean 2015-2019 and its difference between 2020 and five-year mean for ozone indicators AOT40 for vegetation (left) and AOT40 for forests (right)

Country	ISO	Agriculture-weighted concentration AOT40 for vegetation [µg/m³·h]			Forest-weighted concentration AOT40 for forests [µg/m³·h]		
		2020	5-year mean	Differ.	2020	5-year mean	Differ.
Albania	AL	11 585	21 534	-9 949	26 361	43 621	-17 260
Austria	AT	10 032	20 221	-10 188	23 846	35 717	-11 871
Belgium	BE	9 953	11 700	-1 747	25 074	21 303	3 771
Bosnia & Herzegovina	BA	5 277	15 602	-10 325	15 763	31 618	-15 855
Bulgaria	BG	7 647	11 985	-4 338	20 370	30 896	-10 526
Croatia	HR	7 650	17 279	-9 628	21 504	33 381	-11 877
Cyprus	CY	19 649	21 962	-2 312	38 365	45 806	-7 441
Czechia	CZ	9 329	18 846	-9 517	23 993	34 333	-10 340
Denmark (incl. Faroe Islands)	DK	3 218	6 330	-3 112	9 711	11 456	-1 745
Estonia	EE	2 090	3 598	-1 508	4 120	7 177	-3 057
Finland	FI	1 217	2 875	-1 658	2 126	5 144	-3 017
France (metropolitan)	FR	9 185	12 073	-2 887	22 953	26 905	-3 952
Germany	DE	8 895	14 557	-5 662	24 988	28 387	-3 399
Greece	GR	12 929	23 069	-10 139	26 500	44 939	-18 439
Hungary	HU	7 839	15 701	-7 862	19 935	31 650	-11 715
Iceland	IS	892	807	85	3 026	3 009	16
Ireland	IE	3 243	2 564	678	7 036	5 034	2 002
Italy	IT	15 966	25 103	-9 137	32 674	44 671	-11 998
Latvia	LV	1 982	4 291	-2 309	4 661	8 456	-3 795
Liechtenstein	LI	11 491	21 127	-9 636	31 425	38 732	-7 307
Lithuania	LT	2 832	5 624	-2 792	6 562	11 533	-4 972
Luxembourg	LU	10 774	13 952	-3 177	27 795	23 003	4 792
Malta	MT	14 601	23 033	-8 432	36 305	45 991	-9 686
Monaco	MC		9 698	-9 698	42 316	34 976	7 341
Montenegro	ME	7 119	18 240	-11 122	20 480	37 881	-17 401
Netherlands	NL	7 284	8 883	-1 599	19 509	15 600	3 909
North Macedonia	MK	10 553	20 003	-9 449	25 584	43 294	-17 711
Norway	NO	1 662	3 204	-1 543	5 931	7 361	-1 430
Poland	PL	5 853	12 432	-6 579	15 597	23 465	-7 868
Portugal (excl. Azores, Madeira)	PT	10 886	10 844	42	19 627	22 490	-2 864
Romania	RO	6 508	9 570	-3 062	16 187	21 821	-5 634
San Marino	SM	15 104	24 123	-9 020	34 114	41 129	-7 015
Serbia (incl. Kosovo*)	RS	6 549	15 726	-9 177	18 828	33 767	-14 939
Slovakia	SK	7 209	15 582	-8 373	19 485	29 457	-9 971
Slovenia	SI	9 452	20 294	-10 842	24 705	37 058	-12 353
Spain (excl. Canarias)	ES	12 553	18 408	-5 856	19 639	30 547	-10 909
Sweden	SE	2 471	5 263	-2 793	4 987	7 394	-2 408
Switzerland	CH	13 325	20 826	-7 501	31 492	37 100	-5 608
United Kingdom (& Crown dep.)	UK	5 360	4 236	1 124	9 479	6 185	3 294
Total without Türkiye		**8 544**	**13 392**	**-4 849**	**14 584**	**20 651**	**-6 068**
EU-27		**8 876**	**13 967**	**-5 092**	**14 912**	**20 952**	**-6 039**
Kosovo*	KS	8 773	17 907	-9 133	22 967	**38 432**	**-15 464**
Serbia (excl. Kosovo*)	RS-	6 331	15 507	-9 176	18 047	**32 885**	**-14 838**

(*) Under the UN Security Council Resolution 1244/99.
Notes: 5-year mean, i.e. five-year mean 2015-2019. Differ., i.e. difference concentrations between 2020 and five-year mean 2015-2019.

In 2020, the agricultural-weighted concentration of vegetation-related AOT40 shows a decrease of ca. 4 849 µg/m^3·h compared to five-year mean; the forest-weighted concentration of forest-related AOT40 shows a decrease of about 6 068 µg/m^3·h compared to five-year mean. Some slight increases of vegetation-related AOT40 are seen in United Kingdom and Ireland, while the steepest decreases are found in some countries of south-eastern and central Europe (Montenegro, Slovenia, Bosnia and Herzegovina, Austria, and Greece). The highest increases of forest-related AOT40 are seen in the Benelux, United Kingdom and Ireland, while the steepest decreases in Greece and other countries of south-eastern Europe (North Macedonia, Montenegro, and Albania).

A4.3 NO_2 and NO_x

Concentration maps

Map A4.4 presents the difference concentrations between 2020 and five-year average 2015-2019 for NO_2 and NO_x annual averages. Orange and red areas show an increase of concentration in 2020, while blue areas show a decrease.

Map A4.4: Difference concentrations between 2020 and five-year average 2015-2019 for NO_2 annual average (left) and NOx annual average (right)

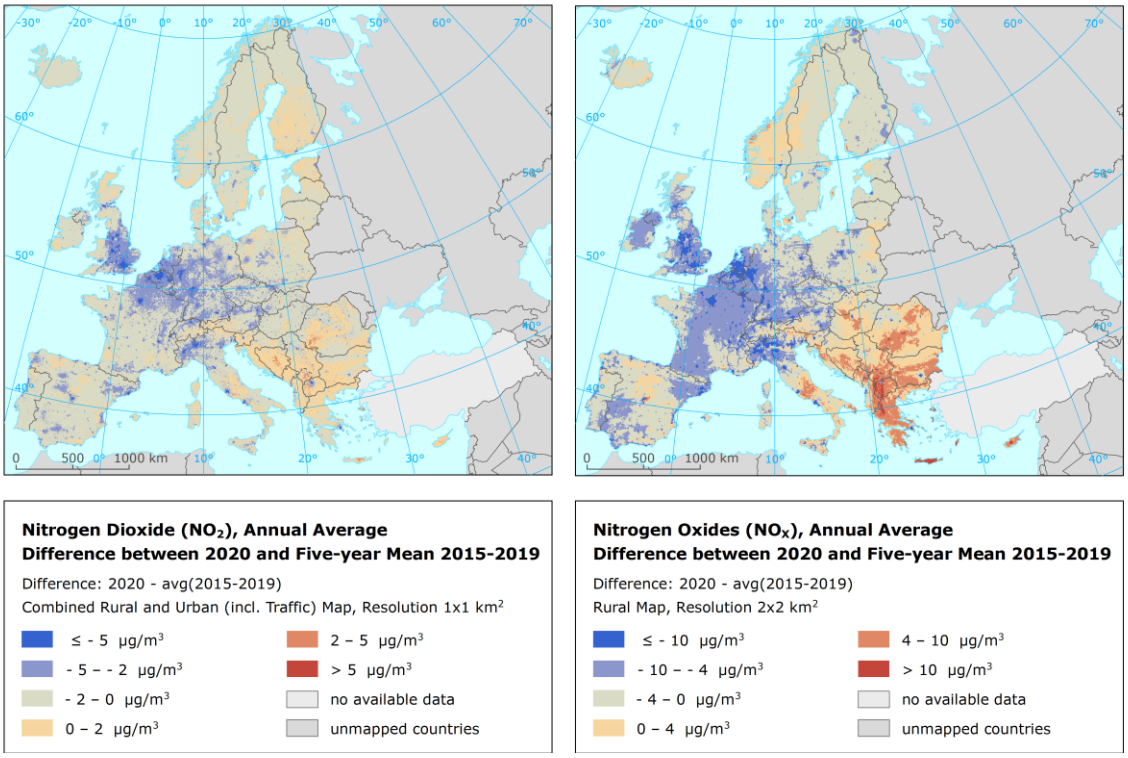

In comparison to five-year mean, general decrease in NO_2 annual concentration is shown. The NO2 concentration (in terms of annual average) shows a decrease of more than 5 µg/m³ per year in areas of London, Paris, Rome, Napoli, Milano, Madrid, and Barcelona. A decrease up to 5 µg/m³ has been observed in some areas of the United Kingdom, Benelux, parts of Spain, France, Italy and countries in central Europe. The main reason for this is the lockdown measures connected with the COVID-19 pandemic, although NO_2 concentrations have been decreasing in the previous years too. The decrease in the road transport, aviation and international shipping intensity during the lockdown resulted in the reduction of the emission and ambient air concentrations of NO_2 and NO_X, mainly in large cities and urbanized parts (EEA, 2020). Some European areas show no change or even increase in annual NO_2 and NO_X concentrations (south-eastern Europe and parts of Poland and northern Europe).

In the case of NO_x, notable decreases are seen in western Europe, Spain, Italy and in parts of countries in central Europe. The highest increases can be seen in Greece, North Macedonia and other countries of south and south-eastern Europe.

Population exposure

Table A4.5 provides the difference between 2020 annual average and five-year mean 2015-2019 for NO_2. In 2020 the overall population-weighted concentration for NO_2 annual average was 14 µg/m³, i.e.

4 µg/m^3 lower than for five-year mean. The steepest decreases are shown in Monaco, Belgium and United Kingdom, while the only slight increase (< 1 µg.m^{-3}) is estimated in Cyprus.

Table A4.5: Population-weighted concentration in 2020 and five-year mean 2015-2019 and its difference between 2020 and five-year mean for NO_2 annual average

Country	ISO	Population-weighted concentration [µg/m³] Annual average			Country	ISO	Population-weighted concentration [µg/m³] Annual average		
		2020	5-year mean	Diff.			2020	5-year mean	Diff.
Albania	AL	12.8	15.7	-2.9	Luxembourg	LU	15.8	19.7	-3.9
Andorra	AD	17.6	19.5	-1.8	Malta	MT	11.0	13.9	-2.9
Austria	AT	14.3	18.3	-4.1	Monaco	MC	18.0	26.4	-8.4
Belgium	BE	14.3	20.5	-6.1	Montenegro	ME	13.7	14.4	-0.6
Bosnia & Herzegovina	BA	14.1	14.7	-0.5	Netherlands	NL	15.8	20.1	-4.3
Bulgaria	BG	16.7	18.3	-1.6	North Macedonia	MK	14.2	18.5	-4.3
Croatia	HR	13.1	15.2	-2.1	Norway	NO	8.0	11.0	-2.9
Cyprus	CY	20.8	20.4	0.4	Poland	PL	13.0	15.1	-2.0
Czechia	CZ	12.5	15.3	-2.9	Portugal (excl. Az., Mad.)	PT	12.5	15.5	-3.0
Denmark (incl. Faroes)	DK	7.4	9.7	-2.3	Romania	RO	15.1	18.0	-2.9
Estonia	EE	5.8	7.4	-1.6	San Marino	SM	13.2	15.4	-2.2
Finland	FI	6.2	8.3	-2.1	Serbia (incl. Kosovo*)	RS	14.8	18.2	-3.4
France (metropolitan)	FR	12.2	16.6	-4.4	Slovakia	SK	11.3	14.7	-3.4
Germany	DE	15.2	19.2	-4.1	Slovenia	SI	12.8	15.4	-2.6
Greece	GR	16.8	20.2	-3.5	Spain (excl. Canarias)	ES	14.6	20.2	-5.6
Hungary	HU	14.9	17.2	-2.3	Sweden	SE	6.5	9.2	-2.7
Iceland	IS	7.1	10.7	-3.6	Switzerland	CH	14.5	18.8	-4.4
Ireland	IE	7.4	9.9	-2.5	United Kingdom (& Cr. dep.)	UK	13.9	19.8	-5.9
Italy	IT	17.6	21.8	-4.2	**Total without Türkiye**		**14.0**	**18.0**	**-4.0**
Latvia	LV	9.6	11.5	-1.9	**EU-27**		**14.1**	**17.9**	**-3.8**
Liechtenstein	LI	15.3	17.9	-2.6	Kosovo*	KS	14.4	16.1	-1.7
Lithuania	LT	10.1	11.6	-1.5	Serbia (excl. Kosovo*)	RS-	14.9	18.7	-3.9

(*) Under the UN Security Council Resolution 1244/99.

Notes: 5-year mean, i.e. five-year mean 2015-2019. Diff., i.e. difference concentrations between 2020 and five-year mean 2015-2019.

Annex 5
Concentration maps including stations

Throughout the report, the concentration maps presented do not include the concentration values measured at the stations. The reason is to better visualise the health-related indicators with their distinct concentration levels at the more fragmented and smaller urban areas.

As presented in Annex 3, the kriging interpolation methodology somewhat smooths the concentration field. Therefore, it is valuable to present in this Annex 5 the indicator maps including the concentration values resulting from the measurement data at the stations. These points provide important additional visual information on the smoothing effect caused by the interpolation. For instance, maps A5.1 and A5.2 present PM_{10} indicators annual average and 90.4 percentile of daily means and include the stations points used in the interpolation. They correspond to Maps 2.1 and 2.2 of the main report, which do not have stations. Table A5.1 provides an overview on the maps of the main report and the corresponding maps including stations point values as presented in this annex.

Both the rural and the urban/suburban background stations and also urban/ traffic stations for PM and NO_2 are included in the maps of the health related indicators, while the rural stations only are shown in the maps of vegetation related indicators. For $PM_{2.5}$ and NO_x, only the stations with relevant measured data (i.e. not the pseudo stations) are presented. For all pollutants, only the validated measurement data (i.e. not the non-validated E2a data from the UK stations) are presented in the maps.

Table A5.1: Overview of maps presented in this Annex 5 and their relation with the maps presented in the main report

Air pollutant	Indicator	Map including stations	Map without stations
PM_{10}	Annual average	A5.1	2.1
	90.4 percentile of daily means	A5.2	2.2
$PM_{2.5}$	Annual average	A5.3	2.3
Ozone	93.2 percentile of maximum daily 8-hour means	A5.4	3.1
	SOMO35	A5.5	3.2
	SOMO10	A5.6	3.3
	AOT40 for vegetation ([a])	A5.7	3.4
	AOT40 for forests ([a])	A5.8	3.5
NO_2	Annual average	A5.9	4.1
NO_x	Annual average ([a])	A5.10	4.2
BaP	Annual average	A5.11	5.1

([a]) Rural map, applicable for rural areas only.

Map A5.1: Concentration map of PM_{10} annual average including station measurement values, 2020

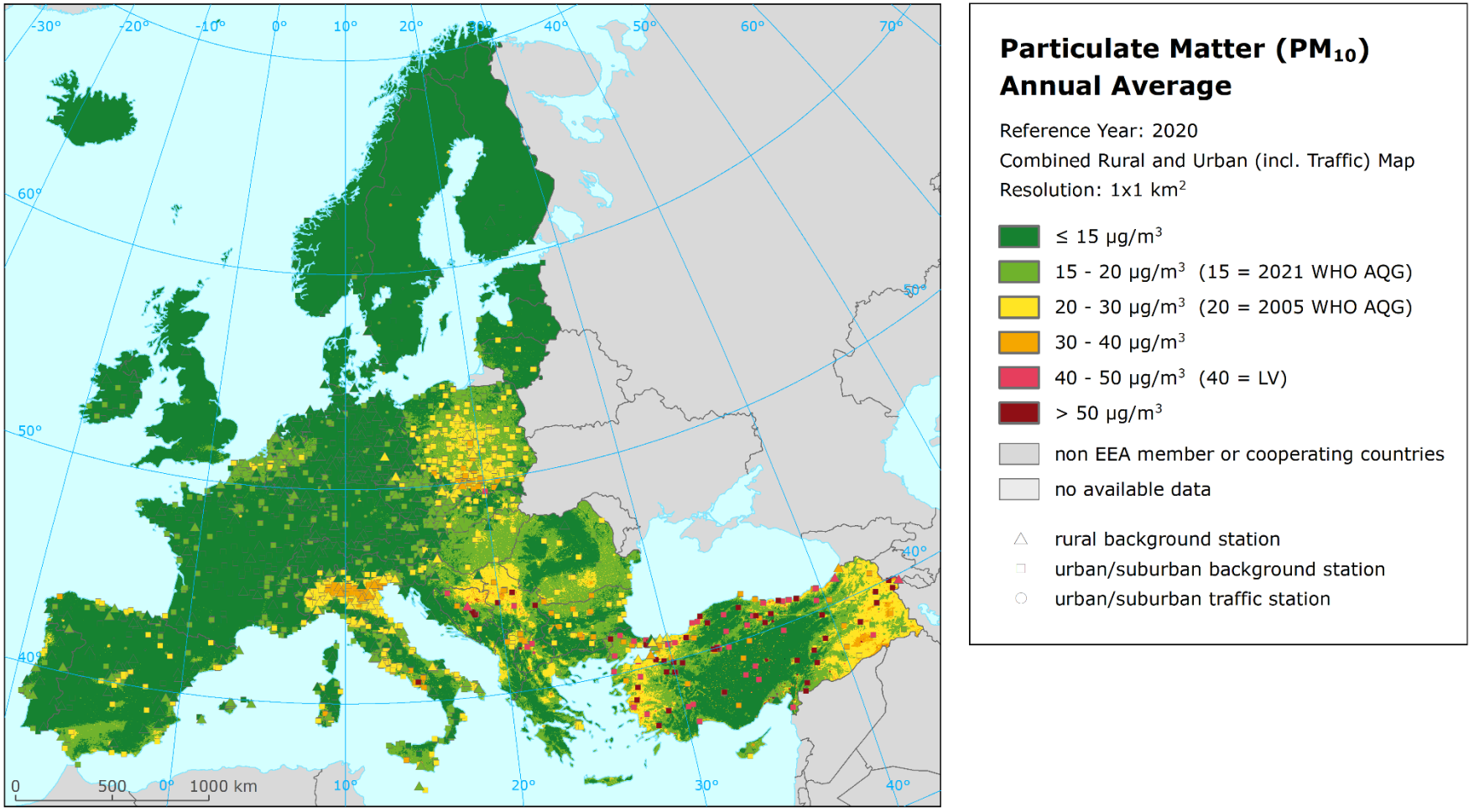

Map A5.2: Concentration map of PM_{10} indicator 90.4 percentile of daily means including station measurement values, 2020

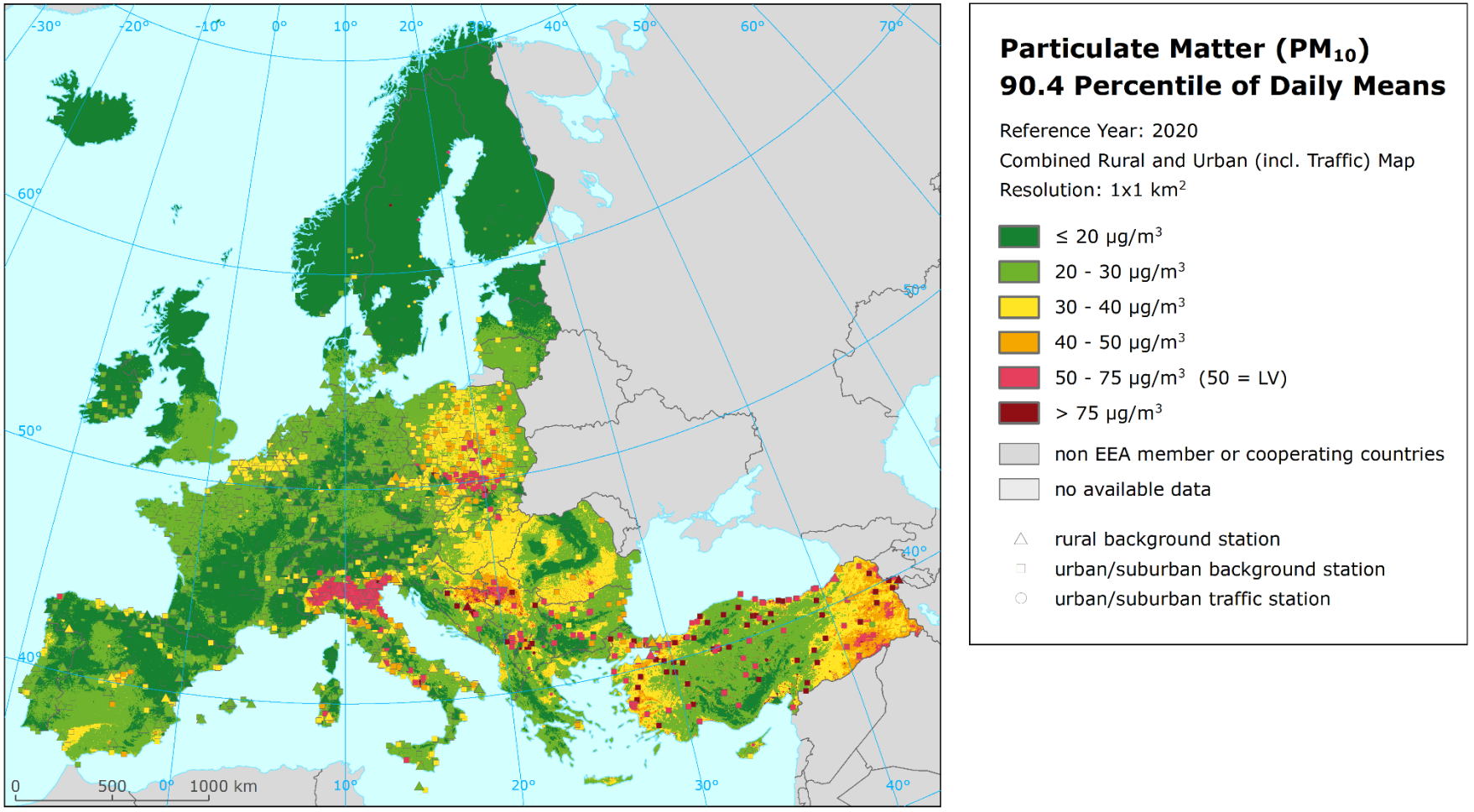

Map A5.3: Concentration map of $PM_{2.5}$ annual average including station measurement values, 2020

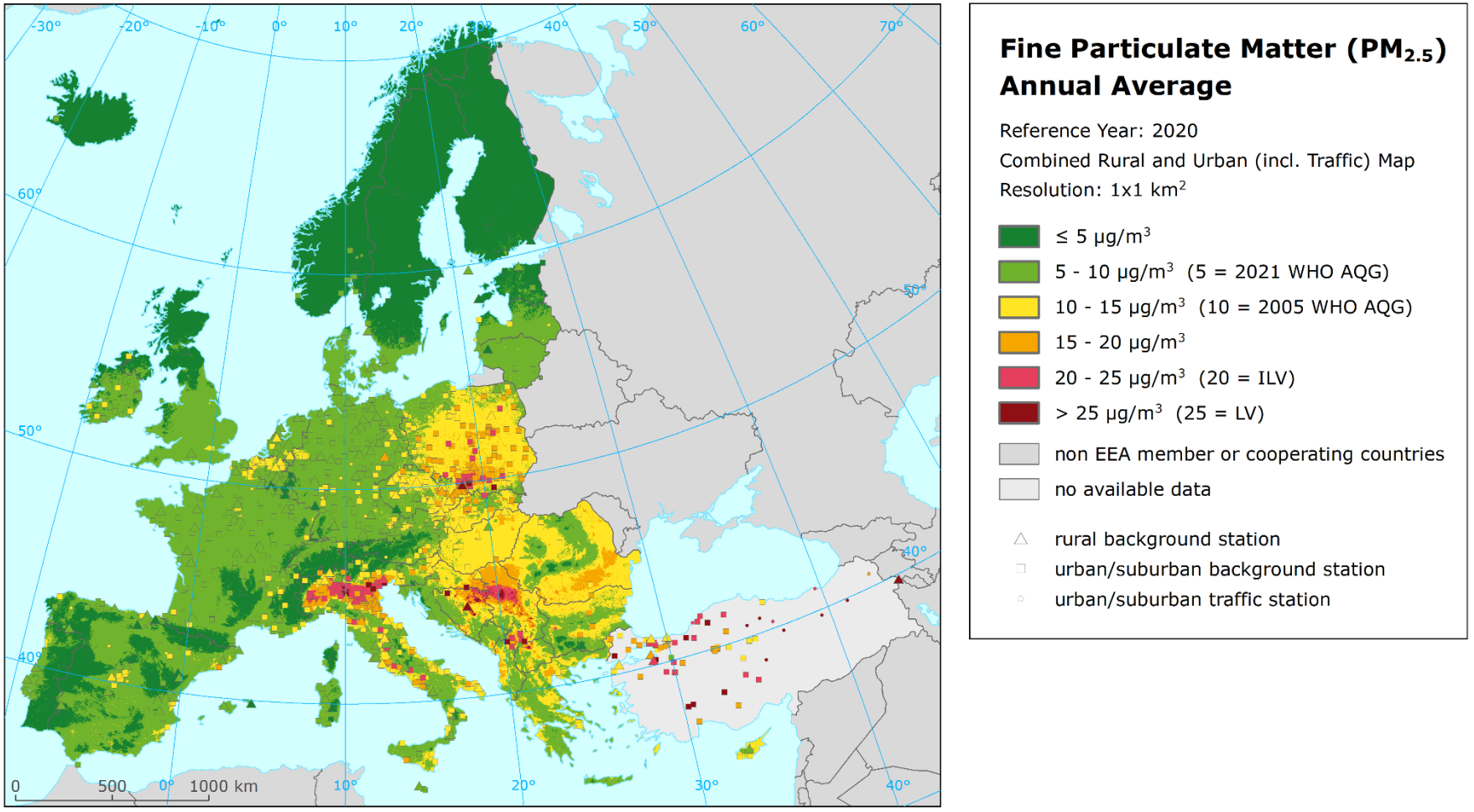

Map A5.4: Concentration map of ozone indicator 93.2 percentile of maximum daily 8-hour means including station measurement values, 2020

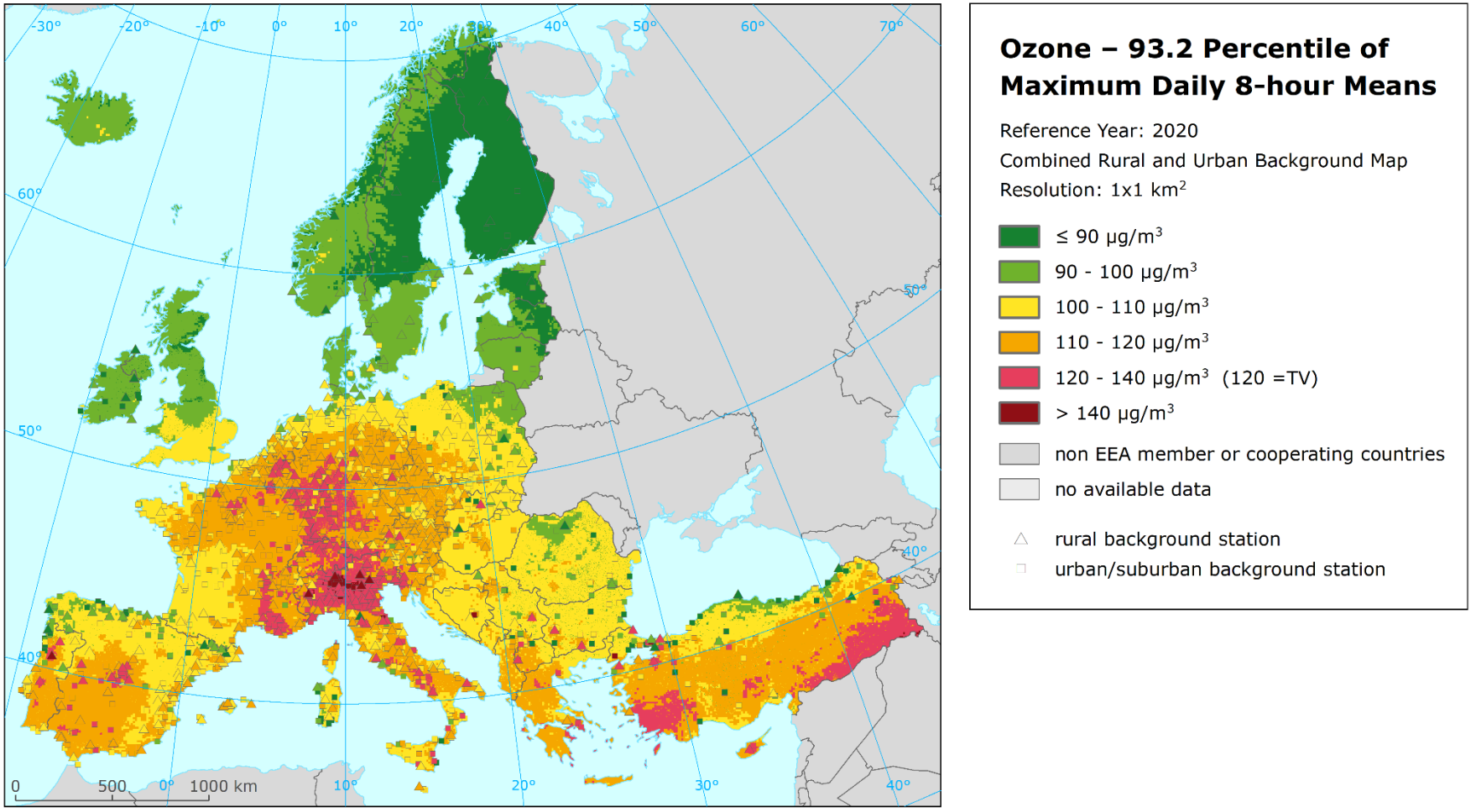

Map A5.5: Concentration map of ozone indicator SOMO35 including station measurement values, 2020

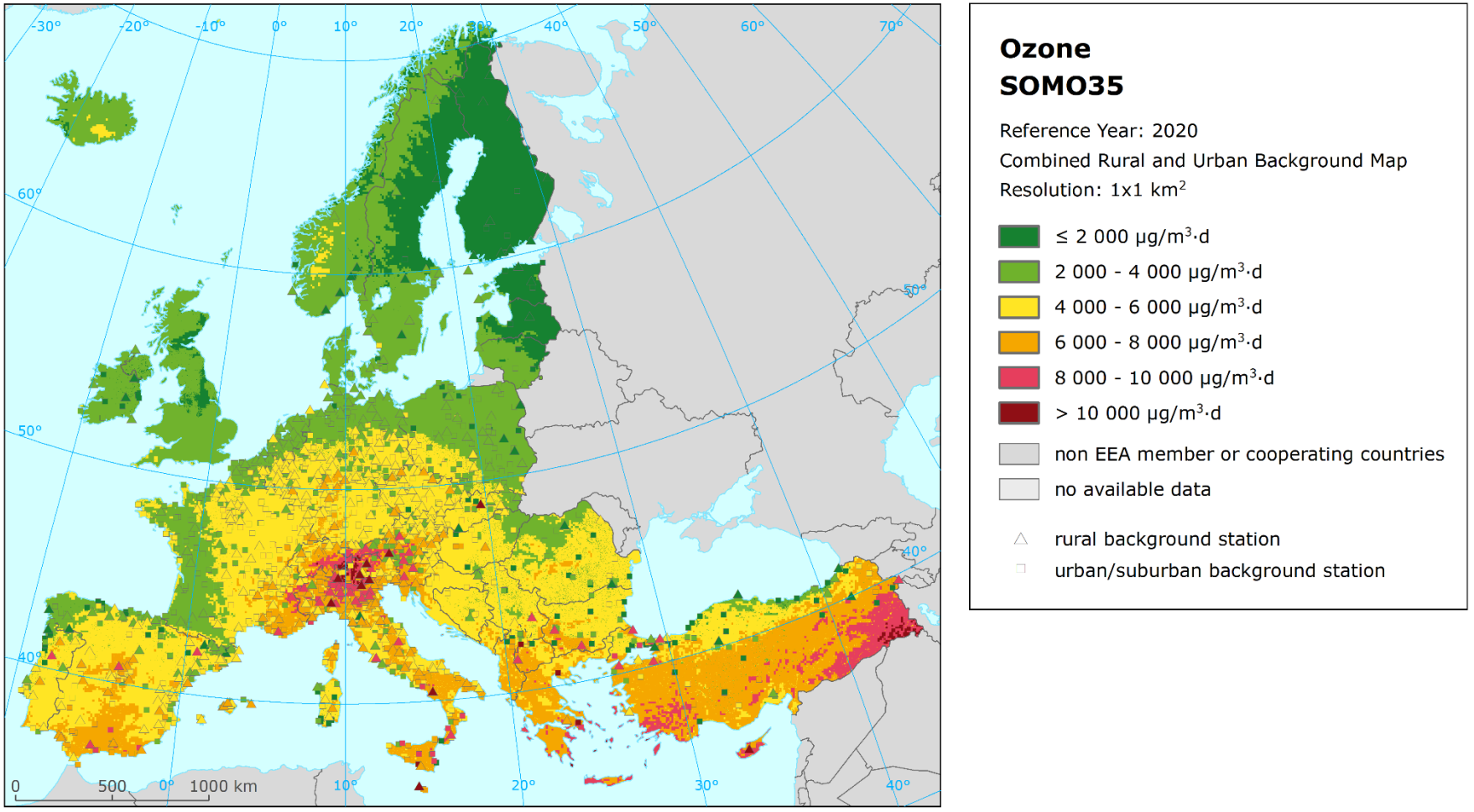

Map A5.6: Concentration map of ozone indicator SOMO10 including station measurement values, 2020

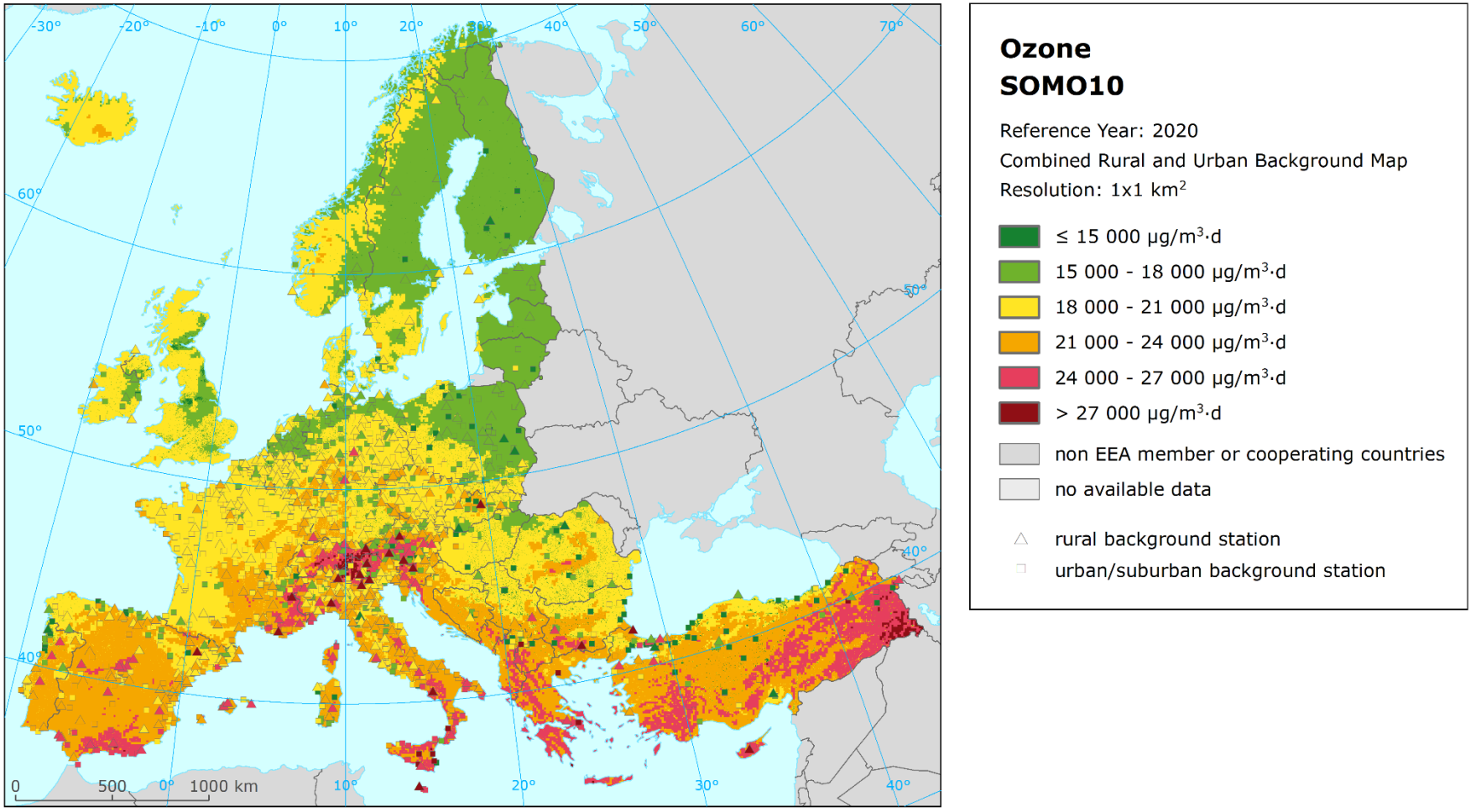

Map A5.7: Concentration map of ozone indicator AOT40 for vegetation including station measurement values, rural air quality, 2020

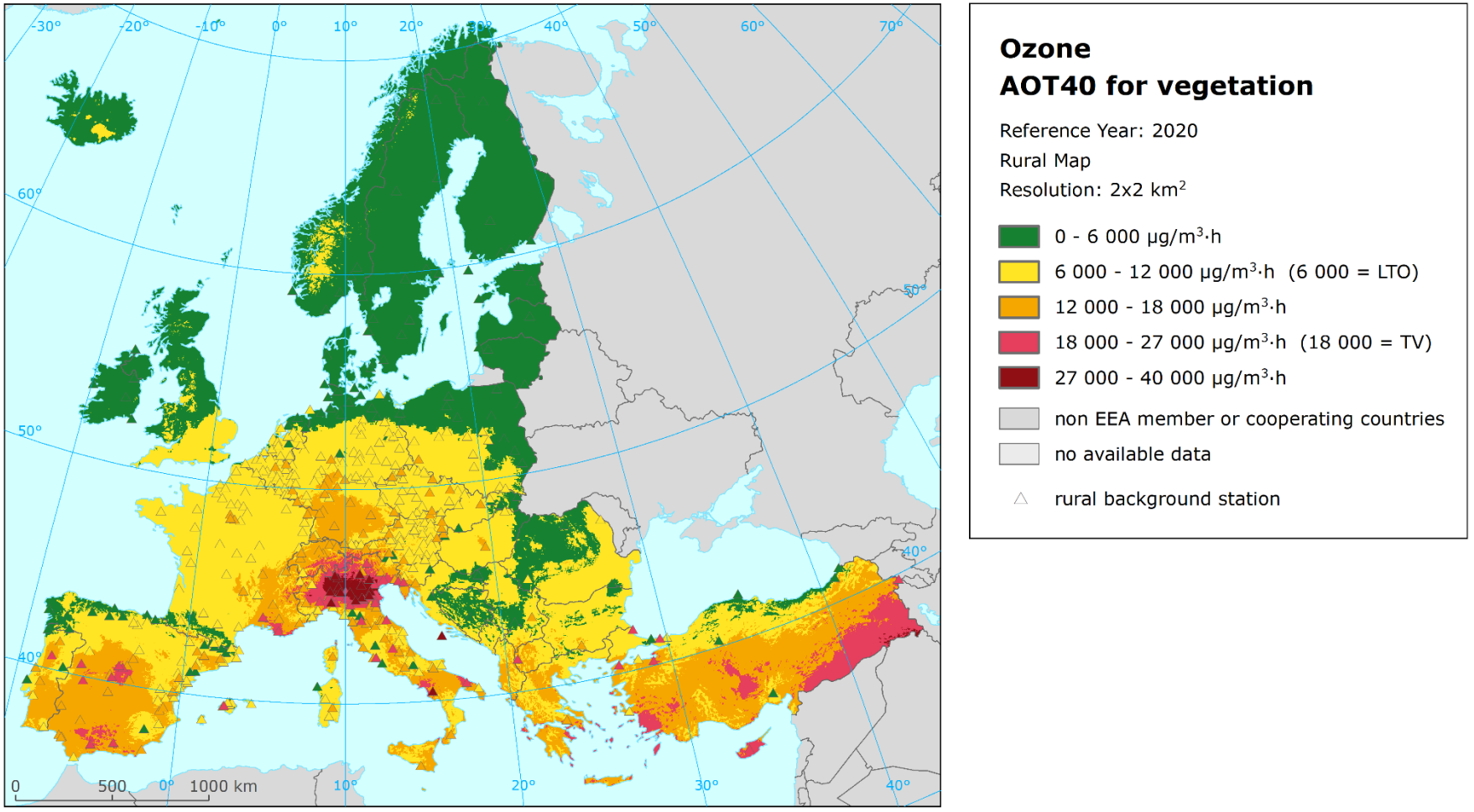

Map A5.8: Concentration map of ozone indicator AOT40 for forests including station measurement values, rural air quality, 2020

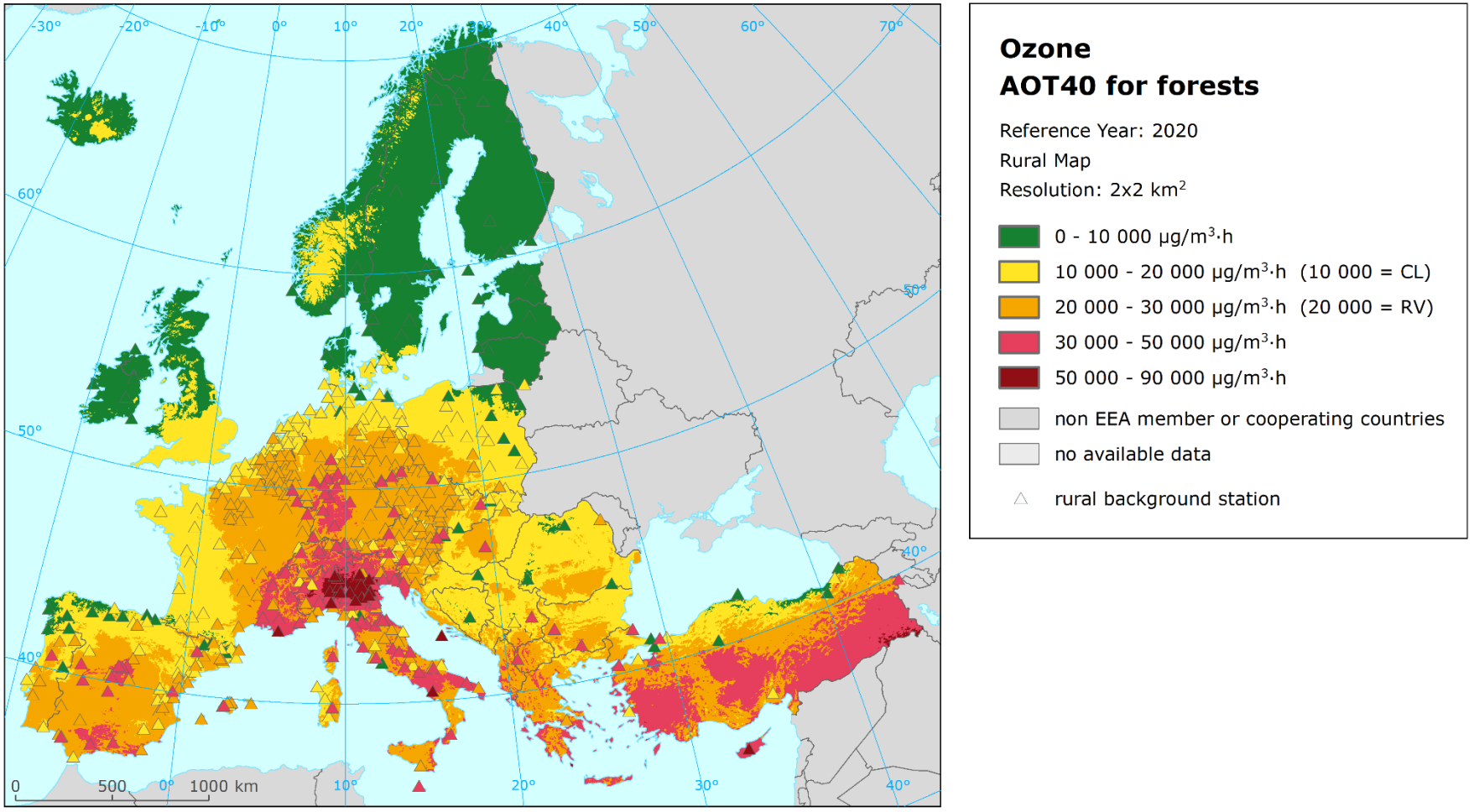

Map A5.9: Concentration map of NO_2 annual average including station measurement values, 2020

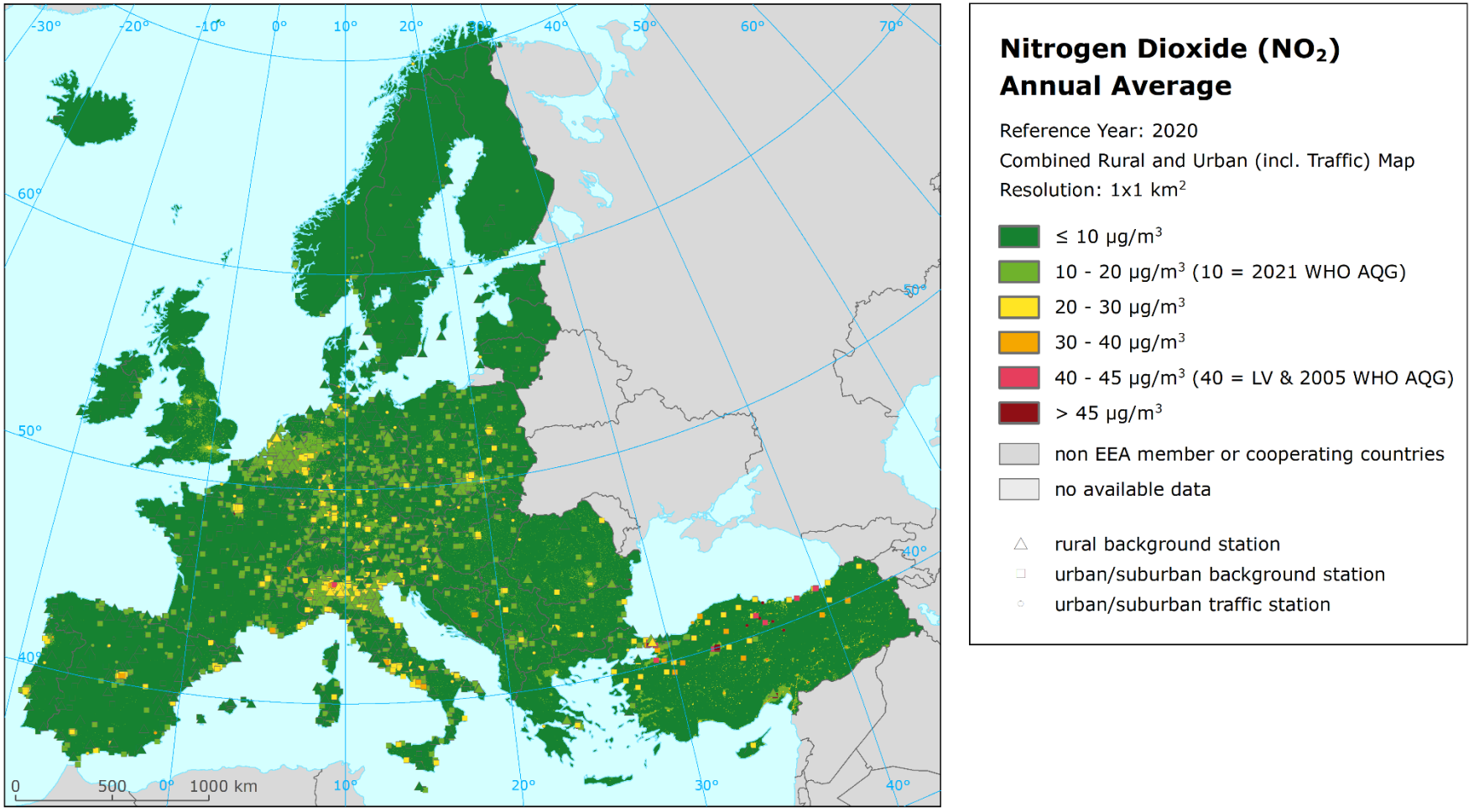

Map A5.10: Concentration map of NO_X annual average including station measurement values, rural air quality, 2020

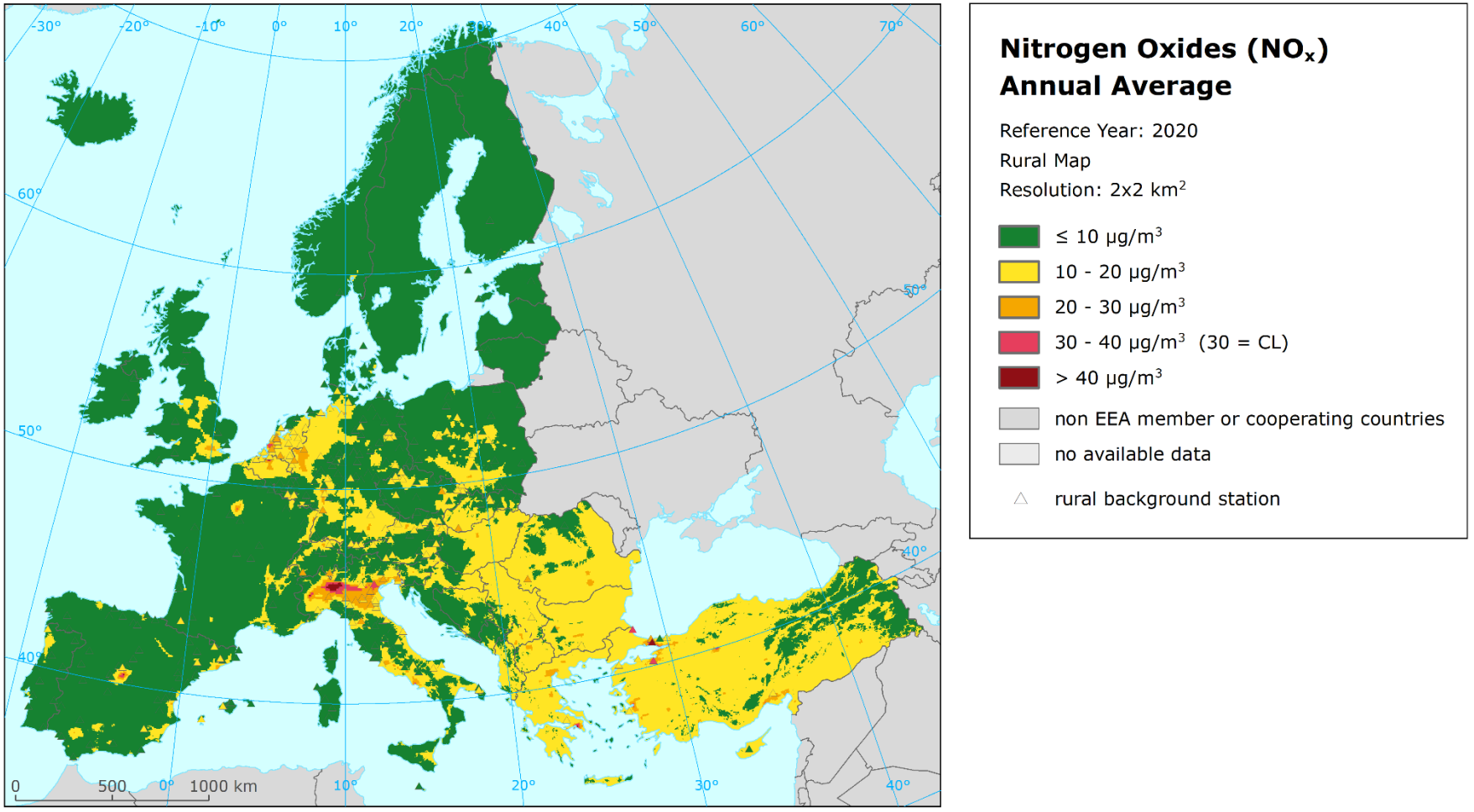

Map A5.11: Concentration map of benzo(a)pyrene annual average including station measurement values, 2020, experimental map

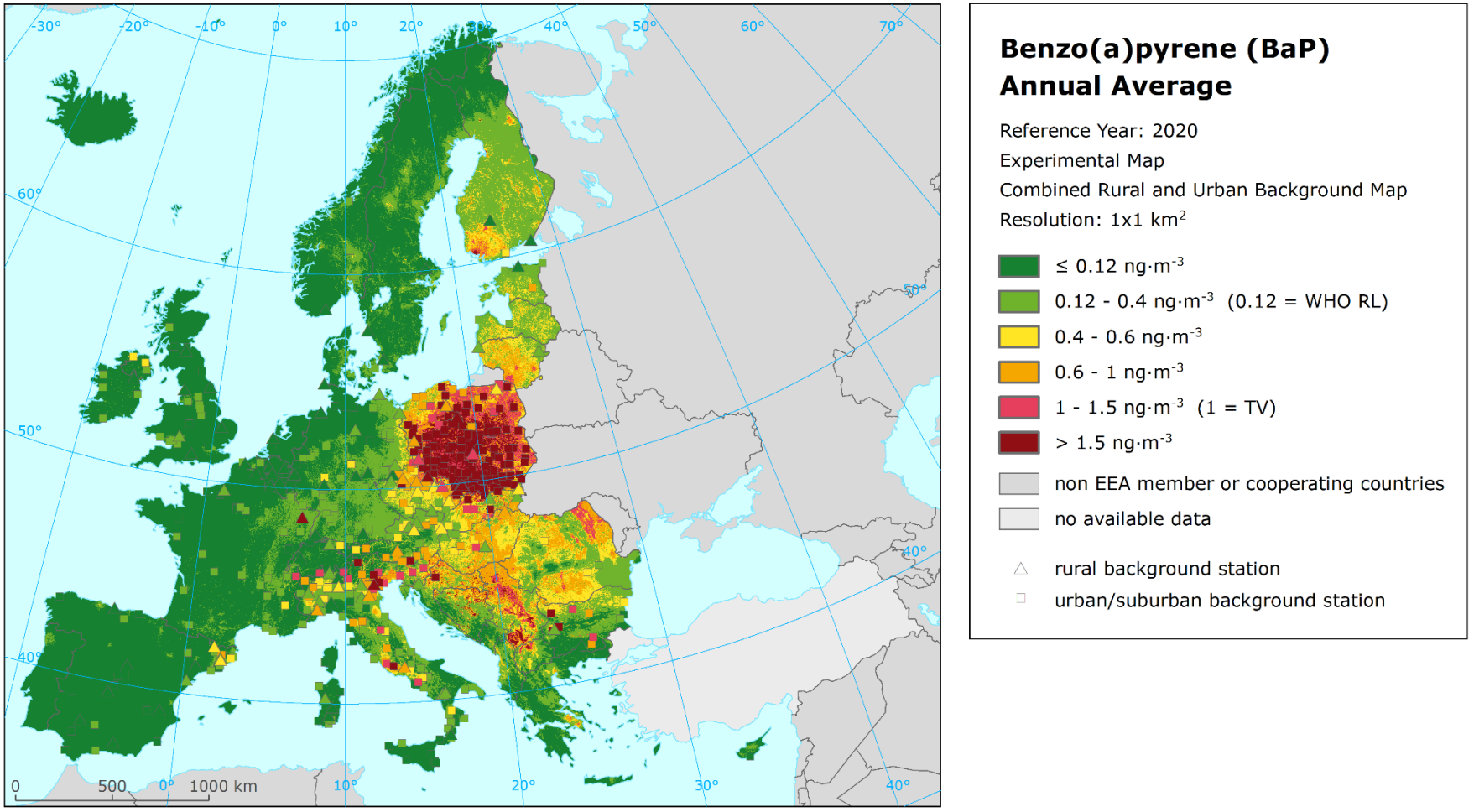

European Topic Centre on
Human Health and the Environment
https://www.eionet.europa.eu/etcs/etc-he

The European Topic Centre on Human Health and the Environment (ETC HE) is a consortium of European institutes under contract of the European Environment Agency.

European Environment Agency
European Topic Centre
Human health and the environment